UNIVERSITÀ
DEGLI STUDI
FIRENZE

DOTTORATO DI RICERCA IN

Farmacologia,Tossicologia e Trattamenti Innovativi

CICLO XXVII

COORDINATORE Prof.ssa Elisabetta Teodori

Gene and microRNA expression profiles in models of brain aging: effects of bioactive phenolic compounds

Settore Scientifico Disciplinare BIO/14

Dottorando

Dott.ssa Elisabetta Bigagli

Tutore scientifico

Prof.ssa Cristina Luceri

Tutore teorico

Prof. Piero Dolara

Coordinatore

Prof.ssa Elisabetta Teodori

Anni 2012/2014

INDEX

Summary of the results of *in vivo* experiments

Age-related diseases have increasingly become the focus of much research interest in recent years, due to the progressive increase in human life expectancy in Western countries and, as a consequence, in the proportion of aged subjects in those populations. Aging is associated with illnesses of many human organs and tissues, but particularly important are those related to the aging of brain cells, which may underlie peculiar susceptibility to acute (e.g., stroke, traumatic events) and neurodegenerative diseases (e.g., Alzheimer's and Parkinson disease) that represent a heavy economic burden and an unmet therapeutic need all over the world (Yankner et al., 2008).

Understanding the mechanisms of age-related changes in the brain and identifying potential modulators may have profound consequences for the prevention and treatment of age-related impairments and diseases (Glorioso and Sibille, 2011). On the other hand, several studies have suggested a role for dietary and lifestyle factors in preventing or delaying, age-related diseases but more evidences to support a role of specific food components in brain aging, are still needed (Barberger-Gateau, 2014).

The first aim of my research was to study the regulatory mechanisms of microRNAs (miRNAs) on genes during the aging process in the brain, by integrating genome-wide miRNA and mRNA expression profiles. The second aim, was to verify whether dietary treatment with olive oil phenols modifies the profile of miRNA and gene expression in the aging mouse brain, and if these changes correlate with the cognitive and motor dysfunction observed in the aged animals.

C57Bl/6J mice fed from middle age to senescence with extra-virgin olive oil rich in polyphenols (H-EVOO, phenol dose/day: 6 mg/kg) showed cognitive and motor maintenance compared to aged-matched controls, fed with the same olive oil but deprived of the phenolic content (L-EVOO). We analyzed two brain areas which are involved in cognitive and motor processes: cortex and cerebellum. Overall, our analyses demonstrated that after 6 months feeding, most of the gene expression changes, were restricted to the cerebral cortex, and for this reason, we later focused on this area alone.

Dietary treatment with H-EVOO was associated with a significant modulation of genes (mostly up-regulated) compared to L-EVOO. Among those, we found Notch1, several bone morphogenetic proteins (BMPs), the nerve growth factor receptor (NGFR) the glucagon-like peptide-1 receptor (GLP1R) and CREB-regulated transcription coactivator 3 (CRTC3) previously associated to brain functioning, synaptic plasticity, motor and cognitive improvements. The

agrin pathway, involved in cholinergic synaptic differentiation and maintenance, was also significantly modulated. We then analyzed global miRNA expression profiles in the cortex harvested from aged and young mice. Overall, H-EVOO-fed mice cortex displayed miRNA expression profiles similar to those observed in young mice. Sixty-three miRNAs, out of 1203 analyzed, were significantly down-regulated compared to the L-EVOO group; among them, mir-484, mir-27, mir-137, mir-30, mir-34 and mir-124. Evidence suggesting that these miRNA are potentially relevant to brain aging, comes from the finding that they are predicted to target the previously mentioned genes and actually, we found an inverse correlation with their target genes. Moreover, many differentially expressed miRNAs were predicted to target pathways and processes relevant to aging such as neurotrophin, axon guidance pathway, and neuro-transmission which regulate synaptic plasticity.

Overall, these results indicate that olive oil phenols exert several beneficial effects in the brain by modulating signaling cascades which impact neuronal function and synaptic plasticity. The modulation of these genes and miRNAs can be thus considered among the molecular mechanism by which olive oil phenols exert their beneficial effects on memory and motor coordination in aging mice.

Summary of the results of *in vitro* experiments

In the last few years, the European Union strongly encouraged the "3Rs" principle (replacement, reduction and refinement) for the protection and spare of animals used for scientific purposes.

In vitro systems, besides sparing animal lives, have the obvious advantage of being often less expensive and shorter in duration and offer a simplified model for shedding light into mechanisms involved in brain aging.

Our purpose was to evaluate long-term neuro-glial co-cultures as a model for investigating senescence in the nervous system and to assess its similarities with *in vivo* models.

To this aim, we maintained the cultures from 15 days in vitro (DIV) (mature cultures) up to 27 DIV (senescent cultures), measuring senescence-associated, neuronal, dendritic and astrocytic markers. Whole miRNA expression profiles were compared to those measured in the cortex of 18- and 24-month-old C57Bl/6J aged mice and of transgenic TgCRND8 mice, a model of amyloid-ß deposition.

Neuro-glial co-cultures displayed features of cellular senescence (increased SA-β-gal activity, oxidative stress, γ-H2AX expression, IL-6 production, astrogliosis) that were concentration-dependently counteracted by the anti-aging compound resveratrol (1-5 µM). Besides

recapitulating some characteristics of cellular senescence, neuro-glial co-cultures also displayed age-associated degenerative changes such as progressive neuronal loss and a decline in the dendritic network. Alterations of senescent cells were also accompanied by changes in miRNA expression. We observed a substantial miRNA down-regulation in neuro-glial co-cultures aged *in vitro* compared to their younger counterparts. The overall effect of resveratrol, was to shift the miRNA expression pattern of senescent neuro-glial co-cultures towards that observed in mature neuro-glial co-cultures (15 DIV). This observation is of particular interest and may indicate new mechanisms by which resveratrol exerts its anti-aging effects. Focusing on those miRNAs that target genes encoding for proteins whose expression was actually measured in our long-term neuro-glial co-cultures, we were able to confirm most of the predicted miRNA–mRNA interactions.

A substantial overlapping was found between age-associated changes in miRNA expression profiles *in vitro* and in TgCRND8 mice but not in physiologically aged mice, indicating that this culture model displays more similarities with pathological than physiological brain aging.

These results demonstrate that neuro-glial co-cultures aged *in vitro* can be useful for investigating the cellular and molecular mechanisms of brain aging and for preliminary testing of protective compounds.

Introduction

Aging is characterized by a progressive loss of physiological integrity, leading to impaired function, increased vulnerability and death. Age-related diseases are increasingly becoming the focus of much research in recent years, due to the progressive rise in human life expectancy in western countries and, as a consequence, to the enlarged number of the proportion of aged subjects in those populations. In 2017 there will be more people over 65 than under 5, and by 2050, two billion of the estimated nine billion people on Earth will be older than 60 (http://unfpa.org/ageingreport/). In this view, maintaining a good health into old age (health-span) has become a new frontier of modern medicine. Aging itself is the primary risk factor for major pathologies, including cancer, diabetes, cardiovascular disorders. Particularly important are the effects of aging in brain cells, which are connected to the susceptibility to acute (e.g., stroke, traumatic events) and neurodegenerative diseases (e.g., Alzheimer's and Parkinson disease) that represent a heavy economic burden and an unmet therapeutic need all over the world (Burch et al., 2014).

Understanding the mechanisms of age-related changes in gene expression and the epigenetic modifications in the aging brain and identifying potential modulators, may have profound consequences for the prevention and treatment of age-related impairments and diseases (Glorioso and Sibille, 2011). On the other hand, several studies have suggested a role for dietary and lifestyle factors in preventing or delaying, age-related diseases but more evidences to support a role of specific food components in brain aging are still needed (Barberger-Gateau, 2014). In this context, the development of whole genome "omic" technologies offers a new strategy to give some new insight into the pathways regulating brain functioning and nutrition which might provide new dietary interventions aimed at prevention and help understanding their effects.

Conserved pathways in organismal and brain aging

Some hallmarks of the aging process have been recently described and involve genomic instability, telomere attrition, epigenetic alterations, loss of proteostasis, deregulated nutrient sensing, mitochondrial dysfunction, stem cell exhaustion and altered intercellular communication (Figure 1) (López-Otín et al., 2013).

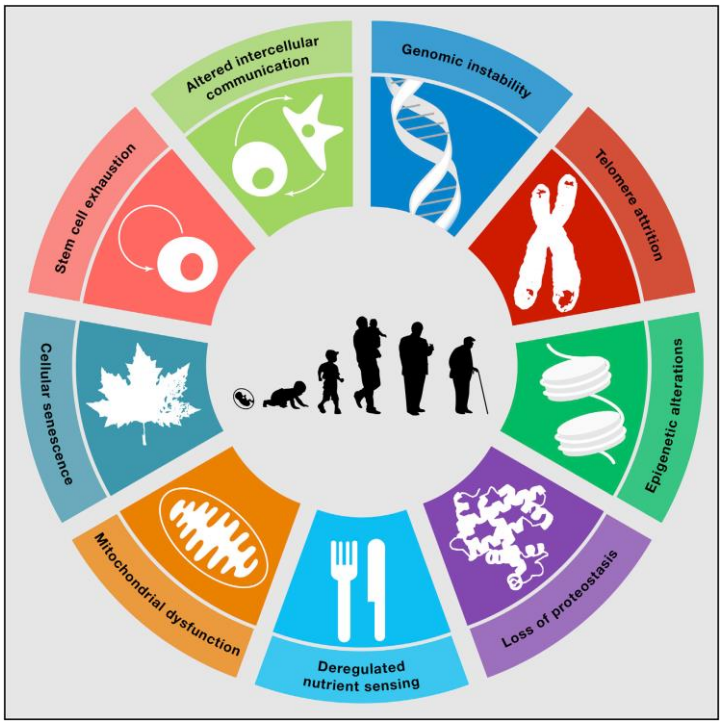

Figure 1. The Hallmarks of aging (Lòpez-Otin et al., 2013)

Genomic Instability

One common denominator of aging is the accumulation of genetic damage throughout life (Moskalev et al., 2013). The integrity and stability of DNA are continuously challenged by exogenous physical, chemical, and biological agents, as well as by endogenous threats, including DNA replication errors, spontaneous hydrolytic reactions and production of reactive oxygen species (ROS) (Hoeijmakers, 2009).

The consequence of genomic instability manifests itself in at least three important ways with age. The first is an erroneous repair of DNA damage that can lead to mutations which are irreversible and perturb tissue homeostasis by essentially promoting the formation of mosaics. Occasionally, mutations could occur in DNA repair factors and this can induce

profound neurodegeneration (Figure 2, red arrow) (Vijg and Suh, 2013). Another way in which DNA damage participates in aging is a decrease in DNA repair activities that can block the transcription of genes encoding for critical neural functions leading to cognitive decline. The formation of DNA damage also elicits epigenetic changes that can accumulate over time as "epi-mutations" and affects gene expression (Madabhushi et al., 2014) (Figure 2).

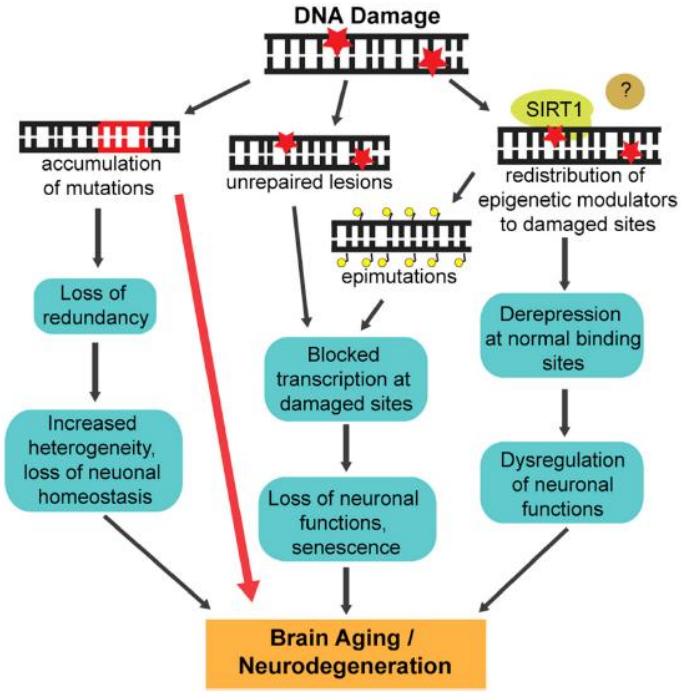

Figure 2. DNA Damage in aging and neurodegeneration (Madabhushi et al., 2014)

Mitochondrial dysfunction and oxidative stress

The classical mitochondrial free radical theory of aging proposes that the progressive mitochondrial dysfunction that occurs with aging results in increased production of ROS, which in turn causes further mitochondrial deterioration and global cellular damage (Harman, 1965).

Gene expression studies suggest that a reduced expression of mitochondrial genes is a strongly conserved feature of aging in organisms ranging from *C. elegans* to humans (Yankner et al., 2008). In particular, organ-specific analysis of brain aging has revealed a progressive decline in mitochondrial gene expression in rats, *rhesus* macaques and humans (Blalock et al., 2003; Lu et al., 2004; Loerch et al., 2008). Mitochondrial function seems to have an important modulating influence on the aging process in all species and it can have either positive or

negative effect on lifespan (Sedensky and Morgan, 2006). Mice that have been engineered to accumulate mitochondrial DNA mutations at an elevated rate show reduced electron chain transport, signs of accelerated ageing and shortened lifespan (Trifunovic et al., 2004). Conversely, overexpression of the antioxidant enzyme catalase specifically in mitochondria, is sufficient to extend mouse lifespan (Schriner et al., 2005).

However, the last 5 years have witnessed an intense re-evaluation of the mitochondrial free radical theory of aging (Hekimi et al., 2011). Of particular impact has been the unexpected observation that increased ROS may prolong lifespan in yeast and *C. elegans* (Van Raamsdonk and Hekimi, 2009). Similarly unexpected are the effects of genetic manipulations in mice that increase mitochondrial ROS and oxidative damage, which do not seem to accelerate aging (Zhang et al., 2009); Likewise, mice with increased antioxidant defenses do not present an extended lifespan (Page et al., 2010). On the other hand in mice a reduced activity of the cytochrome c oxidase complex, a component of the electron transport chain, is associated with increased lifespan. Intriguingly, these mice also exhibit protection against neuronal excitotoxic damage in the brain (Dell'Agnello et al., 2007).

The observation that a modestly reduced mitochondrial function can activate longevity raises the interesting possibility that the initial decline in mitochondrial gene expression observed during brain aging may be part of an active compensatory mechanism that increases stress resistance. In this sense, the primary effect of ROS would be the activation of compensatory homeostatic responses. Beyond a certain threshold, ROS levels betray their original homeostatic purpose and eventually aggravate, rather than alleviate, the age-associated damage (Figure 3)(Hekimi et al., 2011).

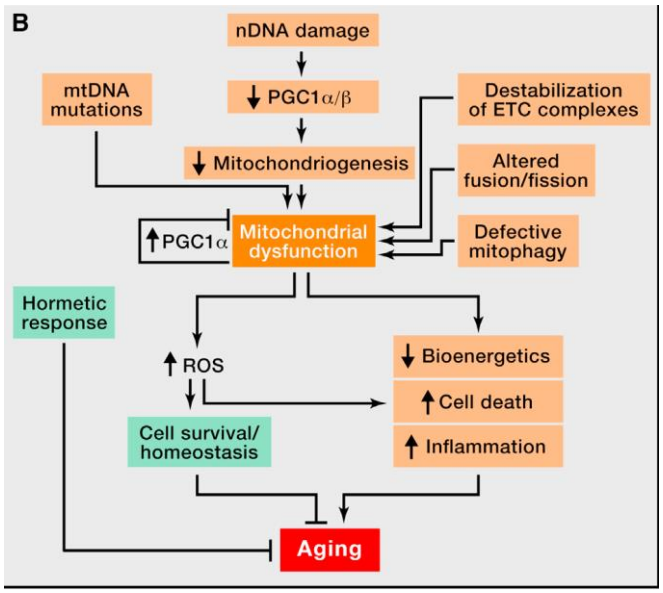

Figure 3. Mitochondrial dysfunction and oxidative stress (Lopez-Otin et al., 2012)

In the brain, declining mitochondrial function may selectively affect neuronal populations with important energy requirements, such as the large pyramidal neurons that degenerate in Alzheimer's disease (AD). With advancing age, there is a progressive accumulation of damaged molecules and impaired energy metabolism in brain cells. In successful brain aging, neurons and glial cells adapt to aging by increasing their ability to cope with stress, and by compensating for lost or damaged cells by remodeling neuronal circuits (hormesis and adaptation). In unsuccessful aging, molecular damage of neurons and inflammatory processes result in synaptic dysfunction, neuronal degeneration and death, without replacement of the lost neurons (Figure 4), (Mattson et al., 2002).

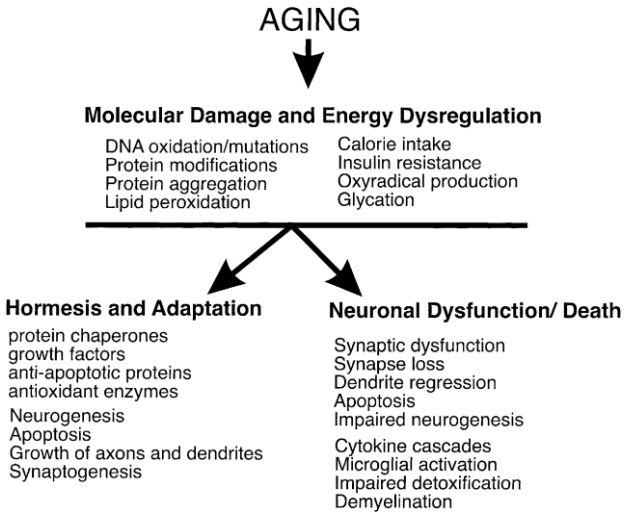

Figure 4. Signal transduction alteration in brain aging (Mattson et al., 2002)

Epigenetic regulation of aging

Epigenetics refers to the study of mechanisms that alter gene expression without altering the primary DNA sequence. Epigenetic mechanisms are reversible and include changes in DNA methylation, histone modifications and variations of small noncoding microRNAs (miRNA) (Kanwal and Gupta, 2012).

Most epigenetic research has converged on the study of modifications of DNA and histone proteins as the mechanisms that directly influence chromatin structure. The basic repeating unit of chromatin is the nucleosome which consists of 146 bp of DNA wrapped around an octamer of histones (two copies of each of H2A, H2B, H3, and H4 monomers). Chromatin can be functionally classified into two forms: heterochromatin and euchromatin (Grewal and Jia, 2007). Euchromatin is decondensed during interphase, is permissive for transcription and replicates early during S-phase. On the other hand, heterochromatin remains condensed during interphase and is mostly transcriptionally silent (Muñoz-Najar and Sedivy, 2011). Different modifications, including DNA methylation and various histone modifications, regulate the constant remodeling of chromatin.

In mammals, nearly all DNA methylation occurs on cytosine residues of CpG dinucleotides and correlates with transcriptional repression (Goll and Bestor, 2005). During aging, global DNA methylation decreases, while some promoters become aberrantly hypermethylated (Waki et al., 2003).

Modifications that are associated with active transcription, such as acetylation of histone 3 (H3) and histone 4 (H4), and dimethylation (Me2) or trimethylation (Me3) of H3K4

and H3K36, are now commonly referred to as euchromatic modifications. Methylations of H3K9, H3K27, and H4K20 are principally localized in inactive genes or regions and are thus regarded as heterochromatic marks; they thus constitute age-associated epigenetic markers (Han and Brunet, 2012) (Figure 5). The role of miRNAs in aging will be discussed in detailed in the section “MicroRNAs as mediators of the ageing process” .

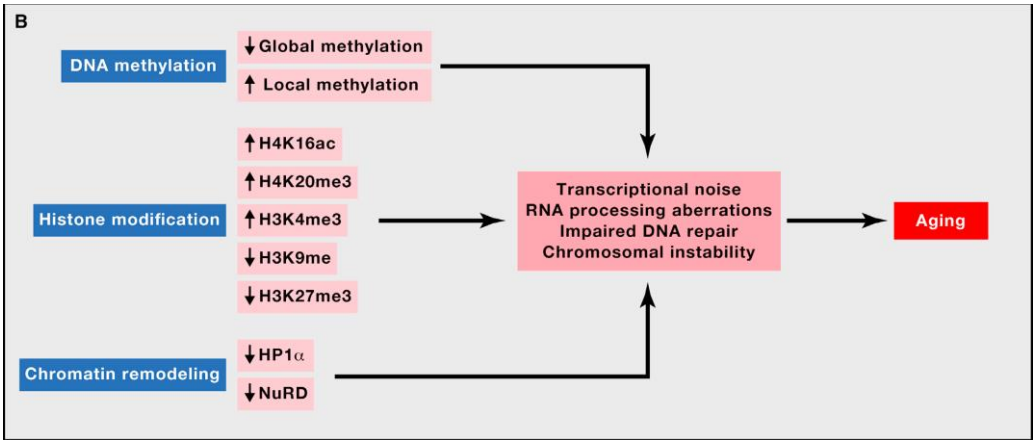

Figure 5. Epigenetic regulation of aging (Lopez-Otin et al., 2012)

Loss of Proteostasis

Proteostasis involves mechanisms for the stabilization of correctly folded proteins, most prominently the heat shock family of proteins, and mechanisms for the degradation of proteins by the proteasome or the lysosome (Hartl et al., 2011; Koga et al., 2011). All these systems function in a coordinated fashion to restore the structure of misfolded polypeptides or proteins to remove and degrade them completely, thus preventing the accumulation of damaged components and assuring the continuous renewal of intracellular proteins. Accordingly, many studies have demonstrated that proteostasis is altered with aging (Koga et al., 2011). Additionally, chronic expression of unfolded, misfolded, or aggregated proteins contributes to the development of age-related pathologies, such as AD, Parkinson’s disease (PD) and cataracts (Powers et al., 2009).

The activities of the two principal proteolytic systems, namely, the autophagy-lysosomal system and the ubiquitin-proteasome system, also decline with aging, supporting the idea that collapsed proteostasis constitutes a common feature of old age (Tomaru et al., 2012) (Figure 6). In flies, increasing autophagy in neurons alone is sufficient to extend lifespan whereas reducing autophagy shortens lifespan and gives rise to neurodegeneration (Simonsen

et al., 2008). Reduced basal autophagy in the mouse nervous system similarly leads to neurodegeneration (Komatsu et al., 2006).

The signaling pathway of mTOR kinase (mammalian target of rapamicin) is a central regulator of protein homeostasis that acts to control autophagy; reduced mTOR signalling has been shown to extend lifespan in yeast, worms and flies (Schieke and Finkel, 2006). Moreover, it was shown that the mTOR inhibitor rapamycin extends lifespan in mice even when treatment is initiated late in life (Harrison et al., 2009). Moreover, rapamycin has been shown to reduce toxic-aggregate formation and disease progression by increasing autophagy in mouse and fly models of Huntington's disease and tauopathy (Ravikumar et al., 2004).

The accumulation of ubiquitylated protein aggregates can also occur during normal human brain ageing and reaches pathological levels in neurodegenerative disorders such as Alzheimer's disease and tauopathies. A mouse model of chronically reduced proteasomal activity in the brain, showed elevated concentrations of several proteins, some of which had previously been found to be altered in the brain of Alzheimer's disease patients. Furthermore, these mice had deficits in spatial memory, consistent with a potential role for defective proteasome function in cognitive decline associated with Alzheimer's disease (Fischer et al., 2009).

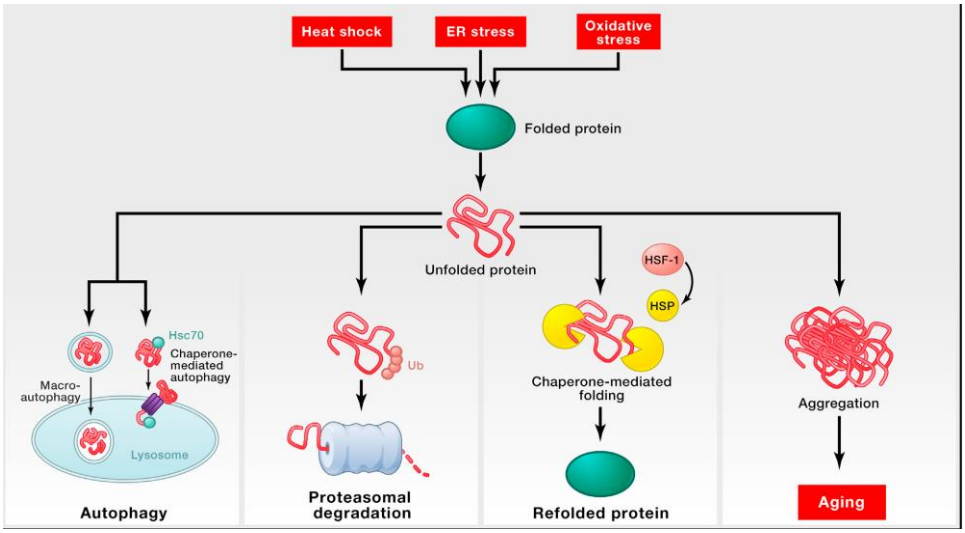

Figure 6. Loss of proteostasis in aging (Lopez-Otin et al., 2012).

Deregulated nutrient sensing pathways: insulin/IGF signaling (IIS) pathway

The insulin/IGF signaling (IIS) pathway is the most conserved aging-controlling pathway in evolution and among its multiple targets, are the FOXO family of transcription factors and the mTOR complexes, which are involved in aging (Barzilai et al., 2012). Reduced IIS pathway is a strongly conserved mechanism of lifespan extension in worms, flies and mammals (Broughton and Partridge, 2009).

Paradoxically, growth hormone and IGF-1 levels decline during normal aging, as well as in mouse models of premature aging (Schumacher et al., 2008). Thus, a decreased IIS is a common characteristic of both physiological and accelerated aging, whereas a constitutively decreased IIS extends longevity. These apparently contradictory observations can be accommodated under a unifying model by which IIS down-modulation reflects a defensive response aimed at minimizing cell growth and metabolism in the context of systemic damage (Garinis et al., 2008). According to this view, organisms with a constitutively decreased IIS can survive longer because they have lower rates of cell growth and metabolism and, hence, lower rates of cellular damage. Along the same lines, physiologically or pathologically aged organisms decrease IIS in an attempt to extend their lifespan.

Importantly, reduced IIS specifically in the nervous system, is sufficient to extend lifespan in several model systems (Iser et al., 2007). Reduction of IIS by neuron-specific knockout of the insulin receptor substrate Irs2 is sufficient to extend mouse lifespan (Taguchi et al., 2007). By contrast, in mammals, insulin and IGF-1 are neurotrophic and promote neuronal survival by inhibiting apoptosis (van der Heide et al., 2006). Insulin and IGF-1 can also promote learning and memory in humans and animal models (Broughton and Partridge, 2009). There is a dichotomy, therefore, between the neuroprotective effects of insulin and IGF-1 signaling and their apparently deleterious effects on organismal lifespan.

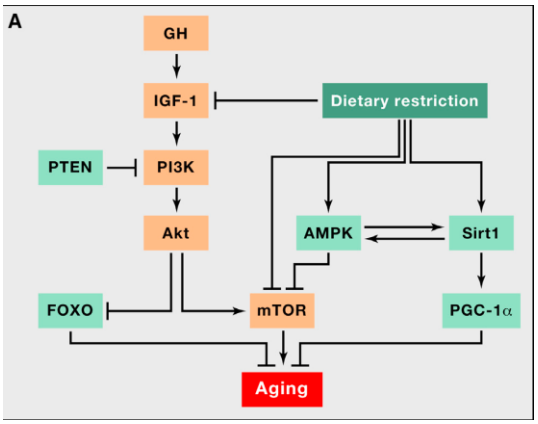

Figure 7. Deregulated nutrient sensing pathways in aging (Lopez Otin et al., 2012).

Deregulated nutrient sensing pathways: caloric restriction and sirtuines

Caloric restriction (CR) that is the reduction of calorie intake without causing malnutrition, is the only known intervention that robustly increases lifespan in many species (Haigis and Guarente, 2006). Recently, CR significantly improves age-related and all-cause survival in monkeys on a long-term ~30% restricted diet since young adulthood (Colman et al., 2014). Caloric restriction has also been widely documented to have beneficial effects on the function of the brain and its vulnerability to age-dependent pathology. It prevents many age-dependent gene expression changes in the mouse brain (Park et al., 2009), reduces age-related brain atrophy in *rhesus* macaques (Colman et al., 2009) and has significant beneficial effects on the age-dependent impairment of learning and memory in rodents (Stewart et al., 1989) and humans (Witte et al., 2009). Unexpectedly, a three-month period of caloric restriction alone in healthy aged humans was sufficient to improve verbal memory by approximately 20% (Witte et al., 2009). There is also evidence that caloric restriction may confer resistance to Alzheimer's-disease-type pathology: caloric restriction was found to reduce amyloid-β deposition and improve learning and memory in transgenic mouse models of Alzheimer's disease (Halagappa et al., 2009).

Since it is unlikely that many would be willing or able to maintain a CR lifestyle, there has been intense interest in mimicking its beneficial effects on health, and potentially on longevity, with drugs.

The sirtuin activator resveratrol, has been proposed as a candidate CR mimetic (See the Resveratrol sections).

In fact, the molecular basis of the beneficial effects of caloric restriction partly depend on sirtuines activation. In fact, in addition to the IIS pathway that participates in glucose sensing, two additional related and interconnected nutrient sensing systems are AMPK and sirtuins that act in the opposite direction to IIS and mTOR, meaning that they signal nutrient scarcity and catabolism instead of nutrient abundance and anabolism. Accordingly, their up-regulation favors healthy aging. In particular, members of the sirtuin family of NAD-dependent protein deacetylases (SIRT) and ADP ribosyl-transferases have been studied extensively as potential anti-aging factors. Interest in this family of proteins in relation to aging stems from a series of studies in yeast, flies and worms, which reported that the sirtuin gene named Sir2, has a remarkable activity on longevity (Guarente, 2011). Overexpression of Sir2 was first shown to extend replicative lifespan in *Saccharomyces cerevisiae* (Kaeberlein et al., 1999), and subsequent reports indicated that enhanced expression of the worm (sir-2.1) and fly (dSir2)

orthologs could extend lifespan in both invertebrate model systems (Rogina and Helfand, 2004; Tissenbaum and Guarente, 2001).

These findings have recently been called into question, however, since lifespan extension originally observed in the worms and flies was mostly due to confounding genetic background differences and not to the overexpression of sir-2.1 or dSir2, respectively (Burnett et al., 2011). In fact, careful reassessments indicate that overexpression of sir-2.1 only results in modest lifespan extension in *C. elegans* (Viswanathan and Guarente, 2011).

Regarding mammals, several of the seven mammalian sirtuin paralogs can modulate various aspects of aging in mice (Houtkooper et al., 2012). In particular, transgenic overexpression of mammalian SIRT1, which is the closest homolog to invertebrate Sir2, improves aspects of health during aging but does not increase longevity (Herranz and Serrano, 2010). Of all the sirtuins, SIRT1 has received most attention. It deacetylates key histone residues involved in the regulation of transcription, including H3-K9, H4-K16, and H1-K26, and multiple non-histone protein targets including p53, forkhead box protein O1/3 (FOXO1/3), peroxisome proliferator-activated receptor gamma coactivator 1α (PGC-1α), and nuclear factor NF-κB. By targeting these proteins, SIRT1 is able to regulate numerous vital signaling pathways, including DNA repair and apoptosis, muscle and fat differentiation, neurogenesis, mitochondrial biogenesis, glucose and insulin homeostasis, hormone secretion, cell stress responses, and circadian rhythms (Hubbard and Sinclair, 2014).

These proteins also play an important role in maintaining neuronal health during aging. In fact, SIRT1 is structurally important, promoting axonal elongation, neurite outgrowth, and dendritic branching. SIRT1 also plays a role in memory formation by modulating synaptic plasticity. Hypothalamic functions that affect feeding behavior, endocrine function and circadian rhythmicity are all regulated by SIRT1. Finally, SIRT1 plays protective roles in several neurodegenerative diseases including Alzheimer's, Parkinson's and motoneuron diseases, which may relate to its functions in metabolism, stress resistance and genomic stability (Herskovits and Guarente, 2014) (Figure 8.)

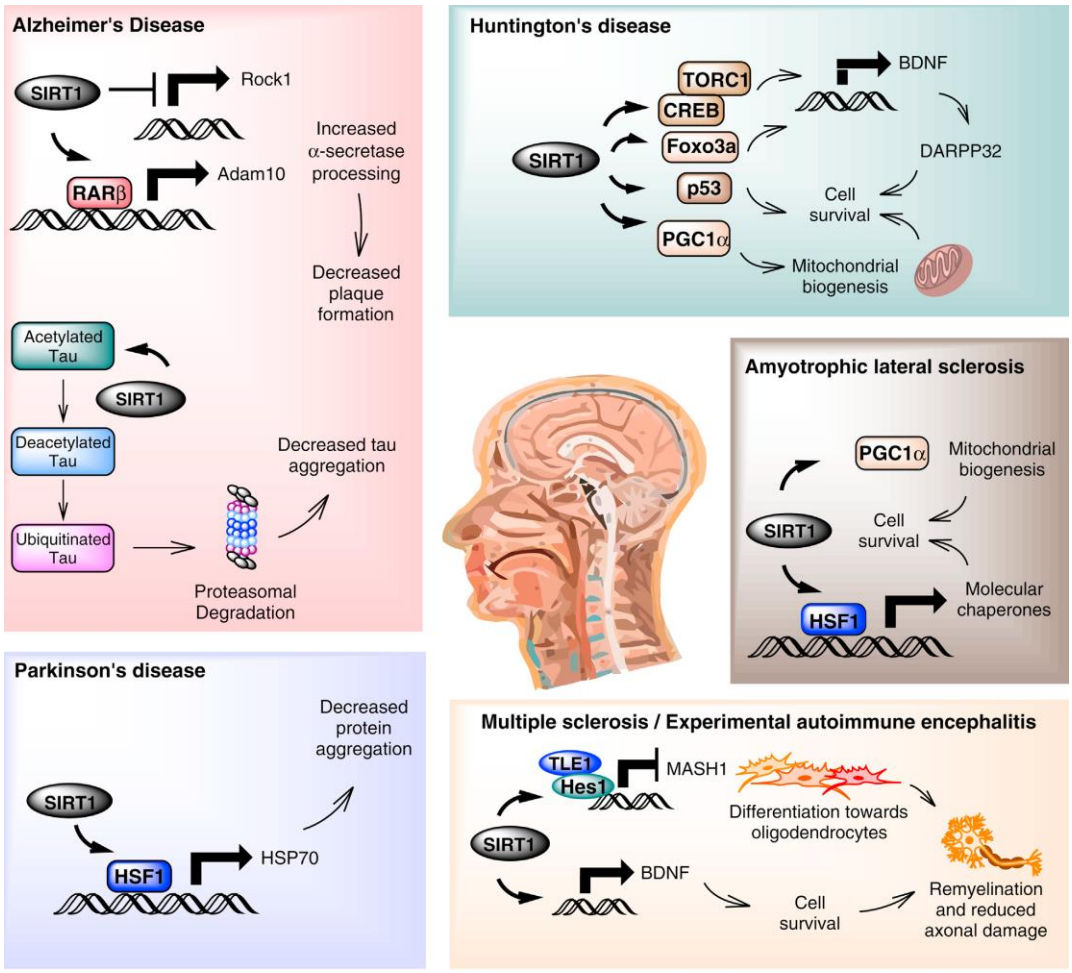

Figure 8. Major targets and mechanisms of SIRT1 in mouse models of neurodegenerative disease (Herskovits and Guarente, 2014).

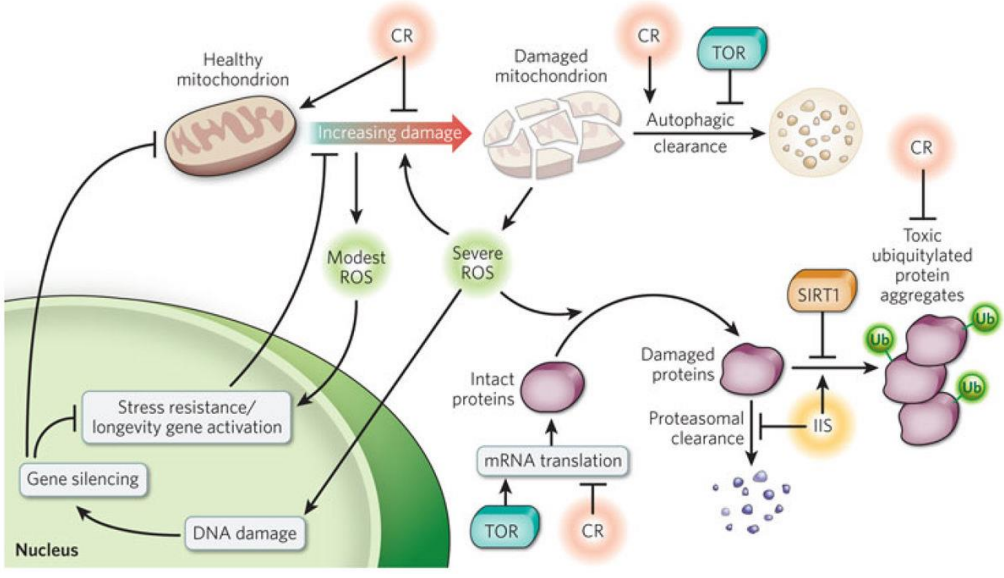

Figure 9. Overview of the pathways that regulate organismal and brain ageing

Cellular senescence

Hayflick observed that human diploid fibroblasts have a limited replication potential in serial cultivation and, beyond that limit, cells will become irreversibly growth-arrested. This cell cycle arrest was called “replicative senescence” (Hayflick, 1965). Limited replication *in vitro* represents only one type of cellular senescence, provoked by telomere shortening and later studies have demonstrated that many different insults can induce cellular stress, e.g. DNA damage and oxidative stress, and thus trigger a senescent phenotype. Thus, more generally, senescence, can be described as a state of stable cell cycle arrest in response to diverse stresses (Campisi and d’Adda di Fagagna 2007).

In young organisms, cellular senescence prevents the proliferation of damaged cells, thus protecting from cancer and contributing to tissue homeostasis. In old organisms, the pervasive damage and the deficient clearance of senescent cells result in their accumulation; this has a number of deleterious effects on tissue homeostasis. Consequently, it has been suggested that cellular senescence contributes to aging by an antagonistic pleiotropic mechanism: cellular senescence would act beneficially early in life by suppressing cancer, but detrimentally later by causing frailty (Figure 10) (Campisi, 2003).

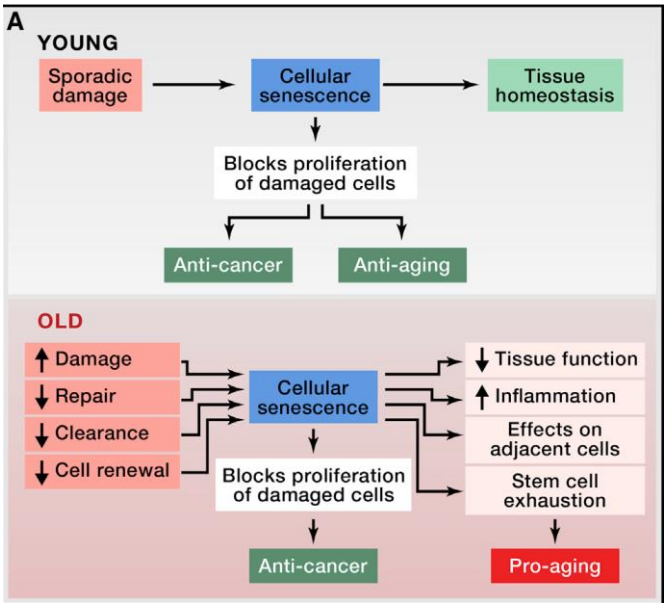

Figure 10. Cellular senescence and antagonistic pleiotropy (Lopez-Otin et al., 2012)

The onset of cellular senescence is regulated, together or sometimes independently, by two tumor suppressor proteins, p53 and retinoblastoma (Rb), whose genes are frequently

lost or mutated in cancer cells, thus promoting indefinite proliferation. In response to stimuli leading to cellular senescence, phosphorylated and stabilized p53 activates its target genes, including the cyclin-dependent kinase inhibitor p21, whose protein product activates Rb through inhibition of a cyclin-dependent kinase complex (E/Cdk2). The hypo-phosphorylated Rb inhibits the transcription of E2F target genes arresting cells in G1 phase of the cell cycle. Rb is also activated by another Cdk inhibitor, p16 acting through cyclin D/Cdk4,6 complex (Campisi, 2001) (Figure 11). Accordingly, senescent cells also show striking changes in gene expression, including up-regulation of cell-cycle inhibitors (p21WAF1 and p16INK4a) and down-regulation of genes that facilitate cell-cycle progression (c-FOS, cyclin-A, cyclin-B, PCNA) or that are involved in cell-cycle (FOXM1, UBE2C, TYMS) (Faraonio et al., 2012)

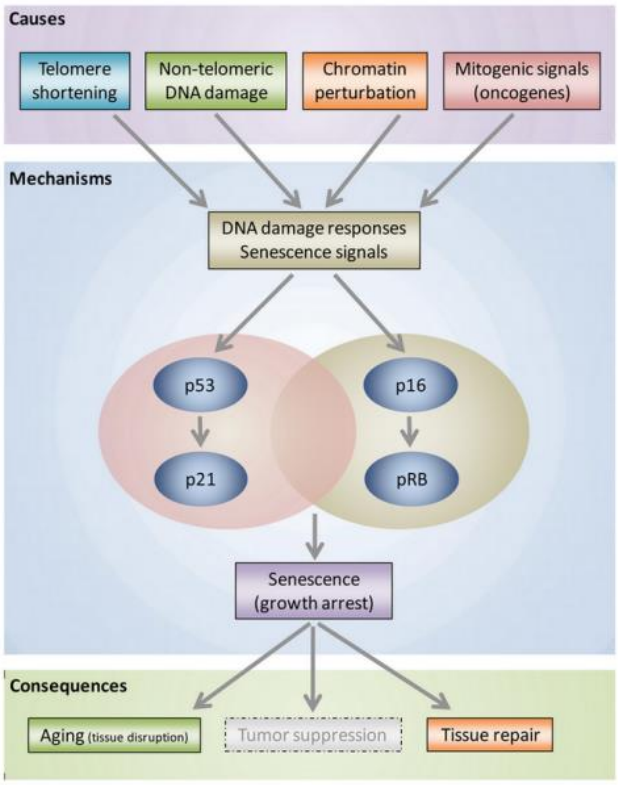

Figure 11. Causes and consequences of senescence (Naesens, 2011).

Morphological and molecular features of cellular senescence

Many morphological and molecular features of cellular senescence have been described in *in vitro* models of proliferating epithelial or mesenchymal cells. *In vivo* senescent cells have been found in human and rodent vascular endothelium and smooth muscle, fat tissue and liver (Jeyapalan and Sedivy, 2008). Senescent cells also accumulate in brain, kidney, liver and heart with advancing age (Sikora et al., 2014) and studies on animal models of accelerated aging have indicated that the premature aging is associated with an increased

level of senescence markers in their tissues (Hinkal et al., 2009) and with many diseases and pathological conditions (Muller, 2009). In the brain, it seems that the accumulation of senescent cells is linked to the decline in the number of progenitor cells and consequently to reduced neurogenesis (Molofsky et al., 2006).

Senescent cells display several characteristic morphological and biochemical features which have been used to identify senescent cells *in vitro* an *in vivo* (Figure 12):

- Altered cellular morphology (often enlarged, flat, multivacuoled and multinucleated cells).
- Increased beta-galactosidase activity (SA-β-GAL).
- Accumulation of foci of DNA damage.
- Accumulation of senescence-associated heterochromatic foci (SAHF) and promyelocytic leukemia nuclear bodies (PML NBs).
- Chromosomal instability.
- Induction of an inflammatory secretome.

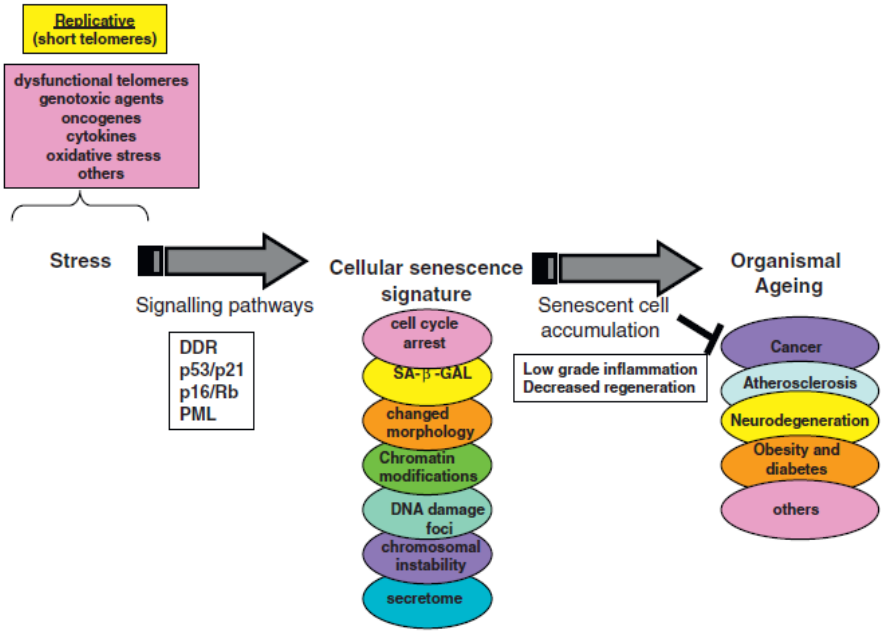

Figure 12. Schematic representation of senescence-associated biomarkers and functional consequences of senescence (Sikora et al., 2011).

Senescence-associated beta-galactosidase (SA-β-Gal)

A typical senescence phenotype consists of enlarged cell with multiple or enlarged nuclei, prominent Golgi apparatus and sometimes a vacuolated cytoplasm. In addition to morphological changes, the most common method used to identify senescent cells is the measurement of the lysosomal beta-galactosidase activity (Debacq-Chainiaux et al., 2009). Due to an expansion of the lysosomes, senescent cells show an increased activity of this enzyme, which is therefore often referred to as senescence associated beta-galactosidase (SA-β-Gal) (Lee et al., 2006). In cultured cells, SA-β-Gal activity has been observed in senescent human diploid fibroblasts (HDFs), and in skin, liver, muscle, and endothelial cells (Giovannelli et al. 2011; Sikora et al., 2011) In addition, SA-β-Gal activity increases upon prolonged culture of both cortical and hippocampal mouse neurons (Chernova, et al., 2006; Dong et al., 2011) (Figure 13).

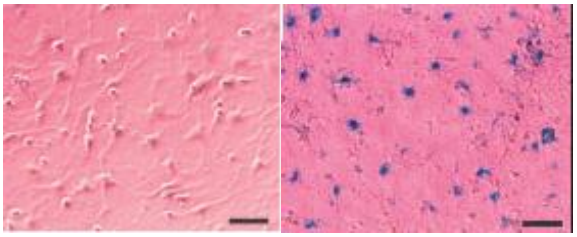

Figure 13. Detection of SA-β-Gal activity (blue staining) in primary culture of hippocampal neurons after 5 and 30 d in vitro (DIV) (adapted from Dong et al., 2011).

Senescence-associated heterochromatic foci (SAHF)

It is thought that alterations of chromatin structure contribute to the irreversible nature of the senescent state. Narita et al. (2003) found that when cells are stained with the DNA-staining dye, 4',6-diamidino-2-phenylindole (DAPI), the senescent cell nucleus is characterized by a number of DAPI foci spreading throughout the nucleus, whereas the young cell nucleus shows an almost uniform staining pattern (Figure 14, panel A, B and C). It is likely that the DAPI foci correspond to highly compacted transcriptionally inactive heterochromatin. Accordingly, the DAPI foci are called senescence-associated heterochromatic foci (SAHFs). Although not all senescent cells exhibit SAHFs, various forms of stress induce SAHF formation as well as other senescence phenotypes, suggesting that SAHFs can be used to identify senescent cells *in vivo* and that SAHF formation contributes somehow to the mechanisms of

cellular senescence (Narita et al. 2003). These heterochromatin spots are also enriched with histone H3-methylated at lysine 9 (H3K9meth), and the phosphorylated form of histone H2AX (γ-H2AX) (Figure 14, panel B and C) (Becker and Haferkamp, 2013).

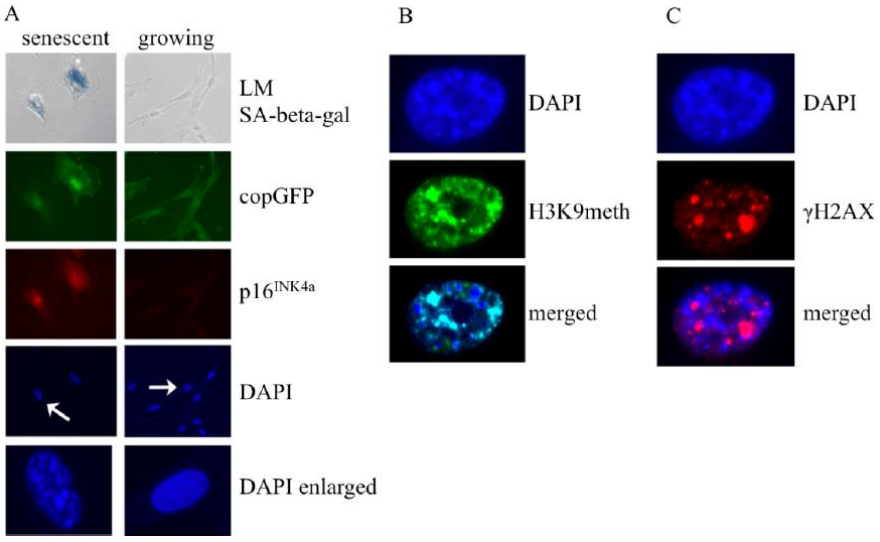

Figure 14. The typical senescent phenotype in fibroblasts (Becker and Haferkamp, 2013)

The DNA damage response and senescence

An extensive literature shows that the aging process is linked to the accumulation of nuclear DNA damage, especially in tissues with limited cell proliferation, such as brain and heart (Madabhushi et al., 2014). In the brain, both single- and double-strand breaks in DNA accumulate during aging, particularly in neurons (Enokido et al., 2008). Several evidence indicates that the DNA damage response (DDR), which is induced by dysfunctional telomeres as well as DNA double strand breaks (DSBs) elsewhere in the genome, is a feature of cellular senescence (d'Adda di Fagagna, 2008). The DDR machinery senses the damage and activates a reversible form of cell cycle arrest to enable repair of the damage. If the DNA damage is too severe, however, cells may remain in a persistent DDR, which often leads to either apoptosis or senescence. The DDR is mediated by DNA damage protein sensors such as the ATM (ataxia telangiectasia mutated), ATR (ATM and Rad3-related), CHK1 and CHK2 (checkpoint kinase 1 and 2). Ultimately, the DDR activates p53, which promotes either apoptosis or senescence via transactivation of its downstream targets, including the cyclin dependent kinase inhibitor, p21 (d'Adda di Fagagna, 2008; Sulli et al., 2012) (Figure 15).

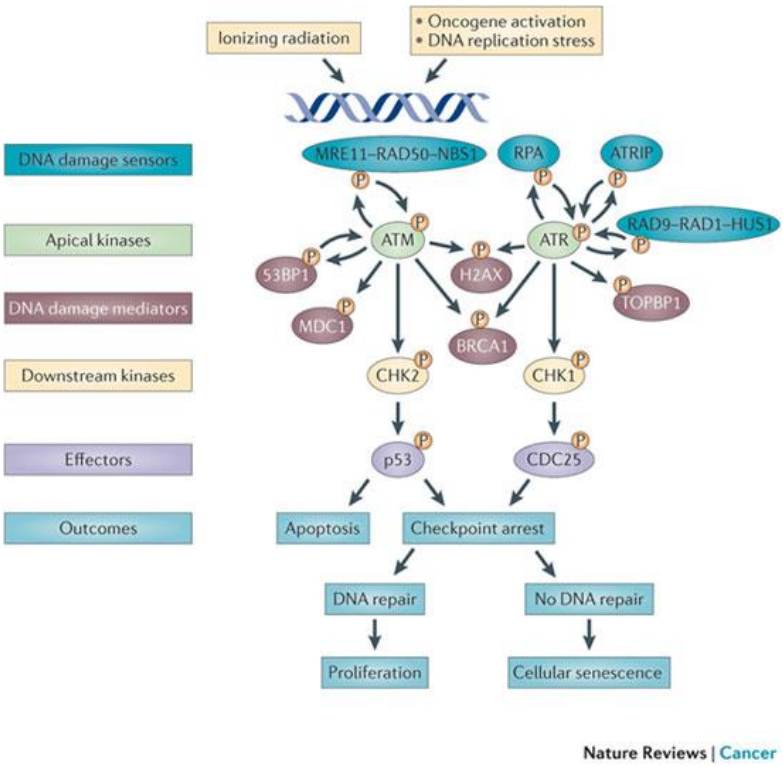

Figure 15. The DNA damage response (Sulli et al., 2012).

Consistent with the concept that the DDR is activated in senescence, the number of γ-H2AX foci (a DSB marker) increases in both mouse and human senescent primary cells (Nakamura et al., 2008), in old mouse brains as well as in other tissues (Mah et al., 2010). SA-β-GAL and γ-H2AX -positive cells co-localize in old mice (Wang et al., 2009) and the number of γ-H2AX foci in lymphocytes in humans increases with age (Sedelnikova et al., 2004). Similarly, the induction of nuclear DDR foci containing activated ATM, H2AX, activated CHK2 and other mediators of DNA damage was detected in post-mitotic primary neurons (Sordet et al., 2009). Moreover, cortical, hippocampal and peripheral neurons in the myenteric plexus from old C57Bl ⁄ 6 mice showed severe DNA damage, activated p38 MAP kinase, high ROS production and oxidative damage, IL-6 production, SAHF and SA-β-Gal activity (Figure 16), (Jurk et al., 2012).

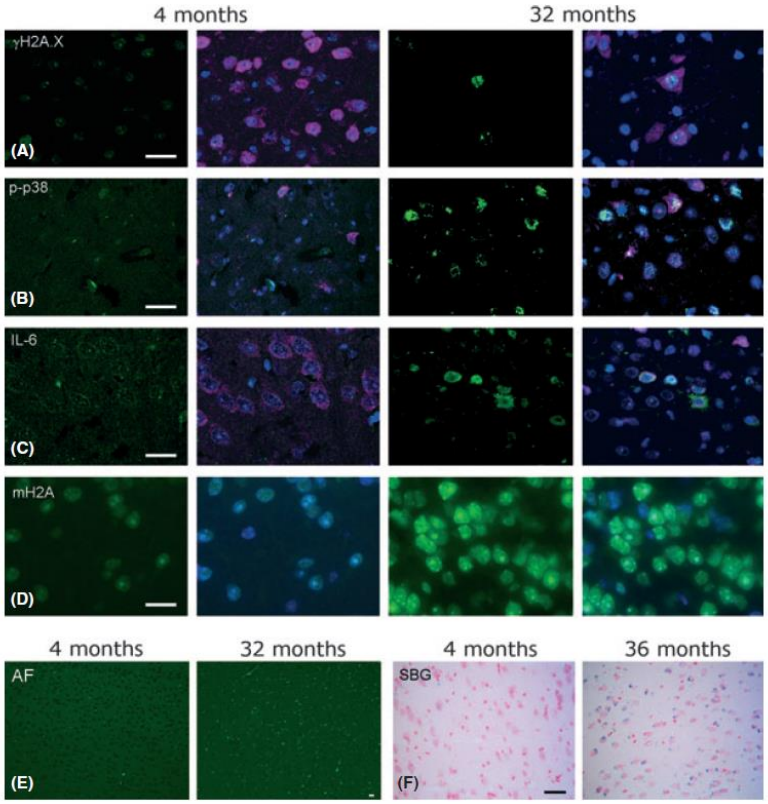

Fig 16. Cortical neurons in old mice are positive for multiple markers of the senescent phenotype.

Representative images from 4 to 32 months old mice are shown. The size marker bars indicate 20 μm. (A–D) Cortical sections were stained with DAPI (blue), the neuronal marker calbindin (purple, omitted in D for clarity) and the antibody of interest (green). Shown are the antibody of interest (left) and the merged image (right). (A) γ-H2A.X, (B) activated p38MAPK, (C) IL-6, (D) mH2A. (E) Autofluorescence on unstained sections. (F) SA-β-Gal (blue) (Jurk et al., 2012).

Inflammation and senescence-associated secretory phenotype (SASP)

Campisi and her collaborators were the first who demonstrated that cellular senescence is linked to the increase in protein secretion and thus the state has been called the SASP (senescence associated secretory phenotype) (Coppe et al., 2010). They observed that pro-inflammatory factors, such as interleukins, chemokines and other inflammatory mediators, such as metalloproteinases and nitric oxide, are the major secreted components in the SASP (Figure 17) and several studies indicated that NF-kB and C／EBPb are the major transcriptional inducers of SASP-related genes (Salminen et al., 2011).

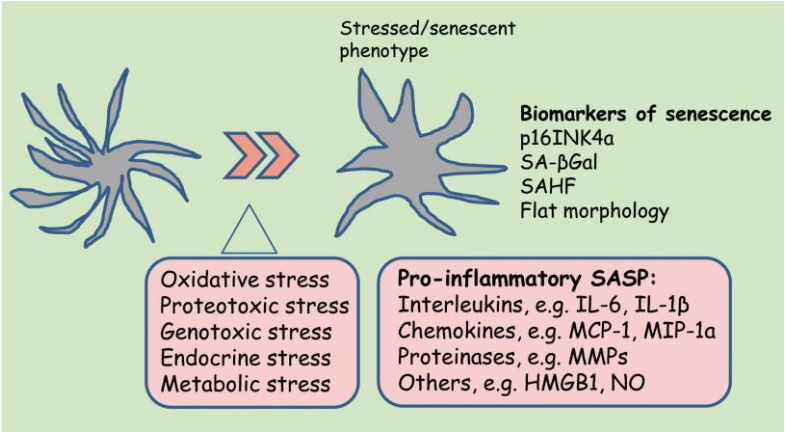

Figure 17. Schematic presentation of the senescence associated pro-inflammatory phenotype (SASP) observed in several cell types (Salminen et al., 2011).

This proinflammatory phenotype has been called ‘‘inflammaging’’ and has a prominent role in regulating intercellular communication; inflammaging may result from multiple causes, such as the accumulation of pro-inflammatory tissue damage, the failure of immune system to effectively clear pathogens and dysfunctional host cells, the propensity of senescent cells to secrete pro-inflammatory cytokines, the enhanced activation of the NF-kB, or the occurrence of a defective autophagy response (Salminen et al., 2011). Global studies on the transcriptional landscape of aged tissues have also emphasized the relevance of inflammatory pathways in aging (Lee et al., 2012).

A novel link between inflammation and aging derives from the recent finding that inflammatory and stress responses activate NF-kB in the hypothalamus and induce a signaling pathway that results in reduced production of gonadotropin-releasing hormone (GnRH) by neurons. This GnRH decline can contribute to numerous aging-related changes such as bone fragility, muscle weakness, skin atrophy, and reduced neurogenesis (Gabuzda and Yankner, 2013).

Several studies have also revealed that, by deacetylating histones and components of inflammatory signaling pathways such as NF-kB, SIRT1 can down-regulate inflammation-related genes (Xie et al., 2013). Consistent with these findings, reduction of SIRT1 levels correlates with the development and progression of many inflammatory diseases, and pharmacologic activation of SIRT1 may prevent inflammatory responses in mice (Hubbard and Sinclair, 2014). Several gene expression profiling studies in brain have revealed that aging is linked to the increase in the expression of inflammatory genes from both neurons and astrocytes and a decrease in gene expression is associated with synaptic transmission, calcium

homeostasis and mitochondrial function (Salminen et al., 2011; Singhal et al., 2014). An inflammatory state has also been documented in senile plaques and surrounding glia in AD patients and animal models, with an increased expression of the acute phase inflammatory protein CRP, as well as pro-inflammatory interleukins such as IL-6 and IL-1 (Finch and Morgan, 2007).

Neuronal and astrocytic morphological alterations in brain aging

Progressive morphological and molecular changes within life-long existing neurons and glia likely underlie age-related cognitive, motor, mood changes and disease susceptibility (Yankner et al., 2008).

Neuronal dendritic arborization affects the formation and maintenance of neural networks; the regulation of synaptic plasticity and the integration of electrical inputs is significantly reduced during aging, whereas the number of neurons is not significantly modified (Yankner et al., 2008) (Figure 18). Age-related changes in the numbers of astrocytes and microglia are also minor and seem to be brain-region and species specific. However, the brain volume decreases, in particular in individuals over the age of 70 years (Esiri, 2007).

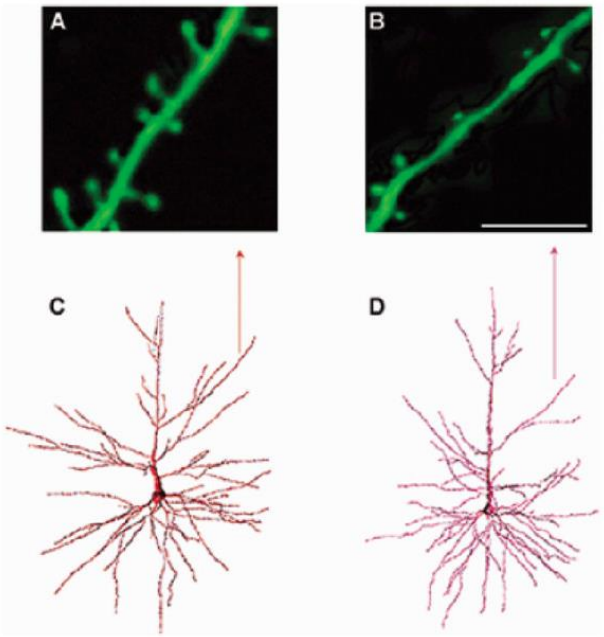

Figure 18. Age-related loss of dendritic spine density. Representative images of spine densities on neocortical pyramidal neurons from young (A and C) and aged (B and D) *rhesus* monkeys are presented (Glorioso and Sibille,2011).

Astrocytes are the most abundant cell type in the brain and provide a supporting structural and functional network; they also have an important role in the neuro-glial crosstalk, being able to propagate the glutamate-induced excitatory signals via Ca^{2+}oscillation even over long distances (Fiacco et al., 2009; Verkhratsky, 2010).

Astrocyte processes interact with the capillary endothelial cells and they can control blood–brain barrier (BBB) permeability and integrity in pathological conditions (Abbott et al., 2006). Astrocytes also mediate the neurovascular coupling between neuronal activity and cerebral blood flow through the regulation of vascular tone (Carmignoto and Gomez-Gonzalo, 2010).

Aging affects many functional characteristics that are regulated by astrocytes, e.g. synaptic plasticity and metabolic balance (Figure 19) and the increase in the expression of glial fibrillary acidic protein (GFAP) has been the most common change observed in astrocytes with aging (Figure 20) (Finch, 2003). In particular, the expression of GFAP increased dramatically after the age of 65 years. Campuzano et al. (2009) demonstrated that the expression of TNF-a, IL-1b and IL-6 is clearly increased in rat brain both in the cortex and the striatum during aging, together with GFAP expression (Campuzano et al., 2009).

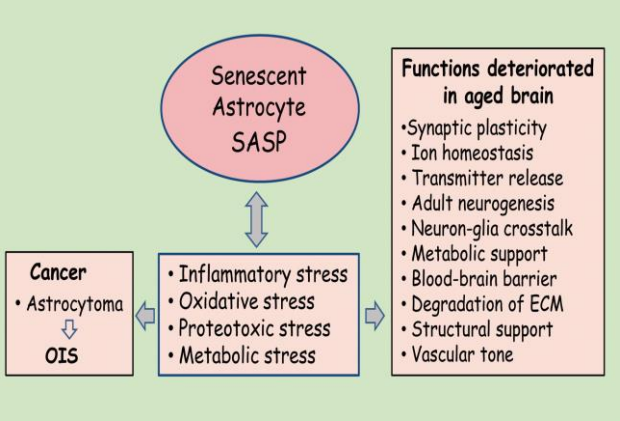

Figure 19. Senescent astrocytes and functional decline (Salminen et al., 2011)

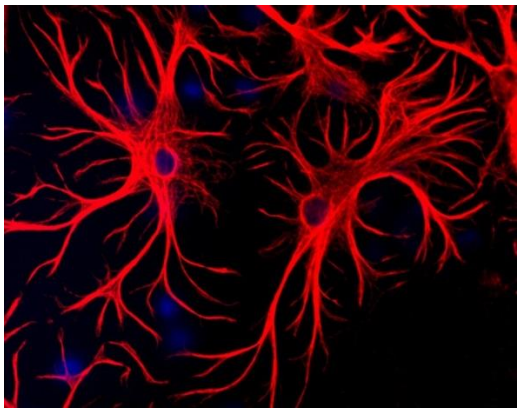

Figure 20. Typical glial fibrillary acidic protein (GFAP) immunofluorescence

Neurochemical changes in brain aging

There is a strong link between dendritic changes and the post-synaptic effects of the cholinergic, serotonergic, dopaminergic and glutamatergic systems which render neurons vulnerable to impaired transmission.

Serotonin shares signaling pathways with other known age-regulatory molecules, such as BDNF and IGF-1 (Mattson et al., 2004), and the selective serotonin reuptake inhibitor antidepressants can modulate neurogenesis (Dranovsky and Hen, 2006). Deficits in serotonergic neurotransmission also correlate with clinical symptoms associated with AD including memory impairment (Rodríguez et al., 2012).

Dopamine, also implicated in several age-related diseases, and components of the dopamine system also decline with age, including the dopamine transporter (DAT) as well as the D1 and D2 receptors (Backman et al., 2006). In humans, pharmacological studies in healthy volunteers have shown that D-amphetamine enhances performance on a variety of tasks and that the D2 receptor agonist, bromocriptine, facilitates spatial working memory, suggesting that D2 receptor down-regulation with age may play a role in age related memory and cognitive decline (Backman et al., 2006). Moreover, monoaminoxidase B, which acts to inactivate dopamine, robustly increases with age (Glorioso and Sibille, 2010) and generates large numbers of ROS. Dopamine also regulates glial dystrophy-related pathways by regulating NFκB and GFAP levels (Luo and Roth, 2000) and interacts with calcium-related pathways and circadian-rhythm pathways through interaction with the gene Clock, amongst others (Rollo, 2009).

Calcium signaling also plays an important role in regulating and maintaining normal neuronal function, including neurotransmitter release, excitability, neurite outgrowth, synaptic

plasticity, gene transcription and cell survival and abnormal elevations of intracellular [Ca2+]i through activation of glutamatergic synapses may lead to cell dysfunction and death (Sun et al., 2013).

Glutamate is the brain predominant excitatory neurotransmitter, it facilitates release of BDNF, is essential for long term potentiation (LTP), synaptic plasticity, neurogenesis, activity-dependent neuronal survival and neural outgrowth during development. With age there is an increase of glutamate levels in the extracellular space of the CNS, which can lead to excessive activation of glutamate receptors and excitotoxicity (Bezprozvanny and Mattson, 2008). It has also been shown that the number of neurons expressing ionotropic glutamate receptors (GludR) and N-methyl-d-aspartate receptor (NMDAR) subunits is significantly reduced during aging (Hof et al., 2002). Brain aging is also subjected to many unique genetic modulators, such as neurotrophins (BDNF) (Mattson, 2008). BDNF is the better characterized modulator of normal brain aging, is neuroprotective against a variety of insults, and is required for changes in spine density underlying learning and memory systems that decline with age (Tapia-Arancibia et al., 2008)(Figure 20).

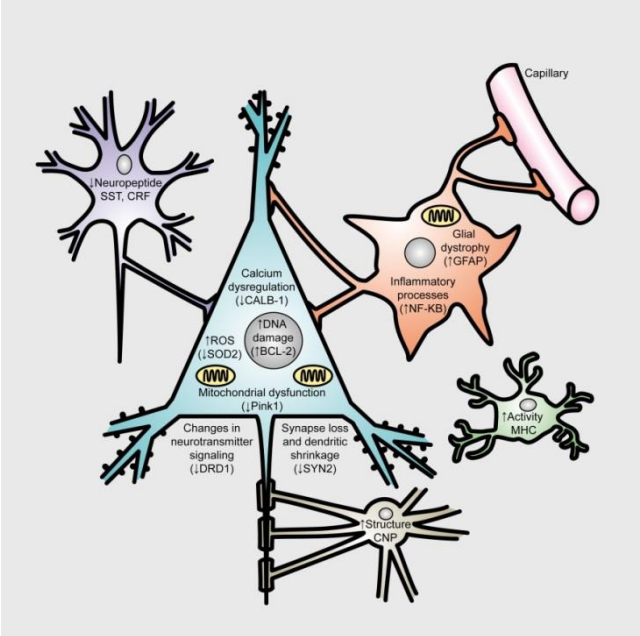

Figure 20. Age-dependent biological changes in brain aging (Glorioso and Sibille,2011).

MicroRNAs as mediators of the ageing process

Epigenetics of ageing is an emerging field involving the mechanisms that affect gene expressions other than inherited DNA sequences regulating the occurrence of ageing. Factors such as DNA methylation, histone modification, chromatin remodeling, the polycomb protein groups, and noncoding RNAs, can all contribute to the broad variety of phenotypes of ageing. Among these, a group of small noncoding RNAs called microRNAs (miRNAs), has been noted with regard to organismal aging as well as brain aging.

MiRNAs have a pivotal role in post-transcriptional regulation of gene expression. MiRNAs associate with the RNA-induced silencing complex (RISC) and bind to the 3' untranslated region (UTR) of their target transcripts, resulting in reduction of gene expression by mRNA degradation or translational blocking (Bates et al., 2009). The specificity of miRNA:mRNA binding is brought about by complementarity of the “seed” sequence of the miRNA (a tract of 7-8 nucleotides at the 5' end of the miRNA molecule) with a complementary sequence within the target mRNA (Lai, 2002). The relatively short region of complementarity between miRNA and target results in many transcripts containing potential binding sites for a given miRNA, and a single miRNA therefore has the potential to regulate hundreds of different mRNA targets (Lewis et al., 2003) (Figure 21). MiRNAs are estimated to regulate as many as 60% of all human mRNAs, which represent practically all cellular and molecular functions such as development, differentiation, cellular proliferation, apoptosis, metabolism and adaptation to environmental stress (Bartel, 2004).

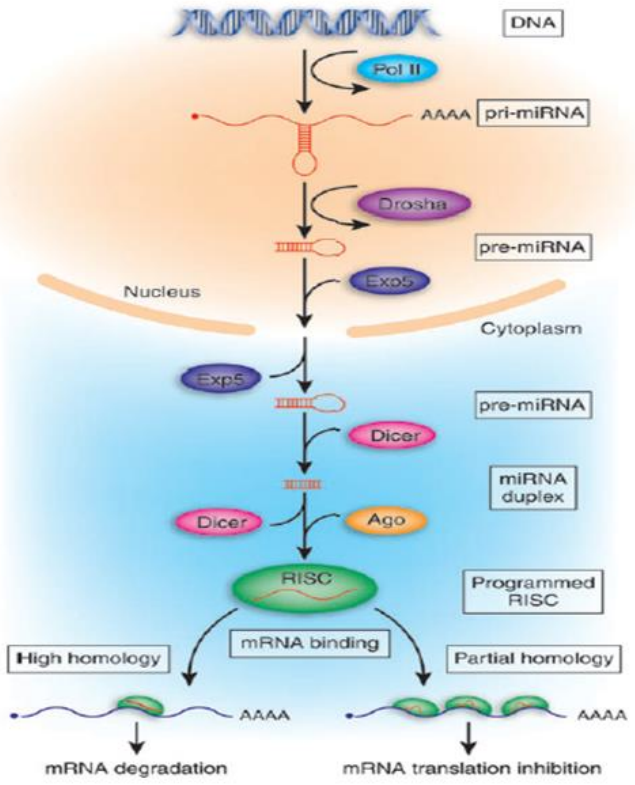

Figure 21. miRNAs biogenesis and mechanism of action (Bates et al., 2009)

MiRNAs influence senescence-relevant pathways

The ability to regulate multiple targets simultaneously makes miRNA a crucial regulator in many physiological conditions, especially in the aging network (Figure 22).

As described above, senescence is mainly governed by the p53 pathway which interacts with miR-34a. In humans, the miR-34 family (miR-34a, miR-34b, miR-34c) is misregulated in many cancer types leading to alteration in the apoptotic process and cell cycle regulation (Wong et al., 2011). MiR-34a is a well-established tumor suppressor and a potent trigger of senescence; these functions are elicited through the growing number of identified mRNAs repressed by miR-34a, including those that encode E2F, c-Myc, sirtuin 1 (SIRT1), Cdk4, Cdk6, B cell leukemia (Bcl)-2, hepatocyte growth factor receptor (Met), and cyclins D1 and E2 (Hermeking, 2010).

Another increasingly recognized group of senescence-regulatory miRNAs targets the RB pathway. Translation of p16, an inhibitor of Cdk4 and Cdk6, was repressed by miR-24 in fibroblast (Lal et al., 2008) while the expression of p21, a broad-spectrum cdk inhibitor, was repressed by miRNAs of the miR-106b family and others with similar seed sequences (miR-

130b, miR-302a-d, miR- 512-3p and miR-515-3p) in human mammary epithelial cells (Borgdorff et al., 2010).

Other genes involved in multiple steps of the DNA damage response pathway are also targeted by miRNAs. First, the DNA damage transducer genes, ATM, is itself targeted by miR-421 in Hela cells (Hu et al., 2010) whilst H2AX is regulated by miR-24 in human blood cells (Lal et al., 2009).

As mentioned above, the SASP is characterized by an elevated secretion of two crucial mediators of inflammation, IL-6 and IL-8. It was recently reported that in HDFs, miR-146a/b reduced the expression of IL-1 receptor-associated kinase 1 (IRAK1), a key component of the IL-1 signal transduction pathway; in turn, reduction of signaling via IRAK blocked the secretion of IL-6 and IL-8 and thus avoided excessive SASP (Bhaumik et al., 2009).

miRNAs are also capable of causing aberrant DNA methylation: silencing of the miR-124a, miR-34, miR-9 and miR-200 gene families by DNA methylation or histone modifications have been noted in several studies (Furuta et al., 2010). The miR-29 gene family directly targets the DNA methyltransferases DNMT3A and DNMT3B in lung cancer cells (Fabbri et al., 2007). Similarly, miR-101, miR-26a, miR-98, miR-miR-124 and miR-144 are involved in histonic modifications (Alajez et al., 2010).

Global profiling approaches have also identified some miRNAs targeting the nutrient sensing pathways: levels of miR-190b,elevated in patients with hepatocellular carcinoma were associated with low serum IGF1 expression and insulin resistance in these patients (Hung et al., 2014). The miR-17-92 clusters target PTEN, and it is thought that their down-regulation during aging causes an increase in PTEN levels, which results in suppression of the IIS pathway (Grillari et al., 2010).

A few miRNAs have been shown to regulate senescence-associated factors in the mitochondria. Along with miR-34a, miR-335 is up-regulated in senescent kidney mesangial cells and these miRNAs target the mitochondrial antioxidative enzymes thioredoxin reductase 2 (TXNRD2) and superoxide dismutase 2 (SOD2), respectively which might contribute to senescence of renal cells (Bai et al., 2011).

More in general, the genome-wide expression analysis of miRNAs in aging individuals revealed a general decline in miRNA levels that was linked to potential loss of control of cancer-associated genes. Nine miRNAs (miR-103, miR-107, miR-128, miR-130a, mIR-155, miR-24, miR-221, miR-496, and mIR-1538) were identified to be significantly lower in the peripheral blood mononuclear cells of old individuals as compared to the young subjects (Persengiev et al., 2012).

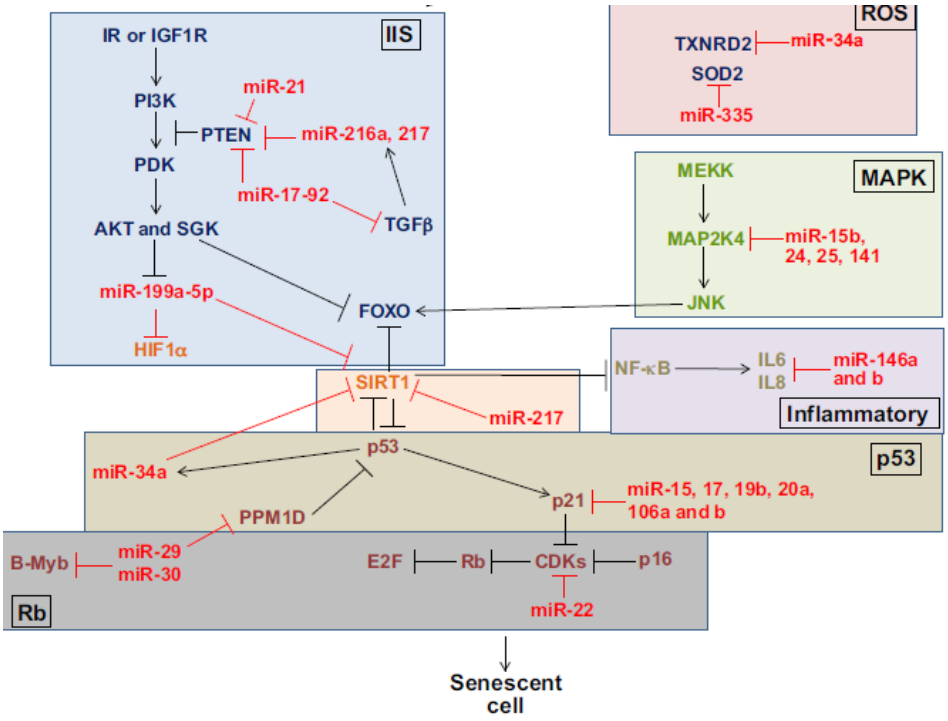

Figure 22. miRNAs involved in senescence-relevant pathways (Smith-Vikos and Slack, 2012).

miRNAs in brain aging and neurodegeneration

The unbalanced equilibrium between up-regulated miRNAs, suppressing unwanted gene expression, and down-regulated miRNAs, whose target genes are important for cellular function, has been noted in the normal aging process in the brain (Liang et al., 2012) and in neurodegenerative diseases (Gascon and Gao, 2012). MiRNAs influence several aspects in neurogenesis, neuronal patterning, neurotransmission and synaptic plasticity (Figure 23) (Salta and De-Strooper,2012). A microarray comparison of synaptosomes with whole-tissue lysates from adult mouse forebrains detected 178 miRNAs, 37 of which were enriched in synapses (Lugli et al., 2008). However, in young mice, a similar study found only 10 miRNAs to be synaptically enriched; interestingly, these miRNAs, were different from those enriched in the synapses of adults (Siegel et al., 2009).

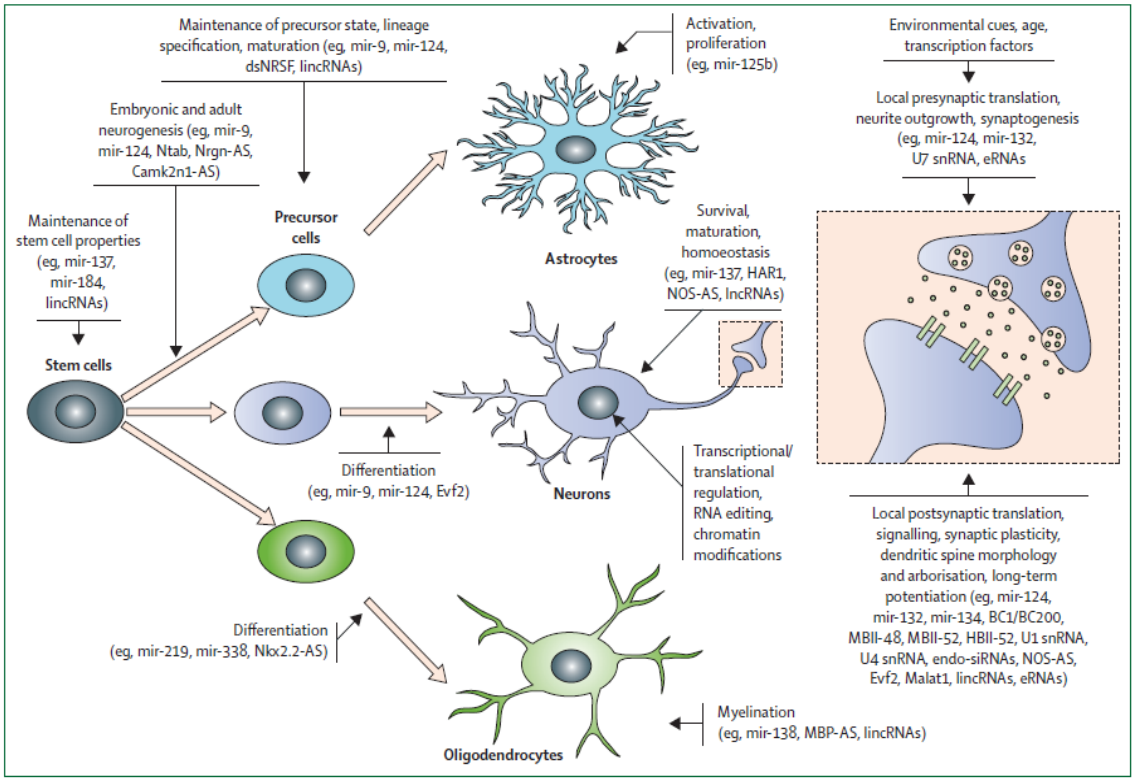

Figure 23. Regulatory miRNAs in the central nervous system (Salta and Strooper, 2012).

In Drosophila, miR-34 is a brain-enriched, adult-onset miRNA and its deletion causes the early onset loss of motor behavior, susceptibility to stress, brain degeneration and a shorter lifespan (Liu et al., 2012). In *C. elegans*, miR-34 impacts lifespan through regulation of autophagy genes (Yang et al., 2011).

MiR-34a/c expression increases with age in the cortex and hippocampus (Khanna et al., 2011) and is also enriched in the cerebral cortex of an AD mouse model and in AD patients (Wang et al., 2009; Zovoilis et al.,2011). Targets include SIRT1, whose regulation by miR-34c is associated with memory impairment in mice (Zovoilis et al.,2011) and is inversely correlated with miR-34a expression in cortex and hippocampus with age (Li et al.,2011). miR-34c also functionally inhibits translation of Bcl-2 in cell studies, an anti-apoptotic protein whose function may also include the modulation of amyloid precursor protein (APP) (Wang et al., 2009). Furthermore, miR-34b is also elevated in the plasma of Huntington's disease (HD) patients (Gaughwin et al., 2011).

About 70 other miRNAs are up-regulated during murine brain aging, starting from 18 months of age. Of these, some are identified both in liver and brain aging studies, whereas others are only up-regulated during brain aging, such as miR-22, miR-101a, miR-720 and miR-

721. Additionally, 27 of the 70 miRNAs are predicted to target components of the mitochondrial electron transport chain, which plays crucial roles during oxidative phosphorylation and decrease in expression during aging, perhaps accounting for decreased respiration rates (Li et al., 2011).

Various miRNAs have also been shown to be up-regulated in the hippocampus of both long-lived Ames dwarf mice and growth-hormone-receptor-knockout strains. Specifically, miR-470, miR-669b and miR-681 suppress expression of IGF1R and AKT, as well as phosphorylation of AKT, which results in decreased phosphorylation of FOXO3, involved in the IIS aging pathway (Liang et al., 2011). However, another study has reported that under conditions of caloric restriction (known to have pro-longevity effects), instead of the expected age-dependent increase in miRNA expression, there is an age-dependent decrease in miR-30e, miR-34a and miR-181a in murine brain tissue (Khanna et al., 2011). These miRNAs have the common target BCL2, a known regulator of apoptosis, and the subsequent increase in BCL2 expression results in a decrease in apoptosis.

A growing list of miRNAs has also been implicated in synaptic function and memory. For example, in cultured neurons, miR-138 affects the morphology of dendritic spines size through its translational target acyl protein thioesterase 1 (Apt1) (Siegel et al., 2009). miR-132 involved in synaptic plasticity, learning and memory, is up-regulated in the hippocampus and cortex in response to novel task learning (Hansen et al., 2013) and synaptic plasticity induction (Nudelman et al., 2010). miR-132 is upregulated through BDNF-dependent and cAMP response element binding protein (CREB)-dependent mechanisms (Magill et al., 2010). One of the targets of miR-132 is MeCP2, the gene implicated in the pathogenesis of the Rett syndrome, a neurologic disorder characterized by cognitive deficiencies (Klein et al., 2007). miR-132 also regulates p250GAP an NMDA receptor associated GTPase-activating protein that is involved in maintaining the morphology of dendritic spines (Wayman et al., 2008). Interestingly, a microarray study that compared miRNA levels throughout the lifespan showed that miR-132 increases with age in the mouse cortex (Eda et al., 2011).

The expression of three miRNAs, miR-182, miR128b, and miR-134, is also regulated in response to the acquisition of fear memory (Griggs et al., 2013). miR-134 is a brain-specific miRNA that works upstream of BDNF and CREB to control synaptic plasticity, learning, and memory (Figure 24). miR-134 expression is controlled in the brain by the deacetylase SIRT1. Brain-specific loss of SIRT1 results in increased expression of miR-134, and deficits in learning and synaptic plasticity through the suppression of CREB and BDNF (Gao et al., 2010). Either SIRT1 activation or miR-134 silencing has a neuroprotective effect in a number of age-dependent neurodegenerative processes (Jimenez-Mateos et al., 2012). A recent study

by Earls et al., (2014) has also shown that mir-185 and miR-25 act in age-dependently to control synaptic plasticity.

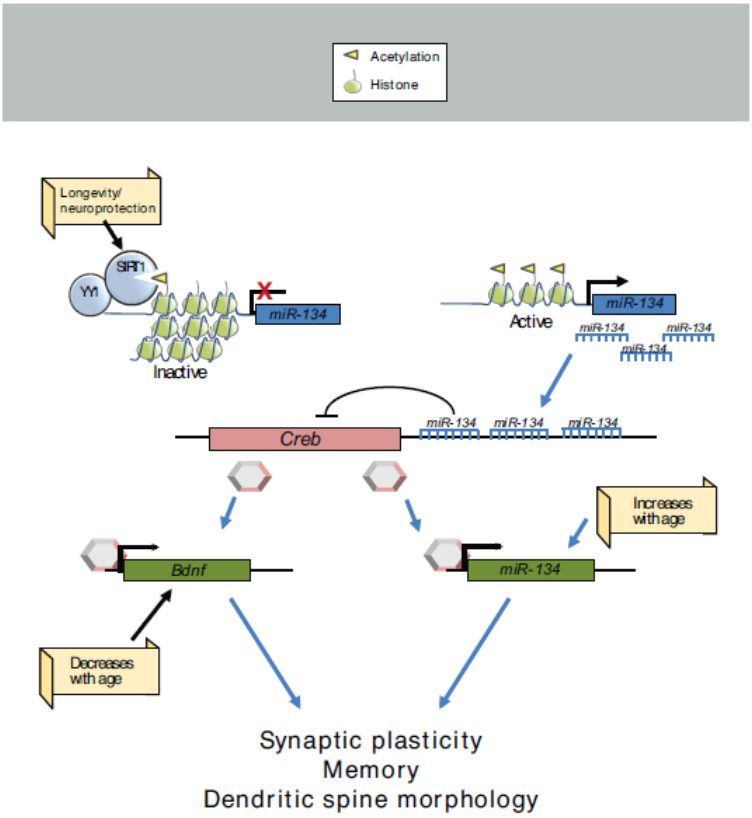

Figure 24. miR-134 in age-related memory pathways (Earls et al., 2014).

Recent reviews also focused on the role of miRNAs on neurodegenerative diseases (Gascon and Gao, 2012). In general, discovering specific miRNAs that target the 3'UTR of key disease genes, and assessing the expression pattern and level of those miRNAs, can uncover the extent to which they may impact the level of the disease protein, and thus pathogenesis (Figure 25). Alzheimer's disease (AD) is the most common neurodegenerative disease and, although predominantly sporadic, analysis of familial cases has identified critical genes for its etiology (Ballard et al.,2011). The pathological features of AD are the deposit of intracellular neurofibrillary tangles containing Tau protein and extracellular plaques containing amyloid-beta (Aβ) peptides in the brain. Various Aβ peptides are produced upon the cleavage of amyloid precursor protein (APP) by β-site APP-cleaving enzyme 1 (BACE1) and γ-secretase. miR-29a/b are down-regulated in a subset of AD patients that show elevated BACE1 protein expression, which is predicted to promote amyloidogenic peptide formation (Hébert et al., 2008). The 3'UTR of BACE1 contains a miR-29a/b target site, and miR-29 targets BACE1. The

BACE1 3'UTR also contains sites for other miRNAs, including miR-107, miR-124, and miR-195 (Fang et al., 2012; Zhu et al., 2012). miR-107 is also down-regulated in AD, and targets cofilin, a component of rod-like actin structures in the AD brain. miR-15a, which belongs to miR-107/103 family, is also down-regulated in AD patients (Wang et al., 2011). Interestingly, the miR-15 family can target extracellular signal-regulated kinase 1 (ERK1), which is a Tau kinase, and this could potentially lead to abnormal Tau phosphorylation *in vivo*, another pathological hallmark of AD (Hébert et al., 2010). Other miRNAs implicated in AD pathology include miR-16, miR-101, miR-106a, miR-520c, and miR-153, which target APP (Long and Lahiri, 2011). Moreover, miR-144 plays a central role in regulating the expression of ataxin 1, the disease-causing gene for the development spinocerebellar ataxia type 1 and was found to have and age-dependent up-regulation in the cortex and cerebellum of humans, chimpanzees and *rhesus* macaques (Persengiev et al., 2011). Overall, these findings highlight the critical impact of select miRNAs on regulation of the expression of central proteins in AD pathogenesis and progression.

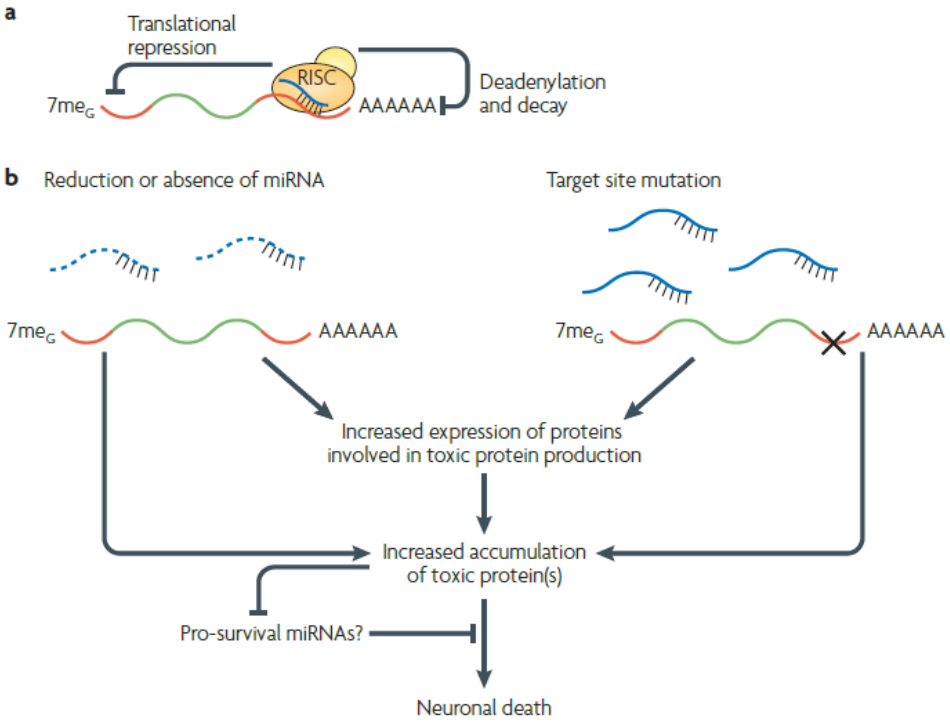

Figure 25. miRNAs effect on neurodegeneration-related toxic proteins (Eacker et al., 2009).

Mediterranean diet and age-related diseases

The dietary pattern that has been most widely studied as possible preventive attempt to control common degenerative diseases, is the Mediterranean diet, characterized by a high intake of vegetables, legumes, cereals, fruits and nuts, a high intake of olive oil, a low intake of saturated lipids, a moderately high intake of fish, a low intake of meat and poultry, and a regular but moderate intake of ethanol, primarily in the form of wine and generally during meals (Figure 26), (Willett et al., 1995). Data from observational, longitudinal, and randomized controlled trials have demonstrated that the Mediterranean diet can improve body mass index and body weight, reduce the incidence of diabetes mellitus and metabolic syndrome, decrease cardiovascular morbidity and coronary heart disease mortality, decreased incidence or mortality from cancer and incidence of Parkinson's and Alzheimer's disease (13%), resulting in a decrease all-cause mortality (Sofi et al., 2008; Estruch et al., 2013). High adherence to Mediterranean diet is also associated with a lower cognitive impairment in non-diabetic subjects (Tsivgoulis et al., 2013), whereas in another large study of older women, no association was found (Samieri et al., 2013).

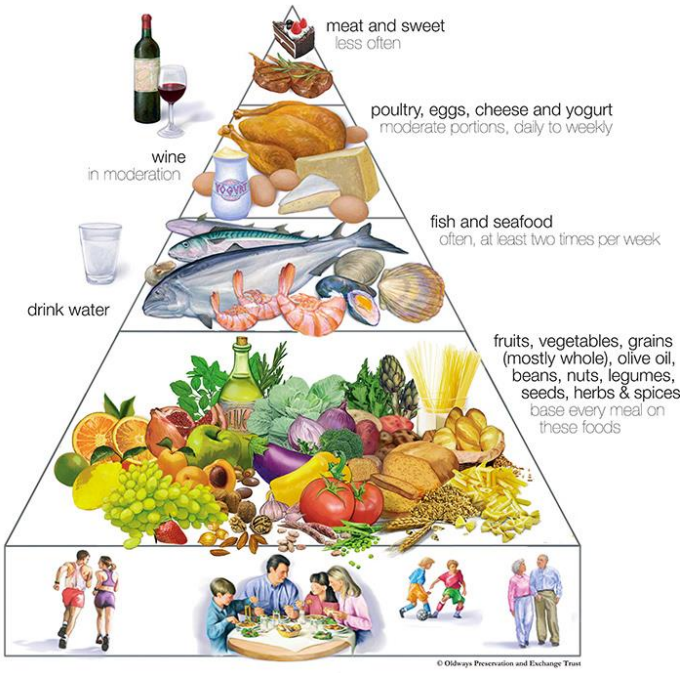

Figure 26. Pyramid of the Mediterranean diet: a cultural model for healthy eating.

Olive oil

Olive oil is produced from the first and second pressings of the olive fruit by the cold-pressing (where no chemicals and only a small amount of heat are applied) of the fruit of *Olea europeae*; it is composed of triacylglycerides (approximately 98%–99% in weight), and a non-glycerol or unsaponifiable fraction (making up 0.4–5% of the olive fruit) which contains phenolic compounds (Tripoli et al., 2005). Studies conducted so far (including human, animal, *in vivo* and *in vitro*) have demonstrated that olive oil phenolic compounds, at first considered important mainly for the shelf-life and flavor of olive oils, have also positive effects on various physiological biomarkers, implicating phenolic compounds as partially responsible for the health benefits associated with the Mediterranean diet (Visioli et al., 1995).

The phenolic fraction of virgin olive oil is heterogeneous, with at least 36 identified structurally distinct phenolic compounds. Variation in the phenolic concentration exists between differing virgin olive oils due to numerous factors including: variety of the olive fruit, region in which the olive fruit is grown, agricultural techniques used to cultivate the olives, maturity of the olive fruit at harvest, and olive oil extraction, processing, storage methods and time since harvest (Bruni et al., 1994; Visioli et al., 2002). The total phenolic content has been reported to be in the range of 196-500 mg/kg. Although the reported levels of phenolic compounds in olive oil vary widely, one consistent conclusion is that extra virgin olive oil (EVOO) has a higher phenolic content than refined virgin olive oil. Owen et al. (2000) showed that this difference was reflected in the levels of individual phenols as well as the total quantity of phenols in the oil.

Phenolic compounds in extra-virgin olive oil (EVOO)

The phenolic fraction of virgin olive oil is formed by a wide range of compounds, including phenolic alcohols (hydroxytyrosol and tyrosol), secoiridoid derivatives (the dialdehydic form of elenolic acid linked to hydroxytyrosol (3,4-DHPEA-EDA, or oleuropein) and the dialdehydic form of elenolic acid linked to tyrosol (p-HPEA-EDA), phenolic acids (vanillic and p-coumaric acids), lignans (pinoresinol and acetoxypinoresinol) and flavonoids (luteolin and apigenin) (Serra et al., 2012). The major phenolic compounds in EVOO are shown in Figure 27. The three phenolic compounds in highest concentration in olive oil are the glycoside oleuropein, hydroxytyrosol (3,4-dihydroxyphenyl ethanol) and tyrosol. These three compounds are related structurally. Hydroxytyrosol and tyrosol are structurally identical except that hydroxytyrosol has an extra hydroxy group in the meta position. Oleuropein is an ester which consists of hydroxytyrosol and elenolic acid. Oleuropein is the major phenolic compound in

olive fruit, which can be as much as 14% in dried fruit, hydroxytyrosol is the major phenolic component in olive oil (Amiot et al., 1996). As the olive fruit matures the concentration of oleuropein decreases and hydroxytyrosol, a hydrolysis product of oleuropein increases (Figure 28), (Cimato et al., 1990). A phenolic compound in EVOO that stands alone in terms of sensory and anti-inflammatory attributes is decarboxy methyl ligstroside aglycone (also known as oleocanthal). Oleocanthal is homologous with the non-steroidal anti-inflammatory drug (NSAID) ibuprofen for its anti-inflammatory properties (Beauchamp et al., 2005), (Figure 27).

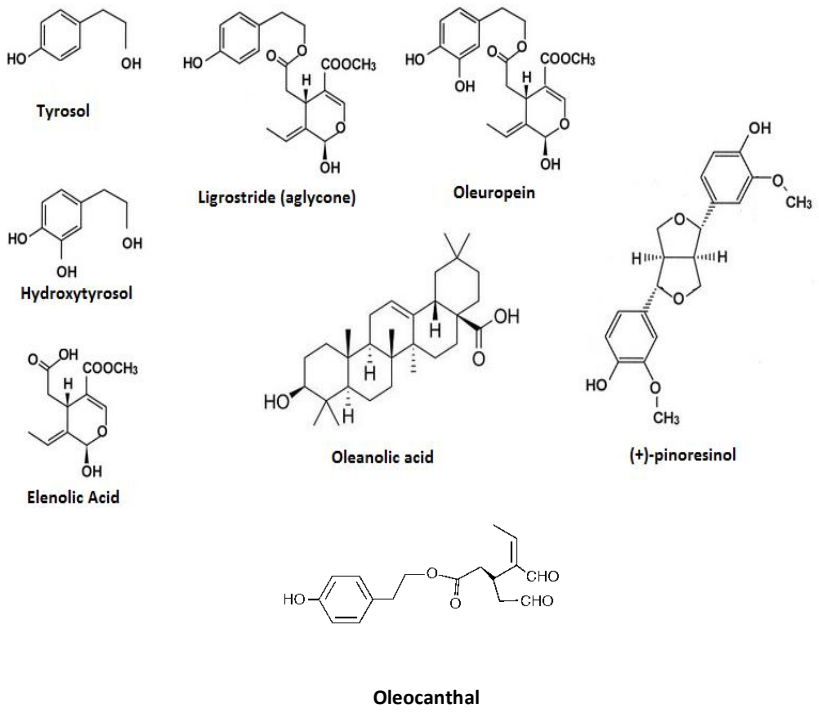

Figure 27. Major phenolic compounds in extra virgin olive oil.

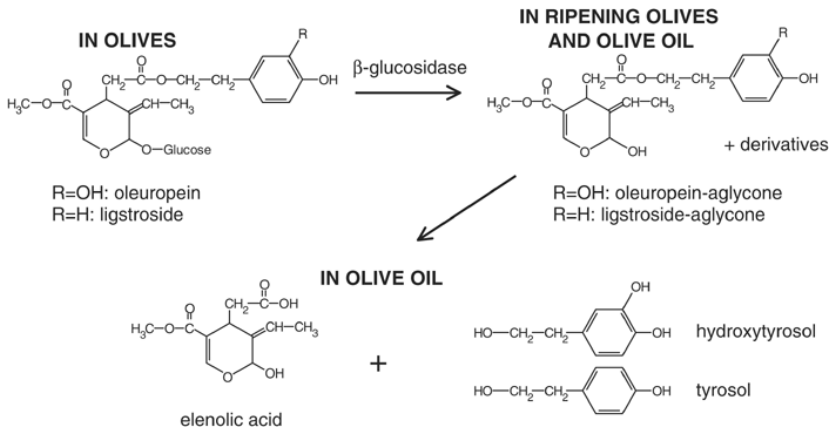

Figure 28. Structures of phenols present in olives and olive oil, their degradation into aglycones during ripening and hydrolysis of aglycones into tyrosol and hydroxytyrosol (Vissers et al., 2004).

Pharmacokinetic of EVOO phenolic compounds

The majority of research regarding the bioavailability of EVOO phenolic compounds has focused on three major phenolics: hydroxytyrosol, tyrosol, and oleuropein. In general, the hydrophilic phenolic compounds of olive oil are absorbed in dose-dependent manner from the gastrointestinal tract in animals and humans and the absorption is usually rapid, the maximum plasma concentration is reached in 5-10 min after ingestion, followed by a rapid decline (Vissers et al., 2004). The phenolics tyrosol and hydroxytyrosol are absorbed by passive diffusion (Manna et al., 2000). It has been proposed that oleuropein-glycoside may diffuse through the lipid bilayer of the epithelial cell membrane and be absorbed via a glucose transporter (Edgecombe et al., 2000).

The quantification of metabolites of the phenolic compounds in the plasma and multiple tissues indicated that after an acute ingestion of olive phenolic compounds, they are absorbed, metabolized and distributed though the blood stream to practically all parts of the body, even across the blood–brain barrier, although in smaller amounts as compared with other organs. Sulfate conjugates of hydroxytyrosol and tyrosol are the main metabolites quantified in the plasma and tissues and free forms of some phenolic compounds, such as oleuropein derivative in the plasma and brain, luteolin in the kidney, testicle, brain and heart, or hydroxytyrosol in the plasma, kidney and testicle (Serra et al., 2012).

Subsequently, phenolics EVOO, are excreted in the urine mainly as sulfate derivatives, followed by glucuronides (Corona et al., 2006). D'Angelo et al. (2001) proposed a metabolic

pathway for hydroxytyrosol in which the action of cathecol-O-methyltransferases (COMT) promotes the appearance of homovanillic acid and its conjugated forms (Figure 28).

Moreover, these phenolic compounds have a low toxicity , with the no observable adverse effect level (NOAEL) being around 2 grams/kg per d (D'Angelo et al., 2001).

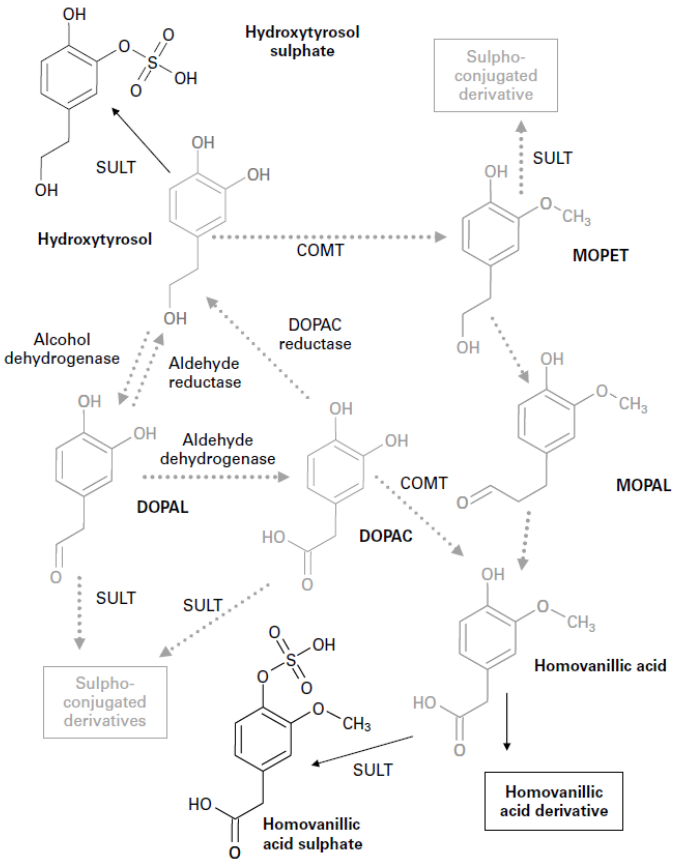

Figure 28. Metabolic pathways of hydroxytyrosol (Suárez et al., 2011).

General mechanisms underlying the biological effects of phenolic compounds

Dietary phenols have been reported to exert their neuronal actions through their potential to protect neurons against injury induced by neurotoxins, their ability to suppress neuro-inflammation and their potential to promote memory, learning and cognitive function. Recent evidence suggests that beyond their anti-oxidative/anti-inflammatory properties, they are also involved in protective signaling and neuro-hormetic effects leading to the expression of genes that encode antioxidant enzymes, phase-2 enzymes, neuro-trophic factors, and cyto-protective proteins. Specific examples of such pathways include the sirtuin-FoxO pathway, the NF-κB pathway, and the Nrf-2/ARE pathway (Figure 29) (Vauzour, 2012).

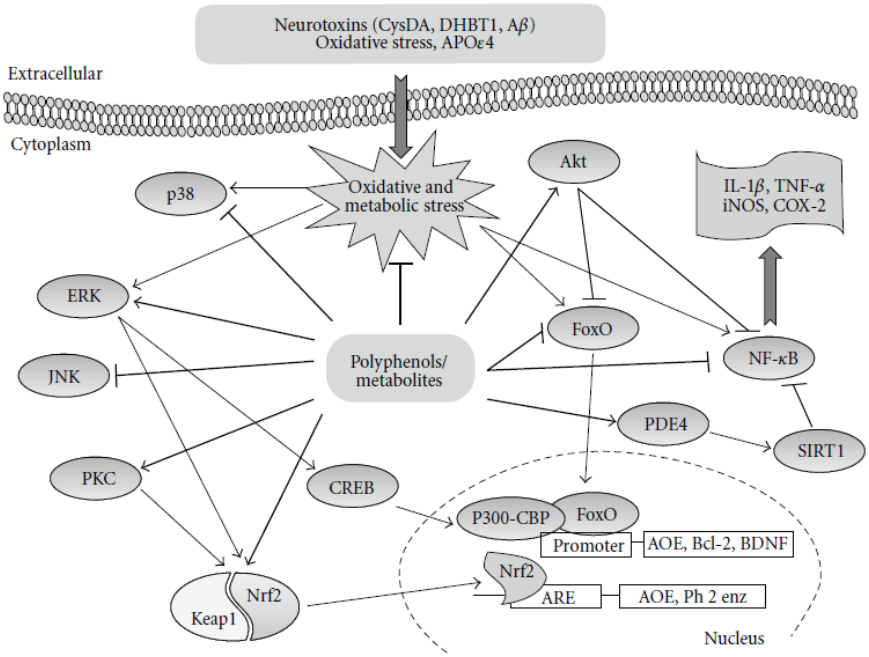

Figure 29. General mechanisms underlying the biological effects of phenolic compounds (Vauzour, 2012)

Phenolic compounds in the brain

It is now understood that the biological actions of phenolic compounds within the nervous system are not due to their direct (i.e., classical) antioxidant effects , but rather through their potential to protect vulnerable neurons, enhance existing neuronal function, stimulate neuronal regeneration, and induce neurogenesis (Spencer, 2010). Indeed, it has become evident that some flavonoids are able to exert neuroprotective actions (at low, physiological concentrations) via their interactions with critical neuronal/glial intracellular signaling pathways, pivotal in controlling neuronal function and survival, resistance to neurotoxins, oxidants and inflammatory mediators, expression of proteins involved in synaptic plasticity and neuronal repair, through their potential to induce changes in blood flow to the brain and to control neuronal differentiation, long-term potentiation, and memory (Spencer, 2007).

Various flavonoid-binding sites on neurons have now been described and include adenosine , GABAA, δ-opioid , nicotinic, estrogen and testosterone receptors, and a specific

brain plasma membrane binding site for polyphenols has been proposed (reviewed in Williams and Spencer, 2012) (Figure 30).

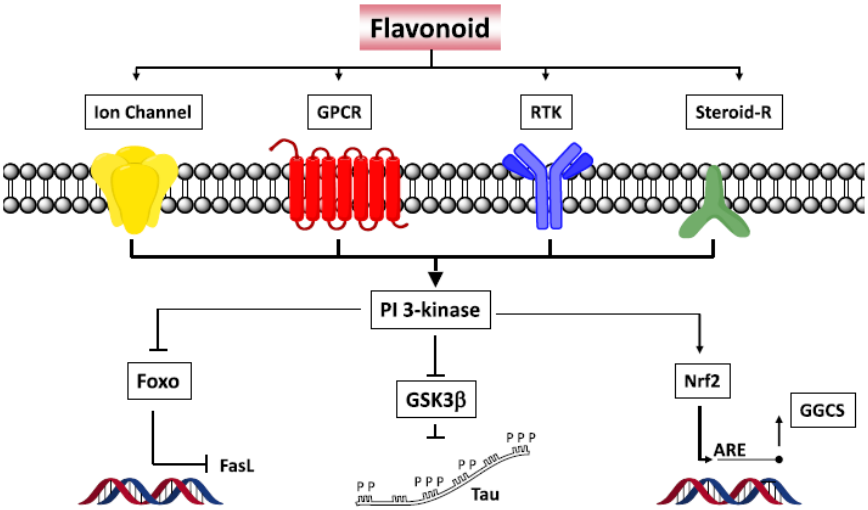

Figure 30. Potential cell surface binding sites for initiating flavonoid signaling to PI3-kinase-dependent neuroprotection.

Receptor binding by flavonoids and their metabolites may underlie the reported changes in the activation status of various downstream kinases, including various members of both the MAP kinase and the PI3-kinase pathways (Spencer, 2010) and the Nf-κB pathway (Goyarzu et al., 2004). Nanomolar concentrations of flavonoids, in particular flavanols and flavanones, have been shown to activate the ERK pathway resulting in downstream cAMP response element binding protein (CREB) activation, which may result in a number of beneficial changes, such as long-lasting changes in synaptic plasticity and memory and the up-regulation of neuroprotective pathways. On the other hand, they are known to inhibiting pro apoptotic signaling through the inhibition of JNK and ASK1. The inhibition of these kinases along with the activation of ERK1/2 leads to a suppression of apoptosis and neuroinflammation and thus the associated neurodegeneration (Figure 31).

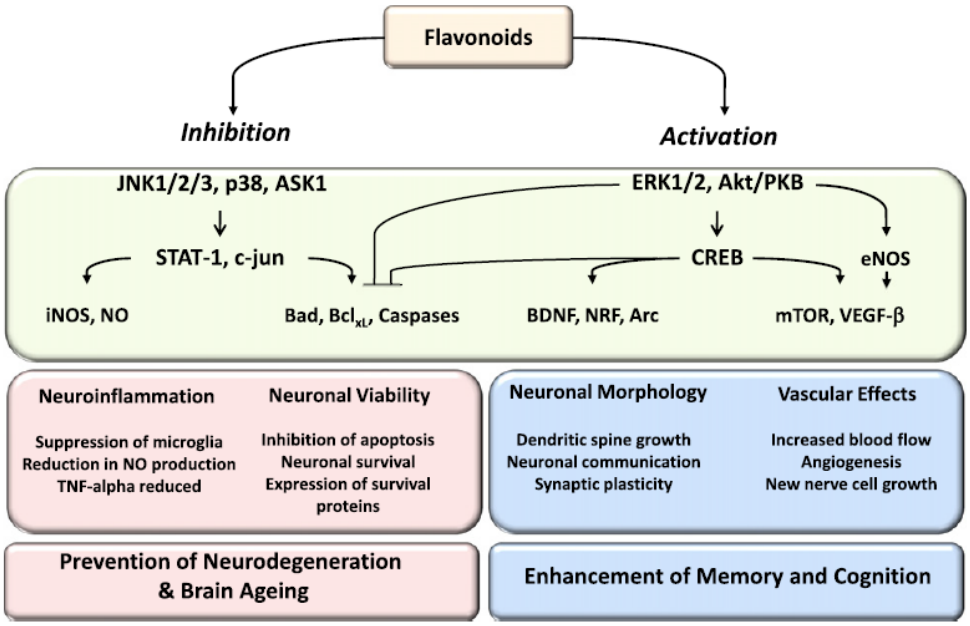

Figure 31. Signaling pathways underlying neuronal survival and cognitive performance (Williams and Spencer, 2012).

Biological and nutrigenomic effects of phenolic compounds in EVOO

Studies (human, animal, *in vivo* and *in vitro*) have demonstrated that olive oil phenolic compounds have antimicrobial activity and positive effects on plasma lipoproteins, oxidative damage, inflammatory markers, platelet and cellular function, and bone health (Cicerale et al., 2010) (Figure 32).

In particular, oleuropein, oleocanthal, hydroxytyrosol, and tyrosol, are inhibitors of oxidative damage and inflammation in a variety of experimental systems. Hydroxytyrosol is a potent radical scavenger and a chelator of metals like iron (Visioli et al., 2011); it reduces platelet aggregation and has anti-inflammatory effects through cyclooxygenase (COX) inhibition. Oleuropein is a radical scavenger and low-density lipoprotein (LDL) oxidation blocker (Visioli et. al.,2002). Oleocanthal, responsible for the pungent taste of new olive oil, has pharmacodynamics properties and potency similar to nonsteroidal anti-inflammatory drugs and blocks both COX-1 and COX- 2 (González-Correa et al., 2008). Recently, effects of oleocanthal on β-amyloid degradation have been described, making this compound of potential interest for the prevention of Alzheimer disease (Abuznait et al., 2013).

More recent studies have indicated that the beneficial effects of the phenolic compounds from EVOO are not due to their anti-oxidant and related activities, since they have a direct impact on the human genome, being able to modify the expression of genes involved

in almost all cellular processes and in particular oxidative stress, inflammation, DNA repair and metabolism. Changes in gene expression may support the beneficial effects observed in phenotypic biomarkers for atherosclerotic processes following olive oil consumption. Within this context, a randomized trial was performed with the aim of assessing the *in vivo* gene expression changes in the lymphocytes of 90 healthy volunteers, showing that the phenols from EVOO have a significant role in the down-regulation of pro-atherogenic genes such as IFN-g, ARHGAP15 and IL7R (Konstantinidou et al., 2010). This result reinforces the importance of including EVOO in the regular diet (the Food and Drug Administration recommends a daily intake of 23 g of olive oil).

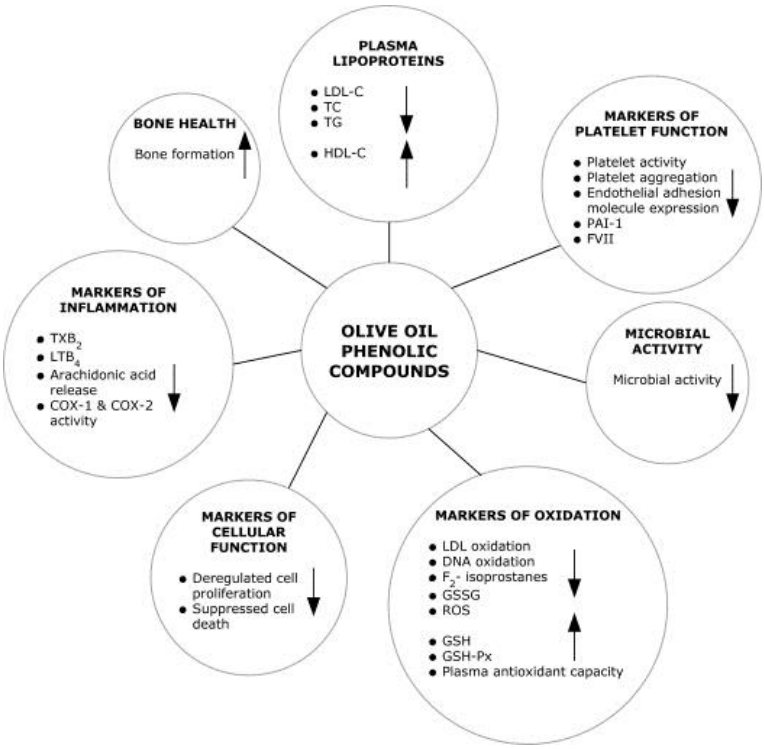

Figure 32. Biological activities of extra virgin olive oil phenolic compounds (Cicerale et al., 2010).

Beneficial effects phenolic compounds in EVOO in aging

Recently, Farr et al. (2012) found that EVOO (210 mg total phenols/kg) has beneficial effects on learning and memory deficits in ageing and diseases related to the overproduction of amyloid-β peptide. In this study, EVOO reversed oxidative damage in the brain of SAMP8 mice, an age-related learning/memory impairment model associated with an increased amyloid-β protein and brain oxidative damage. This effect was augmented by increasing

concentrations of total phenols in EVOO (from 210 to 1050 mg/kg). Moreover, St-Laurent-Thibault et al. (2011) found that tyrosol and hydroxytyrosol (100 µg/mL) serve as neuroprotective agents against Aβ-peptide in cultured neuroblastoma N2a cells. Moreover, hydroxytyrosol, oleuropein and especially oleuropein aglycon, are able to act as Tau aggregation inhibitors at low (10 µM) concentrations, *in vitro* (Daccache et al., 2011).

Published data from my group (Jacomelli et al., 2010; Pitozzi et al., 2010) have shown that rodents fed a diet containing 23% (w/w) extra-virgin olive oil with high polyphenols (EVOO, 700 mg/kg) have decreased systolic blood pressure, lower DNA oxidative damage in blood cells and liver, lower plasma TBARS and a reduced step-through latency in the light-dark box test, indicating lower anxiety. This last effect is associated with decreased glutathione-reductase in the brain, itself associated with decreased anxiety. Pitozzi et al. (2012) also demonstrated that long-term dietary extra-virgin olive oil rich in polyphenols reversed age-related dysfunctions in motor coordination and contextual memory in mice. Grossi et al. (2013) demonstrated that 8 weeks dietary supplementation of oleuropein aglycone (50 mg/kg of diet), improved the cognitive performance in TgCRND8 mice, a model of amyloid-ß deposition, remarkably reduced ß-amyloid levels and plaque deposits and increased autophagy.

Human studies on EVOO

The intake of olive oil, an important component of the Mediterranean diet, has been associated to health benefits in large cohort studies such as the European Prospective Investigation into Cancer and Nutrition (EPIC) study (Buckland et al., 2012). A dietary pattern rich in olive oil and raw vegetables was associated with lower mortality in Italian elderly subjects. After adjustment, overall mortality was reduced by approximately 50% in the highest quartile (Masala et al., 2007). A recent randomized, single-blinded, controlled trial (the PREDIMED (Prevención con Dieta Mediterránea) trial) conducted in high risk patients for cardiovascular disease demonstrated that a Mediterranean diet supplemented with extra virgin olive oil reduced blood pressure and the risk of atrial fibrillation (Martínez-González et al., 2014) and diabetes (Salas-Salvadó et al., 2014). Furthermore, the high intake of both total olive oil and virgin olive oil in older individuals with high cardiovascular risk, was associated with better memory function and global cognition (Valls-Pedret et al., 2012).

Focusing on the CNS effect, evidence from population-based studies in southern Italy indicates that the intake of MUFA is inversely correlated to age-related cognitive decline (Solfrizzi et al., 2006). Epidemiological data in Greece within the European Prospective Investigation into Cancer and Nutrition (EPIC) cohort also suggest that the intake of MUFA is

positively associated with cognitive function, although the association was not statistically significant (Psaltopoulou et al., 2008). Recently, 6.5 years of nutritional intervention with 1 L/week of extra virgin olive oil was also associated to a better cognitive performances (less mild cognitive impairments) (Martínez-Lapiscina et al., 2013).

However, several seed oils (including sunflower, soybean, and rapeseed) containing high quantities of MUFAs, are ineffective in reducing chronic disease risk factors (Harper et al., 2006). In fact, olive oil contains more than MUFA. Olive oil is a functional food which, besides having a high level of MUFA, contains other components with biological properties such as natural antioxidants including phenolic compounds (Covas, 2007). Some antioxidant compounds have been hypothesized to have a protective effect against dementia and cognitive impairment (Gillette-Guyonnet et al., 2007).

Health claims for olive oil constituents

A health claim is defined as any claim that states, suggests or implies that a relationship exists between a food category, a food or one of its constituents and health. Scientific assessment is performed by the European food safety agency (EFSA). Well-performed human intervention trials are particularly important for the successful substantiation of health claims and double-blind, randomized, placebo-controlled trials are considered the gold standard. Several health claim applications for olive oil and its constituents have been assessed in recent years. Phenolic compounds naturally occurring in olive oil were shown to significantly decrease the amount of circulating oxidized LDL particles *in vivo* in a dose-dependent manner in one large and three smaller human intervention studies (Covas et al., 2006; Weinbrenner et al., 2004; Marrugat et al., 2004). On the basis of an established cause-and-effect relationship, the claim that “olive oil polyphenols contribute to the protection of blood lipids from oxidative stress” is now allowed on labels of olive oil, which contains at least 5 mg of hydroxytyrosol and its derivatives (e.g. oleuropein complex and tyrosol) per 20 g of olive oil. Some other claims for olive oil polyphenols have also been evaluated in the last few years (i.e. the role in decreasing potentially pathogenic intestinal microorganisms and anti-inflammatory properties), although stronger clinical evidence is needed before such claims may be used in commercial communications. However, some other claims not related to olive oil polyphenols are currently possible for olive oils (Table 1).

Table 1. General function health claims for olive oil constituents in which a cause-and-effect relationship has been confirmed by the EFSA (www.efsa.europa.eu/).

Health claim	Conditions of use	Reference
Olive oil polyphenols contribute to the protection of blood lipids from oxidative stress.	The claim may only be used for olive oil that contains at least 5 mg of hydroxytyrosol and its derivatives (e.g. oleuropein complex and tyrosol) per 20 g of olive oil. In order to bear the claim, information shall be given to the consumer that the beneficial effect is obtained with a daily intake of 20 g of olive oil.	EFSA NDA Panel, 2011
Vitamin E contributes to the protection of cells from oxidative stress.	The claim may only be used for food, which is at least a source of vitamin E as referred to in the claim "source of vitamin".	EFSA NDA Panel, 2010
Replacing saturated fats with unsaturated fats in the diet contributes to the maintenance of normal blood cholesterol levels.	The claim may only be used for foods where at least 45% of the fatty acids present in the product derive from unsaturated fat on the condition that unsaturated fat provides more than 20% of the energy of the product.	EFSA NDA Panel, 2011

Resveratrol

Resveratrol (3,4',5-trihydroxystilbene) (Figure 33) is a dietary polyphenol present in more than 70 different plants, including red grapes, berries (e.g. cranberries, bilberries, blueberries) and peanuts. It is also present in red wine and, to a much lesser extent, in white wine. The concentration of trans-resveratrol in red wine depends on the type of red wine and its geographic origin, ranging from 0.1 to 14.3 mg/l (i.e. 0.4–57 µM) (Baur and Sinclair, 2006).

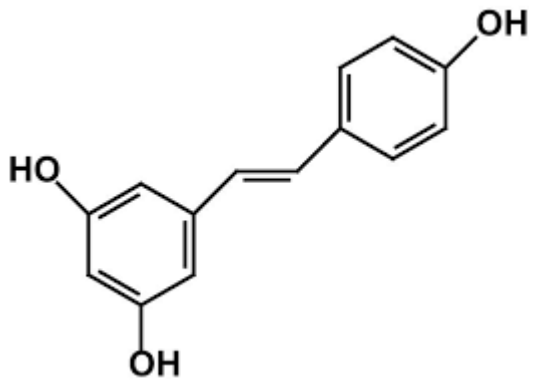

Figure 33. Chemical structure of resveratrol.

Bioavailability of resveratrol

The oral absorption of resveratrol in humans is about 75% and is thought to occur mainly by transepithelial diffusion. Extensive metabolism in the intestine and liver results in an oral bioavailability considerably less than 1%. Dose escalation and repeated dose administration of resveratrol does not appear to alter this significantly. Metabolic studies, both in plasma and in urine, have revealed its major metabolites to be glucuronides and sulfates. Deconjugation enzymes such as β-glucuronidase and sulfatase, as well as specific tissue accumulation of resveratrol, may enhance resveratrol efficacy at target sites (Walle, 2011). Hence, only trace amounts of free resveratrol (approximately 7 μg/l i.e. 30 nM) can be detected in plasma, 30 min after a 25 mg oral dose, whereas the total (free and conjugated) estimated resveratrol quantity is much higher (around 450 μg/l, 2 μM) (Goldberg and Soleas, 2003).

Biological effects of resveratrol

Numerous studies showed its various beneficial biological effects, including its antioxidant, anti-inflammatory activities, release of neurotransmitters and neuromodulators (Granados-Soto, 2003).

In vitro studies have also demonstrated its protective activity against a wide range of stressors, including oxidative stress, inflammation, radiation, ischemia; epidemiological studies indicate that resveratrol consumption can lower the risk of many age-related diseases, including cancer (Sinclair, 2005). This polyphenol has been shown to increase life span in nematodes and fruit flies functioning as caloric restriction mimetic (Wood et al., 2004).

In vivo, resveratrol also showed protective activity against age-related deterioration in mice (Baur et al., 2006; Pearson et al., 2008). In rodents, resveratrol does not extend normal life span but it improves health and prevents the early mortality associated with obesity (Baur, 2010).

The anti-aging effects of resveratrol appear to be related to several biologic actions, such as its ability to function as an antioxidant or to modulate different metabolic and signaling pathways, and have been also associated to its activity as sirtuin activator (Baur and Sinclair, 2006).

Resveratrol ameliorated cognitive decline in Huntington's disease model mice or senescence- accelerated mice (Liu et al., 2012; Ho et al., 2012). More recently, Zhao et al. (2013) demonstrated a positive effect of resveratrol in cognition trough a microRNA-CREB-

BDNF mechanism involving mir-124. Moreover, resveratrol has been shown to increase the clearance of beta-amyloid, a key feature of Alzheimer's disease, and to modulate intracellular effectors associated with oxidative stress (e.g. heme oxygenase), neuronal energy homeostasis (e.g. AMP kinase), program cell death (i.e. AIF) and longevity (sirtuins) (Bastianetto et al., 2014), (Figure 34).

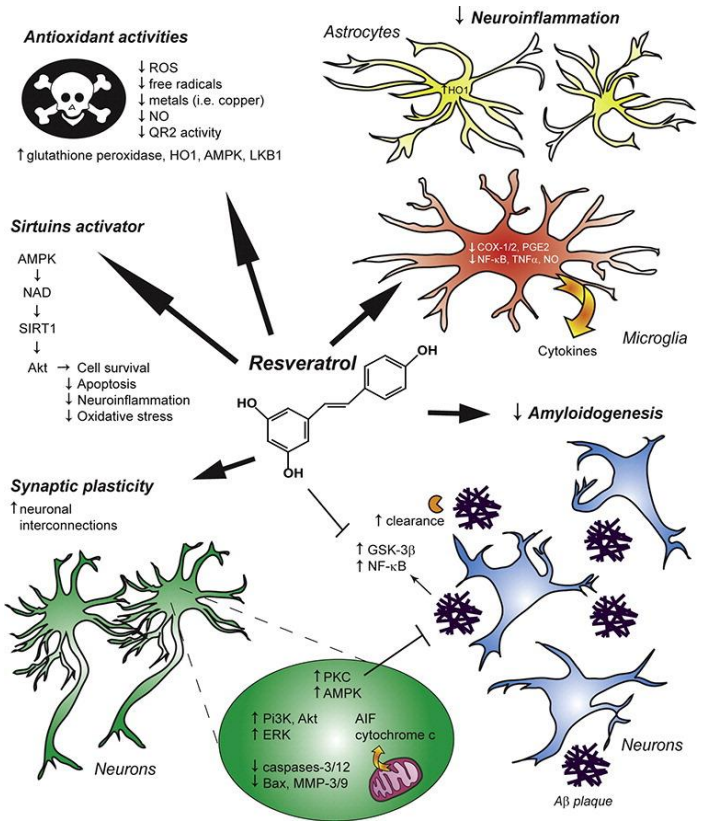

Figure 34. Summary of the neuroprotective actions of resveratrol (Bastianetto et al., 2014).

Resveratrol effects in the brain

Although resveratrol has a poor bioavailability, animal studies have shown that it is able to cross the blood–brain barrier (BBB). For example, a chronic administration of resveratrol (8–30 mg/kg, intraperitoneal, i.p.) significantly protected the hippocampus of rodents exposed to either kainic acid (Virgili and Contestabile, 2000), or to an occlusion of carotid arteries (Wang et al., 2002). In the latest study, the authors found that significant levels of resveratrol were detected in the brain after i.p. injection, reaching its peak at 4 h post-injection, supporting the hypothesis that it can cross the BBB, at least in rodents (Wang et al., 2002). Sinha et al. (2002) reported that a peripheral treatment with trans-resveratrol (20

mg/kg for 21 days) decreased the volume of infarcts in rats subjected to focal ischemia. Finally, similar *in vivo* protective action of resveratrol (5–300 mg/kg) was observed in transgenic models of AD (Frozza et al., 2013). In the latest study, injections of lipid-core nanocapsules containing resveratrol (5 mg/kg, i.p. injections) were able to rescue the deleterious effects of Aβ1–42 while treatment with resveratrol presented only partial beneficial effect. In a randomized, double-blind, placebo-controlled study involving 22 healthy adults, they showed that administration of resveratrol (250 and 500 mg) resulted in dose-dependent increases in cerebral blood flow during cognitive task performance that activates the frontal cortex. However, cognitive functions were not affected. The presence of free resveratrol was confirmed by high performance liquid chromatography, with concentrations, peaking at 5.65 and 14.4 μg/l after 250 and 500 mg, respectively, 90 min after dosing (Kennedy et al., 2010). In contrast, the glucuronidated and sulfated conjugates were present in much higher concentrations 45 min after the start of the cognitive tasks. Concentrations, particularly of the sulfated conjugate, continued to rise to reach about 300 and 700 μg/l for 250 and 500 mg of resveratrol, respectively, at the 90 min post-dose time point that corresponded to the end of the cognitive tasks (Kennedy et al., 2010). Moreover, acute administration of resveratrol has been reported to increase both endothelium-dependent vasodilation and flow-mediated dilation of the brachial artery, an effect that may contribute to enhance cerebrovascular and cognitive functions (Wong et al., 2013). Currently, a clinical study is under way to evaluate resveratrol as a dietary ingredient with beneficial effects in mild to moderate AD. A phase 1, randomized placebo controlled pilot study is under way to determine whether resveratrol (250–1000 mg/day; for 12 to 52 weeks) supplementation is safe and improves memory and physical performance in older adults (ClinicalTrials.gov Identifier: NCT01126229).

Modulatory effects of dietary compounds on miRNA expression

Various diets and dietary interventions including high-fat diets, caloric restriction (CR) and the use of bioactive micronutrients and plant derivatives, have been associated with epigenetic changes that alter cellular signaling (Garcia-Segura et al., 2013; Hardy and Tollefsbol, 2011). These include DNA methylation, histone acetylation, and more recently recognized, changes in miRNAs expression (Garcia-Segura et al., 2013).

In 2010, Li et al. published a review of the modulatory effects of dietary compounds on miRNA expression indicating that a number of miRNAs are up-regulated or down-regulated by natural agents such as curcumin, isoflavone, indole-3-carbinol, 3,3′-di-indolylmethane, epigallocatechin-3-gallate, resveratrol, etc., leading to the inhibition of cancer cell growth,

induction of apoptosis, reversal of epithelium-to-mesenchyme transition or the enhancement of efficacy of conventional cancer therapeutics, while some other natural compounds do the opposite (Li et al., 2010). Other studies asserted that some nutrients in foods, such as amino acid or fatty acids, can modulate miRNA expression (Drummond et al., 2009; Davidson et al., 2009). It has also been described that retinoic acid, folate or curcumin alter the expression of miRNA, an effect that may contribute to the cancer-protective effects of these nutrients (Davis et al., 2008).

Moreover, changes in miRNA expression were observed after polyphenol supplementation, and five miRNAs (miR-291b-5p, miR-296-5p, miR-30c-1*, miR-467b* and miR-374*) counteracted the modulation of miRNA expression induced by apoE mutation in mice (Milenkovic et al., 2012). Mercken et al. (2013) also demonstrated that several miRNAs were differentially expressed in skeletal muscle aging and that CR reversed some of these changes to a younger phenotype (Mercken et al.,2013). Very recently, Sangiao-Alvarellos et al. identified a sets of miRNAs, including let-7a, mir-9*, mir-30e, mir-132, mir-145, mir-200a, and mir-218, whose expression patterns in the hypothalamus were jointly altered by caloric restriction and/or a high-fat diet. The predicted targets of these miRNAs include several elements of key inflammatory and metabolic pathways, including insulin and leptin (Sangiao-Alvarellos et al., 2014).

Very interestingly, Baselga-Escudero et al., 2014 also demonstrated the ability of resveratrol and epigallocatechin gallate to bind miR-33a and miR-122 by using (1)H NMR spectroscopy suggesting a new posttranscriptional mechanism by which polyphenols could modulate metabolism. Finally, over 100 miRNAs, involved in the control of different cellular processes such as inflammation or apoptosis, were identified as modulated by polyphenols in a recent review by Milenkovic (Milenkovic et al., 2013) (Figure 34).

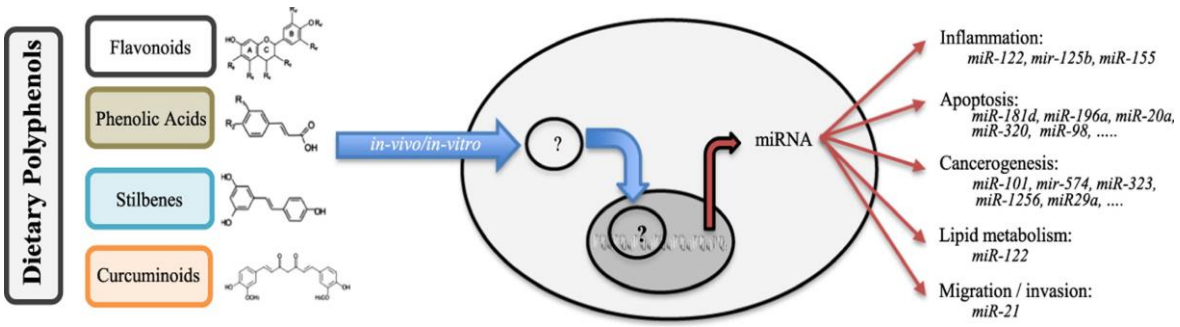

Figure 34. miRNA as molecular target of polyphenols underlying their biological effects (Milenkovic et al., 2013).

Circulating miRNA as potential age-related disease biomarker

Recently, many researchers all over the world have focused on the research of miRNAs as a cost-saving and noninvasive biomarkers in the clinical diagnosis for various diseases. In cell-free serum/plasma, microRNAs have been found in exosome, microvesicles specialized in transporting different types of molecule and currently seen as a short/long range inter-organ communication system (Fabbri et al., 2012). Numerous proteins may be found within exosomes but RNA, with a strong percentage of microRNAs, seems to predominate in these structures; moreover, exosomes prevent miRNAs degradation by RNase (Mitchell et al., 2008).

Serum and plasma contain a large amount of stable miRNAs derived from various tissues/organs, and that the expression profile of these miRNAs shows great promise as a novel non-invasive biomarker for diagnosis of cancer and other diseases (Chen et al., 2008). In particular, altered circulating miRNAs expressions have been reported in acute myocardial infarction, acute coronary syndrome, stable coronary artery disease, heart failure, atherosclerosis, essential hypertension and stroke (Sayed et al., 2014). Significantly higher circulating miR-21 and miR-146a levels in elderly patients with acute myocardial infarction and/or heart failure compared with healthy subjects were also reported (Olivieri et al., 2013). Reduced miR-146a levels were also found in diabetic patients, in association with insulin resistance, poor glycaemia control and high levels of plasma TNFα and IL-6 (Balasubramanyam et al., 2011). In the context of cancer, several circulating miRNAs has been described as potential biomarker for an earlier cancer diagnosis and to predict prognosis and response to therapy (Schwarzenbach et al., 2014).

The study of miRNAs in neurological disease although still in its early days, seems to be a research area of great potential. The ability to detect alterations in miRNAs in the brain by analysis of cerebrospinal fluid, or even better the analysis of plasma, would remarkably improve the diagnostic toolbox for Alzheimer's disease, Parkinson's disease, Huntington's disease, and prion and other neurological diseases.

In 2007, Schipper et al. first reported an overexpression of miRNA in peripheral blood mononuclear cells of AD patients, and their results suggested that miRNAs could be used as biomarkers for AD diagnosis (Schipper et al., 2007). Soon afterward, two specific miRNAs, miR-7 and miR-153, were proven to be able to modulate the transcriptional level of α-synuclein, which is trigger factor of PD (Junn et al.,2009; Doxakis, 2010). Recently, Liu et al. confirmed that miR-384 could regulate the expression of amyloid precursor protein and beta-secretase, which are implicated in the pathological pathway of AD (Liu et al., 2014). In the brain,

circulating microRNAs have been suggested to be vital for neuronal communication (Tsang et al., 2007) and lead microRNAs in blood serve as circulating biomarkers for bipolar disorder and early Huntington's disease (Gaughwin et al., 2011). In aging mice, miR-34a was shown to be upregulated, concomitantly with a decreased mRNA expression of its primary target gene SIRT1, in brain tissue but also in peripheral blood mononuclear cells and plasma (Li et al., 2011). Therefore, it was suggested that circulatory miR-34a may hold great promise as an accessible biomarker for brain aging.

Noren et al. (2010) reported that miR-103, miR-107, miR-128, miR-130a, miR-155, miR-24, miR-221, miR-496, miR-1538 were significantly lower in older individuals suggesting their potential to be diagnostic indicators of age or age-related diseases (Noren et al., 2010). Two sets of circulating brain-enriched miRNAs, the miR-132 family (miR-128, miR-132, miR-874), were also reported to be capable of differentiating mild cognitive impairments from age-matched controls (Sheinerman et al., 2013). In a recent study, five down regulated serum miRNAs (miR-29b, miR-106b, miR-130b, miR-142-5p, and miR-340) and three up regulated miRNAs (miR-92a, miR-222, and miR-375) were also associated to physiological aging (Zhang et al., 2014).

miRNAs therapeutic

miRNAs and miRNA-targeting oligonucleotides have several advantages over traditional small-molecule drugs, most notably they can be chemically modified to enhance their pharmacokinetic and pharmacodynamic profiles and they have the ability to target multiple genes, simultaneously. Not surprisingly, miRNA-targeting therapies are an area of intense interest to pharmaceutical companies, and many of such compounds are in preclinical and clinical development for a variety of indications (Li and Rana, 2014) (Table2).

miR-122 was identified in 2005 as a liver-specific miRNA that can modulate HCV replication. Consistent with this, HCV replication was shown to be inhibited by a 2′-OMe-modified antimiR-122 ASO, paving the way for the development of miR-122 inhibitors as treatments for HCV infection in humans. In a Phase II study, patients with chronic HCV infection received five weekly subcutaneous injections of miravirsen, which resulted in a mean 2–3 log decrease in serum HCV RNA. No serious adverse effects were reported (Lindow and Kauppinen, 2012). These impressive data suggest that miravirsen may become the first anti-miR oligonucleotide drug to enter the market.

On the contrary, miR-34 mimics might be promising therapeutic options for restoring the normal regulation of a range of cell death and survival genes in cancer cells. The leading

therapeutic, MRX34, is a lipid-formulated miR-34 mimic under development by Mirna Therapeutics. MRX34 is the first miRNA mimic to enter clinical trials and is currently in Phase I testing in patients with primary liver cancer or metastatic cancer that has spread to the liver.

Table 2. miRNA-based therapeutic in development (Li and Rana, 2014).

MicroRNA	Oligonucleotide format	Indications	Companies	Developmental stage
miR-122	LNA-modified antisense inhibitor	HCV infection	Santaris Pharma	Phase II
miR-122	GalNAc-conjugated antisense inhibitor	HCV infection	Regulus Therapeutics	Phase I
miR-34	miRNA mimic replacement	Liver cancer or metastasized cancer involving liver	miRNA Therapeutics	Phase I
Let-7	miRNA mimic replacement	Cancer (details undisclosed)	miRNA Therapeutics	Preclinical
miR-21	2′-F and 2′-MOE bicyclic sugar modified antisense inhibitor	Cancer, fibrosis	Regulus Therapeutics	Preclinical
miR-208	Antisense inhibitor	Heart failure, cardiometabolic disease	miRagen/Servier	Preclinical
miR-195 (miR-15 family)	Antisense inhibitor	Post-myocardial infarction remodelling	miRagen/Servier	Preclinical
miR-221	Antisense inhibitor	Hepatocellular carcinoma	Regulus Therapeutics	Preclinical
miR-103/105	Antisense inhibitor	Insulin resistance	Regulus Therapeutics	Preclinical
miR-10b	Antisense inhibitor	Glioblastoma	Regulus Therapeutics	Preclinical

2′-F, 2′-fluoro; 2′-MOE, 2′-*O*-methyoxyethyl; GalNAc, *N*-acetylgalactosamine; HCV, hepatitis C virus; LNA, locked nucleic acid; miRNA, microRNA.

Aims

Genes and epigenetic factors together with environmental variables such as nutrition, generate a sophisticated control network that plays a central role in brain function. However, very little is known on the complex relationships between genome-wide transcriptional responses to the aging process in the brain and their regulation by epigenetic factors such as miRNAs. Moreover, only few studies have explored the effects of specific food components in regulating gene expression and epigenetic patterns during brain aging or neurodegeneration.

Specific aims of *in vivo* studies

The first aim of my research was to study the regulatory mechanisms of miRNAs on genes during the aging process in the brain, by integrating genome-wide miRNA and mRNA expression profiles.

The second aim was to investigate the interactions between specific food components and gene expression, focusing on the significance of epigenetic factors in the nutritional regulation of gene expression; in particular, we verified whether dietary treatment with some olive oil phenols modifies the profile of microRNA and gene expression in the aging mouse brain, and if these changes correlate with the cognitive and motor changes observed in the aging animals.

Specific aims of *in vitro* studies

In the last few years, the European Union strongly encouraged the "3Rs" principle (replacement, reduction and refinement) for the protection and spare of animals used for scientific purposes.

In vitro systems, besides sparing animal lives, have the obvious advantage of being often less expensive and shorter in duration and offer a simplified model for shedding light into mechanisms involved in brain aging.

In this view, we developed an *in vitro* system comprising both neuronal and glial cells as a model for studying the aging process in the brain and for a study of anti-aging/neuro-protective compounds.

To this aim, we first defined the temporal evolution of this system, measuring a series of senescence-associated markers. We then investigated the variation of miRNA expression profiles in this model and assessed its similarities with *in vivo* models of brain aging. Finally, we tested the effects of the anti-aging compound resveratrol on senescence-associated markers and miRNA expression, in order to provide a first evaluation of the predictive potential of anti-aging substances on this model.

Materials and methods

Animals

All procedures were carried out in agreement with the European Union Regulations on the Care and Use of Laboratory Animals (OJ of ECL 358/1, 12/18/1986), according to Italian regulations on the protection of animals used for experimental and other scientific purposes (DM 116/1992), after approval from the Italian Ministry for Scientific Research.

Male C57Bl/6J mice aged 10 months at the beginning of the experiment were used. They were housed in groups of 4 in polypropylene cages equipped with soft wood bedding, a water bottle, and a mouse house in a climate-controlled room with a 12-hr light–dark cycle. The animals were randomly subdivided into three groups of 9 each and fed different diets (about 3 grams/mouse per day) for 12 months. The experimental diets were prepared using components purchased from Piccioni (Gessate, Milan, Italy). Fresh diet was put in the trough every 2 days. We used a modified AIN 76 diet, with lipids providing about 21% of the total energy (kcal), composed of (in grams/100 grams of diet): 44.3 sucrose, 10.0 olive oil, 21.0 casein, 14.0 corn starch, 5.4 cellulose, 3.7 AIN 76 Mineral mix, 1.1 AIN 76 Vitamin mix, 0.3 methionine, and 0.2 choline. This diet provided 407 Kcal/100 grams of weight.

One group of mice fed a diet in which the lipid component was provided by an extra-virgin olive oil high in phenolic antioxidants (H-EVOO group; 718.8 mg of total phenols/kg of olive oil), purchased from Cipolloni and Petesse S.p.A. (Foligno, Perugia, Italy), and another group (negative control) by the same extra-virgin olive oil deprived of phenolic compounds (L-EVOO group; 9.3 mg of total phenols/kg of olive oil). The third group of mice fed a diet containing 10% L-EVOO and resveratrol at a final dose of 22 mg/kg (RESV group). A total of 5 young animals (4–6 months of age) were also analyzed. Mice were sacrificed by cervical dislocation either after 6 or 12 months of treatment, together with a group of young mice (4-6 months of age). Brain samples from young and aged mice were dissected, immediately frozen in liquid nitrogen and stored at −80 °C for further molecular analyses. Frozen samples of cerebral cortex from transgenic hemizygous TgCRND8 (tg) mice (4-6 months of age) were also used. TgCRND8 mice are a mouse model of Alzheimer's disease, displaying a widespread amyloid deposition already detectable at 3 months of age (Bellucci et al., 2006).

Preparation of the oils and analysis of the phenolic content

The H-EVOO was obtained from trees of the Moraiolo cultivar grown in the region of Umbria, in central Italy. The olives were harvested at the early ripening stage (green olives) and processed as follows: The fruit crushing was performed using a tooth grinder, then the olive pastes were malaxed for 40 min at 25 °C and the oil was extracted using a three-phase decanter at low water addition (20 L of water for 100 kg of olive paste). L-EVOO was obtained from H-EVOO as follows: The extra- virgin oil was homogenized for 1 min with water (1:1, vol/vol), and the oil was separated by centrifugation (using a Westfalia separator). This procedure was repeated six times. Then the oil was filtered through a cellulose acetate membrane.

The extraction of H-EVOO and L-EVOO phenols and the high-performance liquid chromatography (HPLC) analysis were conducted using an Agilent Technologies system model 1100 (Agilent Technologies, Palo Alto, CA), composed of a vacuum degasser, a quaternary pump, an autosampler, a thermostated column compartment, a diode array detector (DAD), and a fluorescence detector (FLD). The analysis of the oil extract was performed using C18 columns Spherisorb ODS-1 250 · 4.6mm with a particle size of 5 µm (Phase Separation Ltd., Deeside, UK). The mobile phase was composed of 0.2% acetic acid (pH 3.1) in water (solvent A)/methanol (solvent B) at a flow rate of 1 mL/min, and the gradient was changed as follows: 95% A/ 5% B for 2 min, 75% A/25% B for 8 min, 60% A/40% B for 10 min, 50% A/50% B for 16 min, and 0% A/100% B for 14 min. This composition was maintained for 10 min. Then, the initial conditions were reset, and equilibrium was reached for 13 min; the total running time was 73 min. The oils were stored at room temperature in the dark throughout the experiment, and the bottles were flushed with nitrogen before each recapping.

The antioxidant composition of the olive oils employed is shown in Table 3. At the end of the experiment, the antioxidant content of the study oil was measured again to evaluate the loss of active compounds over time. The results showed that the total content of phenolic antioxidants after 1 year was about 80% of the initial amount. Hydroxytyrosol content was only slightly decreased (- 2%).

Table 3. Antioxidant Composition of the study olive oils (mg/kg).

Components (mg/kg)	H-EVOO	L-EVOO
3,4-DHPEA	15.0 ± 0.5	-
p-HPEA	11.0 ± 0.1	0.1 ± 0.01
3,4-DHPEA-EDA	346.7 ± 3.5	1.1 ± 0.02
p-HPEA-EDA	81.9 ± 1.1	1.7 ± 0.01
(+)-1-Acetoxipinoresinol	17.0 ± 0.02	1.5 ± 0.01
(+)-Pinoresinol	32.3 ± 0.1	2.0 ± 0.02
3,4-DHPEA-EA	214.9 ± 2.1	2.9 ± 0.03
α-tocopherol	131.2 ± 1.1	129.1 ± 1.10

3,4-DHPEA: hydroxytyrosol; p-HPEA: tyrosol; 3,4-DHPEA-EDA: 3,4 dialdehyde form of elenoic acid linked to hydroxytyrosol; p-HPEA-EDA (oleocanthal): dialdehyde form of elenoic acid linked to tyrosol; 3,4-DHPEA-EA: hydroxytyrosol esters of elenoic acid or oleuropein.

Behavioral tests

Behavioral testing was performed at the beginning of the treatment and at 28–35 weeks when the animals were about 18 months old. All of the tests were performed in an acoustically isolated room, kept at 20 °C, starting around 9 a.m. Illumination inside the room was 60 lux. All measurements were done by operators who were blinded.

Motor coordination

On day 1, the mice were given a habituation trial. They were placed on the rotarod apparatus (Ugo Basile, Varese, Italy) initially at speed 0 and then at a constant speed (14 rpm). The mice had to remain on the rotarod for 60 sec. The following day, each mouse was given three trials at three different speeds: 14 rpm, 22 rpm, and 30 rpm. The maximum trial length was 60 sec, and there was a 15-min rest period between each trial. The number of falls and the time to first fall (in sec/100) were recorded.

Contextual memory: step-down inhibitory avoidance test

For the step-down inhibitory avoidance test, the inhibitory avoidance apparatus consisted of an open field gray Plexiglas box (40 · 40 cm) with a steel rod floor. The Plexiglas platform (4 · 4 · 4 cm) was set in the center of the grid floor. Intermittent electric shocks (20 mA, 50Hz) were delivered to the grid floor by an isolated stimulator. In this test, the animals learn to associate exploration of a compartment with a foot shock delivered through the floor grid. On subsequent exposure to the same environment, the mice will avoid stepping down or will increase the latency before ‘‘stepping down’’ onto the floor grid. On the first day (training test), each mouse was gently placed on the platform. When the mouse stepped down from the platform and placed all its paws on the grid floor, an intermittent electric shock was delivered for 3 sec. Responsiveness to the punishment in the training test was assessed by the animal’s vocalization; only those mice that vocalized touching the grid with the four paws were used for the retention test in order to exclude the mice with a different pain threshold. Twenty-four hours (retention test) after training, each mouse was placed on the platform again. The latencies of stepping down were measured, considering 30 sec as the upper cutoff, during the training and retention tests.

Spatial memory: Morris water maze

For the Morris water maze (MWM), we used a circular pool (134 cm diameter and 50cm high) filled with water at 21 – 22°C, made opaque by the addition of nontoxic white paint, and containing a round-shaped transparent acrylic platform (10 cm diameter). In the task, the platform was submerged 1.5 cm below the surface of the water and located in the northwest quadrant of the pool throughout the trials. After a mouse was put into the pool, each had a maximum of 60 sec to locate the platform and climb onto it (one trial). When a mouse located the platform, it was allowed to stay on it for 20 sec. Mice that did not find the platform in the allowed time were placed on it by the experimenter and left there for 20 sec. Latency to reach the platform was registered. Each mouse was subjected to four trials per day. The task consisted of 4 days of trials. Two hours after the last trial, the probe test was carried out. For this test, the platform was removed from the pool and the trial was performed with a cutoff time of 30 sec. The starting point was set in the southeast quadrant. The time spent in the target area, sector, and quadrant (zone radius, 30 cm, three times the target diameter) was recorded by a video tracking/computerized digitizing system (HVS Image, Hampton, UK) as a percentage of the trial time in the pool.

Anxiety: light-dark box

For light–dark preference, we used a light–dark box built in our department, made of two chambers of equal dimensions, one of white opaque plastic, and the other of black opaque plastic. The floors of both chambers were made of stainless steel rods, and the two chambers were separated by a guillotine door. The animals were taken singly from their home cages and brought to the adjacent acoustically insulated room, where the light–dark box apparatus was placed. Each mouse was placed in the lighted chamber, facing away from the closed connecting door. Five seconds later the guillotine door was raised. The time spent by the mouse in the lighted chamber before going into the dark chamber with all four paws (step-through latency) was measured. The total time spent in the light or in the dark chamber and the number of crossings between the two compartments over a period of 3 min were also measured.

Neuromuscular function: grip strength

Neuromuscular function was evaluated by means of a grip strength apparatus measuring the traction exerted by the animals on a pole. The highest force among three attempts was recorded as the force score for the set and the average value from the three highest sets out of five was defined as the forelimb grip strength for each mouse. Mean peak force values (g) were calculated for each animal and normalized to the animal body weight.

RNA extraction for gene expression profiling

For gene expression analysis, total RNA was extracted from 10 (5 for each dietary treatment) samples of cerebral cortex (cc) and 10 samples of cerebellar (cb) harvested from 18 and 24 months-old mice. RNA extraction was performed by using the RNeasy Plus Mini Kit (Quiagen) according to manufacturer's protocol. Brain tissues were lysated in 350 µl of RLT buffer plus β-mercaptoethanol (β-ME), transferred to a gDNA Eliminator spin column and centrifuged for 30 s at ≥8000 x g (≥10,000 rpm) and then, 1 volume of 70% ethanol was added to the flow-through and transferred to an RNeasy spin column and centrifuged for 15 s at ≥8000 x g (≥10,000 rpm). 700 µl Buffer RW1 were then added to the RNeasy spin column and centrifuged for 15 s at ≥8000 x g (≥10,000 rpm) to wash the spin column membrane. Other 500 µl of Buffer RPE were then added to the RNeasy spin column and centrifuged for 15 s at ≥8000 x g (≥10,000 rpm) to perform a second wash of the spin column membrane. This step was repeated two times. Finally, the RNeasy spin column was placed in a new collection tube and centrifuged at full speed for 1 min to eliminate any possible carryover of Buffer RPE. To elute

the RNA, 30µl of RNAse free water were added the RNeasy spin column and centrifuged for 1 min at ≥8000 x g (≥10,000 rpm). To improve the RNA yield, this final step was repeated twice.

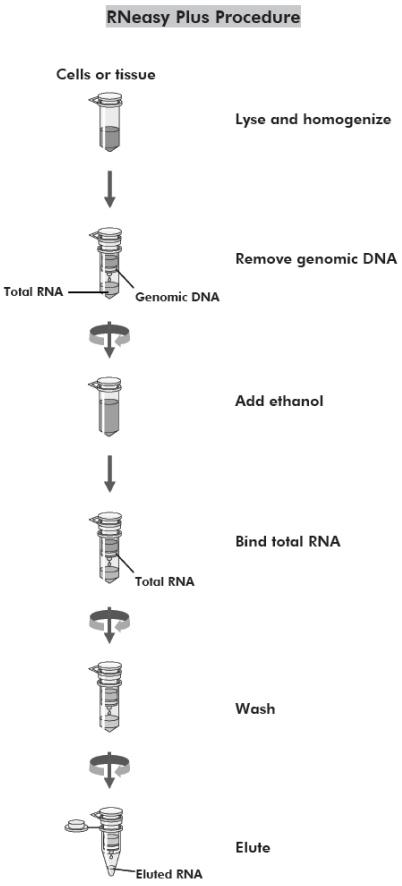

Gene expression microarray protocol

The labeling and hybridization steps were carried out according to the Agilent protocol (Two- Color Microarray-Based Gene Expression Analysis version 5.7), using a two-color microarray protocol in which aged samples were contrasted within each brain region with a reference RNA obtained by pooling equal amount of 9 samples of cc or cb harvested from young mice.

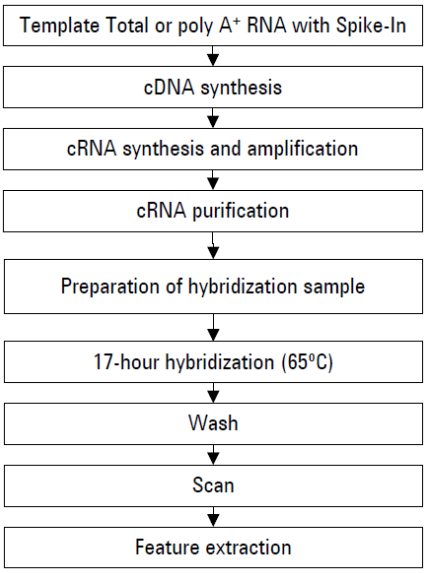

Workflow for sample preparation and array processing

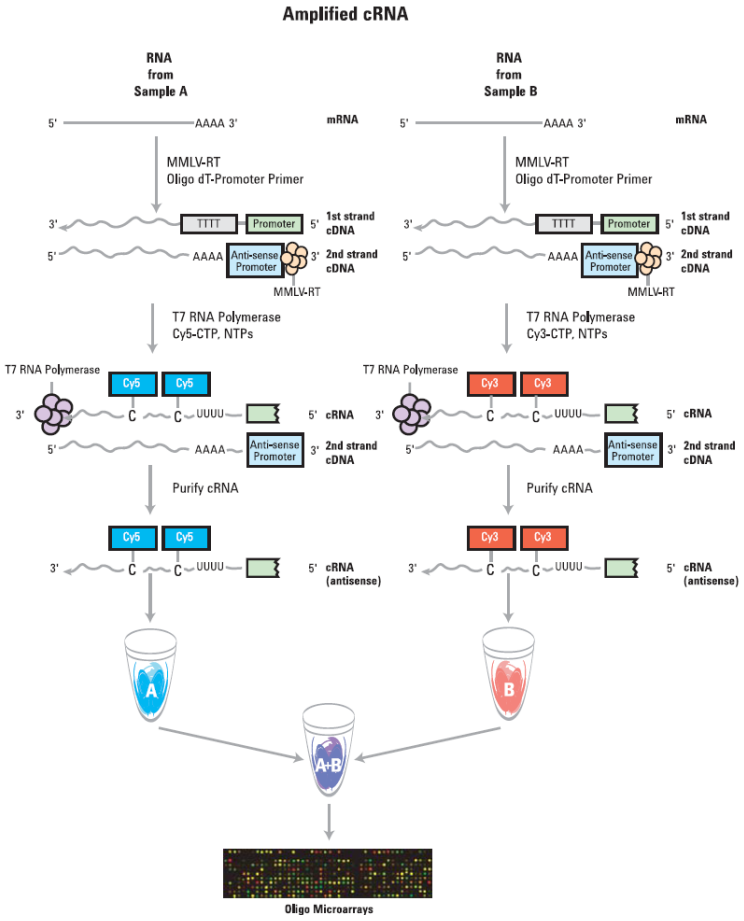

Schematic microarray gene expression procedure

Preparation of Spike A Mix and Spike B Mix

The Agilent RNA Spike-In Kit was developed to provide positive controls for monitoring the microarray workflow from sample amplification and labeling to microarray processing. The Agilent RNA Spike-In Kit contains two spike-in mixtures. Each mixture contains 10 *in vitro* synthesized, polyadenylated transcripts derived from the Adenovirus E1A transcriptome that are premixed at various ratios. The RNA Spike-In Kit consists of two sets of positive control transcript mixtures optimized to anneal to their complementary probes on the microarray, with minimal self-hybridization and cross-hybridization. When the two mixtures are cohybridized onto a microarray, the user can use the expected versus observed log ratios to monitor the system for linearity, sensitivity, and accuracy. Concentrated RNA Spike-In Kit stocks must be diluted with the Dilution Buffer provided in the kit. These are spiked-in directly to the RNA samples prior to amplification and labeling to achieve the final relative amounts indicated in the table below.

Dilutions of Spike A Mix for cyanine 3 and Spike B Mix for cyanine 5 labeling

Starting amount of RNA		Serial dilution			Spike A Mix or Spike B Mix volume to be used (µL)
Total RNA (ng)	PolyA RNA (ng)	First	Second	Third	
50-200		1:20	1:40	1:16	2
201-2000		1:20	1:40	1:4	2
>2000	200	1:20	1:40	0	2

Labeling reaction

50 ng of total RNA, 2 µl of diluted Spike-Mix (A or B) and 1.2 µL of T7 promoter primer were denatured by incubating the reaction at 65°C in a circulating water bath for 10 minutes and then placed on ice for 5 minutes. 8.5 µL of cDNA Master Mix (see table below) were then added to each sample tube, mixed and incubated at 40°C in a circulating water bath for 2 hours. After this, samples were moved to a 65°C circulating water bath and incubated for 15 minutes before being transferred to ice.

cDNA Master Mix

Component	Volume (µL) per reaction	Volume (µL) per 4.5 reactions
5X First Strand Buffer	4	18
0.1 M DTT	2	9
10 mM dNTP mix	1	4.5
MMLV-RT	1	4.5
RNaseOut	0.5	2.3
Total Volume	8.5	38.3

60 µL of Transcription Master Mix were then added to each sample, mixed and incubated in a circulating water bath at 40°C for 2 hours.

Transcription Master Mix

Component	Volume (µL) per reaction	Volume (µL) per 4.5 reactions
Nuclease-free water	15.3	68.9
4X Transcription Buffer	20	90
0.1 M DTT	6	27
NTP mix	8	36
50% PEG	6.4	28.8
RNaseOUT	0.5	2.3
Inorganic pyrophosphatase	0.6	2.7
T7 RNA Polymerase	0.8	3.6
Cyanine 3-CTP or cyanine 5-CTP	2.4	10.8
Total Volume	60	270

Purification

20 µL of nuclease-free water were added to cRNA samples, for a total volume of 100 µL together with 350 µL of Buffer RLT and 250 µL of ethanol (96% to 100% purity), transferred to an RNeasy mini column and centrifuged at 4°C for 30 seconds at 13,000 rpm. The RNeasy column was then transferred to a new collection tube and 500 µL of buffer RPE (containing ethanol) were added to the column. The sample was than centrifuge at 4°C for 30 seconds at 13,000 rpm. Another 500 µL of buffer RPE were added to the column and centrifuged at 4°C

for 60 seconds at 13,000 rpm. The sample were then centrifuged at 4°C for 30 seconds at 13,000 rpm to remove any remaining traces of buffer RPE.

The cleaned cRNA sample was eluted by adding 30 µL RNase-free water directly onto the RNeasy filter membrane. After 60 seconds of incubation, the cleaned cRNA, was collected by centrifugation at 4°C for 30 seconds at 13,000 rpm.

Quantification of the cRNA

cRNA was quantified using the IMPLEN nanophotometer and the following parameters were recorded:

- Cyanine 3 or cyanine 5 dye concentration (pmol/µL)
- RNA absorbance ratio (260 nm/280 nm)
- RNA concentration (ng/µL)

The yield and specific activity of each reaction was calculated as follows:
Yield: (Concentration of cRNA) * 30 µL (elution volume) / 1000 = µg of cRNA
Specific activity: (Concentration of Cy3 or Cy5) / (Concentration of cRNA) * 1000 = pmol Cy3 per µg cRNA
If the yield is <825 ng and the specific activity is <8.0 pmol Cy3 or Cy5 per µg cRNA it is better to not proceed to the hybridization step.

Hybridization

Preparation of hybridization samples

For each microarray, each of the components as indicated in the table below were added in a 1.5 mL nuclease-free microfuge tube and incubated at 60°C for exactly 30 minutes to fragment RNA.

Fragmentation mix

Components	Volume/Mass
cyanine 3-labeled, linearly amplified cRNA	825 ng
cyanine 5-labeled, linearly amplified cRNA	825 ng
10X Blocking Agent	6 µL
Nuclease-free water	bring volume to 28.8 µL
25X Fragmentation Buffer	1.2 µL
Total Volume	30 µL

To stop the reaction 30µl of 2x GEx Hybridization Buffer HI-RPM were added to the fragmentation mix. 55 µl of the sample mixture were loaded into the Agilent Mouse GE 4x44K v2 Oligo 60-mer microarrays, in Agilent microarray chambers (G2534A) at 65° for 18 h.

Bioinformatics methods for Gene expression

GE arrays were scanned using a Genepix 4000B microarray scanner at 5-µm resolution (Axon Instruments, Foster City, CA, USA). Image analysis and initial quality control were performed using Agilent Feature Extraction Software v9.5. Values for control spots and spots that did not meet the quality criteria were flagged. Quality criteria included a minimal spot size, a median/mean ratio of at least 0.9 for each spot, non-saturated intensity for both channels, a signal well above background and a minimal signal intensity for at least one channel.

Initial statistical analysis was performed using unpaired t-test considering Benjamini–Hochberg corrected p-value of 0.05. The pairwise average-linkage cluster analysis was applied to differentially expressed genes using the Cluster 3.0 and Treeview software (Eisen et al., 1998), a method of hierarchical clustering in which relationships among genes and samples (mice) are represented by a tree whose branch lengths reflect the degree of similarity between the genes.

Differentially expressed genes and gene sets between treatments were identified using BRB-Array Tools v.3.8.1 stable release (developed by Dr. Richard Simon and the BRB-array tools development team). Class comparison was performed using a two-sample t-test with random variance model, and a multivariate permutation with a total of 10,000 permutations. A random variance t-test was selected to permit sharing of information among probe sets within

class variation without assuming that all probe sets possess the same variance, at nominal significance level of 0.001. The false discovery rate (FDR) with these conditions for all significant differentially expressed genes was ≤0.1.

Gene Set Expression analysis (GSEA) was used to identify pathways that had more differentially expressed genes than expected by chance among H-EVOO vs. L-EVOO treated mice, in both brain areas, using two statistics (LS and KS). We considered significant gene sets those for which the P value from the LS or KS permutation test was 0.005 or less. Finally, we used the BRB miRNA class comparison tool to group genes into sets predicted to be potential targets of the same miRNA.

Total RNA extraction for miRNAs expression analysis (from brain tissues and cell cultures)

Total RNA including miRNAs was isolated from neuro-glial co-cultures and mice brain cortex by using the Absolutely RNA miRNA Kit (Agilent Technologies, Santa Clara, CA, USA) according to the manufacturer's protocol. miRNA profiling was performed on samples of cerebral cortex harvested from H-EVOO and L-EVOO mice at 6 and 12 months of treatment and from resveratrol treated mice at 6 months of treatment (4 for each diet), from young mice (n=4) and from TgCRND8 mice (n=4).

Brain tissues or cells were lysate with an adequate volume of Lysis Buffer plus β-Mercapto-ethanol and extracted by adding an equal volume of neutral phenol–chloroform [1:1 (v/v)]. The aqueous (upper) phase was then transferred to a fresh tube and extracted by adding an equal volume of chloroform–isoamyl alcohol [24:1 (v/v)] and vortexing for 10 seconds. The mixture was then spinned in a microcentrifuge at maximum speed for 2–3 minutes. The extracted lysate was then transferred to a prefilter spin cup and centrifuged at maximum speed for three minutes. 1.25 volumes of 100% ethanol were then added to the filtrate and vortexed for 15 seconds. The mixture was then transferred to an RNA Binding Spin Cup and centrifuged at maximum speed for 1 minute. RNA binded to the spin cup was washed with 600 µl of 1× Low-Salt Wash Buffer. After that, 55 µl of DNase solution were added directly onto the matrix inside the spin cup and incubated at 37°C for 15 minutes in an air incubator. Two more washes with 600 µl of 1× High-Salt Wash Buffer and with 600 µl of 1× Low-Salt Wash Buffer were performed. A final low salt wash with 600 µl of 1× Low-Salt Wash Buffer was performed and then, the spin cup was centrifuged at maximum speed for 60 seconds. A final centrifuge at maximum speed for 2 minutes was also performed to dry the matrix. The spin cup was transferred to a 1.5-ml microcentrifuge tube and 30 µl of RNasi free water were directly added onto the center of the matrix inside the spin cup. After 1 minute of incubation

the tube was centrifuged at maximum speed for 1 minute at room temperature. To maximize RNA yield, the eluate was reload onto the matrix, incubated for 1 minute and centrifuged at maximum speed for 1 minute at RT.

RNA concentration and purity was determined by using a NanoPhotometer spectrophotometer (IMPLEN, München, Germany). RNA integrity (RIN) was checked with a 2100 Bioanalyzer and RNA 6000 Nano LabChip kit (Agilent Technologies).

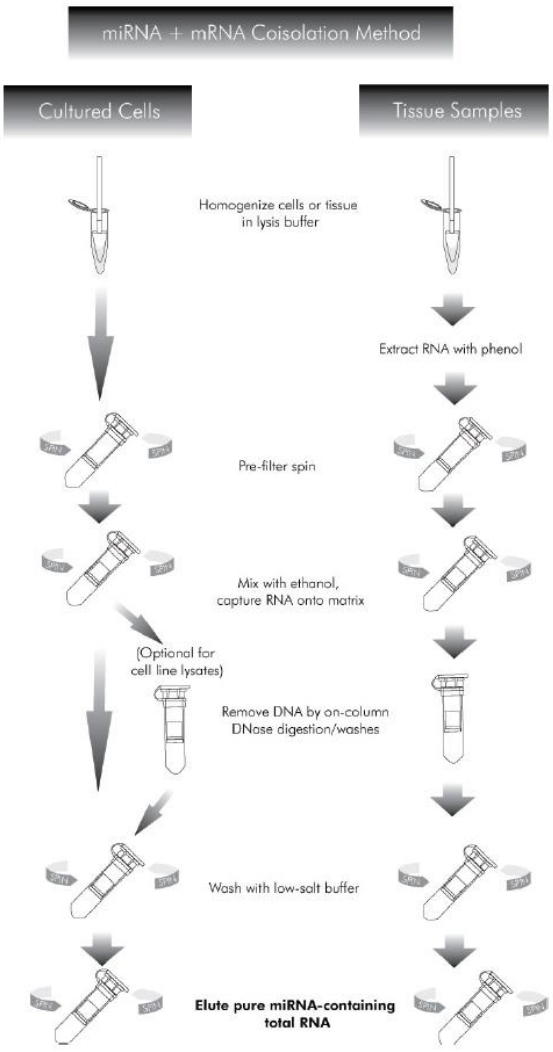

Absolutely RNA miRNA Kit method flow-chart

Preparation of labelled microRNA, microarray hybridization and scanning

To assess the labeling and hybridization efficiencies, total RNA samples were spiked with MicroRNA Spike-In Kit (Agilent Technologies, Santa Clara, USA). After treatment with calf intestine phosphatase (CIP), a labeling reaction was initiated with 100 ng total RNA per sample.

CIP Master Mix with Labeling Spike-In solution

Components	Volume (µL) per reaction	Volume (µL) per 9 reactions
10X Calf Intestinal Phosphatase Buffer	0.4	3.6
Labeling Spike-In	1.1	9.9
Calf Intestinal Phosphatase	0.5	4.5
Total Volume	2.0	18.0

For labeling dephosphorylated RNA, a T4 RNA ligase that incorporates cyanine 3-cytidine bisphosphate (miRNA Complete Labeling and Hyb Kit, Agilent Technologies, Santa Clara, USA) was used.

Ligation Master Mix for T4 RNA Ligase

Components	Volume (µL) per reaction	Volume (µL) per 9 reactions
10X T4 RNA Ligase Buffer	1.0	9.0
Cyanine3-pCp	3.0	27.0
T4 RNA Ligase	0.5	4.5
Total Volume	4.5	40.5

Cyanine 3-labelled miRNA samples were subsequently prepared for one-color hybridization (miRNA Complete Labeling and Hyb Kit).

Hybridization mix for miRNA microarrays with Hyb Spike-In solution

Components	Volume (µL)
Labeled miRNA sample	17
Hyb Spike-In	1
10X GE Blocking Agent	4.5
2X Hi-RPM Hybridization Buffer	22.5
Total Volume	45

The labelled miRNA samples were hybridized to mouse miRNA microarrays (Release 16.0, 8×60K format; Agilent Technologies) at 55 °C for 20 h. Microarray slides were then washed using the Gene Expression Wash Buffers 1 and 2 (Agilent Technologies).

Wash conditions

	Dish	Wash Buffer	Temperature	Time
Disassembly	1	GE Wash Buffer 1	Room temperature	
1st wash	2	GE Wash Buffer 1	Room temperature	5 minutes
2nd wash	3	GE Wash Buffer 2	37°C	5 minutes

Fluorescent signal intensities were detected with the Agilent DNA Microarray Scanner, at a resolution of 2 µm (Agilent Technologies) using the Scan Control A.8.4.1 Software (Agilent Technologies).

Total RNA (100 ng) + Labeling Spike-In (optional)

↓ Phosphatase Treatment, incubate 30 minutes, 37°C*

Dephosphorylated RNA

↓ Add DMSO

↓ Heat, ice

↓ Assemble Labeling Reaction, incubate 2 hours, 16°C*

Labeled RNA

↓ Desalt with Spin Column (optional)*

Desalted Labeled RNA

↓ Dry sample with vacuum concentrator, approximately 2 to 3 hours (with columns), 45°C to 55°C*

↓ Assemble Hybridization Mixture + Hyb Spike-In (optional)

↓ Heat, ice

↓ Hybridize 20 hours, 55°C, 20 RPM

↓ Wash, Scan

miRNA Profile

*The sample can be stored at -80°C after this step, if needed.

Workflow for sample preparation and array processing.

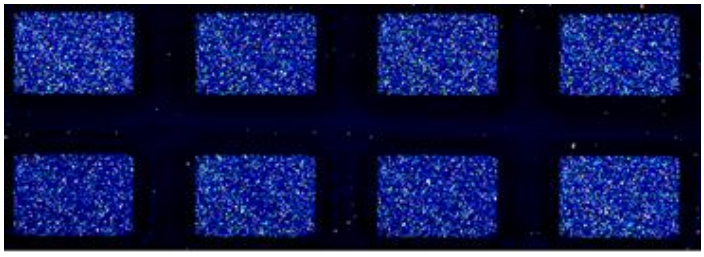

Example of scanned miRNA microarray image

Bioinformatics methods for miRNAs expression

Data were acquired using Agilent Feature Extraction 9.5.3.1 software for miRNA microarray, generating a GeneView file that contains summarized signal intensities for each miRNA by combining intensities of replicate probes and background subtraction. miRNA signal intensities from GeneView files were subjected to quantile normalization; expression differences were compared using the t test unpaired unequal variance between pairs of interest.

miRanda (http://www.microrna.org/microrna/home.do) and DIANA-microT and Target scan databases were used to predict the miRNA target genes. DIANA-miRPath v2.0 (at http://www.microrna.gr/miRPathv2.), a web-based application that performs an enrichment analysis of predicted target genes in all available KEGG pathways, was used to identify biological pathways potentially altered by the expression of the microRNAs simultaneously modulated in neuro-glial co-cultures and in in vivo models of aging and neurodegeneration.

DIANA-mirExTra algorithm was used to identify microRNA effects on gene expression levels, based on the frequency of hexamers in the 3'UTR sequences of genes, using the list of genes and miRNAs whose expression levels were found to be significantly changed comparing H-EVOO to L-EVOO mice fed for six months with the experimental diets, and L-EVOO 18 month-old mice to young mice, in the cortex. This analysis can lead to the identification of miRNAs responsible for the deregulation of large numbers of genes (Alexiou et al., 2010).

MicroRNA Validation: Quantitative real-time reverse transcription–polymerase chain reaction (qRT–PCR)

To confirm the results obtained by microarray miRNAs expression profiling, we performed qRT-PCR in selected affected and not affected miRNAs using SYBR green qRT-PCR assay. All samples were tested in duplicate using 96-well plates. Reverse transcription of RNA was performed using the miScript Reverse Transcription Kit according to manufacturer's instructions (Qiagen, Duesseldorf, Germany). qRT -PCR assays were carried out in 7900HT Fast Real-Time PCR System (Applied Biosystems, California, USA) using miScript SYBR Green PCR Kit and miScript Primer Assay according to manufacturer's instructions (Qiagen, Duesseldorf, Germany). Briefly, each reaction was performed in a final volume of 25 µl containing 2,5 µl of the cDNA, a master mix containing 12.5 µl of 2x QuantiTect SYBR Green PCR Master Mix, 2.5 µl of 10x miScript Universal Primer, 2.5 µl of 10x miScript Primer Assay and RNase-free water. The amplification profile was denaturation at 95°C for 15 min, followed by 40 cycles of 94°C for

15 s, 55°C for 30s, and 70°C for 30s. The expression levels of miRNAs were normalized to RNU6B and calculated as 2^-ΔΔct.

Microarray data are available online at the MIAME public database ArrayExpress (http://www.ebi.ac.uk/arrayexpress/): Experiment name: Olive oil phenols and GE in the aging mouse brain, ArrayExpress accession: E-MTAB-1530; Experiment name: Olive oil phenols and miRNA in the aging mouse brain, ArrayExpress accession: E-MTAB-1549.

Cell cultures

The experimental procedures were in accordance with the standards set forth in the Guide for the Care and Use of Laboratory Animals (published by the National Academy of Science, National Academy Press, Washington, D.C.). The uterus was removed from the gravid rat under anesthesia. Primary cultures of mixed cortical cells containing both neuronal and glial elements were prepared as previously described (Pellegrini-Giampietro et al., 1999). Briefly, cerebral cortices were dissected from fetal mice at 17-18 days of gestation, minced by using medium stock [MS, composed of Eagle's MEM (with Earle's salts, glutamine- and NaHCO3-free) supplemented with 38 mmol/L NaHCO3, 22 mmol/L glucose, 100 U/mL penicillin and 100 μg/mL streptomycin] and incubated for 10 min at 37°C in MS with 0.25% trypsin and 0.05% DNase. Enzymatic digestion was terminated by a second incubation (10 min at 37°C) in MS supplemented with 10% heat-inactivated horse serum and 10% fetal bovine serum, after which the cells were mechanically disrupted and counted. After a brief centrifugation, cells were re-suspended (approximately 4×10^5 cells/mL) and plated in 15 mm multi-well vessels on a layer of confluent astrocytes by using a plating medium of MS supplemented with 10% heat-inactivated horse serum, 10% fetal bovine serum and 2 mmol/L glutamine. Cultures were kept in an incubator at 37°C, with 100% humidity and 95% air and 5% CO2 atmosphere. After 4–5 days in vitro, non-neuronal cell division was halted by the application of 3 mmol/L cytosine arabinoside for 24 h. Cultures were then shifted to a maintenance medium identical to the plating medium but lacking fetal bovine serum, which was then partially replaced twice a week.

During the experiment, neuronal survival was assessed by phase-contrast microscopy and quantified by measuring LDH release. Neurons at 15 days in vitro (DIV) were considered mature and followed over time until cells were viable.

At several time points (15, 21, 23 and 27 DIV) cells were harvested to evaluate different senescence parameters.

Treatments

Cultures were treated with resveratrol 1 and 5 µM (Sigma-Aldrich Chemicals Co., St. Louis, MO, USA) continuously from the maturity stage of 15 DIV (young/adult cultures) to senescence at 27 DIV. The medium was partially changed every 2 days to maintain the concentrations relatively constant over time (24). Concentrations were selected on the basis of the existing literature showing effects of this substance in vitro (24, 25).

LDH release

Cell damage was evaluated by measuring the amount of lactate dehydrogenase (LDH) released from injured cells into the extracellular fluid by using the Citotoxicity Detection Kit (LDH) (Roche Applied Science, Roche, Basilea, CH).

Senescence associated-β-galactosidase activity (SA-β-gal)

Senescence associated-β-galactosidase activity was performed following the protocol of the senescence detection kit (β-galactosidase Staining Kit, Cell Signaling, Danvers, MA, USA). β-Galactosidase is an enzyme that hydrolyzes lactose to glucose and also acts broadly on allyl and alkyl β-D-galactosides. 5-bromo-4-chloro-3-indolyl-β-D-galactopyranoside (X-Gal), which is a substrate of β-galactosidase, is hydrolyzed to galactose and 5-bromo-4-chloro-3-hydroxyindole by the action of the enzyme. 5-bromo-4-chloro-3-hydroxyindole generated by the reaction is oxidized and converts to 5,5'-bromo-4,4'-dichloroindigo, which forms a blue insoluble precipitate.

Briefly, at established time points, cells were washed with PBS, fixed in 1X Fixative Solution (2% formaldehyde, 0.2% glutaraldehyde in PBS) for 15 min at room temperature, and rinsed with PBS. The cells were then incubated with freshly prepared SA-β-gal staining solution (930 µl of Staining Solution (40 mM citric acid/sodium phosphate (pH 6.0), 150 mM NaCl, 2 mM MgCl, 10 µl Staining Supplement A (500 mM potassium ferrocyanide), 10 µl Staining Supplement B (500 mM potassium ferricyanide)) overnight at 37°C. Cells positive for SA-β-gal blue staining were observed under a microscope and counted by two independent investigators with a 20x objective; 10 fields were counted and averaged for each slide.

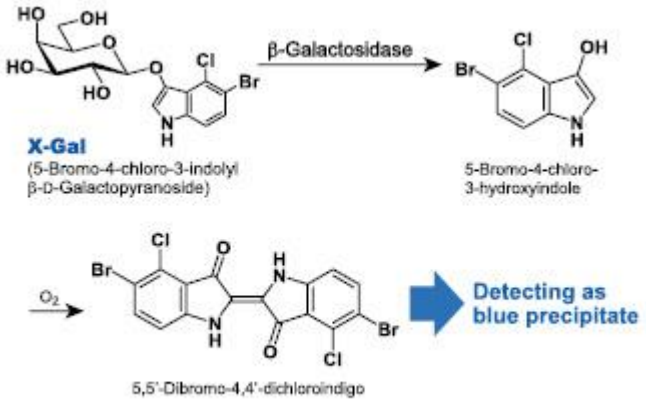

X-Gal hydrolysis with β-galactosidase.

Western blotting

Sample preparation

Harvested cells were lysed in radioimmunoprecipitation assay buffer (RIPA, 25mM Tris–HCl pH 7.6, 150mM NaCl, 1% NP-40, 1% sodium deoxycholate, 0.1% sodium dodecyl sulfate [SDS]) with 1% protease and phosphatase inhibitor Cocktail (Sigma–Aldrich)) and disrupted by sonication for 15 seconds (Microson XL-2000; Misonix, Farmingdale, NY, USA). Lysates were then clarified by centrifugation at 14000 rpm for 5 minutes at 4 °C and supernatants collected and stored at −80°C.

Protein quantification

Protein content was estimated by using the Bio-Rad DC protein assay kit (Bio-Rad, Segrate, Milan, Italy). The Bio-Rad DC Protein Assay is a colorimetric assay for protein concentration following detergent solubilization. The reaction is similar to the well-documented Lowry assay, based on the reaction of protein with an alkaline copper tartrate solution (Reagent A) and Folin reagent (Reagent B). As with the Lowry assay, there are two steps which lead to color development: the reaction between protein and copper in an alkaline medium, and the subsequent reduction of Folin reagent by the copper-treated protein. Color development is primarily due to the amino acids tyrosine and tryptophan, and to a lesser extent, cystine, cysteine, and histidine. Proteins effect a reduction of the Folin reagent by loss of 1, 2, or 3 oxygen atoms, thereby producing one or more of several possible reduced species which have a characteristic blue color with maximum absorbance at 750 nm and minimum absorbance at 405 nm.

BSA standard solutions containing from 0.2 mg/ml to about 2 mg/ml protein were prepared in the same buffer as the samples then 5 µl of standards and samples were pipetted into a clean, dry microtiter plate along with 25 µl of reagent A and 200 µl of reagent B. A 15 minutes incubation was performed at RT and protein content was measured at 650 nm.

Denaturation and reduction of the samples

Antibodies typically recognize a small portion of the protein of interest (referred to as the epitope) and this domain may reside within the 3D conformation of the protein. To enable access of the antibody to this portion it is necessary to unfold the protein, e.g. denature it.

To denature and reduced the disulphide bridges in proteins, we used a loading buffer (Sample buffer 4x, Invitrogen) containing the anionic denaturing detergent sodium dodecyl sulfate (SDS) in the presence of ß-mercaptoethanol and heated samples at 70°C for 10 minutes. Glycerol is also present in the loading buffer to increase the density of the sample to be loaded and hence maintain the sample at the bottom of the well, restricting overflow and uneven gel loading.

To enable visualization of the migration of proteins, the loading buffer also contains a small anionic dye molecule (e.g., bromophenol blue). Since the dye is anionic and small, it will migrate the fastest of any component in the mixture to be separated and provide a migration front to monitor the separation progress.

Electrophoresis protocol

Thirty micrograms of proteins were loaded in pre-cast gels (NuPAGE® Novex® 4-12% Bis-Tris Gels Invitrogen, Carlsbad, CA) along with the MagicMark™ XP protein molecular weight standard and Invitrogen's SeeBlue® Plus2 pre-stained standard for band identification. As running buffer, we used the NuPAGE® MOPS SDS Running Buffer; electrophoresis was performed as follows:

1. 15 min at 100 V (max 100 mA)
2. 15 min at 150 V
3. 15-20 min at 200 V

Pre-cast NuPAGE® Novex® gel

Set-up procedure for the X Cell SureLock® Mini-Cell.

Electro-blotting

Following electrophoresis, the protein must be transferred from the electrophoresis gel to a membrane. The transfer method most commonly used for proteins is the electrophoretic transfer because of its speed and transfer efficiency. This method uses the electrophoretic mobility of proteins to transfer them from the gel to the membrane. Electrophoretic transfer of proteins involves placing a protein-containing polyacrylamide gel in direct contact with a piece to polyvinylidene fluoride (PVDF) membranes (Millipore, Billerica, MA, USA), and "sandwiching" this between two electrodes submerged in a conducting solution. When an electric field is applied, the proteins move out of the polyacrylamide gel and onto the surface of the membrane, where the proteins become tightly attached. The result is a membrane with a copy of the protein pattern that was originally in the polyacrylamide gel. Electro-transfer was performed in the NuPAGE transfer buffer plus methanol (Invitrogen) at 20 V for 60 minutes

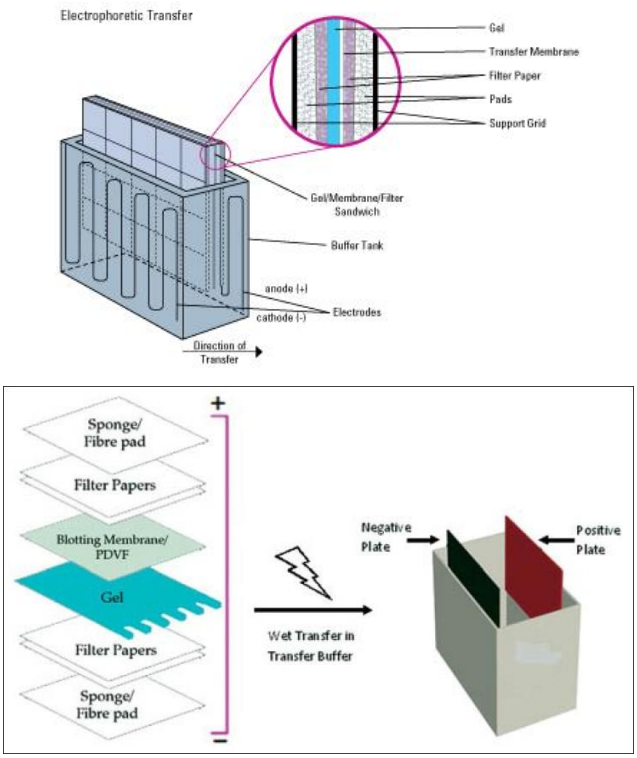

Western blot transfer apparatus and "sandwich" principle

Visualization of proteins in membranes: Ponceau Red

To check for success of transfer, the membrane was washed in PBS 1X, then a solution of Ponceau Red 0.1% in trichloroacetic acid 1% was added and incubated on an agitator for 5 min. The membrane was then de-stained completely by repeated washing in water and re-activated with methanol.

Blocking of the membrane

Blocking the membrane prevents non-specific background binding of the primary and/or secondary antibodies to the membrane. We incubated the membrane with a solution of non-fat milk at 6% for 1 hour at RT.

Immunostaining

Immunostaining was performed with the following specific primary antibodies incubated over night at 4 °C under agitation:

- NeuN mouse monoclonal antibody, clone A60 (Millipore), 1:1000
- MAP-2 Antibody (Cell Signaling), 1:1000

- Polyclonal Rabbit Anti-Glial fibrillary Acidic Protein (Dako, Glostrup, Denmark.), 1:3000
- Phospho-Histone H2A.X (Ser 139) Antibody (Cell Signaling), 1:500
- GAPDH (14C10) Rabbit mAb (Cell Signaling), 1:3000
- Drebrin A/E Polyclonal Antibody (Millipore), 1:5000
- Post Synaptic Density Protein 95 Antibody, PSD-95 (Millipore), 1:5000

The next day, membranes were washed three times in PBS and incubated for 2 hours at RT with the following suitable secondary antibodies:

- Anti-Rabbit IgG HRP-linked Antibody (Cell Signaling), 1:4000
- Goat Anti Mouse IgG (H & L) Peroxidase Conjugated Affinity Purified Antibody (Chemicon International), 1:5000

Incubation and washes were performed by using the SNAP i.d.® 2.0 Protein Detection System (Millipore).

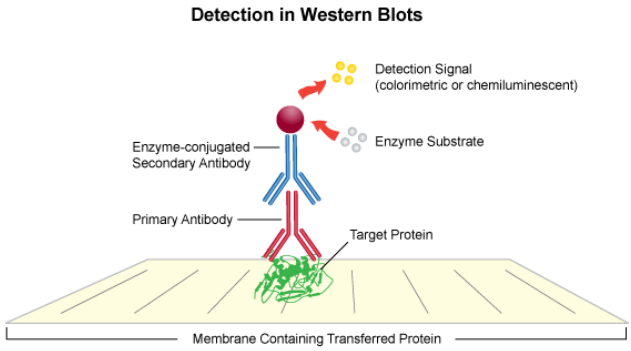

Diagram 2: *Illustration of detection in Western Blots.*

Schematic illustration of western blotting detection and SNAP i.d.® 2.0 Protein Detection System and holders

Immunodetection

Enhanced chemiluminescence (ECL) is the most commonly used method for routine protein detection in Western blots. ECL is based on the emission of light during the horse radish peroxides (HRP)- and hydrogen peroxide-catalyzed oxidation of luminol. The emitted light is then captured by a CCD camera, for qualitative or semi-quantitative analysis.

Our proteins were visualized using the enhanced chemiluminescence procedure with Immobilon Horseradish Peroxidase Substrate (Millipore) by mixing equal volumes (500µl) of Luminol Reagent and Peroxide Solution and incubating 5 minutes at RT.

Immune-reactive bands were acquired through the Image Quant 350 (GE Healthcare Life sciences, Buckinghamshire, UK) and quantified by densitometric analysis using the Quantity-One software (Bio-Rad Laboratories). Each density measure was normalized by using the corresponding GAPDH level as internal control.

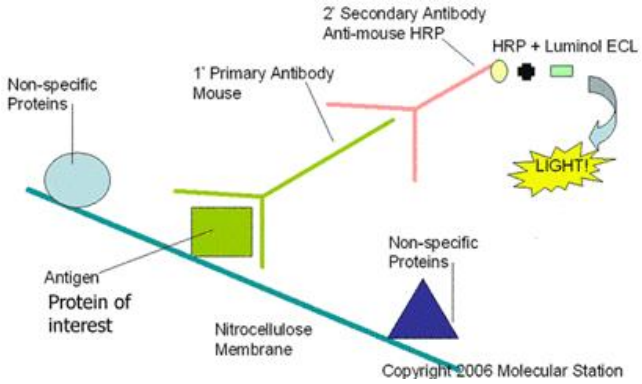

ECL immuno -detection principle

Dot blotting

Protein detection using the dot blot protocol is similar to western blotting in that both methods allow for the identification and analysis of proteins of interest. Dot blot methodology differs from traditional western blot techniques by not separating protein samples using electrophoresis. Sample proteins are instead spotted onto membranes and hybridized with an antibody probe. Semi-quantitative measurements can be made of the spots.

Equal aliquots (30 µg) of protein were applied to a nitrocellulose membrane (Millipore) and allowed to dry for 30 min at RT. After blocking with 6% non-fat dry milk for 1 h at RT, the membranes were incubated overnight at RT with the Anti-HNE-Michael Adducts, reduced rabbit pAb Calbiochem® (Millipore), 1:500, Anti-Nitrotyrosine Antibody, clone 2A8.2, Chemicon (Millipore) 1:500 followed by incubation with Anti-Rabbit IgG HRP-linked Antibody (Cell

Signaling), 1:4000 for 1 h at RT. Chemiluminescence was developed by Immobilon Horseradish Peroxidase Substrate (Millipore) and immunoreactive spots were quantified using Quantity-One software (Bio-Rad Laboratories).

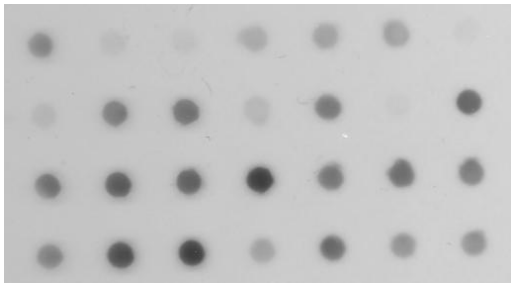

Example of a dot blotting immuno detection

Immunocytochemistry

For immunocytochemistry, cells were growth in sterile coverslips; the culture medium was then aspirated from each well and washed twice in PBS at RT. The cells were then fixed in 4% (v/v) paraformaldehyde in PBS for 20 minutes at RT. Before performing the immunodetection, especially if the target protein is intracellular expressed, it is very important to permeabilize the cells. This procedure was performed by incubating the samples for 30 min with PBS containing 0.25% Triton X-100. The cells were then washed in PBS three times for 5 min and incubated with non-fat milk (6%) for 1 hour at RT.
Cells were then were incubated over night at 4°C with the following primary antibodies:

- NeuN mouse monoclonal antibody, clone A60 (Millipore), 1:100
- MAP-2 Antibody (Cell Signaling), 1:100
- Polyclonal Rabbit Anti-Glial fibrillary Acidic Protein (Dako), 1:500
- Phospho-Histone H2A.X (Ser 139) Antibody (Cell Signaling), 1:50
- Anti-Drebrin A/E Antibody, Polyclonal Antibody (Millipore), 1:50
- Anti-Post Synaptic Density Protein 95 Antibody, PSD-95 (Millipore),1:50

The next day, the primary antibody solution was removed and the cells were washed three times in PBS, 5 min each in the dark. Then the cells were incubated with the suitable

secondary fluorescent antibody for 2 hours at RT in the dark and washed three times with PBS for 5 min each in the dark.

The following suitable fluorescent secondary antibodies were used:

- AlexaFluor 488 goat anti-mouse (Invitrogen), 1:200
- AlexaFluor 594 goat anti-rabbit (Invitrogen), 1:200

Image acquisition and analysis

Microscopic analysis was performed with a fluorescence microscope (Labophot-2, Nikon, Tokyo, Japan) connected to a CCD camera. Densitometric analyses on digitalized images were performed with the freely available ImageJ NIH software. Results were expressed in arbitrary units (AU).

Carbonyl residues assay

Carbonyl residues were spectrophotometrically determined by the method of Correa-Salde and Albesa (Correa-Salde and Albesa,). Harvested cells were lysed in radioimmunoprecipitation assay buffer (RIPA, 25mM Tris–HCl pH 7.6, 150mM NaCl, 1% NP-40, 1% sodium deoxycholate, 0.1% SDS) with 1% protease and phosphatase inhibitor Cocktail (Sigma–Aldrich)) and disrupted by sonication (Microson XL-2000; Misonix, Farmingdale, NY, USA). Lysates were clarified by centrifugation and supernatants collected at −20°C. Protein content was estimated by using the Bio-Rad DC protein assay kit (Bio-Rad, Segrate, Milan, Italy).

Cell lysates (0.25 ml) were treated for 1 h with 1 ml of 0.1% dinitrophenylhydrazine in 2 M HCl and precipitated with 10% trichloroacetic acid before being centrifuged 20 min at 10 000g. The pellets were then extracted with 1 ml of ethanol:ethyl acetate mixture (1:1) three times and then dissolved in 2 ml of 6 M guanidine HCl in 20 mM potassium phosphate buffer (PBS) pH 7.5. The solutions were incubated at 37 °C for 30 min and insoluble debris was removed by centrifugation. The absorbance was measured at 370 nm and carbonyl content was estimated using a molar absorption coefficient of 22,000 M-1 cm-1.

Detection of advanced glycation end products (AGEs)

AGEs determination was carried out in the culture media according to the method described by Musolino et al. (2012). The fluorescence intensity of culture media was measured

at 440 nm after excitation at 370 nm, using a fluorescence spectrophotometer (Multilabel Counter 1240 Victor 3, Perking Elmer, Waltham, MA, USA) at RT. Results were expressed as fluorescence intensity/mg of proteins.

Comet assay

The comet assay procedure was used to measure the level of strand breaks (SBs) in neuro-glial co-cultures at 15, 27 and 27 DIV treated with resveratrol 1 and 5 µM. Cells were counted and the vitality assessed by means of the Trypan Blue exclusion test. Twenty µl of cell suspension containing about 12500 cells, were then mixed with 75 µl of 0.7 % low-melting point agarose (maintained at 37°C) and kept for 10 min on ice in order to solidify the agarose. After this time, a further layer of agarose was added on each slide and left again to solidify for 10 min on ice. The slides were subsequently transferred to a lysis solution [1 % N-lauroyl-sarcosine, 2.5 mM NaCl, 100 mM Na2EDTA, 1% TritonX-100, 10% dimethylsulfoxide (DMSO)] and incubated 1 h at 4°C in order to obtain lysis of the cytoplasms and deproteinisation of the nuclei.

After this, the slides were subjected to electrophoresis. All the slides of the experiment were placed in an ice cold electrophoresis chamber (model GNA–200, Pharmacia, Milan, Italy) in an alkaline electrophoresis buffer (300 mM NaOH, 1mM Na2EDTA) for 40 min to allow DNA unwinding. At the end of this time, current was switched on and the electrophoresis was conducted for 30 min at 1.8 V/cm and 300 mA.

At the end of this time the slides were removed from the electrophoresis chamber and washed three times, 5 min each, with neutralisation buffer (40 mM tris-HCl, pH 7.4). Finally, the slides were stained with ethidium bromide (20 µg/ml) overnight and analysed on the following day. Microscopical analysis was carried out by means of a Labophot–2 microscope (Nikon, Japan) provided with epifluorescence and equipped with a rhodamine filter (excitation wavelength 546 nm; barrier 580 nm).

Each experimental point was run in duplicate and the images of 50 randomly chosen nuclei per slide were captured and analysed using the Comet Assay IV imaging software (Perceptive Instruments, UK). Data were expressed as % DNA in tail (i.e. the average % of DNA migrated in the tail over 100 nuclei).

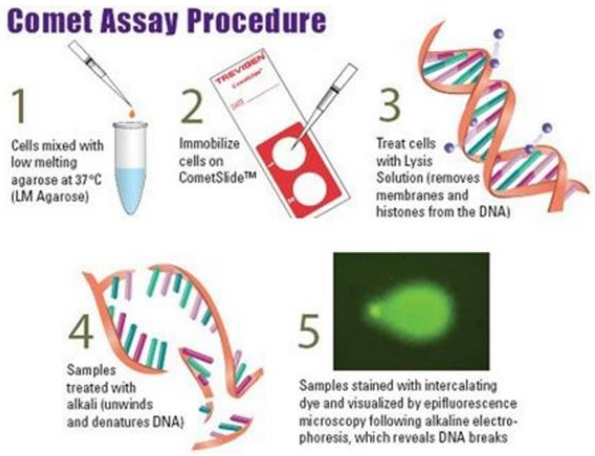

Schematic procedure for comet assay

Cytokine determination

Neuro-glial co-culture supernatants were collected at the different time points and stored at -80°C for cytokine determination by ELISA (MCYTOMAG-70K, MILLIPLEX MAP Mouse Cytokine/Chemokine Magnetic Bead Panel - Immunology Multiplex Assay, Merck-Millipore, Darmstadt, Germany).

PGE2

PGE2 levels were measured in the supernatants using an immunoenzymatic method (Cayman Chem, Mich., USA) according to the manufacturer's specifications, and expressed as ng of PGE2 per mL of supernatant.

Statistics

Statistical analyses were carried out using GRAPHPAD Prism 5 software. For in vitro analysis, as the number of observations did not allow the application of a test to evaluate normal distribution, we performed comparisons among groups using the non-parametric Mann-Whitney U test ($p<0.05$ was considered statistically significant). Data are means ± SE.

With the exception of the microarray data, results of *in vivo* experiments were analyzed using one-way ANOVA ($p<0.05$ was considered statistically significant). Data are means ± SE. The correlation among the different variables was analyzed by means of the Spearman non-parametric test.

Results

Experimental models *in vivo*

Animal growth and survival

During the six months treatment, the animals grew from an initial average weight of 27.31 ± 0.32 grams to a final of 46.21 ± 0.93 grams (means ± SE). No difference was observed among the growth and survival curves of the experimental groups.

Behavioral tests

Motor coordination: rota-rod test

As shown in Figure 1, young animals performed better than aged animals in L-EVOO group; in this group the ability to remain on the rota-rod was decreased at 18 months of age compared to young mice ($p<0.01$). However, mice in the H-EVOO group, showed a better performance as compared to L-EVOO, with a 74 % increase in the time spent on the rota-rod ($p<0.05$). Animals fed resveratrol, were able to remain on the rota-rod for the same time as young animals ($p<0.01$ vs L-EVOO).

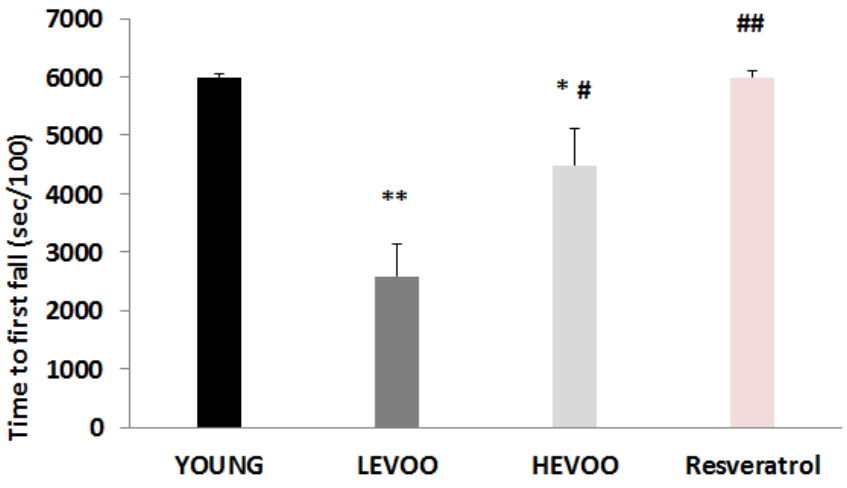

Figure 1. Performance in the rota-rod test of young mice, H-LEVOO, L-EVOO and resveratrol-fed old mice. The behavioral parameter was the latency to first fall (s/100), at a speed of 14 rpm, expressed as mean ± SE. Lower times correspond to worst performance, i.e. reduced motor coordination. * $p<0.05$ vs YOUNG; ** $p<0.01$ vs YOUNG; # $p<0.05$ vs L-EVOO; ## $p<0.01$ vs L-EVOO.

Contextual memory: step down test.

In the step-down inhibitory avoidance test, animals learn to suppress the exploratory tendency to avoid aversive stimuli. Figure 2 shows that the latency to step down on the electrified grid after the training phase, was strongly reduced in 18-month-old animals fed L-EVOO compared to young mice, indicating an impaired contextual memory. In the H-EVOO group, the latency was increased (+63%) compared with L-EVOO, although this difference did not reach a statistical significance. Resveratrol treated mice also performed better (+46%) than L-EVOO but this difference was also not significant.

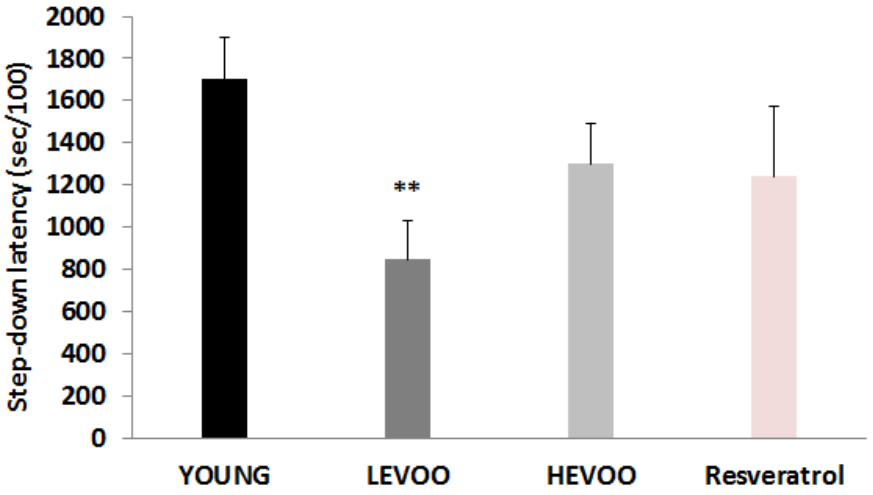

Figure 2. Performance in the step-down test of young mice, H-LEVOO, L-EVOO and resveratrol-fed old mice. The behavioral parameter was latency to step down (s/100), expressed as mean ± SE. Lower times correspond to bad performance, i.e. reduced memory. ** $p<0.01$ vs YOUNG.

Spatial memory: Morris water maze

The groups of aged mice did not differ from the young in their learning ability to find the platform in the Morris water maze during the 4 d of training (data not shown). However, in the probe test the H-EVOO animals spent longer time in the quadrant, sector, and platform position, and entered more times into the platform position, compared to the L-EVOO, reaching or even overtaking the young mice values (Table 1). Of these differences, only the one relative to time spent in platform sector reached significance ($p<0.05$). Resveratrol treated mice did not performed better than L-EVOO.

Table 1. Morris Water Maze Parameters: Probe Test

	Time spent in platform quadrant (sec)	Time spent in platform sector (sec)	Time spent in platform position (sec)	Number of entries in platform position
YOUNG	**10.03±1.29**	**5.13±0.81**	**0.45±0.21**	**0.9±0.2**
L-EVOO	**9.53±0.87**	**2.60±0.59 ***	**0.30±0.30**	**0.75±0.5**
H-EVOO	**12.50±0.96**	**6.27±0.39 #**	**0.38±0.32**	**1.33±0.51**
Resveratrol	**7,35±3.85**	**2,75±0.88 ***	**0,30±0.07**	**1.00±0.01**

Values are means of 5 animals ± SE. * p<0.05 vs young mice; # p<0.05 vs L-EVOO.

Anxiety-related behavior: light–dark box

The test is based on the natural aversion of mice to brightly illuminated areas and on their spontaneous exploratory behavior in novel environments. Old animals showed a decreased initial latency to pass into the dark compartment compared to young mice (11.50 *vs* 70.10 sec, p < 0.01), indicating an age-related increase in the level of anxiety (Figure 3). However, mice in the H-EVOO group showed an increased latency to step into the dark (+76%) as compared to L-EVOO (p<0.05). Resveratrol did not modify the level of anxiety compared to L-EVOO group (Figure 3).

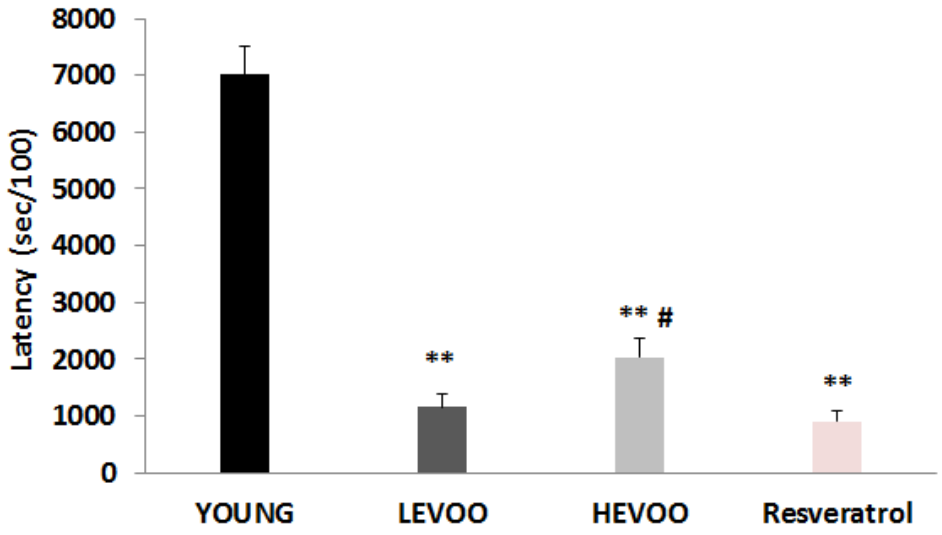

Figure 3. Performance in the light-dark test of young mice, H-LEVOO, L-EVOO and resveratrol-fed old mice. The behavioral parameter was latency to step into the dark compartment (s/100), expressed as mean ± SE. Lower times correspond to worse performance, i.e. increased anxiety. **p<0.01 vs YOUNG; # p<0.05 vs LEVOO.

Muscular function: grip strength test

Muscular strength was decreased in all aging mice, despite the dietary treatment, compared with young animals, declining from 4.2 ± 0.12 to 2.3 ± 0.15 g/body weight ($p<0.01$). The H-EVOO animals displayed only a slightly increased strength compared to L-EVOO (+7%,) (Figure 4).

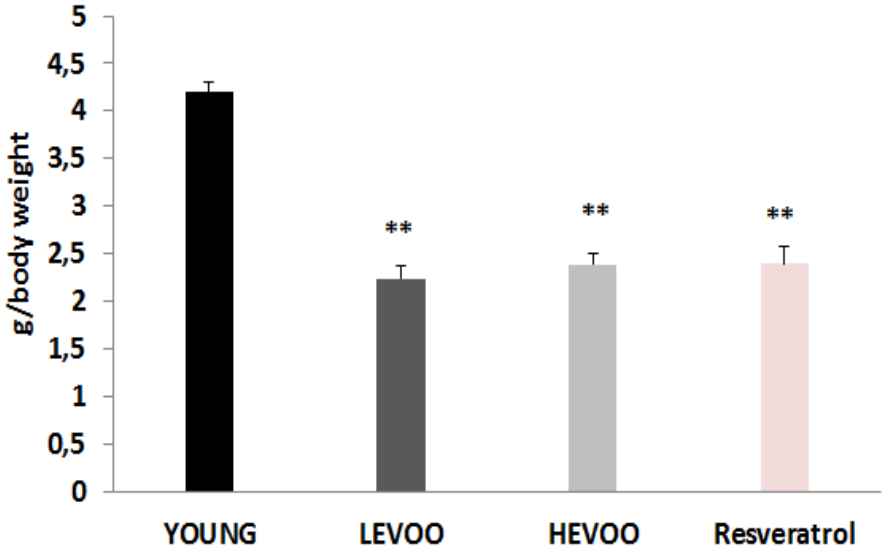

Figure 4. Mean peak of measured force (g)/ mouse body weight (g) expressed as mean ± SE, **p<0.01 vs YOUNG.

Effects on gene expression

To establish the diet-related changes in gene expression we first compared the gene expression profile in the cortex and cerebellum of H-EVOO mice receiving for 6 months diets containing extra virgin olive oil rich in phenols or of L-EVOO mice fed the same diet, for the same period, but containing olive oil deprived of polyphenol content, both compared to young mice. After 6 months of feeding we observed that, most of the age-related and diet-related changes of gene expression were restricted to the cerebral cortex. In fact, in the cerebellum, only a limited number of genes was differentially expressed in aged mice compared to the young animals, 4 % in the H-EVOO and nearly 2 % in L-EVOO group. In the cerebral cortex, on the contrary, a larger number of genes were significantly regulated: more than 20 % in the H-EVOO group and nearly 7 % in L-EVOO, compared to young mice. In this area, H-EVOO treatment significantly ($p<0.05$) modulated 3622 genes (1239 up-regulated with a fold change (FC) >2 and 2383 down-regulated with a FC <0.5 ; L-EVOO modulated a total of 1275 genes (393 up-regulated with a FC >2 and 882 down-regulated with a FC<0.5) (Figure 5).

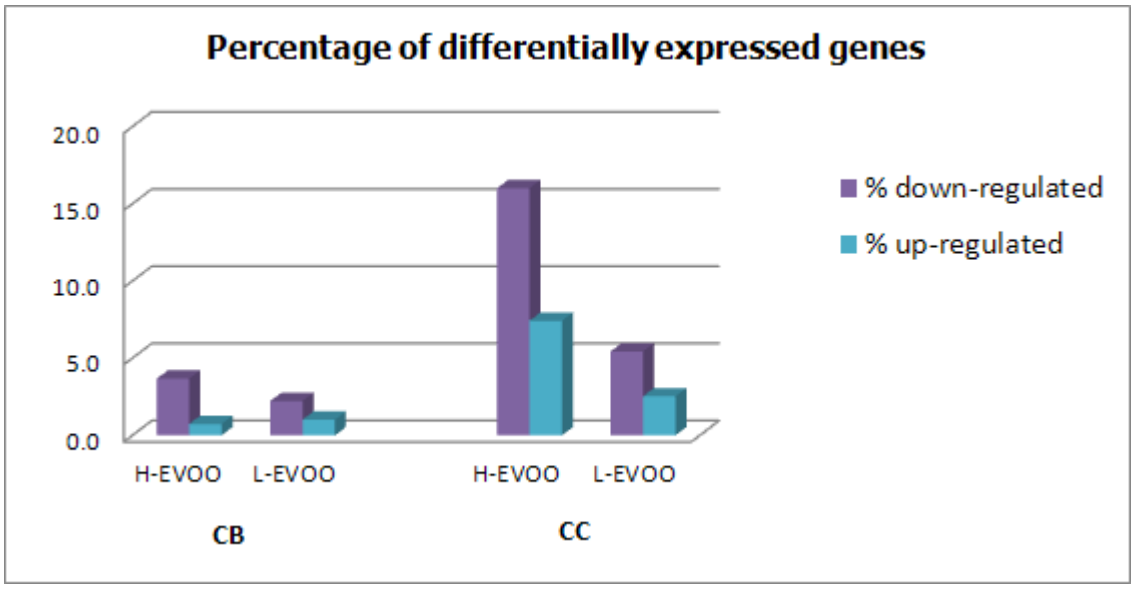

Figure 5. Percentage of significantly ($p<0.05$) up-regulated or down-regulated genes in the cerebellum and cerebral cortex of aged mice, comparing H-EVOO and L-EVOO to young mice.

Age-related gene expression changes and pathway analysis

In order to characterize the gene expression profile of aging mice, we compared the cortex gene expression profile of aging mice irrespective of the dietary treatment, to those of young mice. By this analysis, we found that several genes were significantly down-regulated ($p< 0.05$) by aging: ATP-binding cassette proteins, ATP-ases, calcium voltage dependent channels, calcium calmodulin kinases, ADP-ribosylation factors, carbonic anhydrases, catalase and superoxide dismutase 3, several cyclines, autophagy-related proteins and beclin-1, proteasome-related proteins and chaperonines, ionotropic and metabotropic glutamate receptors and several synaptotagmins, poly (ADP-ribose) polymerase family, member 1 (Parp1), mitogen-activated protein kinases (MAPKs), dentritic spine density protein drebrin, NOS3. The down-regulation of ephrin and fibroblast growth factor receptor, previously linked to motor deficits, was also found. Genes up–regulated by aging included caspase-1 and 4, DNA cross-link repair proteins, glyoxalase 1, superoxide dismutase 1, insulin-like growth factor 1, IL-1β, IL-21R and prostaglandin E synthase 3 (Ptges3), MAOA, phosphodiesterase 5A (Pde5a), peroxisome proliferator activated receptor alpha (Ppara) and peroxisome proliferative activated receptor, gamma (Ppargc1a), the purinergic receptor P2rx7, PTEN and NOS1 (Table 2).

Table 2. Significantly (p<0.05) modulated genes comparing old mice to young mice (FC=fold change).

GeneName	Description	FC ODL mice vs YOUNG
Abca14	ref|Mus musculus ATP-binding cassette, sub-family A (ABC1), member 14 (Abca14), mRNA [NM_026458]	0,46
Abcb9	ref|Mus musculus ATP-binding cassette, sub-family B (MDR/TAP), member 9 (Abcb9), mRNA [NM_019875]	0,47
Arf4	ref|Mus musculus ADP-ribosylation factor 4 (Arf4), mRNA [NM_007479]	0,35
Arfgap1	ref|Mus musculus ADP-ribosylation factor GTPase activating protein 1 (Arfgap1), transcript variant 1, mRNA [NM_145760]	0,47
Atg4b	ref|Mus musculus autophagy-related 4B (yeast) (Atg4b), mRNA [NM_174874]	0,48
Atg7	ref|Mus musculus autophagy-related 7 (yeast) (Atg7), mRNA [NM_028835]	0,28
Atp1a1	ref|Mus musculus ATPase, Na+/K+ transporting, alpha 1 polypeptide (Atp1a1), mRNA [NM_144900]	0,46
Atp2b2	ref|Mus musculus ATPase, Ca++ transporting, plasma membrane 2 (Atp2b2), transcript variant 1, mRNA [NM_009723]	0,41
Atp6ap1	ref|Mus musculus ATPase, H+ transporting, lysosomal accessory protein 1 (Atp6ap1), mRNA [NM_018794]	0,31
Atp6v1h	ref|Mus musculus ATPase, H+ transporting, lysosomal V1 subunit H (Atp6v1h), mRNA [NM_133826]	0,29
Atxn7	ref|Mus musculus ataxin 7 (Atxn7), mRNA [NM_139227]	6,10
Becn1	ref|Mus musculus beclin 1, autophagy related (Becn1), mRNA [NM_019584]	0,22
Cacna1a	ref|Mus musculus calcium channel, voltage-dependent, P/Q type, alpha 1A subunit (Cacna1a), mRNA [NM_007578]	0,34
Camk1	ref|Mus musculus calcium/calmodulin-dependent protein kinase I (Camk1), mRNA [NM_133926]	0,40
Car12	ref|Mus musculus carbonic anyhydrase 12 (Car12), mRNA [NM_178396]	0,48
Car2	ref|Mus musculus carbonic anhydrase 2 (Car2), mRNA [NM_009801]	0,39
Car4	ref|Mus musculus carbonic anhydrase 4 (Car4), mRNA [NM_007607]	0,43
Casp1	ref|Mus musculus caspase 1 (Casp1), mRNA [NM_009807]	3,31
Casp4	ref|Mus musculus caspase 4, apoptosis-related cysteine peptidase (Casp4), mRNA [NM_007609]	2,24
Cat	ref|Mus musculus catalase (Cat), mRNA [NM_009804]	0,26
Ccnd1	ref|Mus musculus cyclin D1 (Ccnd1), mRNA [NM_007631]	0,49
Ccnd2	ref|Mus musculus cyclin D2 (Ccnd2), mRNA [NM_009829]	0,50
Cct3	ref|Mus musculus chaperonin containing Tcp1, subunit 3	0,38

	(gamma) (Cct3), mRNA [NM_009836]	
Cct6a	ref|Mus musculus chaperonin containing Tcp1, subunit 6a (zeta) (Cct6a), mRNA [NM_009838]	0,25
Cct8	ref|Mus musculus chaperonin containing Tcp1, subunit 8 (theta) (Cct8), mRNA [NM_009840]	0,33
Dbn1	ref|Mus musculus drebrin 1 (Dbn1), transcript variant 1, mRNA [NM_001177371]	0,45
Dclre1c	ref|Mus musculus DNA cross-link repair 1C, PSO2 homolog (S. cerevisiae) (Dclre1c), transcript variant 2, mRNA [NM_175683]	4,92
Dnaja1	ref|Mus musculus DnaJ (Hsp40) homolog, subfamily A, member 1 (Dnaja1), transcript variant 1, mRNA [NM_001164671]	0,46
Dnajb2	ref|Mus musculus DnaJ (Hsp40) homolog, subfamily B, member 2 (Dnajb2), transcript variant 2, mRNA [NM_178055]	0,40
ENSMUST00000111939	ens|nitric oxide synthase 1, neuronal Gene [Source:MGI (curated);Acc:MGI:97360] [ENSMUST00000111939]	2,35
Epha2	ref|Mus musculus Eph receptor A2 (Epha2), mRNA [NM_010139]	0,40
Epha4	ref|Mus musculus Eph receptor A4 (Epha4), mRNA [NM_007936]	0,27
Eps15l1	ref|Mus musculus epidermal growth factor receptor pathway substrate 15-like 1 (Eps15l1), transcript variant 1, mRNA [NM_007944]	0,42
Eps8	ref|Mus musculus epidermal growth factor receptor pathway substrate 8 (Eps8), mRNA [NM_007945]	0,45
Fgfr1	ref|Mus musculus fibroblast growth factor receptor 1 (Fgfr1), transcript variant 1, mRNA [NM_010206]	0,45
Fgfr2	ref|Mus musculus fibroblast growth factor receptor 2 (Fgfr2), transcript variant 1, mRNA [NM_010207]	0,46
Glo1	ref|Mus musculus glyoxalase 1 (Glo1), transcript variant 1, mRNA [NM_025374]	2,42
Gria4	ref|Mus musculus glutamate receptor, ionotropic, AMPA4 (alpha 4) (Gria4), transcript variant 1, mRNA [NM_019691]	0,39
Grid1	ref|Mus musculus glutamate receptor, ionotropic, delta 1 (Grid1), mRNA [NM_008166]	0,41
Grin2b	ref|Mus musculus glutamate receptor, ionotropic, NMDA2B (epsilon 2) (Grin2b), mRNA [NM_008171]	0,48
Grm1	ref|Mus musculus glutamate receptor, metabotropic 1 (Grm1), transcript variant 2, mRNA [NM_001114333]	0,39
Grm1	ref|Mus musculus glutamate receptor, metabotropic 1 (Grm1), transcript variant 2, mRNA [NM_001114333]	0,33
Grm5	ref|Mus musculus glutamate receptor, metabotropic 5 (Grm5), transcript variant b, mRNA [NM_001143834]	0,47
Hdac2	ref|Mus musculus histone deacetylase 2 (Hdac2), mRNA [NM_008229]	0,17
Hdac8	ref|Mus musculus histone deacetylase 8 (Hdac8), mRNA [NM_027382]	0,48

Igf1	ref|Mus musculus insulin-like growth factor 1 (Igf1), transcript variant 2, mRNA [NM_184052]	2,51
Il1b	ref|Mus musculus interleukin 1 beta (Il1b), mRNA [NM_008361]	3,65
Il1rl1	ref|Mus musculus interleukin 1 receptor-like 1 (Il1rl1), transcript variant 1, mRNA [NM_001025602]	2,84
Il21r	ref|Mus musculus interleukin 21 receptor (Il21r), mRNA [NM_021887]	4,04
Insr	ref|Mus musculus insulin receptor (Insr), mRNA [NM_010568]	0,29
Kcna1	ref|Mus musculus potassium voltage-gated channel, shaker-related subfamily, member 1 (Kcna1), mRNA [NM_010595]	0,50
Kcnc1	ref|Mus musculus potassium voltage gated channel, Shaw-related subfamily, member 1 (Kcnc1), transcript variant B	0,39
Kcnh4	ref|Mus musculus potassium voltage-gated channel, subfamily H (eag-related), member 4 (Kcnh4), mRNA [NM_001081194]	0,44
Maoa	ref|Mus musculus monoamine oxidase A (Maoa), nuclear gene encoding mitochondrial protein, mRNA [NM_173740]	2,56
Map2k1	ref|Mus musculus mitogen-activated protein kinase kinase 1 (Map2k1), mRNA [NM_008927]	0,36
Map2k2	ref|Mus musculus mitogen-activated protein kinase kinase 2 (Map2k2), mRNA [NM_023138]	0,47
Map3k1	ref|Mus musculus mitogen-activated protein kinase kinase kinase 1 (Map3k1), mRNA [NM_011945]	2,15
Map3k1	ref|Mus musculus mitogen-activated protein kinase kinase kinase 1 (Map3k1), mRNA [NM_011945]	2,11
Ncam1	ref|Mus musculus neural cell adhesion molecule 1 (Ncam1), transcript variant 2, mRNA [NM_010875]	0,31
ND6	ens|mitochondrially encoded NADH dehydrogenase 6 Gene [Source:MGI Symbol;Acc:MGI:102495] [ENSMUST00000082419]	3,09
Negr1	ref|Mus musculus neuronal growth regulator 1 (Negr1), transcript variant 2, mRNA [NM_177274]	8,58
Nkap	ref|Mus musculus NFKB activating protein (Nkap), mRNA [NM_025937]	2,04
nos1	ens|nitric oxide synthase 1, neuronal Gene [Source:MGI (curated);Acc:MGI:97360] [ENSMUST00000111939]	2,35
Nos3	ref|Mus musculus nitric oxide synthase 3, endothelial cell (Nos3), mRNA [NM_008713]	0,43
Nqo1	ref|Mus musculus NAD(P)H dehydrogenase, quinone 1 (Nqo1), mRNA [NM_008706]	2,09
P2rx7	ref|Mus musculus purinergic receptor P2X, ligand-gated ion channel, 7 (P2rx7), transcript variant 4, mRNA [NM_001038887]	2,65
P2ry2	ref|Mus musculus purinergic receptor P2Y, G-protein coupled 2 (P2ry2), mRNA [NM_008773]	2,83
Parp1	ref|Mus musculus poly (ADP-ribose) polymerase family,	0,41

	member 1 (Parp1), mRNA [NM_007415]	
Pde5a	ref|Mus musculus phosphodiesterase 5A, cGMP-specific (Pde5a), mRNA [NM_153422]	9,26
Ppara	ref|Mus musculus peroxisome proliferator activated receptor alpha (Ppara), transcript variant 1, mRNA [NM_011144]	2,78
Ppargc1a	ref|Mus musculus peroxisome proliferative activated receptor, gamma, coactivator 1 alpha (Ppargc1a), transcript variant 1	2,45
Psma4	ref|Mus musculus proteasome (prosome, macropain) subunit, alpha type 4 (Psma4), mRNA [NM_011966]	0,50
Psmb7	ref|Mus musculus proteasome (prosome, macropain) subunit, beta type 7 (Psmb7), mRNA [NM_011187]	0,42
Pten	ref|Mus musculus phosphatase and tensin homolog (Pten), mRNA [NM_008960]	3,59
Ptgdr	ref|Mus musculus prostaglandin D receptor (Ptgdr), mRNA [NM_008962]	9,86
Ptges3	ref|Mus musculus prostaglandin E synthase 3 (cytosolic) (Ptges3), mRNA [NM_019766]	2,01
Sod1	ref|Mus musculus superoxide dismutase 1, soluble (Sod1), mRNA [NM_011434]	2,41
Sod3	ref|Mus musculus superoxide dismutase 3, extracellular (Sod3), mRNA [NM_011435]	0,48
Syt1	ref|Mus musculus synaptotagmin I (Syt1), mRNA [NM_009306]	0,49
Syt12	ref|Mus musculus synaptotagmin XII (Syt12), mRNA [NM_134164]	0,32

The functional analysis, performed using the GO-Elite software, identified the pathways associated to the genes found to be affected by aging such as the proteasome degradation and the senescence and autophagy processes (Table 3 and Figure 6).

Table 3. Significantly ($p<0.05$) modulated pathways comparing old mice to young mice

Gene-Set Name	Number Changed	Number Measured	Number in Gene-Set	PermuteP	gene symbols
Proteasome Degradation:WP519	15	33	62	0	H2afx|Nedd4|Psma4|Psma6|Psmb1|Psmb2|Psmb7|Psmd12|Psmd6|Psmd8|Psmd9|Rpn1|Ube2b|Ube2d3|Uchl1
Cytoplasmic Ribosomal Proteins:WP163	6	13	97	0.002	Rpl13a|Rpl24|Rpl31|Rps25|Rps6ka3|Rpsa
Senescence and Autophagy:WP1267	12	34	61	0	Becn1|Bmi1|Braf|Creg1|Hras1|Il6st|Irf7|Lamp2|Map1lc3a|Map2k1|Map2k3|Plat
Exercise-induced Circadian Regulation:WP544	9	26	47	0.004	Azin1|Gfra1|Hspa8|Psma4|Qk|Tob1|Tubb4|Ugp2|Zfr
Circadian Exercise:WP544	9	26	47	0.004	Azin1|Gfra1|Hspa8|Psma4|Qk|Tob1|Tubb4|Ugp2|Zfr
Keap1-Nrf2:WP1245	4	9	14	0.0125	Gclc|Nfe2l2|Nqo1|Pik3ca
Fatty Acid Beta Oxidation:WP1269	8	23	35	0.0055	Acadl|Acads|Acsl1|Acsl5|Acsl6|Dld|Lpl|Slc25a20

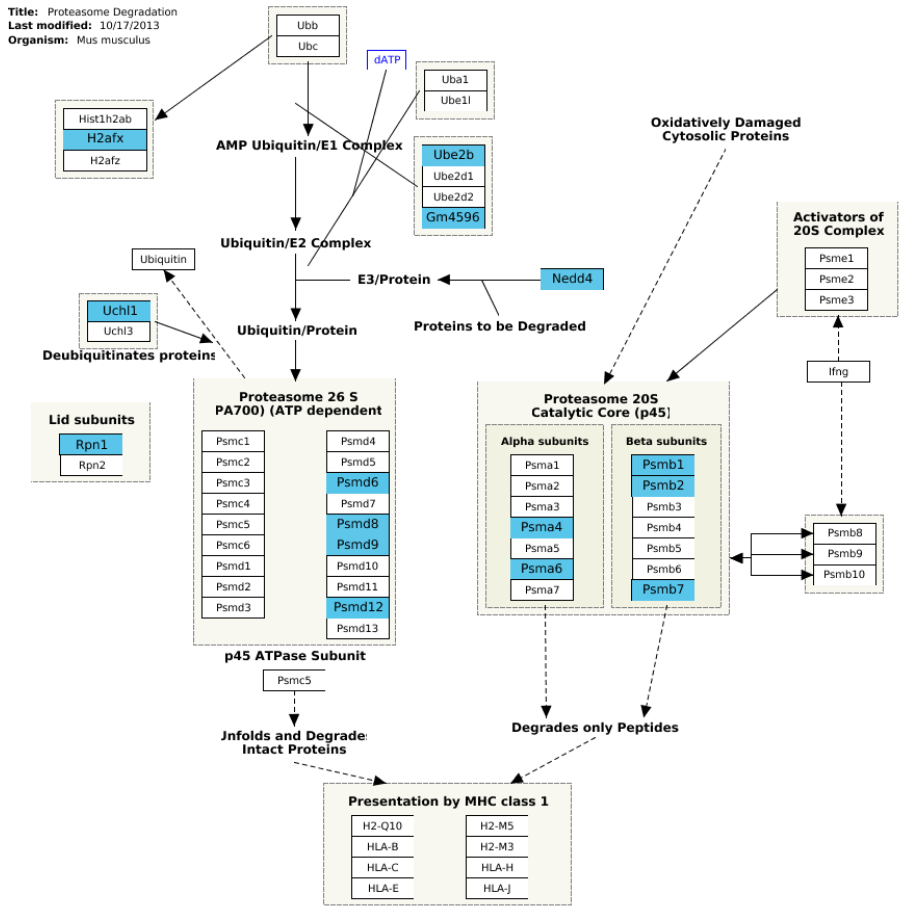

Figure 6. Pathway associated to the proteasome degradation. The genes reported in light-blue are those found down-regulated in the cortex of aged mice, compared to the young.

Diet-related gene expression changes

Unsupervised hierarchical clustering analysis was performed in order to evaluate the degree of changes in gene expression observed in H-EVOO and L-EVOO compared to the same brain area from young mice. The results are shown in the form of a tree whose branch lengths reflects the degree of similarities among the experimental groups; thus, similar expression profiles are closer to each other. This analysis distinguished different expression profiles in cortex and cerebellum but not between dietary groups (Figure 7).

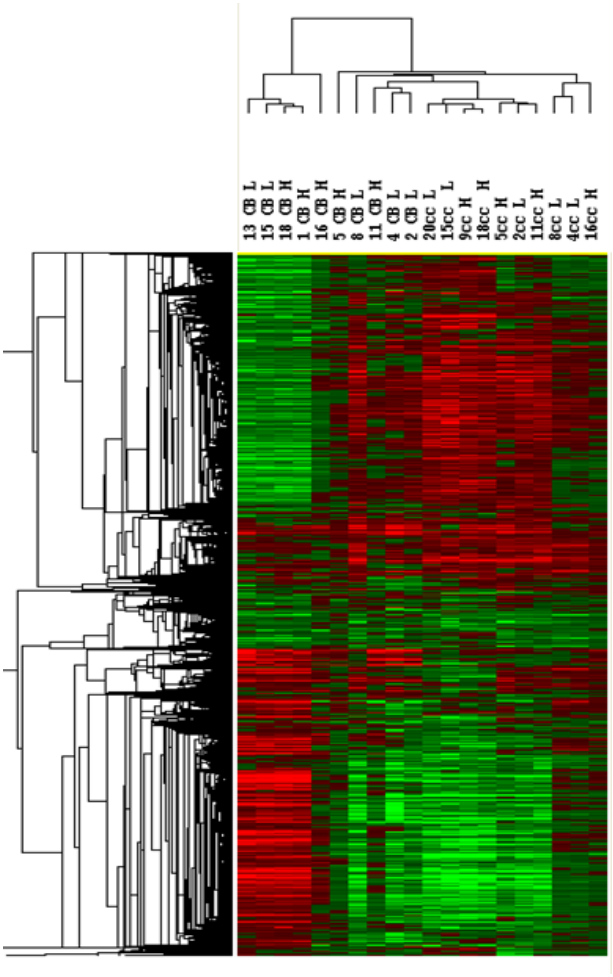

Figure 7. Hierarchical cluster analysis of the gene expression profiles of cortex and cerebellum from old mice (fed with H-LEVOO (H) or L-EVOO diet (L)), compared to the same brain area harvested from young mice. Each column represents a different mouse and each row a different gene; the color code indicates down-regulation (green) or up-regulation (red). CB= cerebellum; CC=cortex.

We next compared directly the gene expression changes observed in the cortex of H-EVOO and L-EVOO mice and found that 743 genes were differentially expressed ($p<0.05$) in these two groups. The most interesting data are summarized in Table 3; differences involve genes related to brain function such as Notch1, CREB regulated transcription coactivator 3 (Crtc3), several bone morphogenetic proteins (Bmp 4, 7 and 8), several members of forkhead box transcription factors (FOX), histamine receptor H4, insulin receptor (Insrr), glucagon-like peptide 1 receptor (Glp1r), nerve growth factor receptor (NGFR), histone acetyltransferase (Myst3), neuronal navigator (nav1), laminins and utrophins, all up-regulated in H-EVOO fed mice. Several heat shock proteins and ubiquitin conjugating enzymes were, on the contrary, down-regulated in H-EVOO group compared to L-EVOO (Table 4).

Table 4. List of differentially (p<0.05) expressed genes between H-EVOO (H) and L-EVOO (L) mice. FC=fold change

GeneName	Description	FC H vs L
Adrbk2	adrenergic receptor kinase, beta 2 (Adrbk2), transcript variant 2, mRNA	1,6
Aldh1a2	aldehyde dehydrogenase family 1, subfamily A2 (Aldh1a2), mRNA	2,1
Aldh4a1	aldehyde dehydrogenase 4 family, member A1 (Aldh4a1), mRNA	1,6
Apoc2	apolipoprotein C-II (Apoc2), mRNA	3,1
Apol10b	apolipoprotein L 10b (Apol10b), mRNA	1,7
Bmp4	bone morphogenetic protein 4 (Bmp4), mRNA	1,5
Bmp7	bone morphogenetic protein 7 (Bmp7), mRNA	1,6
Bmp8a	bone morphogenetic protein 8a (Bmp8a), mRNA	1,6
Cabp5	calcium binding protein 5 (Cabp5), mRNA	1,8
Chat	choline acetyltransferase (Chat), mRNA	1,4
Chrna2	cholinergic receptor, nicotinic, alpha polypeptide 2 (Chrna2), mRNA	1,2
Cnn1	calponin 1 (Cnn1), mRNA	2,2
Col18a1	collagen, type XVIII, alpha 1 (Col18a1), transcript variant 1, mRNA	1,8
Col1a2	collagen, type I, alpha 2 (Col1a2), mRNA [NM_007743]	1,6
Col25a1	collagen, type XXV, alpha 1 (Col25a1), transcript variant 1, mRNA	2,6
Cpped1	calcineurin-like phosphoesterase domain containing 1 (Cpped1), mRNA	0,9
Crtc3	CREB regulated transcription coactivator 3 (Crtc3), mRNA	1,6
Dnaja3	DnaJ (Hsp40) homolog, subfamily A, member 3 (Dnaja3), mRNA	0,8
Dnaja4	DnaJ (Hsp40) homolog, subfamily A, member 4 (Dnaja4), mRNA	0,3
Dnajc14	DnaJ (Hsp40) homolog, subfamily C, member 14 (Dnajc14), mRNA	0,7
Dnajc5	DnaJ (Hsp40) homolog, subfamily C, member 5 (Dnajc5), mRNA	0,8
Ercc3	excision repair cross-complementing rodent repair deficiency, complementation group 3 (Ercc3), mRNA	0,6
Ermn	ermin, ERM-like protein (Ermn), mRNA	2,8
Foxc1	forkhead box C1 (Foxc1), mRNA	1,8
Foxc2	forkhead box C2 (Foxc2), mRNA	2,1
Foxi1	forkhead box I1 (Foxi1), mRNA	1,6
Gab3	growth factor receptor bound protein 2-associated protein 3 (Gab3), mRNA	2,7
Gcm1	glial cells missing homolog 1 (Drosophila) (Gcm1), mRNA	3,4
Glp1r	glucagon-like peptide 1 receptor (Glp1r), mRNA	2,4
Grinl1a	glutamate receptor, ionotropic, N-methyl D-aspartate-like 1A (Grinl1a), transcript variant 1, mRNA	1,1
Grm1	glutamate receptor, metabotropic 1 (Grm1), transcript variant 2, mRNA	0,3
Gstm4	glutathione S-transferase, mu 4 (Gstm4), transcript variant 1, mRNA	0,6
Gstt2	glutathione S-transferase, theta 2 (Gstt2), mRNA	0,7
Hap1	huntingtin-associated protein 1 (Hap1), transcript variant 1, mRNA	1,5
Hip1	huntingtin interacting protein 1 (Hip1), mRNA	1,3
Hrh4	histamine receptor H4 (Hrh4), mRNA	1,6
Insrr	insulin receptor-related receptor (Insrr), mRNA	3,2

Kcnk10	potassium channel, subfamily K, member 10 (Kcnk10), mRNA	1,6
Kcnq2	potassium voltage-gated channel, subfamily Q, member 2 (Kcnq2), mRNA	1,5
Lama4	laminin, alpha 4 (Lama4), mRNA	1,6
Lamc3	laminin gamma 3 (Lamc3), mRNA	1,6
Lrp6	low density lipoprotein receptor-related protein 6 (Lrp6), mRNA	2,0
Mmp24	matrix metallopeptidase 24 (Mmp24), mRNA	2,1
Mpzl2	myelin protein zero-like 2 (Mpzl2), mRNA	2,0
Myst3	MYST histone acetyltransferase (monocytic leukemia) 3 (Myst3), mRNA	1,5
Nav1	neuron navigator 1 (Nav1), mRNA	1,5
Nfasc	neurofascin (Nfasc), transcript variant 1, mRNA	1,5
Ngfr	nerve growth factor receptor (TNFR superfamily, member 16) (Ngfr), mRNA	1,7
Notch1	Notch gene homolog 1 (Drosophila) (Notch1), mRNA	3,1
Npb	neuropeptide B (Npb), mRNA	1,2
Nr1i3	nuclear receptor subfamily 1, group I, member 3 (Nr1i3), mRNA	2,7
Ntsr2	neurotensin receptor 2 (Ntsr2), mRNA	1,4
Nutf2	nuclear transport factor 2 (Nutf2), mRNA	0,7
P2ry2	purinergic receptor P2Y, G-protein coupled 2 (P2ry2), mRNA	1,5
Pcolce	procollagen C-endopeptidase enhancer protein (Pcolce), mRNA	1,8
Pinx1	PIN2/TERF1 interacting, telomerase inhibitor 1 (Pinx1), mRNA	2,7
Slc13a4	solute carrier family 13/4 (sodium/sulfate symporters), (Slc13a4), mRNA	2,3
Slc16a7	solute carrier family 16/7 (monocarboxylic acid transport), (Slc16a7), mRNA	2,9
Slc6a13	solute carrier family 6/13 (GABA transporter,) (Slc6a13), mRNA	2,3
Tgm2	transglutaminase 2, C polypeptide (Tgm2), mRNA	2,0
Tgm3	transglutaminase 3, E polypeptide (Tgm3), mRNA	1,3
Tnnc2	troponin C2, fast (Tnnc2), mRNA	1,9
Tns1	tensin 1 (Tns1), mRNA	1,6
Tpm2	tropomyosin 2, beta (Tpm2), mRNA	1,9
Trpm1	transient receptor potential cation channel, (Trpm1), mRNA	3,0
Txndc11	thioredoxin domain containing 11 (Txndc11), mRNA	0,9
Txnl4a	thioredoxin-like 4A (Txnl4a), transcript variant 2, mRNA	0,8
Ube2q2	ubiquitin-conjugating enzyme E2Q (putative) 2 (Ube2q2), mRNA	0,7
Ube2ql1	ubiquitin-conjugating enzyme E2Q family-like 1 (Ube2ql1), mRNA	0,7
Ube2w	ubiquitin-conjugating enzyme E2W (putative) (Ube2w), mRNA	0,7
Utrn	utrophin (Utrn), mRNA	2,0

We next applied a more stringent criteria ($p<0.001$) for statistical analysis by using the class comparison tool of BRB-Array Tools, to identify differentially modulated genes in the cortex of H-EVOO treated mice compared to L-EVOO fed mice ($p<0.001$; Table 5, Figure 8). This analysis found out 53 differentially expressed genes among which again Notch1 (Figure 9), GABA transporter Slc6a13, sodium/sulfate symporters Slc13a4, anion exchanger Slc4a1ap,

transient receptor potential cation channel Trpm1, the apolipoprotein C-II (Apoc2), ermin and the aldehyde dehydrogenase 1 (Aldh1a2), up-regulated in the cortex of H-EVOO mice.

Only 2 genes were down-regulated in the cortex of H-EVOO mice: Xlr3b and Zbtb8a. On the contrary, this analysis did not find differentially expressed genes in the cerebellum.

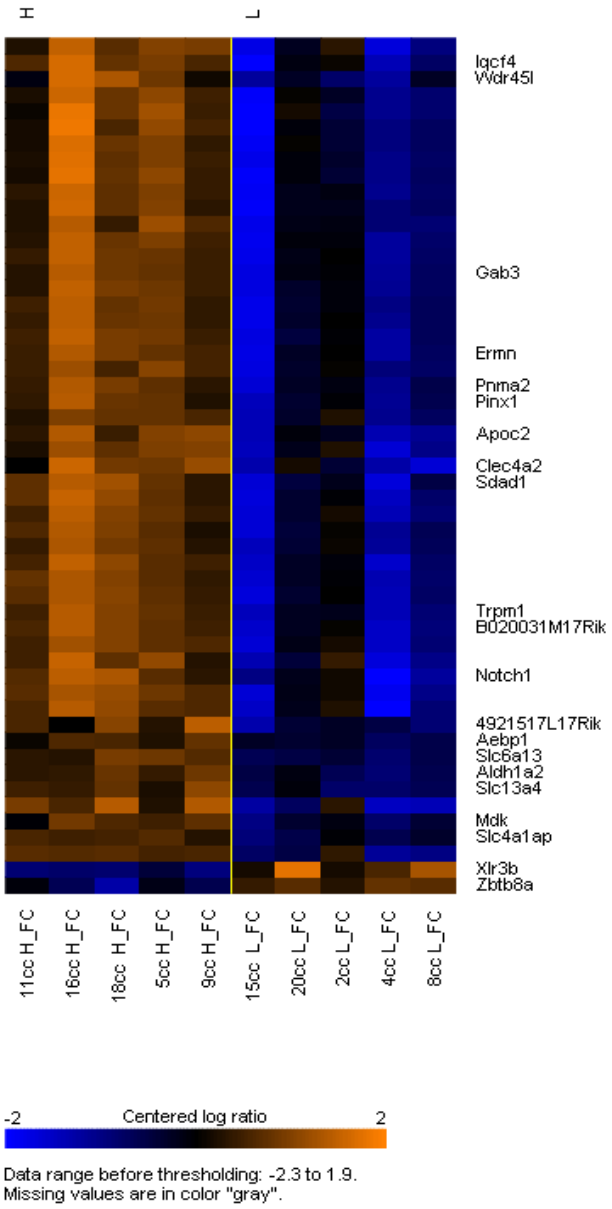

Figure 8. Heat map showing the expression profiles of the 53 genes differentially expressed in the cerebral cortex comparing H-LEVOO to L-EVOO-fed mice, by class comparison. Each column represents a different mouse and each row a different gene (gene name are on the right side when known, with empty spaces if unknown; for the detailed gene list see Table 2; the color code indicates down-regulation (blue) or up-regulation (brown).

Table 5. List of genes with known function found differentially expressed in mice cortex between H-EVOO and L-EVOO, as identified by class comparison analysis.

p-value	Geometric mean of ratios in H-EVOO mice	Geometric mean of ratios in L-EVOO	Gene Description
5.93e-05	2.86	1.24	ref|Mus musculus solute carrier family 6 (neurotransmitter transporter, GABA), member 13 (Slc6a13), mRNA [NM_144512]
0.0001264	3.88	1.23	ref|Mus musculus transient receptor potential cation channel, subfamily M, member 1 (Trpm1), transcript variant 2, mRNA [NM_001039104]
0.0001405	4.23	1.2	ref|Mus musculus SDA1 domain containing 1 (Sdad1), mRNA [NM_172713]
0.0001889	2.68	0.84	ref|Mus musculus apolipoprotein C-II (Apoc2), mRNA [NM_009695]
0.0002096	2.8	1.31	ref|Mus musculus aldehyde dehydrogenase family 1, subfamily A2 (Aldh1a2), mRNA [NM_009022]
0.0002367	2.9	1.29	ref|Mus musculus solute carrier family 13 (sodium/sulfate symporters), member 4 (Slc13a4), mRNA [NM_172892]
0.0002502	0.59	1.78	ref|Mus musculus X-linked lymphocyte-regulated 3B (Xlr3b), mRNA [NM_001081643]
0.0002507	4	1.24	ref|Mus musculus RIKEN cDNA B020031M17 gene (B020031M17Rik), mRNA [NM_001033769]
0.0002574	2.74	0.78	gb|Mus musculus 15 days embryo head cDNA, RIKEN full-length enriched library, clone:D930018D02 product:unclassifiable, full insert sequence. [AK142804]
0.0003568	3.17	1.04	ref|Mus musculus ermin, ERM-like protein (Ermn), mRNA [NM_029972]
0.0003842	4.66	1.33	ref|Mus musculus C-type lectin domain family 4, member a2 (Clec4a2), transcript variant 1, mRNA [NM_001170333]
0.0004007	3.37	1.19	ref|Mus musculus paraneoplastic antigen MA2 (Pnma2), mRNA [NM_175498]
0.0004336	2.05	1.03	ref|Mus musculus solute carrier family 4 (anion exchanger), member 1, adaptor protein (Slc4a1ap), mRNA [NM_009206]
0.0004503	3.22	1.19	ref|Mus musculus PIN2/TERF1 interacting, telomerase inhibitor 1 (Pinx1), mRNA [NM_028228]
0.0005997	1.98	0.83	ens|predicted gene 10304 Gene [Source:MGI Symbol;Acc:MGI:3642623] [ENSMUST00000094945]
0.000604	2.83	0.93	gb|Mus musculus 3 days neonate thymus cDNA, RIKEN full-length enriched library, clone:A630025K03 product:unclassifiable, full insert sequence. [AK080285]
0.0006247	4.35	1.3	ens|RIKEN cDNA 4932431P20 gene Gene [Source:MGI Symbol;Acc:MGI:2149781] [ENSMUST00000141713]
0.0006312	0.41	0.9	ref|Mus musculus zinc finger and BTB domain containing 8a (Zbtb8a), mRNA [NM_028603]

0.0006538	2.76	1.08	ref|Mus musculus RIKEN cDNA 4921517L17 gene (4921517L17Rik), mRNA [NM_027585]
0.000709	4.61	1.34	ref|Mus musculus Notch gene homolog 1 (Drosophila) (Notch1), mRNA [NM_008714]
0.0007352	1.73	0.82	ref|Mus musculus midkine (Mdk), transcript variant 1, mRNA [NM_010784]
0.0007373	3	1.05	ref|Mus musculus growth factor receptor bound protein 2-associated protein 3 (Gab3), mRNA [NM_181584]
0.0008548	1.98	0.57	ref|Mus musculus IQ motif containing F4 (Iqcf4), mRNA [NM_026090]
0.0009226	2.5	0.86	ref|Mus musculus Wdr45 like (Wdr45l), mRNA [NM_025793]
0.0009579	2.3	1.25	ref|Mus musculus AE binding protein 1 (Aebp1), mRNA [NM_009636]

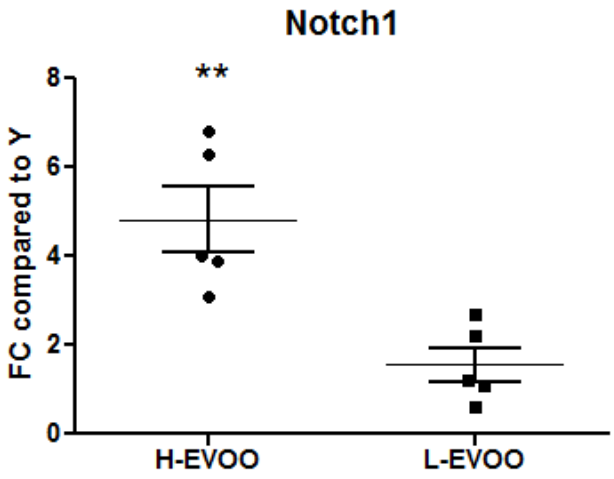

Figure 9. Notch1 gene expression (Fold change (FC) *vs* YOUNG), in H-EVOO and L-EVOO mice after 6 months of feeding. ** p<0.01

Pathway analysis

In order to evaluate the effects of H-EVOO feeding on biological processes, we also performed a biological pathway analysis by means of the Gene Set Enrichment Analysis (GSEA). This analysis measures the cumulative effect of small but consistent changes in gene expression within a biological pathway. This method is very sensitive, as it can show whether the overall regulation of a pathway is significantly changed even when gene expression changes of individual in a pathway are not. In fact, single-gene analysis may miss important effects on pathways and cellular processes, often affect sets of genes acting in concert.

After H-EVOO feeding GSEA found 2 significant variations of gene sets in cerebellum and 6 in cortex, out of 231 gene sets investigated (Table 6). In cerebellum, the beta-arrestin pathway was down-regulated, whereas genes associated with the MEF2D signaling were up-regulated by H-EVOO feeding. Among the six pathways differentially modulated in cortex, 31 genes were associated to the agrin-related postsynaptic differentiation (Figure 10) (such as laminin alpha 1, 2, 3 and 4, utrophin, agrin, and the cholinergic receptor muscarinic 1, mostly up-regulated in H-EVOO cortex) and 16 with the prion pathway (Figure 11). Interestingly, the receptor tyrosine kinase ephrinA4 pathway was also up-regulated in H-EVOO (Figure 12).

Table 6. Gene sets identified by GSEA, comparing H-EVOO to L-EVOO mice cortex and cerebellum.

Biocarta pathway description	Number of genes	LS permutation p-value	KS permutation p-value	Efron-Tibshirani's GSA test p-value
CORTEX				
m_agrin Pathway	31	0.00184	0.00482	< 0.005 (-)
m_ion Pathway	5	0.02692	0.06371	< 0.005 (-)
m_plc d Pathway	7	0.03082	0.29067	< 0.005 (-)
m_ephA4 Pathway	6	0.046	0.043	< 0.005 (+)
m_prion Pathway	16	0.07607	0.00429	0.03 (-)
m_cbl Pathway	10	0.148	0.16894	< 0.005 (-)
CEREBELLUM				
m_b Arrestin Pathway	14	0.05007	0.06687	< 0.005 (+)
m_mef2d Pathway	15	0.07862	0.00394	0.105 (-)

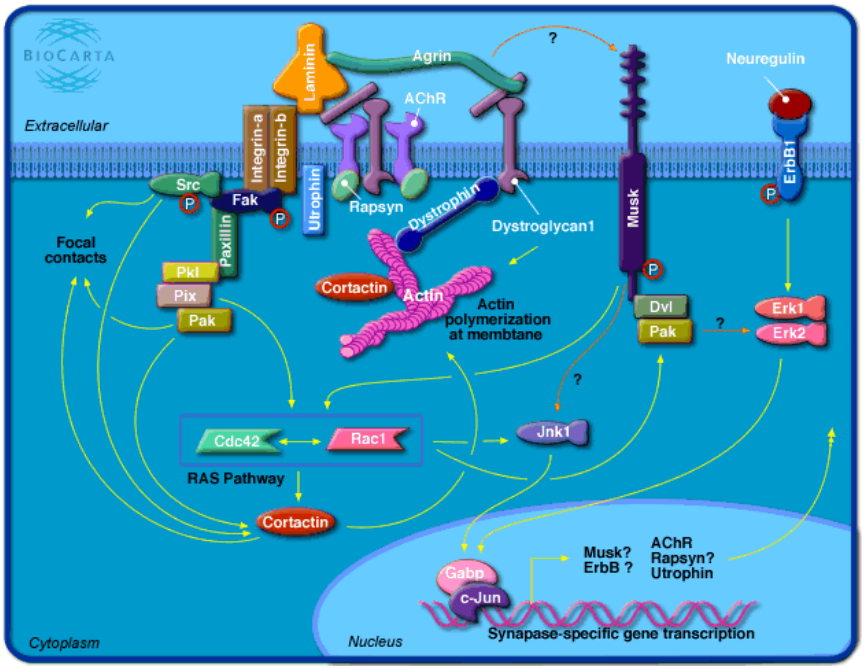

Figure 10. Agrin pathway from Biocarta

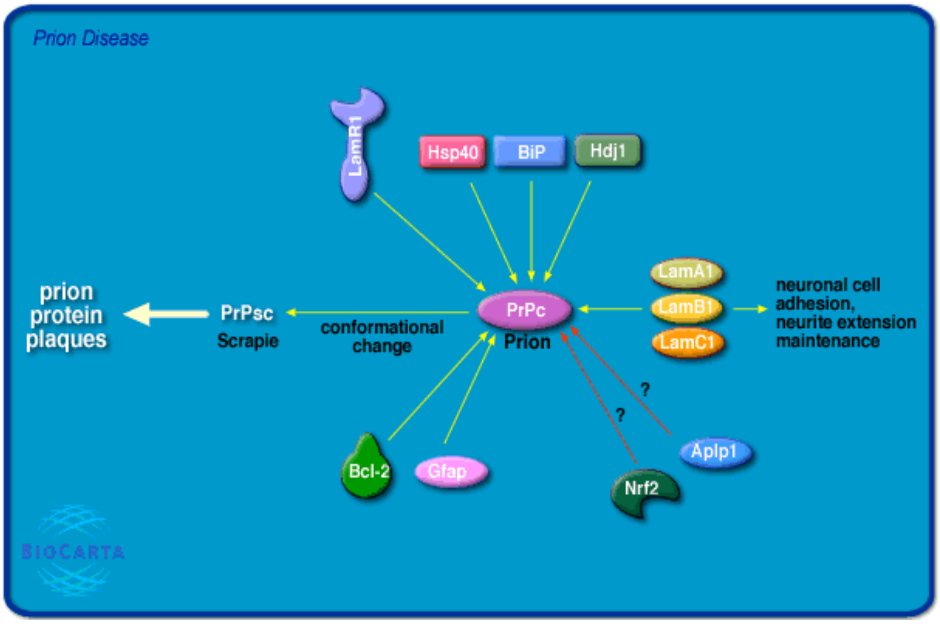

Figure 11. Prion pathway from Biocarta

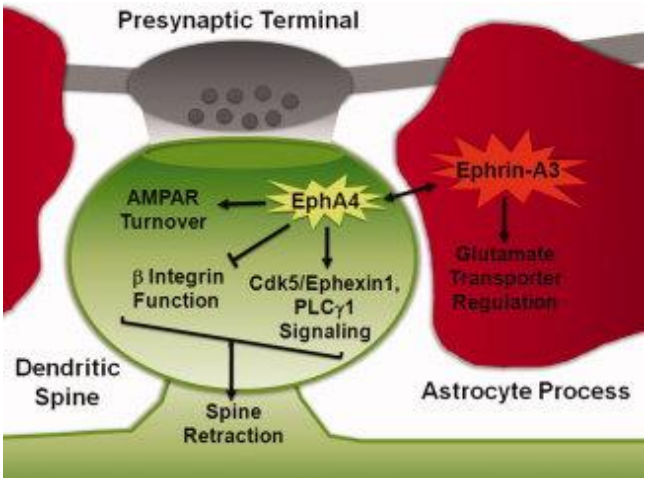

Figure 12. Ephrin (ephA4) pathway: neuron–astrocyte communication through EphA4 and ephrin-A3. EphA4 signaling causes spine retraction by reducing β integrin function and promoting signaling through Cdk5/Ephexin1 and PLCγ1. EphA4 activation also causes the turnover of the AMPA receptor (AMPAR) subunit GluR1 through the ubiquitin–proteasome pathway (Willi et al., 2012).

miRNA class comparison

The miRNA class comparison identified 9 gene sets differentially expressed comparing H-EVOO to L-EVOO mice; these were predicted to be targets of the same miRNA (Table 7); among these 9 miRNAs, miR-15a, miR-30e and miR-30b were significantly down-regulated in the cortex of H-EVOO mice (see below for details).

Table 7. Gene sets differentially expressed between the two groups of mice, computationally predicted to be targets of the same miRNA

MicroRNA Gene Sets	Number of genes	LS permutation p-value	KS permutation p-value	Efron-Tibshirani's GSA test p-value
hsa-miR-373	258	0.02515	0.12292	< 0.005 (-)
mmu-miR-30e_star	265	0.02625	0.04346	< 0.005 (+)
mmu-miR-15a_star	146	0.05358	0.08049	< 0.005 (+)
mmu-miR-30b_star	235	0.0679	0.06072	< 0.005 (-)
hsa-miR-612	297	0.08684	0.00183	0.215 (-)
mmu-miR-452	201	0.23091	0.11503	< 0.005 (+)
mmu-miR-15a	452	0.38261	0.63794	< 0.005 (+)
hsa-miR-614	224	0.59667	0.40016	< 0.005 (-)
mmu-miR-770-5p	305	0.70649	0.39922	< 0.005 (-)

miRNA expression profiles

We checked for the expression of 1203 different mouse miRNA types annotated in miRBase (release 18) including alternate miRNA products (denoted as −5p/−3p).

In order to understand potential contributions of miRNAs to gene expression changes in the mouse brain, we first examined their expression on samples of cerebral cortex harvested from aging mice treated for 6 or 12 months with olive oil rich or deprived of phenols.

Cluster analysis of these data revealed that after 12 months of treatment, the cortex miRNA expression profiles were very similar among groups; on the contrary, after 6 months, unsupervised clusterization was able to distinguish between mice fed extra virgin olive oil rich in phenols and mice fed the same extra-virgin olive oil deprived of phenols (Figure 13).

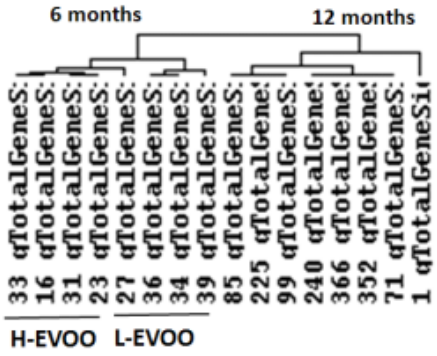

Figure 13. Hierarchical cluster dendrogram of miRNAs expression profiles of H-LEVOO and L-EVOO cortex harvested from mice fed for 6 or 12 months with the experimental diets.

We next extended our analysis to miRNA expression on samples of cerebral cortex harvested from aging mice treated with resveratrol for 6 months.

Unsupervised hierarchical cluster analysis was able to distinguish the expression profiles of the three experimental groups; one mouse in L-EVOO group had different profiles. Resveratrol-fed mice showed an overall miRNAs down regulation compared to young mice and clusterized next to H-EVOO fed mice (Figure 14).

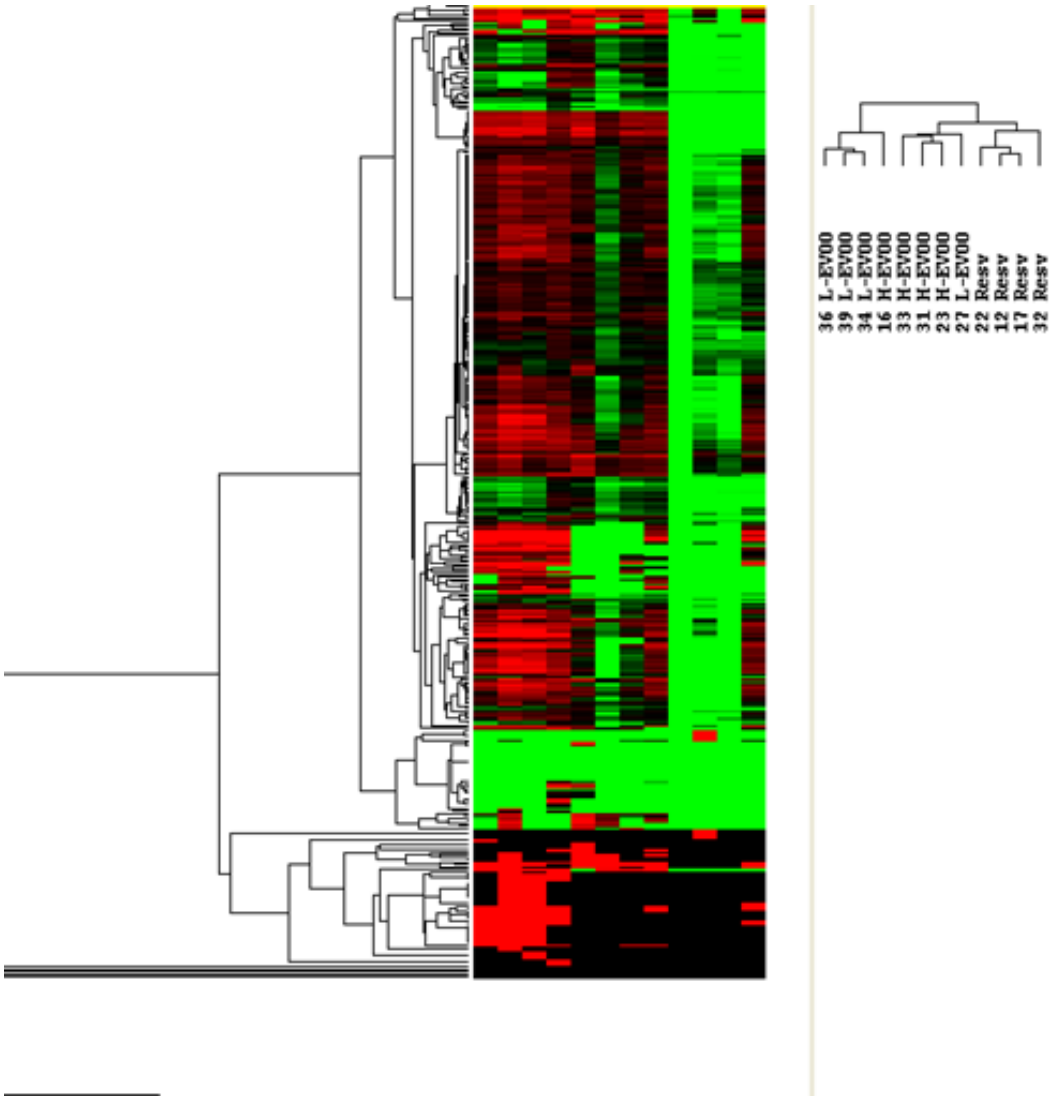

Figure 14. Hierarchical cluster dendrogram of miRNAs expression profiles in H-EVOO, L-EVOO and resveratrol in cortex harvested from mice fed 6 months the different experimental diets. Color code: red: up-regulated miRNAs; green: down-regulated miRNAs.

Age-related and diet-related miRNA expression changes

In order to characterize the miRNA expression profile of aging mice, we compared the miRNA expression profile of aging mice in H-EVOO, L-EVOO and resveratrol groups, to those of young mice.

Many miRNAs expressed in the brain demonstrated expression changes with age: 166 miRNAs were significantly ($p < 0.05$) modulated in L-EVOO group compared to young. While some miRNAs were down-regulated in expression with increased age, most of them demonstrated increased expression (151 up-regulated, 16 down-regulated). In H-EVOO group a very few miRNAs were significantly modulated compared to young mice: 10 miRNAs were

up-regulated and 7 were down-regulated compared to young mice. Resveratrol-treated mice showed 112 miRNAs differentially expressed compared to young mice, all down-regulated.

Venn diagram in figure 15 shows the degree of overlapping among the results obtained from the three experimental groups. miR-712-5p, miR-720, miR-134-5p were down-regulated in all three groups, thus were related to the aging process *per se*. H-EVOO and resveratrol treated mice showed miR-340-5p, miR-29b-3p and miR-29c-3p in common. H-EVOO and L-EVOO showed 8 miRNA in common. Interestingly, H-EVOO treatment was able to modulate only 2 miRNAs *per se*, confirming that these mice had similar miRNA profiles compared to young; on the contrary, resveratrol and L-EVOO group induced a larger number of modulated miRNAs.

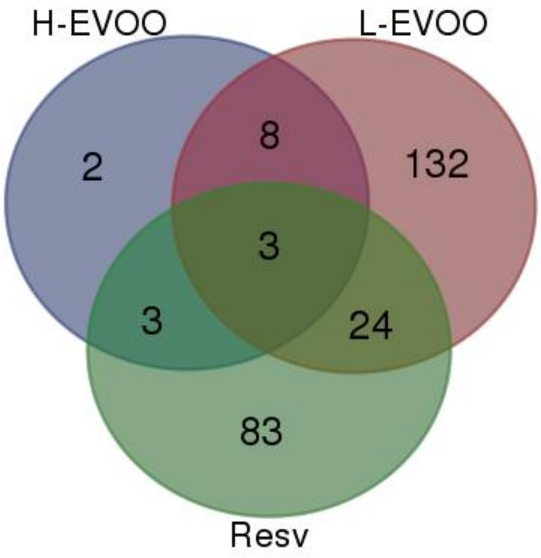

Figure 15. Venn diagram showing the degree of overlapping between the miRNA expression profile of H-EVOO, L-EVOO and resveratrol-treated mice compared to young mice.

Significance analysis of microarrays (SAM)

SAM analysis confirmed that the miRNAs expression profiles of the H-EVOO-fed mice cortex were very similar to those of young mice, whereas those of L-EVOO-fed mice and young animals were very different: only two miRNAs were in fact differentially expressed between these two groups of animals; on the contrary, 295 miRNAs were differentially expressed comparing the cortex of L-EVOO-fed mice and young mice. Moreover, we found 151 miRNA, all down-regulated, comparing the miRNA expression profiles of the cortex harvested from aged mice fed resveratrol and the cortex of young mice (Figure 16).

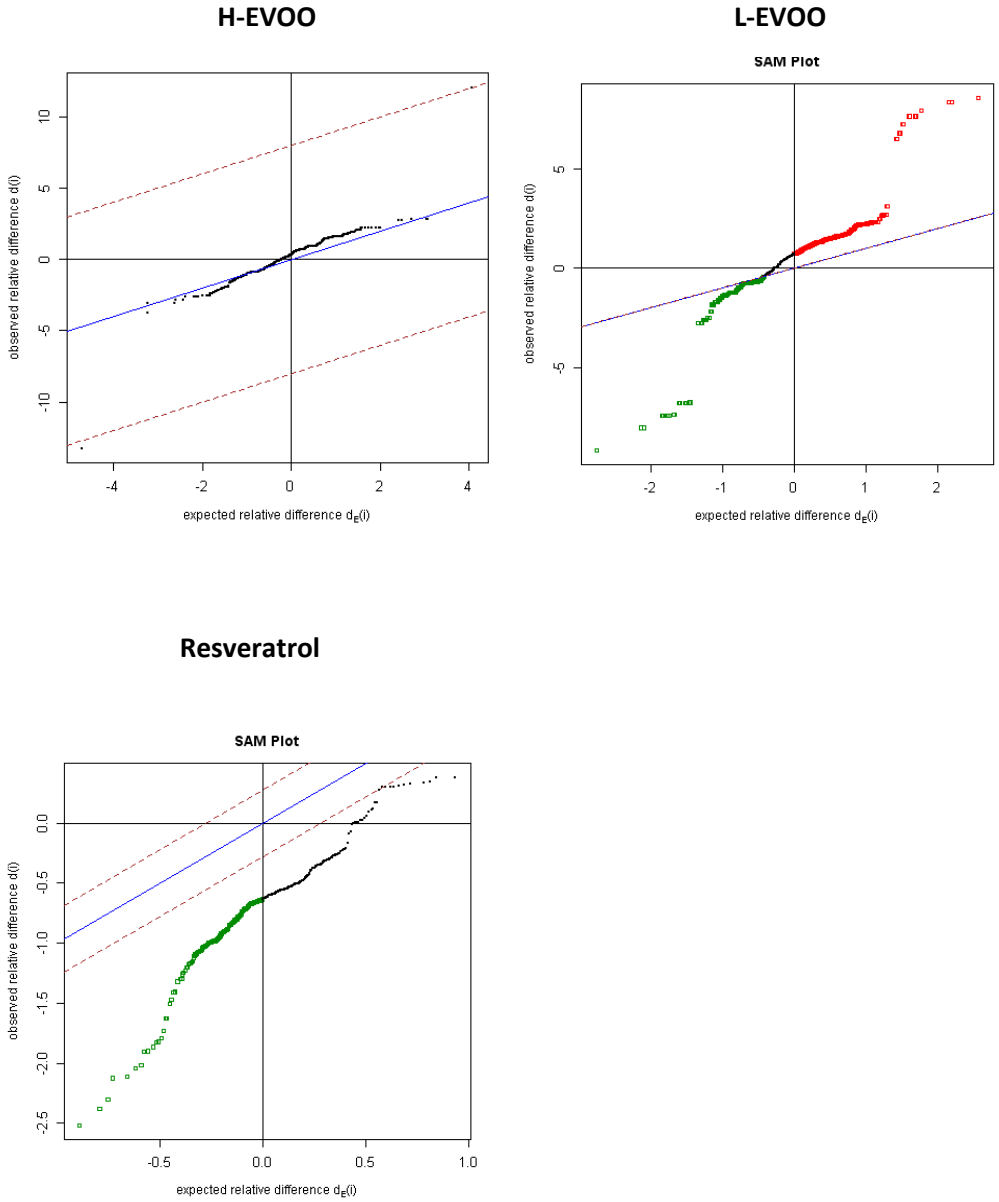

Figure 16. SAM plots: dots colored green or red represent genes up- or down-regulated, comparing old mice (H-EVOO, L-EVOO or Resveratrol group) to young animals. The remaining unchanged genes are shown in black.

In order to characterized the diet-related effects on miRNA expression profiles, we then compared directly the expression profile of H-EVOO to L-EVOO and those from resveratrol treated mice to L-EVOO.

Statistical analysis found 63 miRNA differentially modulated (out of the 1203 analyzed) by the two dietary treatments after 6 months (Table 8) and 289 miRNAs were differentially expressed ($p<0.05$) comparing resveratrol treated mice with L-EVOO. Interestingly, both H-

EVOO and resveratrol-associated miRNAs were down-regulated compared to L-EVOO and all miRNAs modulated in H-EVOO were also modulated in resveratrol treated mice (Figure 17).

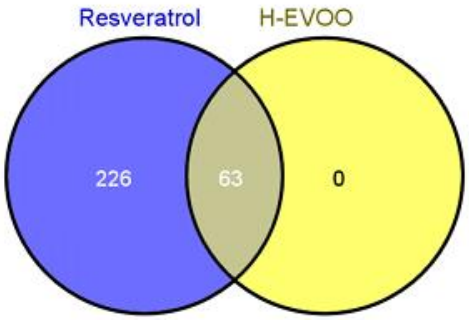

Figure 17. Venn diagram showing the degree of overlapping between miRNA expression profile in H-EVOO and resveratrol treated mice compared to L-EVOO.

Table 8. List of miRNAs differentially expressed in the cerebral cortex of mice fed with H-EVOO or L-EVOO diet for 6 months ($p<0.05$).

ID	Name	H-EVOO group mean (gTotalGeneSignal)	L-EVOO group mean (gTotalGeneSignal)
MIMAT0000665	mmu-miR-223-3p	**16.1**	**22.2**
MIMAT0012774	mmu-miR-664-3p	**12.9**	**20.5**
MIMAT0000674	mmu-miR-181c-5p	**48.7**	**78.4**
MIMAT0003127	mmu-miR-484	**11.8**	**21.4**
MIMAT0000219	mmu-miR-24-3p	**513.8**	**964.6**
MIMAT0000237	mmu-miR-204-5p	**85.7**	**161.8**
MIMAT0000533	mmu-miR-26a-5p	**1507.1**	**2846.2**
MIMAT0000378	mmu-miR-300-3p	**155.2**	**300.9**
MIMAT0000134	mmu-miR-124-3p	**3312.3**	**6565.2**
MIMAT0000514	mmu-miR-30c-5p	**341.9**	**683.7**
MIMAT0000142	mmu-miR-9-5p	**995.7**	**2010.9**
MIMAT0003453	mmu-miR-497-5p	**43.3**	**88.2**
MIMAT0000131	mmu-miR-99a-5p	**176.3**	**363.3**
MIMAT0000126	mmu-miR-27b-3p	**98.7**	**203.9**
MIMAT0000128	mmu-miR-30a-5p	**168.5**	**384.2**
MIMAT0003890	mmu-miR-551b-3p	**52.4**	**121.5**
MIMAT0000746	mmu-miR-381-3p	**23.6**	**55.0**
MIMAT0000130	mmu-miR-30b-5p	**136.8**	**326.5**
MIMAT0000537	mmu-miR-27a-3p	**66.5**	**164.3**
MIMAT0000536	mmu-miR-29c-3p	**440.9**	**1116.7**
MIMAT0003388	mmu-miR-376b-5p	**7.8**	**20.6**
MIMAT0000534	mmu-miR-26b-5p	**63.8**	**176.6**
MIMAT0001093	mmu-miR-411-3p	**11.4**	**34.8**
MIMAT0003456	mmu-miR-495-3p	**18.7**	**57.1**

MIMAT0000248	mmu-miR-30e-5p	**52.5**	**164.1**
MIMAT0000138	mmu-miR-126-3p	**90.3**	**283.4**
MIMAT0003185	mmu-miR-369-5p	**16.5**	**52.0**
MIMAT0001421	mmu-miR-434-5p	**11.0**	**35.2**
MIMAT0004747	mmu-miR-411-5p	**11.3**	**36.7**
MIMAT0000582	mmu-miR-338-3p	**68.8**	**223.4**
MIMAT0004745	mmu-miR-384-5p	**17.0**	**55.5**
MIMAT0000658	mmu-miR-210-3p	**6.2**	**20.3**
MIMAT0000743	mmu-miR-379-5p	**17.9**	**59.2**
MIMAT0000148	mmu-miR-136-5p	**21.1**	**71.0**
MIMAT0000527	mmu-miR-16-5p	**105.1**	**354.2**
MIMAT0000386	mmu-miR-106b-5p	**9.7**	**32.7**
MIMAT0000663	mmu-miR-218-5p	**130.9**	**443.5**
MIMAT0014943	mmu-miR-3107-5p	**3.6**	**12.4**
MIMAT0000526	mmu-miR-15a-5p	**33.9**	**122.8**
MIMAT0000149	mmu-miR-137-3p	**52.9**	**203.7**
MIMAT0000740	mmu-miR-376a-3p	**29.4**	**124.8**
MIMAT0004651	mmu-miR-340-5p	**7.4**	**31.4**
MIMAT0017080	mmu-miR-379-3p	**2.1**	**9.0**
MIMAT0000143	mmu-miR-9-3p	**141.6**	**628.7**
MIMAT0014805	mmu-miR-1843-5p	**2.6**	**11.7**
MIMAT0000225	mmu-miR-195-5p	**15.0**	**82.7**
MIMAT0000605	mmu-miR-350-3p	**5.1**	**30.4**
MIMAT0000151	mmu-miR-140-5p	**3.4**	**20.8**
MIMAT0003738	mmu-miR-496-3p	**2.4**	**14.9**
MIMAT0001092	mmu-miR-376b-3p	**7.3**	**52.1**
MIMAT0001632	mmu-miR-451	**9.2**	**67.8**
MIMAT0000612	mmu-miR-135b-5p	**3.9**	**29.1**
MIMAT0000529	mmu-miR-20a-5p	**2.1**	**15.5**
MIMAT0019349	mmu-miR-101c	**5.4**	**45.9**
MIMAT0000133	mmu-miR-101a-3p	**6.1**	**53.2**
MIMAT0000247	mmu-miR-143-3p	**1.6**	**15.7**
MIMAT0003732	mmu-miR-668-3p	**0.9**	**11.5**
MIMAT0000381	mmu-miR-34c-5p	**0.1**	**6.3**
MIMAT0000382	mmu-miR-34b-5p	**0.1**	**6.9**
MIMAT0000379	mmu-miR-301a-3p	**0.1**	**8.4**
MIMAT0000513	mmu-miR-19b-3p	**0.1**	**8.5**
MIMAT0000741	mmu-miR-377-3p	**0.1**	**9.0**
MIMAT0004537	mmu-miR-154-3p	**0.1**	**18.5**

Only 10 miRNA after 12 months of feeding were differentially modulated (Table 9). mir-136-5p was the only miRNA significantly modulated both after 6 and 12 months of treatment, but in an opposite way.

Table 9. List of miRNAs differentially expressed in the cerebral cortex of mice fed with H-EVOO or L-EVOO diet for 12 months (p<0.05).

ID	Name	H-EVOO group mean (gTotalGeneSignal)	L-EVOO group mean (gTotalGeneSignal)
MIMAT0000551	mmu-miR-323-3p	**6,4**	**0,1**
MIMAT0001419	mmu-miR-433-5p	**5,7**	**0,1**
MIMAT0004578	mmu-miR-300-5p	**9,9**	**1,0**
MIMAT0014814	mmu-miR-3058-3p	**25,1**	**4,7**
MIMAT0000678	mmu-miR-7b-5p	**27,7**	**5,8**
MIMAT0003450	mmu-miR-488-3p	**19,7**	**5,5**
MIMAT0000148	mmu-miR-136-5p	**137,1**	**45,5**
MIMAT0003741	mmu-miR-674-3p	**26,8**	**11,5**
MIMAT0022503	mmu-miR-344i	**33,4**	**17,0**
MIMAT0000144	mmu-miR-132-3p	**1575,6**	**940,7**

Among miRNAs low/not expressed in the cortex of young and H-EVOO and resveratrol treated mice and highly expressed in L-EVOO animals, we found miR-101, miR-30, miR-181, miR-29, miR-34, miR-124,mir-137, mir-484, mir-340, mir-9, mir-27 and mir-24 (Table 8).

Microarray results validation : qPCR

A few miRNAs were selected for validation by qRT-PCR. Microarray results were confirmed by qPCR of miR-101, miR-30, miR-124 and miR-34 (Table 7), using RNU1A as stable reference (Table 10).

Table 10. Expression of miR-101, miR-34a, miR-30a and miR-124, evaluated by microarray analysis (expressed as gTotalGeneSignal) and by q-PCR, using RNU1A as reference.

gTotalGeneSignal	**miR-101a**	**miR-34a**	**miR-30a**	**miR-124**
H-EVOO	6.11±6	285±53.7	168±48.8	3312±739.8
L-EVOO	*53.22±15.4	461±103.2	*384±71.8	*6565±907.8
young mice	0.10±0.0	212±73.0	185±22.8	4131±361.7
2−ΔΔCT				
H-EVOO	2.6±1	0.6±0.1	0.9±0.4	1.2±0.4
L-EVOO	*18.8±5.6	9±3.6	*12.1±3	*14.7±4.9
young mice	1.1±0.4	1.1±0.3	1.03±0.3	1.01±0.1

*p<0.05 vs. young and H-EVOO mice.

Target prediction analysis

We predicted targets for putative miRNAs using a combination of miRanda and TargetScan (see Methods). Many genes are predicted to be targeted multiple times by a single miRNA, and conversely, many miRNAs are predicted to target a single gene.

Mir-484 is predicted to target Crtc3 gene, mir-137-3p is predicted to target BMP7 gene, mir-27a-3p targets NGFR and GLP1R, mir-340 is predicted to target Aldh1a2 gene and actually, we found an inverse correlation with their target genes (Figure 18, 19, 20, 21).

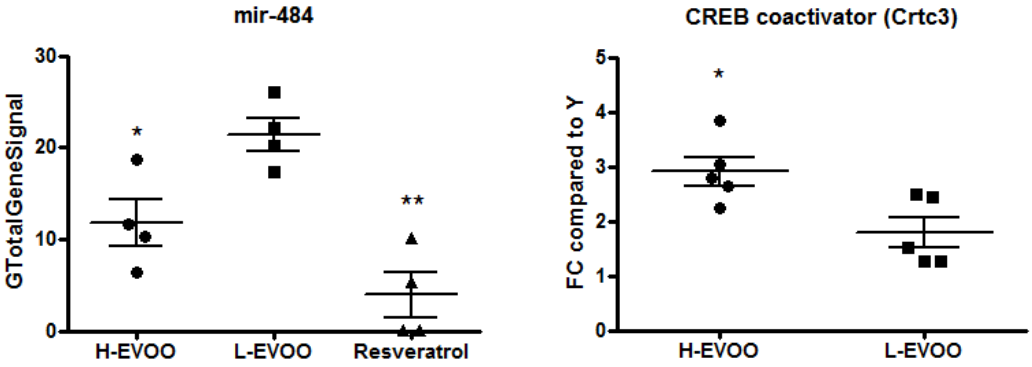

Figure 18. Mir-484 levels and those of its target CREB coactivator Crtc3.

An inverse, borderline significant correlation between mir-484 and the performances on the Morris water maze test for spatial memory was found when resveratrol treated mice were not included in the analysis (Figure 18a).

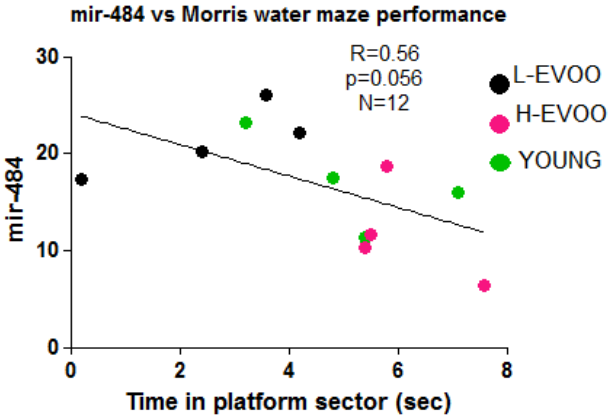

Figure 18a. Correlation between miR-484 and the results on Morris water maze test for spatial memory.

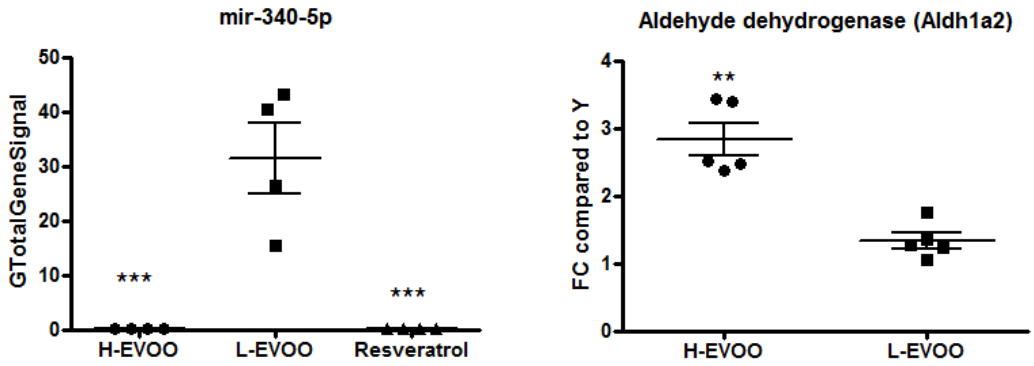

Figure 19. Mir-340-5p levels and those of its target Aldehyde dehydrogenase (Aldh1a2).

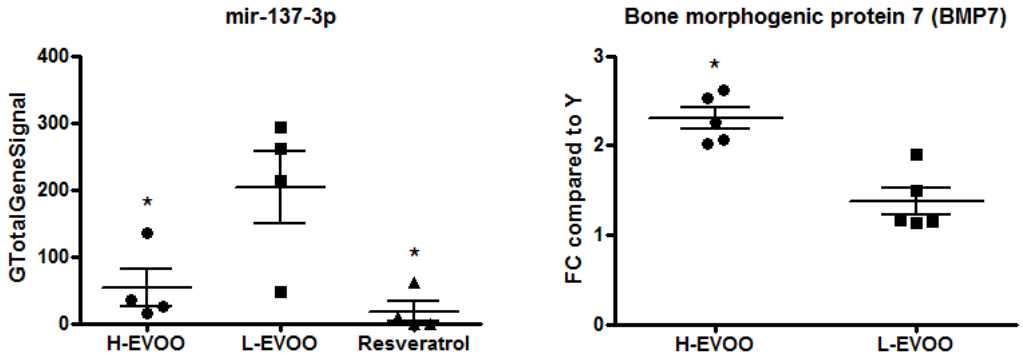

Figure 20. Mir-137-3p levels and those of its target Bone morphogenic protein 7 (BMP7).

Interestingly, an inverse correlation between mir-137-3p and motor coordination was found (Figure 20a).

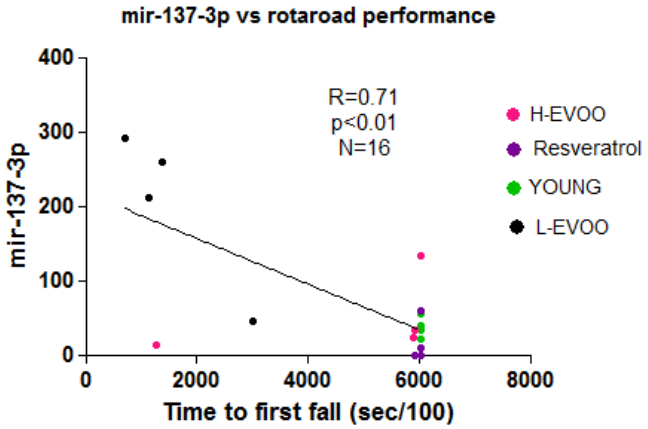

Figure 20a. Correlation between mir-137-3p expression levels and the results on rota-road for motor coordination.

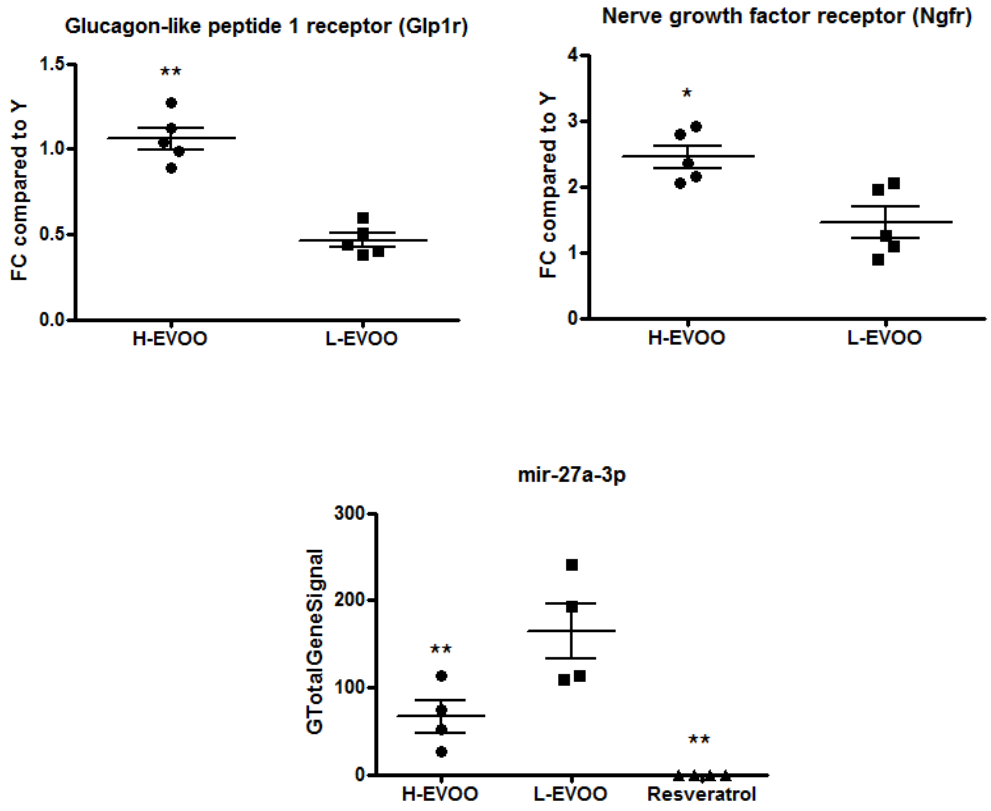

Figure 21. Mir-27a-3p levels and those of its targets Glucagon-like peptide-1 receptor (Glp1r) and nerve growth factor receptor (NGFR).

Mir-27a-3p levels were inversely correlated to the results of rota-rod performances of all mice groups and to those of light-dark box for anxiety when considering only aging mice in L-EVOO and H-EVOO group (Figure 21a).

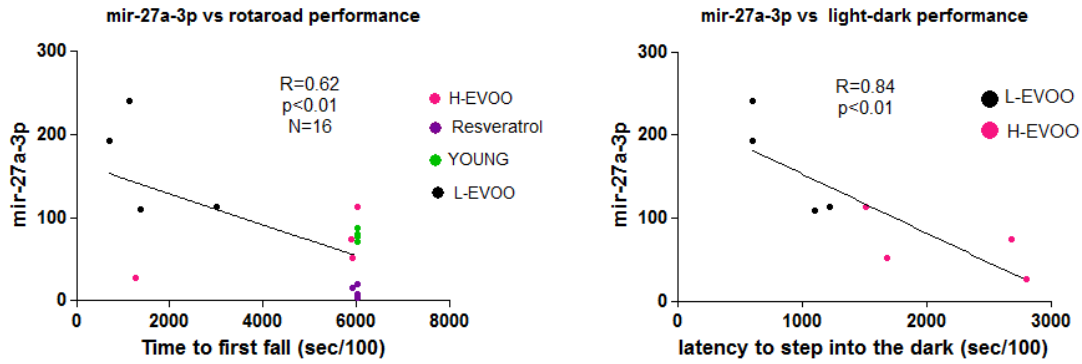

Figure 21a. Correlation between miR-27a-3p the results on behavioural tests (rotaroad for motor coordination, light-dark for anxiety).

miR-30c-b/5p and miR-34a-b-c/5p and mir-124 are predicted to target Notch1 gene and, indeed, their expression was inversely correlated with Notch1 expression (Figure 22).

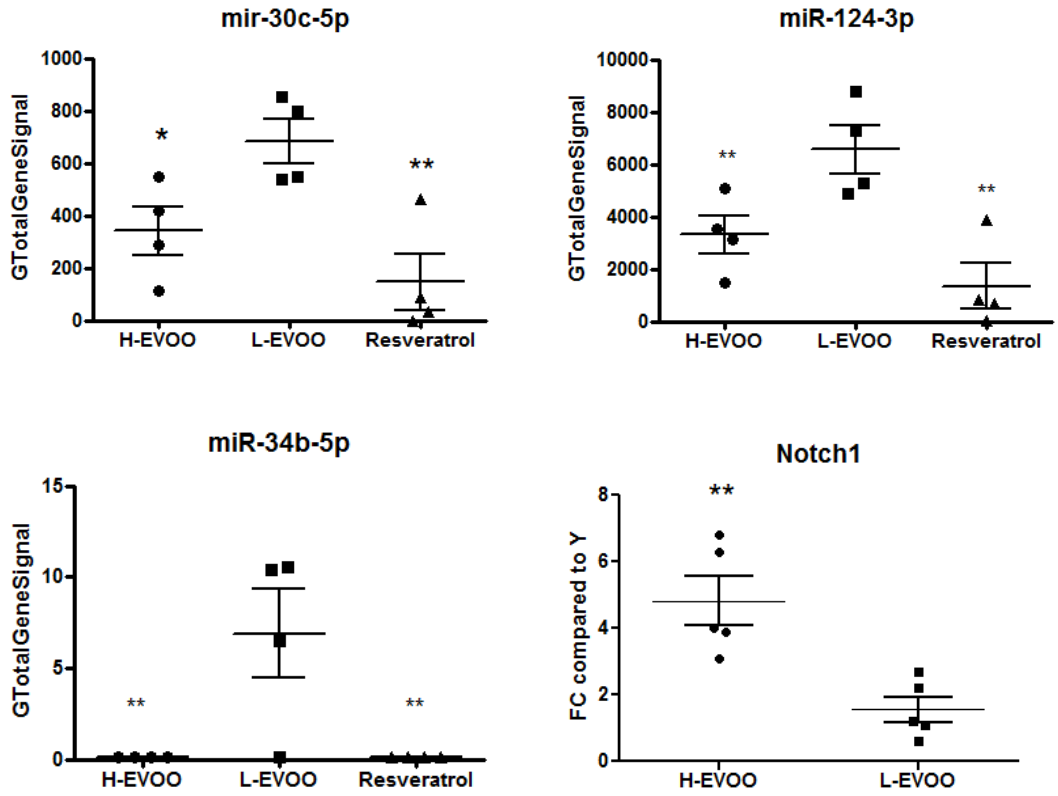

Figure 22. miR-30c-5p, mir-124-3p and miR-34a-5p expression levels and those of their predicted target Notch1 gene.

We also observed a significant correlation between rota-rod performances of all mice and the cortex miR-30c-5p expression ($p<0.05$), a borderline correlation between mir-34a-5p and step-down performances only in aging mice ($p=0.067$) and a significant correlation ($p<0.01$) between mir-30a-5p and light dark box performances in aging mice in H-EVOO and L-EVOO groups. mir-124 is also predicted to target CREB1, and a borderline significant correlation between mir-124-3p and performances in the Morris water maze was found. The correlation between mir-124-3p and the performances in the light-dark box was highly significant in H-EVOO and L-EVOO groups (Figure 22a).

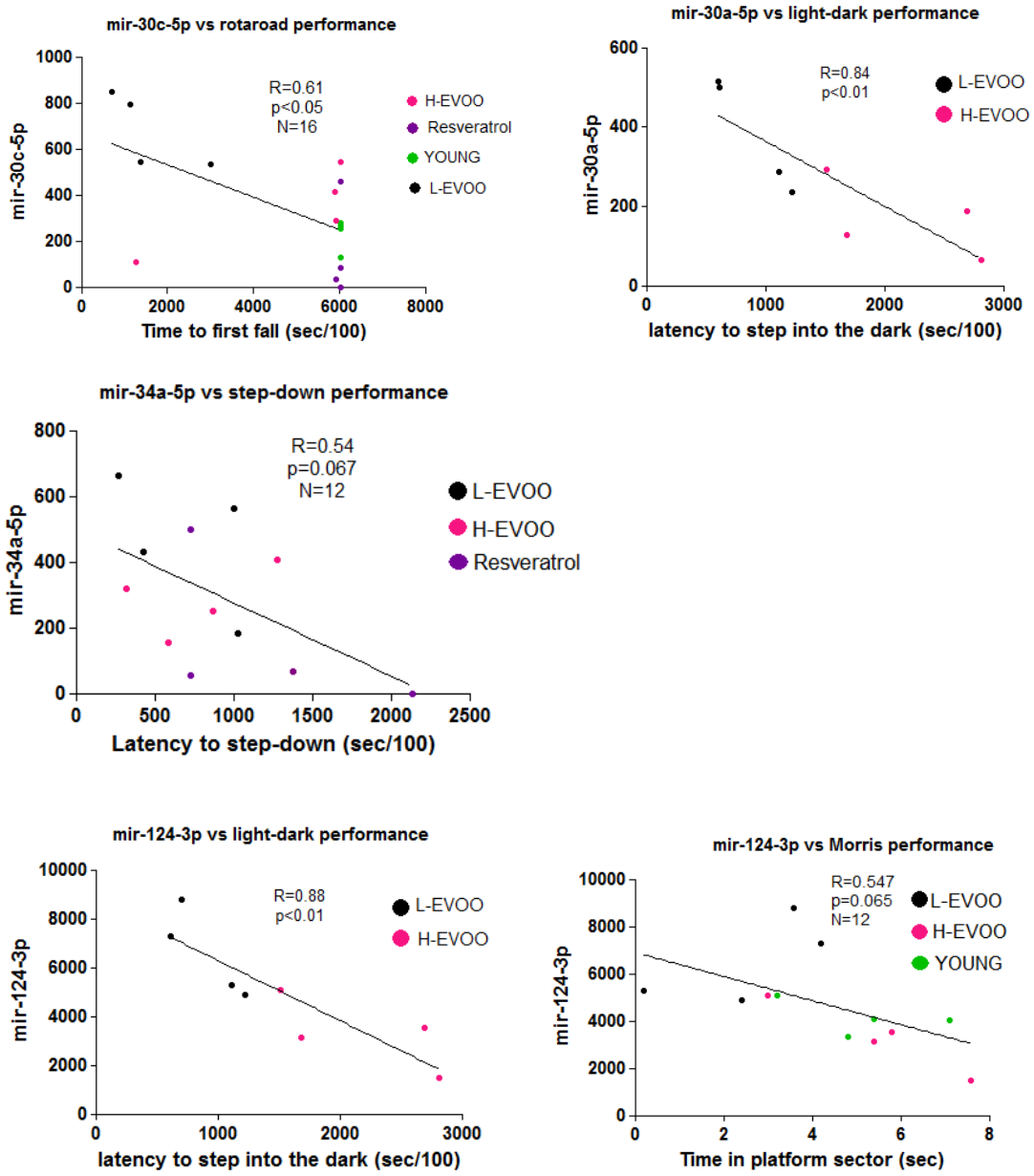

Figure 22a. Correlation between miR-30c-5p, mir-124-3p and miR-34a-5p expression levels and the results on behavioural tests (rotaroad for motor coordination, step-down for contextual memory, light-dark for anxiety and Morris water maze for spatial memory).

Targeted Pathways of miRNAs

To further elucidate the possible functional relevance of age and diet affected miRNAs, we next looked for significantly overrepresented KEGG (Kyoto Encyclopedia of Genes and Genomes) pathways among the predicted target genes of miRNAs. The KEGG pathway

database contains information on molecular interactions in known metabolic and regulatory pathways and allows functional characterization of an input gene list.

By means of DIANA-miRPath v2.0 analysis we examined the collective targets of up- and down-regulated miRNA to consider cooperative targeting of pathways by multiple co-expressed miRNAs. We found 39 significantly targeted KEGG pathways as significantly enriched ($p<0.01$) for the 63 miRNA group targets. As is seen in Table 7, many of the identified pathways are categorized under biological processes connected with central functions such as neurotrophin signaling, axon guidance pathway, mTOR signaling pathway, long-term potentiation and depression, insulin signaling, protein processing, dopamine and glutamate signaling (Table 11).

Indeed, many key genes implicated in these pathways are predicted to be targeted by multiple miRNAs that are differentially expressed between L-EVOO and H-EVOO. Among all, mir-27, mir-181, mir-24, mir-124, mir-29, mir-30, mir-34 and mir-101 are involved in the modulation of most of the above mentioned pathways.

Table 11. Pathways enriched with gene targets of miRNAs differentially expressed in the cortex of HEVOO compared to L-EVOO fed mice. p-value depicts the probability that the examined pathway is significantly enriched with gene targets of at least one selected miRNA.

KEGG pathway	p-value	genes	miRNAs
ECM-receptor interaction	<1e-16	17	2
Mucin type O-Glycan biosynthesis	<1e-16	15	11
Endocytosis	<1e-16	74	11
Glycosphingolipid biosynthesis	<1e-16	10	12
Regulation of actin cytoskeleton	<1e-16	79	13
VEGF signaling pathway	<1e-16	31	14
mTOR signaling pathway	<1e-16	35	15
Long-term potentiation	<1e-16	39	15
Insulin signaling pathway	<1e-16	56	15
Ubiquitin mediated proteolysis	<1e-16	63	16
Wnt signaling pathway	<1e-16	72	16
TGF-beta signaling pathway	<1e-16	46	16
Focal adhesion	<1e-16	106	17
Neurotrophin signaling pathway	<1e-16	62	17
PI3K-Akt signaling pathway	<1e-16	149	18
Glioma	<1e-16	36	18
MAPK signaling pathway	<1e-16	124	20
ErbB signaling pathway	<1e-16	53	20
Axon guidance	<1e-16	82	23
Protein processing in endoplasmic reticulum	2,22E-10	46	10
Lysine degradation	4,44E-10	16	8
Circadian rhythm	3,11E-09	18	14
Dopaminergic synapse	5,17E-07	47	9
Gap junction	7,82E-07	22	10
Glutamatergic synapse	2,08E-05	46	9
Small cell lung cancer	8,11E-04	35	6
Calcium signaling pathway	9,62E-02	46	11
Adherens junction	7,43E+00	33	8
Jak-STAT signaling pathway	3,40E+01	27	6
Prion diseases	6,15E+01	1	1
Phosphatidylinositol signaling system	9,11E+01	22	8
Long-term depression	0.000146718	19	5
Glycosaminoglycan biosynthesis	0.0001721187	7	4
Fatty acid biosynthesis	0.0004441118	1	2
N-Glycan biosynthesis	0.0006285946	14	9
Adipocytokine signaling pathway	0.0007053327	20	6
Protein digestion and absorption	0.001709413	23	3

Using the list of genes and miRNAs differentially modulated in the cortex after six months of feeding, and comparing either L-EVOO to young mice or H-EVOO to L-EVOO, DIANA-mirExTra algorithm calculated the most significantly over-represented hexamers and the combined score produced by the values of three hexamers (Table 12 and Table 13); this allowed to obtain a list of 14 miRNAs modulated by aging, and a list of 6 miRNAs modulated by the treatment with olive oil phenols, based on the correlation between the expression level of each miRNA and of its target genes (Table 5). We thus identified 5 miRNAs that were modulated in an opposite way by aging and by dietary treatment: at the top ranking score we found miR-30a-5p. We also found one miRNA, miR-484, modulated by the treatment but not by aging.

Table 12. List of miRNAs differentially modulated comparing L-EVOO to H-EVOO cortex and correlated with the expression changes of their target genes

miRNA	Score	hexamer1	hexamer2	hexamer3
mmu-miR-30a-5p	12.9	TTTACA	GTTTAC	TGTTTA
mmu-miR-484	10.586	GCCTGA	AGCCTG	GAGCCT
mmu-miR-434-5p	4.494	CGAGCT	TCGAGC	GTCGAG
mmu-miR-369-5p	4.01	CGATCT	TCGATC	GTCGAT
mmu-miR-451	0.85	CGGTTT	ACGGTT	AACGGT
mmu-miR-126-3p	0.166	GTACGA	GGTACG	CGGTAC

miRNAs differentially modulated comparing L-EVOO to H-EVOO cortex, sorted according to the combinatorial score produced by the values of hexamers 1, 2 and 3.

Table 13. List of miRNAs differentially modulated comparing L-EVOO to YOUNG mice cortex and correlated with the expression changes of their target genes

miRNA	Score	hexamer1	hexamer2	hexamer3
mmu-miR-681	62.284	AGGCTG	GAGGCT	CGAGGC
mmu-miR-709	55.092	GCCTCC	TGCCTC	CTGCCT
mmu-miR-706	32.116	TTCTCT	TTTCTC	GTTTCT
mmu-miR-30a-5p	31.23	TTTACA	GTTTAC	TGTTTA
mmu-miR-129-5p	20.924	AAAAAG	CAAAAA	GCAAAA
mmu-miR-434-3p	19.942	TTCAAA	GTTCAA	GGTTCA
mmu-miR-380-3p	19.138	TACATA	CTACAT	ACTACA
mmu-miR-30a-3p	16.902	TGAAAG	CTGAAA	ACTGAA
mmu-miR-434-5p	15.094	CGAGCT	TCGAGC	GTCGAG
mmu-miR-433-3p	14.786	CATGAT	TCATGA	ATCATG
mmu-miR-451	8.614	CGGTTT	ACGGTT	AACGGT
mmu-miR-720	8.372	CGAGAT	GCGAGA	AGCGAG
mmu-miR-126-3p	5.872	GTACGA	GGTACG	CGGTAC
mmu-miR-369-5p	4.462	CGATCT	TCGATC	GTCGAT
mmu-miR-451	8.614	CGGTTT	ACGGTT	AACGGT

miRNAs differentially modulated comparing L-EVOO to young mice cortex, sorted according to the combinatorial score produced by the values of hexamers 1, 2 and 3.

miRNA in neurodegeneration

We also extended our examination, analyzing the cortex of 4 TgCRND8 mice, a model of Alzheimer's disease, aged 4-6 months, corresponding to a middle stage of Aß deposition. TgCRND8 mice showed 237 miRNAs significantly modulated compared young mice ($p<0.05$). SAM analyses revealed that these animals had an extensive down-regulation of miRNA expression compared to wild type mice (Figure 23).

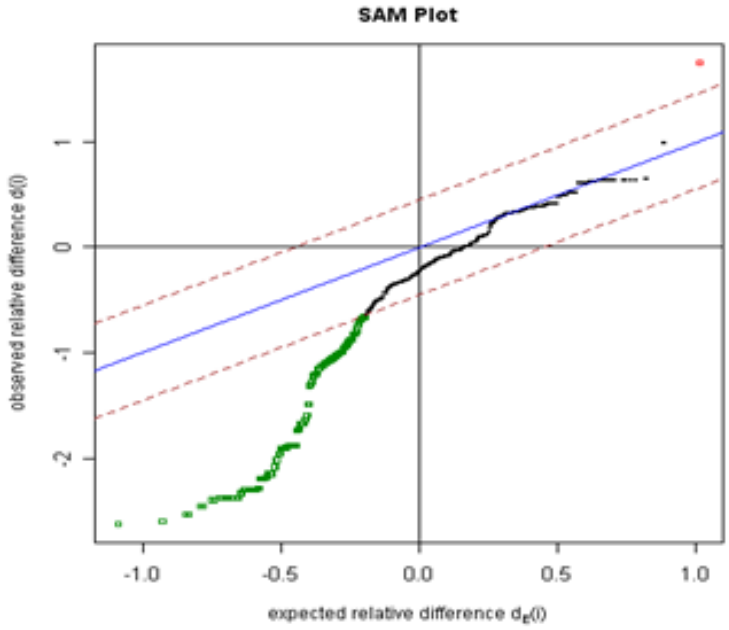

Figure 23. SAM plot: dots in green represent genes down-regulated, comparing TgCRND8 mice to young animals. The remaining unperturbed genes are shown in black.

We specifically examined the expression of miRNAs previously associated to aging or neurodegenerative disorders such as such as miR-34b and c, mir-181b and mir-146, over-expressed in TgCRND8 and in L-EVOO mice cortex, compared to young mice. Interestingly, mir-29 was significantly down-regulated in TgCRND8 mice and in L-EVOO mice (Figure 24).

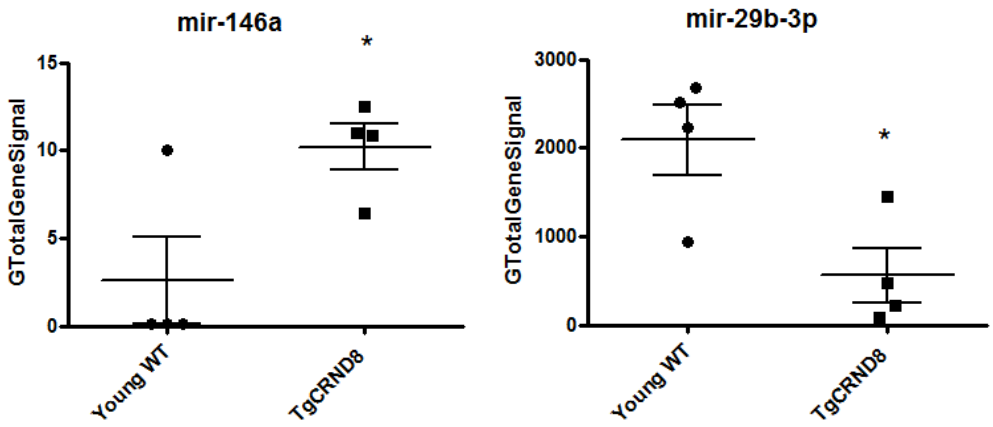

Figure 24. miRNA expression profiles of miR-146a and miR-29 in the cortex of TgCRND8 transgenic mice and young animals. *p<0.05 vs. young.

Results

Experimental model *in vitro*

Cell culture morphology and cytotoxicity

Measuring LDH release in the medium, we found a low and constant level of not modified by resveratrol (Figure 25, panel A). Demonstrative microscopy images indicate that 15 DIV represents a stage of maturation in which neurons form neuronal clusters and an extensive network of neuritis. At 27 DIV, no visible sign of neuronal deterioration was detected (Figure 25, panel B).

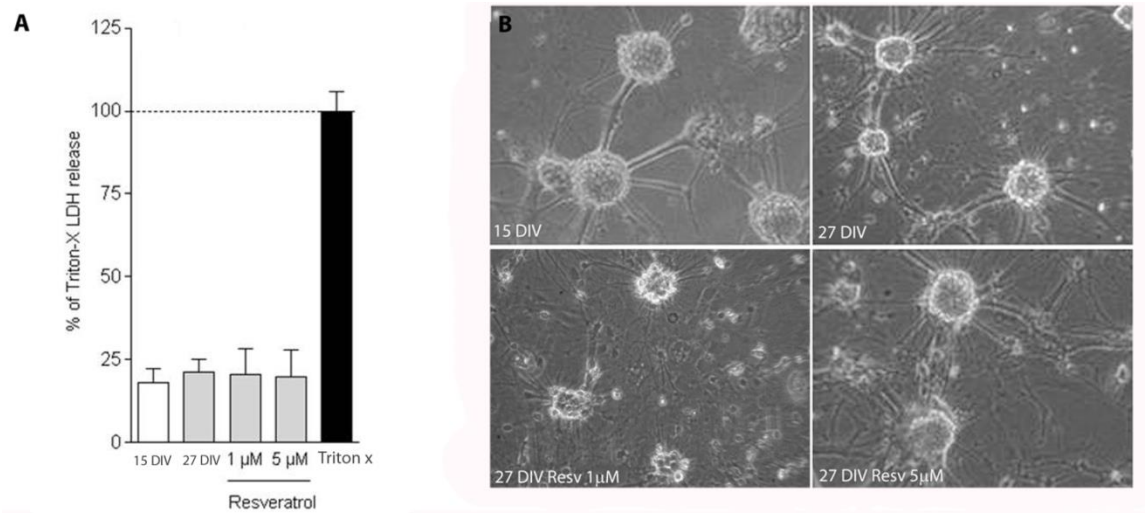

Figure 25. Panel A: percentage of LDH release in the medium in neuro-glial co-culture at 15 DIV, 27 DIV and in 27 DIV treated with resveratrol 1 and 5 µM. Results are expressed as a percentage of Triton-X induced LDH release and calculated as mean ± SE of three independent experiments. Panel B: representative microscopic images of neuro-glial co-culture at 15 DIV, 27 DIV and 27 DIV treated with 1 and 5 µM resveratrol.

Senescence-related markers

Cytochemical determination of senescence associated-β-galactosidase activity (SA-β-gal)

The appearance of senescence was evaluated starting from 15 DIV (the maturity stage) until 27 DIV. Neurons positive for SA-β-gal increased as a function of time, reaching the maximum between 23 and 27 DIV ($p<0.01$, 27 DIV vs 15 DIV). Beyond 27 DIV, neuro-glial co-cultures were not viable and we considered this stage as full senescence (Figure 26, panel A). Microscopy images indicate that at 15 DIV, almost no neuronal cell was positive for SA-β-gal whereas at 27 DIV neuro-glial co-culture showed a widespread blue staining in neurons inside the clusters and a more intense staining outside the clusters (Figure 25, panel B). At 27 DIV, a light blue and diffuse staining for SA-β-gal appeared also in the underlying astrocytic layer (Figure 26, panel B). Resveratrol (1-5 µM) administered from 15 to 27 DIV, reduced SA-β-gal activity in 27 DIV neuro-glial co-culture at levels below those of 15 DIV ($p<0.01$ vs 27 DIV) (Figure 26, panel A and B).

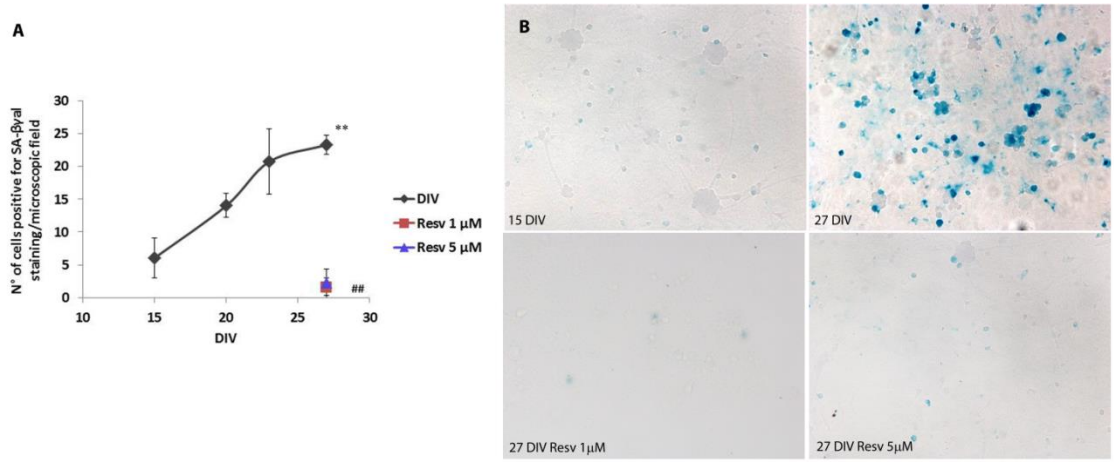

Figure 26. Panel A: number of cells positive for SA-βGal blue staining/microscopic field in neuro-glial co-culture at 15 DIV, 20 DIV, 23 DIV, 27 DIV and at 27 DIV treated with 1 and 5 µM resveratrol. Results are expressed as mean ±SE from three independent experiments. ** $p<0.01$ vs 15 DIV; ##$p<0.01$ vs 27 DIV. Panel B: representative microscopic images of neuro-glial co-culture at 15 DIV, 27 DIV and 27 DIV treated with resveratrol 1 and 5 µM.

Western blotting and immunocytochemistry for γ-H2AX

In neuro-glial co-cultures at 15, 20, 23 and 27 DIV we observed a time-dependent increase of γH2AX, a marker of senescence-related DNA damage ($p<0.05$, 27 DIV vs 15 DIV). Resveratrol, concentration-dependently reduced the senescence-associated increase of γH2AX ($p<0.05$, 27 DIV Resv 5 vs 27 DIV)(Figure 27, panel A). Representative immunofluorescence images for γH2AX (in red) and the neuronal marker NeuN (in green) show the co-localization of γH2AX with NeuN positive neurons (in yellow) (Figure 27, panel B).

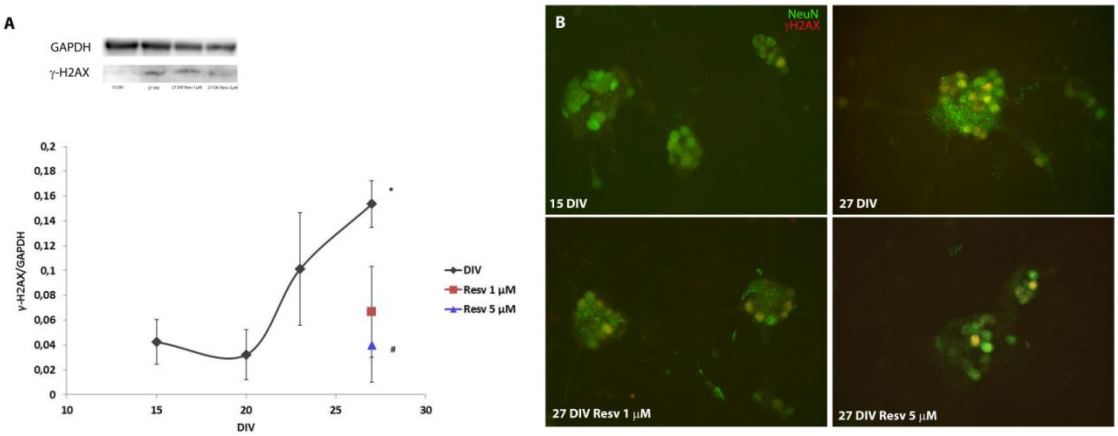

Figure 27. Panel A: γ-H2AX protein expression in neuro-glial co-culture at 15 DIV, 20 DIV, 23 DIV and 27 DIV and at 27 DIV treated with resveratrol 1 and 5 µM. Results are expressed as mean ±SE from three independent experiments. * $p<0.05$ vs 15 DIV; # $p<0.05$ vs 27 DIV. Panel B: representative immune-fluorescence images of γ-H2AX (in red) and of the neuronal marker NeuN (in green) in neuro-glial co-cultures at 15 DIV, 27 DIV and 27 DIV treated with resveratrol 1 and 5 µM.

Western blotting and immunocytochemistry for neuronal (NeuN), dendritic (MAP2) and astrocytic (GFAP) markers

The neuronal marker NeuN decreased from 15 DIV to 20 DIV, remained stable from 20 DIV to 23 DIV, and significantly decreased at 27 DIV ($p<0.05$, 27 DIV vs 15 DIV (Figure 27, panel A). Moreover, immune-fluorescent images showed the progressive emptying of neuronal clusters at 27 DIV (Figure 28, panel B). Immuno-reactivity for MAP 2 (in green), a marker of dendritic spines, indicated the presence of smaller processes in 27 DIV co-cultures (Figure 29, panel B). The relative protein quantifications further supported this result; in fact, the shape of MAP2 protein expression levels was quite similar to that observed for NeuN, displaying a constant loss of MAP2 protein expression levels from 15 DIV to 20, 23 and 27 DIV ($p<0.05$ 27 DIV vs 15 DIV) (Figure 28, panel A). Resveratrol did not modify the senescence-dependent loss neither in NeuN nor in MAP2 protein expressions (Figure 28, panel A and Figure 29, panel A).

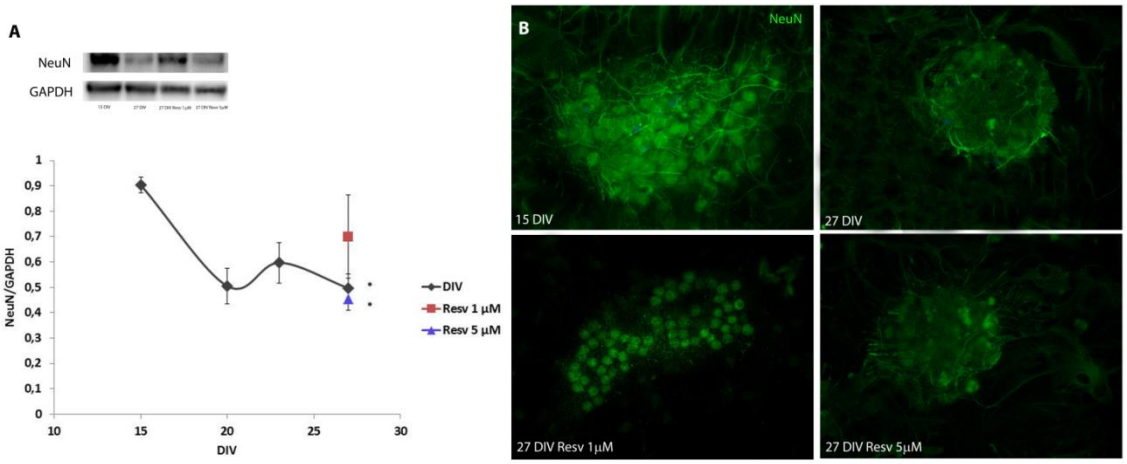

Figure 28. Panel A: NeuN protein expression levels in neuro-glial co-culture at 15 DIV, 20 DIV, 23 DIV, 27 DIV and at 27 DIV treated with resveratrol 1 and 5 µM. Results are expressed as mean ±SE from three independent experiments. * p<0.05 vs 15 DIV. Panel B: representative immune-fluorescent images of neuronal clusters (NeuN positive cells in green) at 15 DIV, 27 DIV and 27 DIV treated with 1 and 5 µM resveratrol.

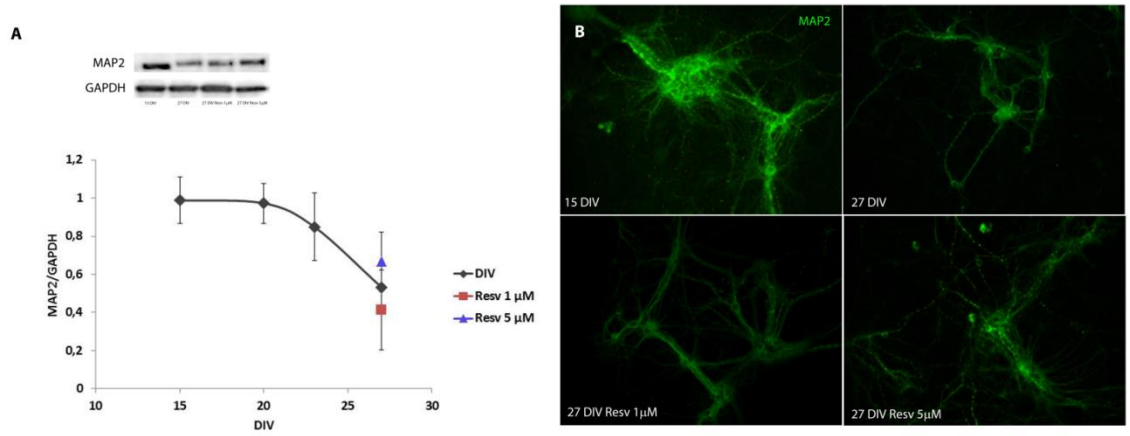

Figure 29. Panel A: MAP2 protein expression levels in neuro-glial co-culture at 15 DIV, 20 DIV, 23 DIV, 27 DIV and at 27 DIV treated with resveratrol 1 and 5 µM. Results are expressed as mean ±SE from three independent experiments. Panel B: representative immune-fluorescent images of MAP2 (in green) in neuro-glial co-cultures at 15 DIV, 27 DIV and 27 DIV treated with 1 and 5 µM resveratrol.

In order to evaluate the appearance of senescent characteristics in the underlying astrocytic layer, astrocyte cell morphology and the astrocytic protein GFAP were also examined. In 27 DIV neuro-glial co-cultures, astrocytes became hypertrophic, exhibited an intensive immuno-staining for GFAP and displayed an extensive network of large processes (Figure 30, panel B). Results of GFAP protein expression levels were consistent with those of immunofluorescence showing an increase in GFAP protein expression from 15 DIV to 20, 23

and 27 DIV (Figure 30, panel A). Resveratrol concentration-dependently reduced GFAP protein expression to levels below those of 15 DIV neuro-glial co-cultures (Figure 30, panel A).

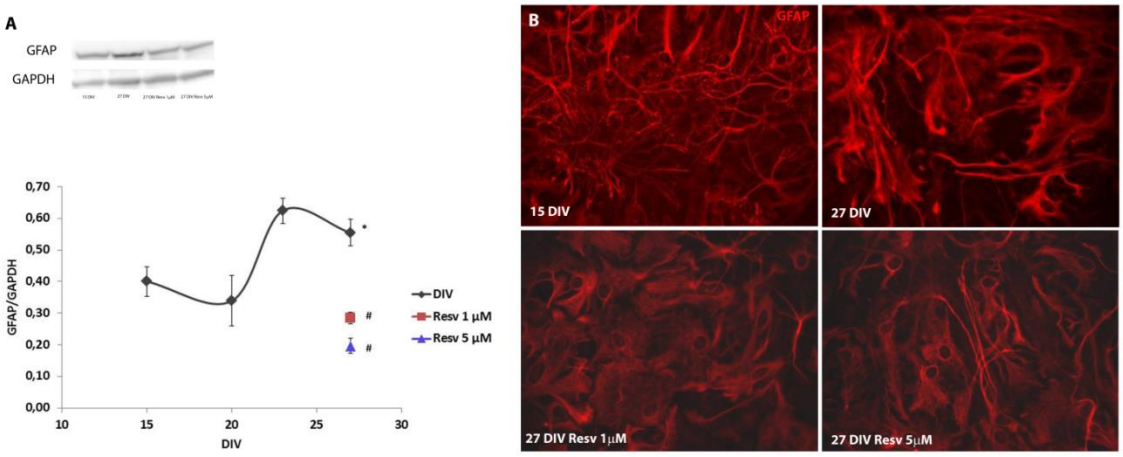

Figure 30. panel A: GFAP protein expression levels in neuro-glial co-culture at 15 DIV, 20 DIV, 23 DIV, 27 DIV and at 27 DIV treated with 1 and 5 µM resveratrol. Results are expressed as mean ±SE from three independent experiments. * $p<0.05$ vs 15 DIV; # $p<0.05$ vs 27 DIV. Panel B: representative immune-fluorescent images of GFAP (in red) in neuro-glial co-cultures at 15 DIV, 27 DIV and 27 DIV treated with resveratrol 1 and 5 µM.

Immunocytochemistry for the dendritic marker drebrin and post-synaptic density protein PSD-95

In neuro-glial co-cultures at 27 DIV, we observed a significant reduction of both the dendritic spine marker drebin and the post-sinaptic density protein PSD-95. Resveratrol, concentration dependently counteract the senescence dependent loss in PSD-95 but prevented the senescence dependent loss of drebrin only at 5 µM (Figure 31 and Figure 32).

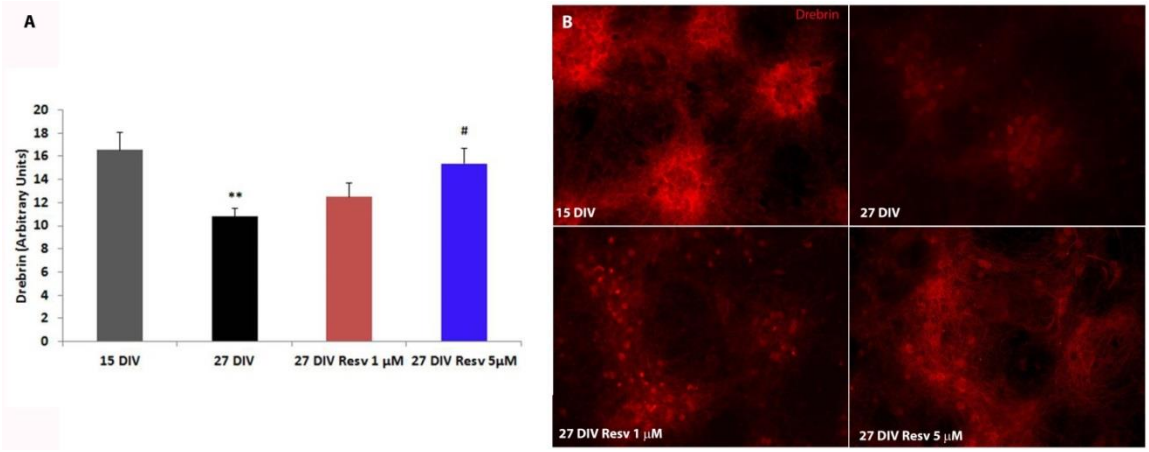

Figure 31. Panel A: densitometric analysis of Drebrin in neuro-glial co-culture at 15 DIV, 27 DIV and at 27 DIV treated with resveratrol 1 and 5 µM. Results are expressed as mean ±SE from three independent experiments. ** p<0.01 vs 15 DIV; # p<0.05 vs 27 DIV. Panel B: representative immune-fluorescent images of Drebrin (in red) in neuro-glial co-cultures at 15 DIV, 27 DIV and 27 DIV treated with resveratrol 1 and 5 µM.

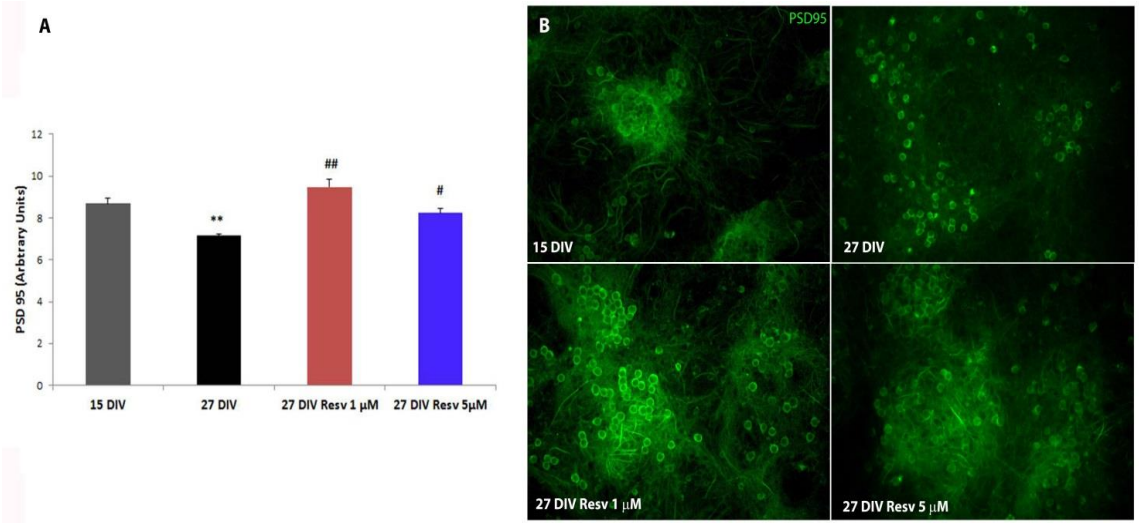

Figure 32. Panel A: densitometric analysis of PSD-95 in neuro-glial co-culture at 15 DIV, 27 DIV and at 27 DIV treated with resveratrol 1 and 5 µM. Results are expressed as mean ±SE from three independent experiments. ** p<0.01 vs 15 DIV; ## p<0.01 vs 27 DIV; # p<0.05 vs 27 DIV. Panel B: representative immune-fluorescent images of PSD-95 (in green) in neuro-glial co-cultures at 15 DIV, 27 DIV and 27 DIV treated with 1 and 5 µM resveratrol.

Oxidative stress: carbonyl residues

Protein oxidation, measured as carbonyl residues, progressively increased from 15 DIV to 20, 23 and 27 DIV. At 27 DIV, we detected the highest levels of protein oxidation compared

to 15 DIV neuro-glial co-cultures; this effect was reduced by 1 µM resveratrol ($p<0.05$)(Figure 33).

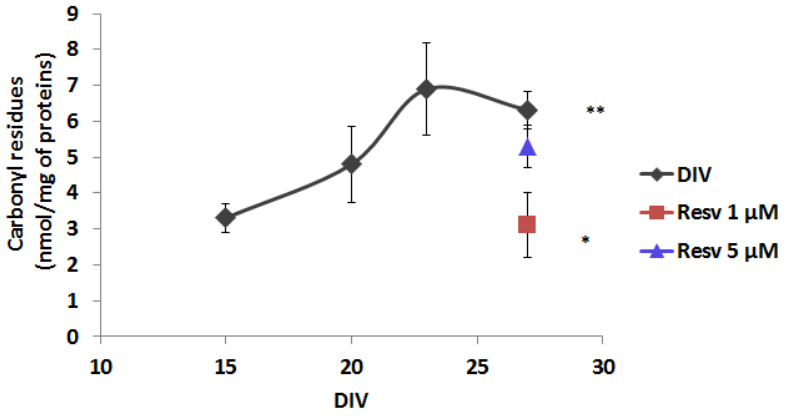

Figure 33. Carbonyl residues in neuro-glial co-cultures at 15, 20, 23, 27 DIV and in 27 DIV cells treated with 1 and 5 µM resveratrol (mean ± SE of three experiments). * $p<0.05$ vs 15 DIV; ** $p<0.01$ vs 15 DIV; # $p<0.05$ vs 27 DIV.

Oxidative stress: 4-hydroxynonenal

Lipo-peroxidation, measured as 4-hydroxynonenal (4-HNE) levels, was significantly increased in neuro-glial co-cultures at 27 DIV. Resveratrol, reduced 4-HNE expression to levels similar to those of 15 DIV neuro-glial co-cultures (Figure 34, Panel A). Panel B: representative immune-fluorescent images of 4-HNE (in red) in neuro-glial co-cultures at 15 DIV, 27 DIV and 27 DIV treated with 1 and 5 µM resveratrol.

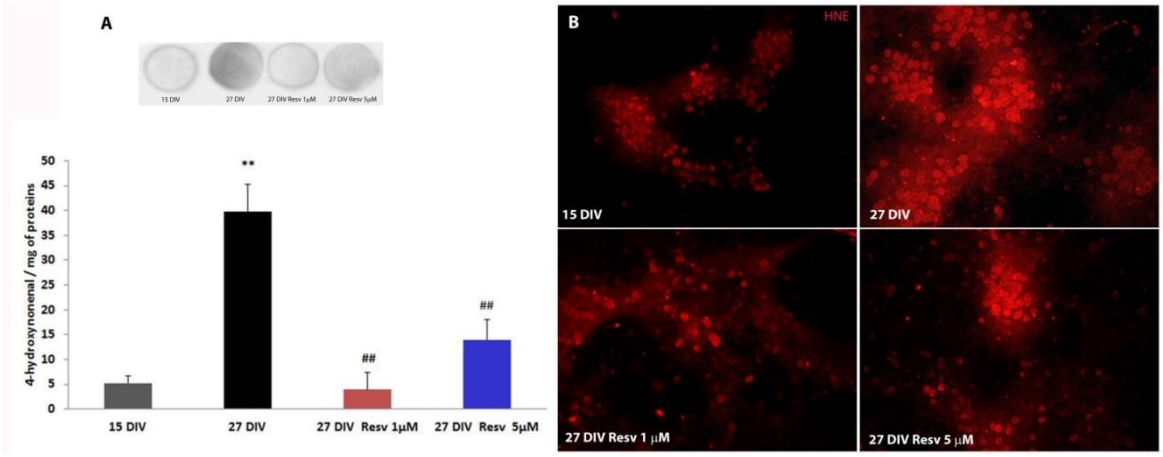

Figure 34. Panel A: 4-hydroxynonenal (4-HNE) levels in neuro-glial co-cultures at 15, 27 DIV and 27 DIV treated with 1 and 5 µM resveratrol. Panel B: representative immune-fluorescent images of 4-HNE (in red) in neuro-glial co-cultures at 15 DIV, 27 DIV and 27 DIV treated with 1 and 5 µM resveratrol.

Oxidative stress: nitrotyrosine

Protein oxidation was also measured by means of nitrotyrosine immunocytochemical detection. No differences were observed among the experimental groups (Figure 35).

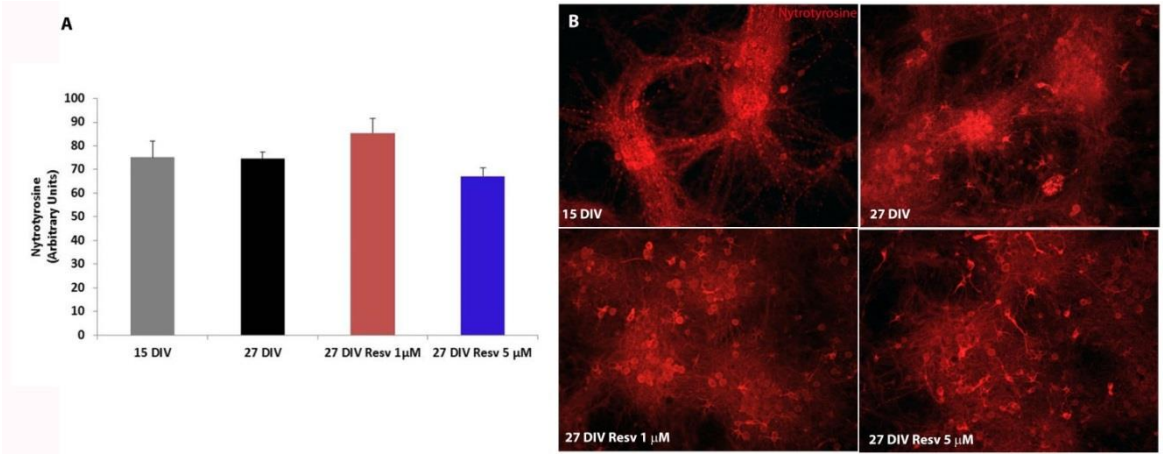

Figure 35. Panel A: nitrotyrosine levels in neuro-glial co-cultures at 15, 27 DIV and 27 DIV treated with 1 and 5 µM resveratrol. Panel B: representative immune-fluorescent images of nitrotyrosine (in red) in neuro-glial co-cultures at 15 DIV, 27 DIV and 27 DIV treated with 1 and 5 µM resveratrol.

DNA damage

DNA damage was significantly increased in senescent neuro-glial co-cultures and not modified in resveratrol treated cells (Figure 36).

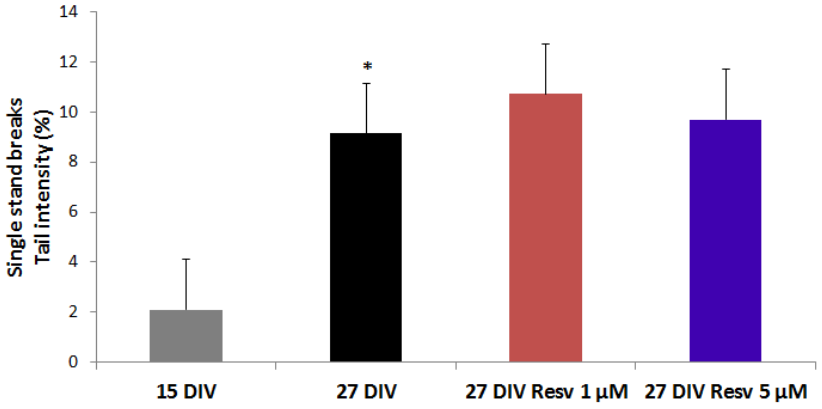

Figure 36. Single strand breaks measured as tail intensity (%) in neuro-glial co-cultures at 15, 27 DIV and 27 DIV treated with 1 and 5 µM resveratrol. * p<0.05 vs 15 DIV.

Inflammation

The production of the pro-inflammatory cytokine IL-6 was strongly increased in 27 DIV compared to 15 DIV and resveratrol 1-5 µM counteracted this effect (p<0.01, 15 DIV vs 27 DIV; p<0.01, 27 DIV Resv 5 vs 27 DIV; p< 0.01 27 DIV Resv 1 vs 27 DIV) (Figure 37). The levels of PGE2 showed a time-dependent increase which reached significance at 27 DIV. Resveratrol (1-5 µM) had no significant effects (Figure 38).

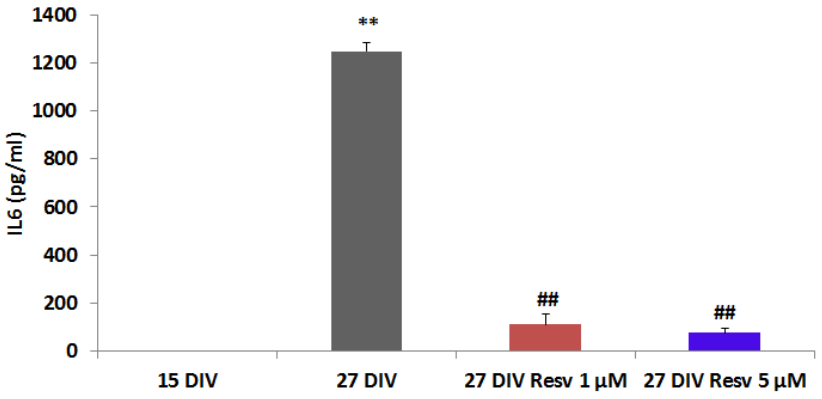

Figure 37. IL-6 levels in the culture media of neuro-glial co-cultures at 15, 27 DIV and 27 DIV treated with 1 and 5 µM resveratrol. ** p<0.01 vs 15 DIV; ## p<0.01 vs 27 DIV.

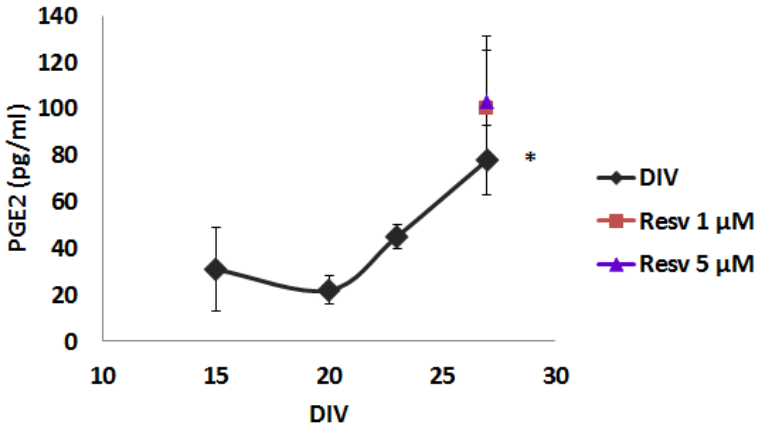

Figure 38. PGE2 levels in the culture media of neuro-glial co-cultures at 15, 20, 23, 27 DIV and 27 DIV treated with 1 and 5 µM resveratrol. * p<0.05 vs 15 DIV.

MiRNA expression profiles in neuro-glial co-cultures

miRNA profiling was performed on neuro-glial co-cultures at 15 DIV and 27 DIV and in 27 DIV treated with 1 and 5 µM resveratrol. 335 of the 1080 miRNAs analysed were differentially expressed (down-regulated or completely absent) between 15 and 27 DIV. Resveratrol reversed the extensive down-regulation observed in 27 DIV neuro-glial co-cultures and this effect was concentration-dependent for 202 miRNAs. An unsupervised hierarchical cluster analysis (Figure 39, panel A) shows the relationships among the experimental groups as a tree with branch lengths reflecting the similarity between experimental groups. miRNA expression profiles of senescent neuro-glial co-cultures treated with resveratrol were similar to those of young cells (Figure 39, panel A). Among the miRNAs down-regulated in senescent co-cultures and restored after resveratrol treatment, we found several members of the mir-466-467-669 cluster, mir-7, mir-24-3p, mir-328-3p, miR-17-92 cluster and mir-204-5p. Putative gene targets of some miRNAs down-regulated in senescent cultures were identified by DIANA-microT and are shown in Table 14. miR-715, miR-199a-5p and miR-199a-3p were the only 3 found to be up-regulated in 27 DIV cells, with a >2 fold-change.

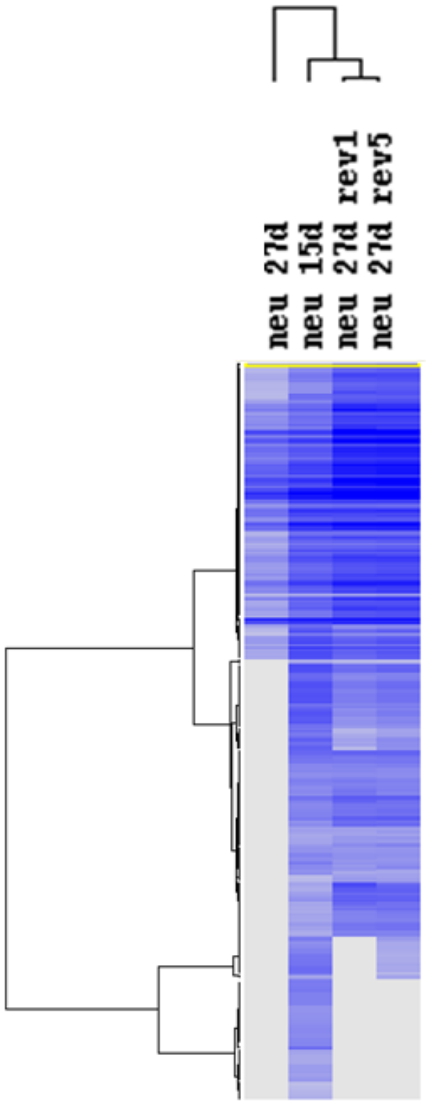

Figure 39. Unsupervised hierarchical clustering of miRNA expression profiles in neuro-glial co-cultures at 15 DIV, 27 DIV and 27 DIV treated with 1 and 5 µM resveratrol. Each row represents a different miRNA; the color code indicates not-expressed miRNAs (grey) or expressed miRNAs (blue).

Table 14: List of miRNA down-regulated in 27 DIV compared to 15 DIV cells, with a FC<0.5, their predicted target and biological significance

miRNA	Predicted gene target	Biological significance
miR-17-92	p21	Cell cycle regulation, senescence, apoptosis
mir-669c-3p	GLB1	Marker of senescence
mir-466	ATM	DNA damage response cascade
mir-24-3p/mir-124-3p	H2AX	Senescence, DNA damage
mir-7a-5p	PARP-1	Senescence, DNA damage, neurodegeneration
miR-204-5p /mir-669h-3p	GFAP	Astrocytes activation
miR-188-5p	Nrp-2	Dendritic spine reduction
miR-23b	Apaf-1	Neuronal death
mir-26b-5p	E2F7	Senescence

Comparison between *in vitro* and *in vivo* miRNA expression profiling

MiRNA profiling was used to compare *in vitro* and *in vivo* models. The age-associated changes in miRNA profiles of neuro-glial cultures were compared with those occurred in the cortex of aged C57Bl/6J mice (18 and 24 months of age) and TgCRND8 mice aged 4-6 months (corresponding to a middle stage of Aß deposition). 85 miRNAs resulted in being down-regulated (with an FC<0.5) in 27 DIV cultures and in TgCRND8 mice, compared to their respective young counterparts (15 DIV and wild-type mice). Instead, only 8 miRNAs were down-regulated both in 27 DIV and in 24-month-old C57Bl/6J mice, and 17 miRNAs in 27 DIV and in 18-month-old C57Bl/6J mice, each compared to their respective young counterparts (15 DIV and young mice). These data and the degree of overlap among the different groups are represented in the Venn diagram in Figure 40.

Interestingly, 3 miRNAs down-regulated in 27 DIV were simultaneously down-regulated in 18- and 24-month-old C57Bl/6J mice and in TgCRND8 mice (mir-7b-3p, mir-452-5p, mir-290-5p). We found mir-29a and mir-29-b, mir-466, mir-467 and mir-669 among the miRNAs exclusively down-regulated in 27 DIV and the TgCRND8 mouse cortex (Figure 40).

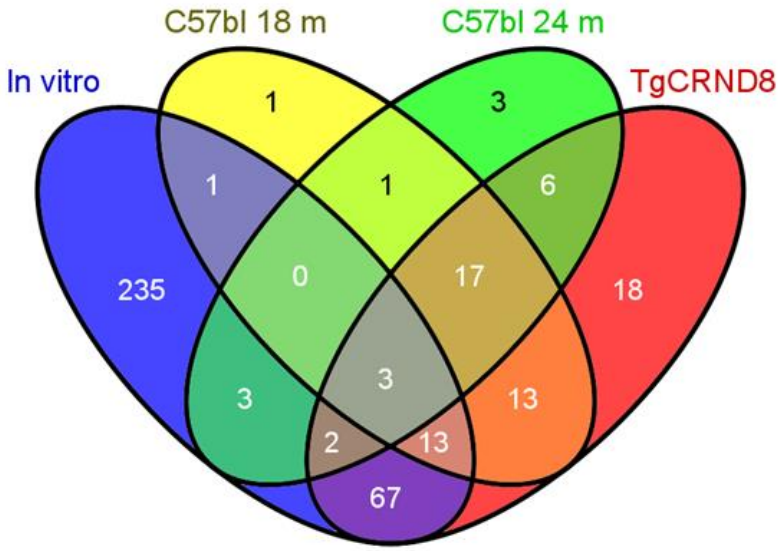

Figure 40. Venn diagram showing the overlapping among the age-related changes in miRNAs expression profiles among neuro-glial co-cultures (27 DIV compared to 15 DIV) (*in vitro*, blue circle), physiological aging in C57bl mice cerebral cortex (18 and 24 months-old compared to 3 months-old) depicted in the yellow and green circles respectively, and pathological aging in TgCRND8 cortex (transgenic compared to wild type) depicted in the red circle. Only down-regulated miRNAs are shown (Fold change<0.5).

Target prediction analysis

Putative gene targets for some of these down-regulated miRNAs were identified by DIANA-microT and are shown in Table 15.

Table 14: List of miRNA down-regulated in 27 DIV, compared to 15 DIV cells and in TgCRND8 mice, compared to C57Bl/6J young mice, with a FC<0.5, their predicted target and biological significance

miRNA	Predicted gene target	Biological significance
mir-7b-3p	histone H3.3 PAI-1	Regulation of chromatin Senescence
mir-452-3p	GLUD1	Loss of neurons, dendritic spines
mir-290-5p	Histone demethylase UTX	Aging
mir-29/mir-328	BACE-1	APP processing
mir-669h-3p	Contactin 4	Axon guidance
mir-466m-5p	APP	Amiloyd plaques
mir-467	HIF-1 E2f7	Hypoxia p53-dependent cell cycle arrest
mir-669c-3p	Beclin 1	Autophagic process
mir-181b/d-5p	HMGB-1, IL-6	Stress response in astrocytes, inflammation

miRNA expression by qRT-PCR analysis

qRT-PCR confirmed the down regulation (indicated as fold change (FC)) of miR-17 (FC 27 DIV/15DIV: 0.09), miR-124 (FC 27 DIV/15DIV: 0.115), let-7a (FC 27 DIV/15DIV: 0.27), mir-29b: (FC 27 DIV/15DIV: 0.35). Given that mir-29b was among the miRNAs down-regulated in 27 DIV cultures and in TgCRND8 mice, its down-regulation was also confirmed in the cortex of TgCRND8 mice with an FC TgCRND8/ young of 0.27 . Mir-34a was also chosen as one of the non-affected miRNAs and also in this case, qRT-PCR confirmed the microarray results demonstrating that this miRNA was expressed only at very low levels and that it was not modified in senescent cultures compared to the young ones. With the same approach we also confirmed the effect of resveratrol in reverting the down-regulation observed in 27 DIV for the above mentioned miRNAs: mir-17: FC 27 DIV Resv 1 µM/15DIV: 1.29 and FC 27 DIV Resv 5 µM/15DIV: 1.52; miR-124: FC 27 DIV Resv 1 µM/15DIV: 3.2 and FC 27 DIV Resv 5 µM/15DIV

3.7; let-7a: FC 27 DIV Resv 1 µM/15DIV: 4.2 and FC 27 DIV Resv 5 µM/15DIV: 5.2; mir-29: FC 27 DIV Resv 1 µM/15DIV: 1.8 and FC 27 DIV Resv 5 µM/15DIV: 4.4.

Pathway analysis

DIANA-miRPath v2.0 analysis identified several pathways as significantly enriched ($p<0.01$) for the 85 miRNAs down-regulated in 27 DIV cultures and in TgCRND8 mice. As it can be seen in Table 16, many of the identified pathways are categorized under core biological processes in the brain, such as neurotrophin signaling, axon guidance pathway, dopaminergic, GABAergic and glutamatergic transmission as well as long-term depression and potentiation. Moreover, mTOR and the PI3K-Akt signaling pathway were also significantly modulated. The list of miRNAs belonging to these pathways is shown in Table 17.

Table 16. Pathways enriched with targets of miRNAs found to be down-regulated in in 27 DIV (vs 15 DIV) and in TgCRND8 mice (vs young C57BL/6J), with a FC<0.5; p-value depicts the probability that the examined pathway is significantly enriched with gene targets of at least one selected miRNA

KEGG pathway	p-value	number of genes	number of miRNAs
MAPK signaling pathway	0	83	15
mTOR signaling pathway	0	38	17
Wnt signaling pathway	0	69	17
TGF-beta signaling pathway	0	42	17
PI3K-Akt signaling pathway	0	119	19
Axon guidance	0	68	22
Endocytosis	1,27E-08	47	10
Neurotrophin signaling pathway	1,95E-08	29	11
GABAergic synapse	2,34E-08	33	15
Glutamatergic synapse	2,44E-08	36	12
Ubiquitin mediated proteolysis	2,00E-04	38	9
Dopaminergic synapse	4,20E-04	29	7
Retrograde endocannabinoid signaling	1,82E-03	35	12
Circadian rhythm	8,91E-03	19	11
Phosphatidylinositol signaling system	4,79E-02	20	10
Long-term depression	1,24E-06	20	10
Glioma	2,02E-06	21	9
Regulation of actin cytoskeleton	5,35E-06	53	4
Lysine degradation	9,01E-06	15	8
Long-term potentiation	9,25E-06	19	5
Calcium signaling pathway	1,41E-05	45	8
Endocrine and other factor-regulated calcium reabsorption	2,22E-05	14	9
Protein processing in endoplasmic reticulum	3,48E-05	28	6
Gap junction	0.0002971512	19	7
Insulin signaling pathway	0.000509933	30	4
Chemokine signaling pathway	0.002399127	29	7
Protein digestion and absorption	0.003412517	17	2

Table 17. List of miRNAs down-regulated in in 27 DIV, compared to 15 DIV cells, and in TgCRND8 mice compared to C57B6J young mice cortex, with a FC<0.5 and their enriched pathways.

mTOR signaling pathway	**PI3K-Akt signaling pathway**	**Axon guidance**	**Neurotrophin signaling pathway**
mmu-miR-7b-3p	mmu-miR-17-3p	mmu-miR-467b-3p	mmu-miR-467b-3p
mmu-miR-467b-3p	mmu-miR-134-5p	mmu-miR-467f	mmu-miR-467f
mmu-miR-467g	mmu-miR-467b-3p	mmu-miR-467g	mmu-miR-467g
mmu-miR-1839-3p	mmu-miR-467f	mmu-miR-1897-5p	mmu-miR-32-3p
mmu-miR-2137	mmu-miR-467g	mmu-miR-1904	mmu-miR-669f-3p
mmu-miR-669f-3p	mmu-miR-2137	mmu-miR-3099-3p	mmu-miR-669p-3p
mmu-miR-466i-5p	mmu-miR-669f-3p	mmu-miR-32-3p	mmu-miR-467c-3p
mmu-miR-149-3p	mmu-miR-328-5p	mmu-miR-467c-3p	mmu-miR-467a-3p
mmu-miR-467c-3p	mmu-miR-3077-5p	mmu-miR-466m-3p	mmu-miR-181d-5p
mmu-miR-466m-3p	mmu-miR-467c-3p	mmu-miR-3096b-3p	mmu-miR-466f-3p
mmu-miR-467a-3p	mmu-miR-466m-3p	mmu-miR-669c-3p	mmu-miR-467d-3p
mmu-miR-669c-3p	mmu-miR-3096b-3p	mmu-miR-770-3p	
mmu-miR-29b-3p	mmu-miR-467a-3p	mmu-miR-721	
mmu-miR-92a-3p	mmu-miR-669c-3p	mmu-miR-212-3p	
mmu-miR-181b-5p	mmu-miR-29b-3p	mmu-miR-320-3p	
mmu-miR-181d-5p	mmu-miR-92a-3p	mmu-miR-181b-5p	
mmu-miR-467d-3p	mmu-miR-34a-5p	mmu-miR-181d-5p	
	mmu-miR-467d-3p	mmu-miR-466g	
	mmu-miR-500-3p	mmu-miR-466h-5p	
		mmu-miR-467d-3p	
		mmu-miR-500-3p	
GABAergic synapse	**Glutamatergic synapse**	**Dopaminergic synapse**	**Long-term depression**
mmu-miR-467b-3p	mmu-miR-7b-3p	mmu-miR-467b-3p	mmu-miR-452-5p
mmu-miR-669h-3p	mmu-miR-467b-3p	mmu-miR-1894-3p	mmu-miR-467b-3p
mmu-miR-1892	mmu-miR-32-3p	mmu-miR-32-3p	mmu-miR-669h-3p
mmu-miR-1894-3p	mmu-miR-466m-5p	mmu-miR-3102-5p	mmu-miR-32-3p
mmu-miR-32-3p	mmu-miR-669f-3p	mmu-miR-467c-3p	mmu-miR-3102-5p
mmu-miR-466m-5p	mmu-miR-467c-3p	mmu-miR-467d-3p	mmu-miR-467c-3p
mmu-miR-669f-3p	mmu-miR-466m-3p	mmu-miR-500-3p	mmu-miR-706
mmu-miR-466i-5p	mmu-miR-467a-3p		mmu-miR-181b-5p
mmu-miR-3102-5p	mmu-miR-705		mmu-miR-181d-5p
mmu-miR-467c-3p	mmu-miR-181b-5p		mmu-miR-467d-3p
mmu-miR-467a-3p	mmu-miR-181d-5p		
mmu-miR-34a-5p	mmu-miR-467d-3p		**Long-term potentiation**
mmu-miR-466g			mmu-miR-669h-3p
mmu-miR-466h-5p			mmu-miR-1906
mmu-miR-467d-3p			mmu-miR-32-3p
			mmu-miR-181b-5p

Discussion of the experimental model *in vivo*

Aging is a complex process which manifests a variety of characteristics and changes from early ages some of which seem to be evolutionarily conserved. In humans, aging is often accompanied by cognitive and motor decline and is the primary risk factor for neurodegenerative disorders including Alzheimer's and Parkinson disease and trinucleotide repeat disorders (Yankner et al., 2008). While some physiological differences between young and aged brains have been described, the mechanisms involved in brain aging at the molecular level, are not yet well understood.

Gene expression profiling of the brain have been conducted in mice, rats, chimpanzees and humans and have shown that specific genes and pathways are affected by aging (Blalock et al., 2003; Lu et al., 2004). Studies in mice have reported that genes involved in inflammatory and stress responses, as well as proteases involved in neuropeptide metabolism, show altered expression (Jiang et al., 2001; Lu et al., 2004;). However, how the many affected pathways and processes are regulated in the overall picture of brain aging remains to be elucidated. In this respect, understanding the genomic basis of the phenotypic changes observed in aging brain, could yield insights into the underlying networks affecting these processes. However, genotype does not necessarily determine the aging phenotype which could also be affected by the epi-genome modulation of gene expression in response to endogenous and exogenous regulators during the life span.

Diet is an important factor for human health and its effects are being to be understood in molecular terms with the help of the nutrigenomic research. Diet has been linked to the general health status through its ability of modulating several biological pathways and gene response (García-Cañas et al., 2010). It is also well recognized that numerous bioactive dietary components mediate epigenetic modifications associated with the pathophysiology of several diseases (Li et al., 2010). However, only few studies have explored the effects of specific food components in regulating epigenetic patterns during brain aging or neurodegeneration (Khanna et al., 2010).

The intake of olive oil, an important component of Mediterranean diet, has been associated to health benefits in large cohort studies such as the European Prospective Investigation into Cancer and Nutrition (EPIC) studies (Buckland et al., 2012). Furthermore, high intake of olive oil and specifically virgin olive oil in older individuals with high cardiovascular risk, was associated with better memory function and global cognition (Valls-Pedret et al., 2012). In agreement, data from my research group demonstrated that mice fed from middle age to senescence with extra-virgin olive oil rich in phenols maintained contextual

memory (evaluated with the step-down test) to levels similar to young animals, and displayed a significant reduction of age-related impairment in motor coordination (measured by the rota-rod test), (Pitozzi et al., 2012).

In this study, we focused on a subgroup of animals (mice) from the previous study, in order to verify whether the cognitive and motor changes induced by the treatment with extra virgin olive oil rich in phenolic compounds, were associated to changes in gene expression and how miRNAs were involved in these processes.

In this small subgroup of animals we confirmed the strong improvement induced by the high-phenols extra virgin olive oil and by 22 mg/kg resveratrol on motor coordination; moreover, extra-virgin olive oil feeding was also able to modulate the spatial memory (assessed with the Morris Water Maze) and the anxiety-related behavior (evaluated with the light-dark box), effects not observed in the resveratrol-treated group. The results on the step-down test showed a tendency towards improved contextual memory, which, however, did not reach statistical significance, in both groups.

Farr and co-authors have reported that 11-month-old SAMP8 mice fed for 6 weeks with a polyphenol-rich extract from extra-virgin olive oil showed improved memory in the T-maze foot shock avoidance test and in the object recognition test (Farr et al., 2012).

Other authors have reported beneficial effects on memory of other antioxidant–anti-inflammatory dietary components. Shan et al. demonstrated that purple sweet potato, a source of anthocyanins with powerful antioxidant activity, could attenuate in 4 weeks the impairment in passive avoidance memory in a model of mouse aging (Shan et al., 2009) while 50 mg/kg curcumin ameliorated spatial memory in SAMP8 mice by decreasing oxidative stress in the hippocampus (Sun et al., 2013).

In our experiment both phenols from olive oil and resveratrol led to an improvement in the memory of mice to remember the electric shock. In the literature, there are data that show that resveratrol, at doses of 10 and 20 mg / kg, results in an improvement of the loss of memory induced by streptozotocin in diabetic rats, evaluated with the step-down test (Schmatz et al., 2009) , while very few data are reported relative to phenols of olive oil.

Grossi et al. (2013) demonstrated that 8 weeks dietary supplementation of oleuropein aglycone (50 mg/kg of diet), improved the cognitive performance in TgCRND8 mice assessed with the step down test.

The antioxidant and anti-inflammatory properties of polyphenols contained in vegetable food, such as spinach, strawberries, or blueberries extracts, and their ability to reduce motor deficits in aged animals have been reported previously (Joseph et al., 1999). The same group has shown that diets rich in antioxidants, administered to aged rats for 8 weeks,

can improve performance in a motor learning task and reverse the age-induced decline in cerebellar b-adrenergic receptor function (Bickford et al., 2000). Moreover, in our previous study we observed a reduced levels of TBARs in the cortex and in the cerebellum only in the H-EVOO group (Pitozzi et al., 2012).

For our transcriptomic analyses we concentrated on two brain areas which are involved in cognitive and motor processes: cortex and cerebellum. Overall, our analyses demonstrated that after 6 months, most of the gene expression changes, were restricted to the cerebral cortex, and for this reason we later focused on this area alone.

In the cerebral cortex, several genes were modulated by the aging process *per se,* irrespective of the dietary treatment; among those, we found several down –regulated genes associated to biological processes largely involved in aging such as ionotropic and metabotropic glutamate receptors, calcium channels and synaptic proteins, some antioxidant enzymes and DNA repair factors, several autophagy related proteins and cyclines. Inflammation and apoptosis-related genes together with MAO-A and Igf-1 were, as expected, up-regulated in the cortex of aging mice.

Our research, however, focused on genes with different expression in mice fed oil rich in phenolic compounds (H-EVOO) compared to those treated with oil phenols-deprived (L-EVOO). Dietary supplementation with H-EVOO was associated with a significant modulation of genes (mostly up-regulated) compared to L-EVOO. Among those, we found several bone morphogenetic proteins (BMPs), the nerve growth factor receptor (NGFR) the glucagon-like peptide-1 receptor (GLP1R) and CREB-regulated transcription coactivator 3 (CRTC3).

BMPs are members of the transforming growth factor-β (TGFβ) family which is critical for controlling cell differentiation and apoptosis. BMPs exert a neuro-protective function in models of ischemic stroke and in neurodegeneration and improve motor function in stroke of rats (Chang et al., 2003; Heinonen et al., 2014). The neuro-protective effects of BMPs, seems to involve the activation of MAPK, protein kinase C and SMAD signaling cascade (Cox et al., 2004).

NGF and its receptors, play a critical trophic and protective role on cholinergic neurons that degenerate during brain aging and neurodegenerative disorders; it has been linked to improved memory or decreased cognitive deficit (Markowska et al., 1994) while CREB-dependent gene expression is essential for long-term memory and neuronal plasticity and CRTCs are its crucial coactivators (Nonaka et al., 2014).

Another interesting finding in our work was the up-regulation of the glucagon-like peptide 1 receptor (Glp1r) by H-EVOO; in fact, Glp1r, besides being involved in the regulation

of insulin signaling, also plays important roles in neuroprotection; in particular, mice lacking this receptor display impairments in synaptic plasticity and memory deficit (Abbas et al., 2009).

When we applied a more stringent criterion for statistical analysis, we found that dietary intervention with H-EVOO was associated with a significant up-regulation of Notch1. Notch pathway is a highly conserved controller of neural development and it is also involved in neurogenesis, neuritic growth (Sestan et al., 1999), neural stem cell maintenance (Hitoshi et al., 2002), synaptic plasticity (Poirazi and Mel, 2001) and long term memory (Shors et al., 2001). Loss of function mutations in Notch1, are also associated to deficits in spatial learning and memory (Costa et al., 2003).

We also found increased expression of several transporter proteins, as well as cation and anion channels, which might contribute to improve neuronal and glial function.

Among the ones over-expressed in H-EVOO treated mice, we also found apolipoprotein C-II (ApoC-II) a component of very low density lipoproteins involved in lipid metabolism, whose levels are decreased in spinocerebellar ataxias, a neurodegenerative disease characterized by neurological symptoms such as loss of balance and motor coordination (Swarup et al., 2012). Interestingly, aldehyde dehydrogenase 1 (Aldh1a2) was also up-regulated in mice fed H-EVOO: Aldh1a2 is the rate-limiting retinoic acid-synthesizing enzyme; it has been reported that decreased retinoic acid levels in the hippocampus lead to impaired neurogenesis and performance in cognitive tasks (Jacobs et al., 2006) and in spatial learning and memory (Cocco et al., 2002). Moreover, Aldhs play an important role in detoxifying aldehydes; mice lacking Aldh1 exhibit age-dependent deficits in motor performance assessed on an accelerating rotarod (Wey et al., 2012). Finally, a common loss of function genetic polymorphism (ALDH2*2) has been identified as a risk factor for Alzheimer's disease (Hao et al., 2011).

The modulation of the above mentioned genes, might represent a previously un-reported mechanism by which olive oil phenols exert their beneficial effects on motor and cognitive behavior in aging mice.

We also performed gene pathway analysis in order to evaluate the effects of small, but consistent changes in gene expression within a biological process and found out that the pathway of agrin was significantly up-regulated in H-EVOO treated mice; in peripheral ganglia, agrin mediates the acetylcholine receptor clustering at the neuromuscular junction (Gingras et al., 2007) ; agrin is also expressed in the brain where it acts as a synapse-organizing molecule and activates ERK1/2 and CREB signaling (Chiamulera et al., 2008; Rimer, 2011).

Another pathway up-regulated by H-EVOO is the prion pathway (PrP). PrP serves as a receptor for a variety of ligands, including heparan sulfate, laminin, nerve cell adhesion

molecule, various synaptic and stress-inducible proteins, suggesting that it possesses physiological, neuro-protective functions (Onodera et al., 2014).

Interestingly, the Ephrin (EphA4) signaling pathways was also modulated in mice treated with H-EVOO; EphA4 signaling in neurons regulates spine size and density, synaptic strength and is involved in neuronal-astrocytic communication (Murai et al., 2011). Mice lacking EphA4, display deficits in motor coordination and reduced spatial memory (Willi et al., 2012), suggesting that H-EVOO-induced improvements in motor coordination and spatial memory might be associated to the modulation of this pathway.

We did not find any significant specific gene modulation in the cerebellum; however, pathway analysis found that β-arrestin signaling was down-regulated while Myocyte enhancer factor 2 (MEF2) pathway was up-regulated in the cerebellum of H-EVOO treated mice. MEF2 proteins are important regulators of gene expression during the development of skeletal, cardiac and smooth muscle. MEF2 proteins are also present in the brain and have been implicated in cerebellar neuron survival and differentiation (Li et al., 2001). β-arrestins represent a small family of G protein-coupled receptors (GPCRs) regulators, which provide modulating effects by facilitating desensitization and internalization of GPCRs as well as initiating their own signaling. Recent reports have demonstrated that β-arrestins levels correlated with neuronal loss and amyloid-β peptide pathology in brains of Alzheimer patients and animal models (Jiang et al., 2013).

Overall, these results indicate that olive oil phenols exert several beneficial effects in the brain by modulating signaling cascades which impact neuronal function and synaptic plasticity. The modulation of these genes and pathways can be thus considered among the molecular mechanism by which olive oil phenols exert their beneficial effects on memory and motor coordination in aging mice.

Fine-tuning of gene expression is a fundamental requirement for development and function of cells and organs. This requirement is particularly obvious in the central nervous system where function depends not only on static circuitries, but on plastic changes at the synaptic level allowing both learning and memory. It is evident that these processes necessitate flexibility and stability at the same time. These two features can be achieved by complex molecular networks between regulatory mechanisms and interactions between microRNAs (miRNAs) and their target genes.

MiRNAs represent a class of small regulatory noncoding RNAs ~22 bp in length that mediate post-transcriptional silencing of gene expression through the recognition of specific sequences in target messenger RNAs (Lai, 2002). The mechanism by which miRNAs regulate gene expression is complex, since one miRNA can target several thousand mRNAs, and one

mRNA can be regulated by several miRNAs. miRNAs are involved in different functional processes, including memory and cognitive functions and are often deregulated during cellular senescence, aging and disease; many miRNAs are highly expressed in the adult nervous system in a spatially and temporally controlled manner in normal physiology, as well as in certain pathological conditions (Bates et al., 2009). These findings emphasize that gene regulation networks based on miRNA activities may be particularly important for brain function and perturbation of these networks may result in abnormal brain function.

However, neither miRNA specific function nor the gene regulatory networks with which they are associated have been studied in detail; also incompletely understood is how miRNAs affect the aging brain.

In this study, we used whole genome expression analyses to investigate the expression changes of miRNAs during aging in the mouse brain; we also tried to understand if these changes can be counteracted by a dietary treatment. In our case we used supplementation with extra virgin olive oil rich in phenolic compounds (H-EVOO) administered from middle age to senescence.

It is worth highlighting that gene expression changes that occur in the cortex of old mice were mainly down-regulated; in accordance, miRNA were mostly up-regulated with growing age. These results indicate that the aging process is accompanied by deep changes in the transcriptional regulation.

Overall, cortex of H-EVOO-fed mice displayed miRNA expression profiles similar to those observed in young mice. Sixty-three miRNAs, out of 1203 analyzed, were significantly down-regulated compared to the L-EVOO group; evidence suggesting that these miRNA are potentially relevant to brain aging comes from their predicted targets: mir-484 targets Crtc3 gene, mir-137-3p BMP7 gene, mir-27 the NGFR and GLP1R gene, mir-340 targets Aldh1a2 gene. Actually, we found an inverse correlation with their target genes. miR-30c-b/5p and miR-34a-b-c/5p are predicted to target Notch1 gene and, indeed, their expression was inversely correlated with Notch1 expression.

The analysis of miRNAs performed on mice fed resveratrol, showed a very different profile from that observed in young mice, characterized by an extensive miRNA down-regulation. This result was not seen in the group treated with H-EVOO and suggests that resveratrol is capable of modulating a wide range of biological processes with respect to H-EVOO. Further analyses on the gene expression profiles of the cortex harvested from these mice will permit to better explore the consequences of this widespread miRNA down-regulation.

We also searched correlations between miRNA expression and behavioral performances. For example, mir-484, which control the expression of Crtc3, was inversely associated to spatial memory performances when resveratrol fed mice which did not performed better, were not included in the analysis.

Mir-27 and mir-137 control the expression of NGFR and GLP1R and of BMP, respectively, and were correlated to motor coordination in all mice and to the emotional behavior of aging mice in L-EVOO and H-EVOO groups.

The expression of mir-30c-5p and mi-34a-5p which control Notch1 gene, was inversely correlated to the rota-rod and step-down performances, the former in both young and old mice and the last only in aging mice. Mir-30a-5p and mir-124-3p were correlated to the performances in the light-dark box. miR-124 targets glucocorticoid receptors, an important component of stress responses and thus might be involved in influencing processes with a stress component. This correlation resulted to be strong in the old animals but was no longer observed when taking into account both young and old mice, indicating an age-specific role of these miRNAs in the modulation of anxious behavior.

Furthermore, miR-124 also targets plasticity related genes, like cAMP response element-binding protein (CREB) which might contribute to enhanced spatial memory performances in all mice but not in resveratrol fed ones.

Li and co-workers have identified age-associated increases of miR-30d, miR-34a, miR-468, miR-669b and miR-709 in C57Bl/6 mouse brain and liver, and of miR-22, miR-101a, miR-720, miR-721 in brain (Li et al., 2011). The same group has shown that the age-dependent increased expression of miR-181a-1, miR-30e and miR-34a can be counteracted by calorie restriction (Khanna et al., 2011), along with down-regulation of pro-apoptotic and up-regulation of anti-apoptotic genes. MiR-34a increases have been associated to aging and learning dysfunctions in animal models and Alzheimer disease (Liu et al., 2012; Zovoilis et al., 2011). miR-34 and miR-124 expression have been reported to gradually increase during brain development and aging (Eda et al., 2011); it is important to mention that the inhibition of miR-34c improved memory functions in aged mice (Zovoilis et al., 2011). Accordingly, we detected no expression of this miRNA in the cortex of H-EVOO mice which performed better in the in the step down test.

The health effects of polyphenols have been often correlated to changes in gene expression (Park et al., 2009; Bayram et al., 2012) and these modifications might be the result of interactions with signaling cascades as well as consequences of epigenetic mechanisms.

A large part of the studies focusing on miRNAs as mediators of polyphenol effects were obtained *in vitro*, mainly on cancer cells, testing single compounds such as epigallocatechin

gallate (Li et al., 2010; Tsang et al., 2010) or resveratrol (Bae et al., 2011) or extracts (Bladé et al., 2013). The ability of dietary polyphenols to modulate miRNAs expression has also been reported in a few *in vivo* studies: in the liver of rats treated with grape seed proanthocyanidins (Baselga-Escudero et al., 2012) or with several individual polyphenols (Milenkovic et al., 2012). Among the miRNAs found to be affected by these compounds, miR-30 family members have been described in several studies: miR-30b was reported to be down-regulated in HepG2 cells treated with proanthocyanidin extracts from cocoa and grape seed (Arola-Arnal and Bladé, 2011) and miR-30c was down-regulated in the liver of C57B6/J mice treated with different polyphenols, among which quercetin, hesperidin, naringenin, anthocyanin, catechin and curcumin (Milenkovic et al., 2012). The miR-30 family is involved in the regulation of several pathways including the NF-kappa-B pathway, mitochondria activities, oxidative phosphorylation and glutathione metabolism and their expression is up-regulated during Rb-dependent senescence in HeLa cervical carcinoma cells and in primary human fibroblasts undergoing replicative senescence (Martinez et al., 2011). In our study, most of the miR-30 family members were expressed at lower level in H-EVOO compared to L-EVOO-treated mice, suggesting that they can have an important role in the molecular, biochemical and behavioral effects observed in these animals.

Moreover, many differentially expressed miRNAs were predicted to target pathways and processes relevant to aging such as neurotrophin, axon guidance pathway, dopamine and glutamate transmission which regulate synaptic plasticity (Tanaka et al., 2008; Scharfman and Chao, 2013).

When we extended our examinations on miRNA expression profiles of a mouse model of Alzheimer's disease, we found that miR-146, mir-101, mir-328, mir-181 and miR-29, which were significantly down-regulated in our dataset, have been linked to neuro-inflammation and Alzheimer's disease (Kim et al., 2014).

Because miRNAs expression profiles can be easily studied in in human plasma samples by PCR, these findings indicate a potential importance of measuring circulating miRNAs as a tool for the identification of neuronal aging and for testing the effectiveness of anti-aging therapies.

In conclusion, our work has shown that a long-term administration of olive oil phenols can modify gene and miRNA expression profiles in the cerebral cortex of aged mice along with cognitive, motor and emotional behavior. We have previously shown a correlation between a reduction in lipid peroxidation in the cerebellum and improved motor coordination (Pitozzi et al., 2012). In light of the very limited gene expression changes found in this brain area, we hypothesize that this treatment affects the cerebellum mainly through the protection from

oxidative stress. Instead, in the cerebral cortex the modulation of the genome was significant and involved pathways related to synaptic plasticity and neuronal function, that might be associated with the memory, motor and emotional improvements found in these animals.

The pattern of altered miRNA expression observed in our work suggests that multiple gene regulation relationships are affected in aging; they could, therefore, be counteracted by treatments with olive oil phenols. It is interesting to underline that the changes in both behavior and cerebral gene and miRNAs expression induced by the treatment with olive oil rich in phenols were already evident after 6 months of treatment , when the animals were still middle-aged.

Our nutraceutical approach, suggests that long term treatment with olive oil phenols could be considered a neuroprotective strategy for the prevention of brain aging by the induction of health-promoting genes and the coordinated modulation of miRNAs.

Discussion of the experimental model *in vitro*

Neurons are particularly vulnerable to age-related changes which affect their function and contribute to the onset of age-related neurodegenerative pathologies. Neuro-glial co-cultures are an integrated model accounting for the reciprocal and profound interactions between neurons and glia, currently used only for short-term experiments. Here we studied the temporal evolution and senescence of this integrated system. We observed a significant variability in obtaining long-term cell survival *in vitro,* possibly due to variations in cell isolation procedures, or to frequent medium changes. However, once the system is functioning it can provide useful information. In fact, we were able to demonstrate that a relatively long period in culture determines the appearance of a senescent phenotype, offering the possibility of investigating age-related changes.

Interestingly, neuro-glial co-cultures show some of the senescence features observed in proliferating peripheral cells such as the progressive accumulation of SA-β-gal. This observation is in line with Bhanu et al. (2010) who reported a significant increase in the SA-β-gal in cerebellar granular neurons aged *in vitro* for 30 DIV and with Geng et al. (2010) after 20 DIV and Dong et al. (2011) in hippocampal neurons after 30 DIV; resveratrol induces a strong, concentration-dependent decrease in the number of cells positive for SA-β-gal when administered to neuro-glial co-cultures from 15 to 27 DIV. We reported similar effects in human fibroblasts undergoing replicative senescence (Giovannelli et al., 2011). Other than SA-β-gal, several data suggest that during senescence the signaling pathway that responds to DNA damage (DDR) is activated and γ-H2AX is among the markers of such activation (Jurk et al., 2012). Consistently, we found a progressive increase in γ-H2AX protein expression as a function of days *in vitro*. *In vivo* results also support the notion of the DDR activation during senescence; Jurk et al. (2012) reported that old mice displayed multiple markers of the senescent phenotype including ROS production, interleukin secretion, SA-β-gal activity and γ-H2AX. Barral et al. (2014) also reported that the cerebral cortex was a major site of expression of γ-H2AX in both neurons and astrocytes in fully mature and senescent mice and that the appearance of γ-H2AX was primarily related to a DDR occurring in post-mitotic neurons and glial cells. Interestingly, resveratrol was able to strongly reduce γ-H2AX protein levels thus reducing the DNA damage signaling cascade in senescent neuro–glial co-cultures. This effect was similar to that reported by Halicka et al. (2012) in several proliferating cell lines and in human lymphocytes (Halicka et al., 2012).

In our model of neuro-glial co-cultures, we observed an increase in the level of oxidative damage to proteins as a function of days *in vitro*. Increased oxidative damage on

proteins was previously reported in neurons upon aging (Aksenova et al., 1999) and carbonyl residues were considered among the contributors to the onset of age-related neurodegenerative diseases (Rahmadi et al., 2011). Oxidation damaged proteins have been shown to increase as a function of age and a number of age-related diseases have been associated with elevated levels of these proteins (Baraibar and Friguet, 2013). Instead, no difference in nitrotyrosine levels was found in senescence *in vitro*, in agreement with previous data in a similar model (Lesuisse and Martin, 2002) showing that some proteins accumulate nitration, whereas others show a reduced nitration profile in cortical neurons. *In vivo*, nitrotyrosine was found to be decreased (Cakatay et al., 2001) or increased (Shin et al., 2002) in aged rats.

Lipid peroxidation is another major outcomes of free radical-mediated injury which directly damages membranes and generates a number of secondary neurotoxic products such as 4-hydroxynonenal (4-HNE) which binds to synaptosomal proteins and changes protein conformation and function. Accordingly, we found increased levels of 4-HNE as a prominent marker of aging in neuro-glial co-cultures and a strong protective effect of resveratrol in line with the neuroprotective effects of this compounds (Bastianetto, 2014).

Senescent cultures are also characterized by a strong increase in the production of the proinflammatory cytokine, IL-6, which is completely counteracted by resveratrol. Several reports indicate that senescent cells express a senescence-associated secretory phenotype (SASP) consisting of an increased secretion of growth factors, inflammatory cytokines and proteolytic enzymes, and involved in microenvironment remodeling (Coppe et al., 2010). As a whole, neuro-glial co-cultures show features typical of *in vivo* aging and a well-established anti-aging molecule, such as resveratrol, reverses these changes.

Besides recapitulating some characteristics of cellular senescence, neuro-glial co-cultures also display age-associated degenerative changes such as progressive neuronal loss and a decline in the dendritic network. A reduction in synaptic and dendritic markers has been described in hippocampal neurons aged *in vitro* (Bertrand et al., 2011). Dong et al. reported that the number of neurons decreases after DIV 25 *in vitro* with a concomitant increase in SA-β-gal (Dong et al., 2011). In our experiments we demonstrated that changes in neurons are accompanied by activation of glial cells, resulting in hypertrophy of astrocytes and age-associated gliosis.

The activation of astrocytes produces a state of low-level inflammation, playing an important role both in aging and in age-related neurological diseases (Middeldorp and Hol, 2011). Aged astrocytes do not support neuronal survival in mixed neuronal-glial cultures as efficiently as young cells Pertusa et al. (2007). Kremsky et al. (2012) demonstrated that primary

mixed glial cultures show age-related increased expression of genes related to inflammatory processes, and that these changes were modulated by the presence of co-cultured microglial cells or neurons. *In vivo* data also indicate that aged astrocytes show features of the senescence-associated secretory phenotype, as described in fibroblasts and endothelial cells (Salminen et al., 2011). We can thus conclude that in neuro-glial co-cultures *in vitro,* some neurons undergo senescence while others are progressively lost, as indicated by the time-dependent decrease in markers of neuronal nuclei and synaptic contacts. In this context, it is feasible that the activated astrocytes lose their function of supporting neurons.

Resveratrol, has been reported to be neuro-protective in rodent models of neurodegeneration and central nervous system injury (Huber and Superti-Furga, 2011). Resveratrol also prevented ageing-related cognitive decline in rodent models (Murase et al., 2009 and Oomen et al., 2009) and humans (Kennedy et al., 2010). In our model resveratrol failed to counteract the senescence-dependent loss of neuronal cell bodies and connections but exerted a clear and concentration-dependent effect in reducing astrogliosis. An analogous effect was reported by Genade and Lang who found that resveratrol prevents the aging-associated dysregulation of GFAP expression without avoiding the loss of neurons in the midbrain of the fast-aging fish *Nothobranchius guentheri* (Genade and Lang 2013).

Alterations of senescent cells are accompanied by changes in miRNA expression. miRNAs act as master negative regulators of gene expression and a single miRNA can target many mRNAs in parallel, thus having the potential to simultaneously modify multiple cell pathways such as proliferation, differentiation, senescence and death (Ambros, 2004).

We observed a substantial miRNA down-regulation in neuro-glial co-cultures aged *in vitro* compared to their younger counterparts.

A general decline of miRNA expression was previously associated to the aging process in peripheral proliferating cells *in vitro*: experiments from Brosh and colleagues demonstrated that the onset of cellular senescence significantly decreases miRNA expression in fibroblasts (Brosh et al., 2008). Moreover, genome-wide expression analysis in aging individuals revealed a general decline in miRNA levels in peripheral blood mononuclear cells as compared to young individuals (Noren et al., 2010; El Sharawy et al., 2012). Interestingly, several miRNAs down-regulated in 27 DIV neuro-glial co-culture (such as miR-17, miR-19b, miR-20a and miR-106a) were previously found to be less abundant in cells from older humans (Hackl et al., 2010). The miR-17-92 cluster has been reported to target several proteins involved in cell cycle, such as p21 and has also been found as a commonly down-regulated microRNA cluster in human replicative and stress-induced senescence (Hackl et al., 2010; Li et al., 2009). Furthermore, an increased level of miR-17-92 was associated with a protection against ROS and DNA damage in

RB mutated tumor cells (Ebi et al., 2009). We can assume that a decrease in miR-17-92, as detected in our neuro-glial co-cultures aged *in vitro*, results in increased oxidative stress and DNA damage and thus contributes to senescence-associated neuronal alterations.

The overall effect of resveratrol in our experiments, was to shift the miRNA expression pattern of senescent neuro-glial co-cultures towards that observed in mature neuro-glial co-cultures (15 DIV). This observation is of particular interest and may indicate new mechanisms by which resveratrol exerts its anti-aging effects.

The gene encoding for β-galactosidase (*GLB*) was also predicted by the DIANA microT to be up-regulated, based on the down-regulation of mir-669c-3p in aged co-cultures; this is in agreement with the increased β-galactosidase activity found at senescence. This miRNA is among the most down-regulated in our 27 DIV neuro-glial co-cultures and resveratrol concentration-dependently restored its expression al levels quite below those of the 15 DIV neuro-glial co-cultures, suggesting a role for mir-669c-3p in the control of SA-β-gal and thus in the appearance of senescence. This result is also supported by the finding that several members of its clustered miRNAs, such as mir-466, were also down-regulated in 27 DIV and concentration-dependently increased after resveratrol treatment; searching for mir-466 family targets, we found that some are capable to target the ataxia telangiectasia mutated (ATM) kinase. ATM is one of the major proteins involved in the DNA damage response and in the induction of senescence, through its downstream effect on H2AX. Interestingly, the expression of this family of miRNAs was restored by resveratrol, which also reduced β-galactosidase staining and γ-H2AX protein expression in aged cultures. Moreover, γ-H2AX has been reported to be a target for mir-24 in blood cells (Lal et al., 2009), similarly to what we observed in neuro-glial co-cultures. Another finding supporting the role of miRNAs in regulating the senescence phenotype is that miR-26a-5p and mir-26b-5p, are predicted to target the transcription factor E2F7, which has been reported to cooperate with RB to promote senescence in fibroblasts (Aksoy et al., 2012).

γ-H2AX is also predicted to be targeted by mir-7a-5p which is another miRNAs with this behavior. miR-7a-5p is also predicted to target the Poly(ADP-ribose) polymerase-1 (PARP-1), a nuclear enzyme that contributes to inflammation and neuronal death under stress conditions; PARP-1 accumulation has been identified in human Alzheimer's disease (Strosznajder et al., 2012). miR-7 was also previously shown to control the growth of the developing cerebral cortex by targeting genes in the p53 pathway and its functional knockdown reduces neurogenesis and the number of NeuN positive neurons (Pollock et al., 2014). miR-188-5p, also decreased in 27 DIV, was reported to be involved in the reduction in dendritic spine density induced by up-regulating Nrp-2 expression in hippocampal neurons

from rat primary cultures (Lee et al., 2012). Moreover, we also found both mir-23a and mir-23b to be down-regulated; a reduced expression of miR-23b was inversely correlated with an elevation of Apaf-1 expression during neuronal apoptosis (Chen et al., 2014).

We investigated if some of the miRNAs down-regulated in senescent neuro-glial co-cultures might be linked to the induction of GFAP protein expression and astrogliosis. Interestingly, we found that miR-149-3p and mir-669h-3p, which are not expressed in 27 DIV but restored after resveratrol treatment, were predicted to target GFAP gene. This is the first report suggesting a link between the activation of astrocytes and miRNAs expression.

Focusing on those miRNAs that target genes encoding for proteins whose expression was actually measured in our long-term neuro-glial co-cultures, we were able to confirm most of the predicted miRNA–mRNA interactions. In fact, the up-regulation of the genes encoding for GFAP, IL-6 and H2AX, predicted on the basis of the down regulation of the respective targeting miRNAs 149-3p, let-7a/b/c/g-5p and 124-3p/24-3p, were actually confirmed by western blotting, showing increased levels of the three proteins.

Similarly, the predicted up-regulation of Nrp-2 and Apaf-1 genes, encoding for proteins involved in dendritic spine reduction and neuronal death, was supported by the finding that MAP-2 and NeuN proteins were down-regulated in senescent cultures.

In conclusion, our data disclose previously unknown putative miRNA-mRNA relationships and suggest a functional role for these interactions in the frame of the senescence process. The global effect of resveratrol was to shift the miRNAs expression patterns of senescent neuro-glial co-cultures towards those of mature neuro-glial co-cultures at 15 DIV. Several miRNAs, involved in the control of different cellular processes such as inflammation, apoptosis, senescence and neurodegeneration, were modulated by resveratrol. The modulation of miRNAs expression by resveratrol could constitute a new pathway by which this compound exerts its health-promoting effect.

By comparing age-associated changes in the expression profiles of miRNAs in the *in vitro* model with those measured in the cortex of physiologically aged 18- and 24-month-old mice, we found only a few similarities, such as the down-regulation of mir-7b-3p, mir-452-5p and mir-290-5p. These were not exclusively related to aging, being observed also in the cortex of TgCRND8 mice. Histone H3.3, a regulator of chromatin, is constitutively expressed throughout the cell cycle and in quiescence and it is incorporated into chromatin in a DNA synthesis-independent manner. This histone accumulation was reported in non-dividing differentiated and mature rat brain cortical neurons (Bosch and Suau, 1995). Chromatin structure is extensively remodeled upon senescence entry, as exemplified by the formation of senescence-associated heterochromatin foci (SAHF) which were suggested to involve the

histone variant H3.3 (Zhang et al., 2005). Interestingly, among mir-7b-3p targets we also found the plasminogen activator inhibitor 1 precursor (PAI-1), which other than being considered a marker of senescence, was suggested to be necessary and sufficient for the induction of replicative senescence downstream of p53 (Kortlever et al., 2006). Moreover, PAI-1 expression increases with age in the brain of wild type and APP/PS1 transgenic mice and in AD patients and is correlated to the increase in Aβ accumulation during aging and in AD (Liu et al., 2011). Importantly, miR-7-induces the down-regulation of α-synuclein in the MPTP-induced neurotoxin model of Parkinson's disease, in cultured cells and in mice, suggesting its role in several neurodegenerative diseases (Junn et al., 2009). Mir-452-3p was predicted to target the glutamate dehydrogenase GLUD1. In transgenic mice over-expressing GLUD1 a loss of neurons, dendritic spines and nerve endings during the aging process was previously observed (Michaelis et al., 2011.). In another work by Bao et al, reported that GLUD1 overexpressing mice exhibited an overall significant decrease in dendrites and neurons (Bao et al., 2009). Mir-290-5p was predicted to target the histone demetilase UTX. The expression of human UTX was reported to be increased in the human brain and *C. elegans* during the aging process and has been linked to insulin signaling and to an aging-related decline in cellular functions (Jin et al., 2011).

Interestingly, DIANA-miRPath analysis indicates that miR-7b-3p and miR-452-5p are involved in mTOR and HIF-1 signaling pathways, key modulators of aging and age-related disease (Ogunshola and Antoniou, 2009; Johnson et al., 2013).

The expression profiles of miRNAs in this cellular model appears to resemble more closely to the expression profiles of TgCRND8 in mice cortex, an *in vivo* model of pathological aging and neurodegeneration. Among the 67 miRNAs down-regulated by aging both in long-term neuro-glial co-cultures and in TgCRND8 mice cortex, the miR-29 family members were previously reported to have target sites on the gene encoding for β-amyloid cleavage enzyme 1 (BACE-1), which is one of two critical enzymes required for the cleavage of amyloid precursor protein and the generation of toxic Aβ species; the loss of this cluster is negatively correlated with BACE1 expression in sporadic Alzheimer disease (Hébert et al., 2008). Both mir-328-3p and 5p were also down-regulated in 27 DIV neuro-glial co-culture and in our transgenic mice, consistently with the results by Provost who demonstrated that decreased expression levels of miR-328 in the hippocampus of aging APPSwe/PS1 mice, correlated to higher BACE-1 protein expression and enhanced Aß formation, suggesting a role for miRNAs in the development of AD (Provost, 2010). Since miRNA in clusters may share a common gene promoter and may be regulated as a whole transcriptional unit, it could be of interest to determine whether any entire cluster changed in the same direction. We found that the

majority of the miRNAs in mir-669-mir-466-mir-467 cluster changed in the same directions being down-regulated in 27 DIV and in TgCRND8 mice. In particular, mir-669h-3p was predicted to target contactin 4 protein (Cntn4), an axon-restricted protein involved in synaptogenesis and axon guidance and found to be a ligand for APP suggesting to affect the processing of APP to Aβ (Osterfield et al., 2010). Overall, the DIANA miRPath pathway enrichment analysis indicated that the most significant set of miRNAs deregulated both in senescent neuro-glial co-cultures and in TgCRND8 mice cortex is involved in pathways related to the control of aspects of survival, development, function and senescence of neurons.

In conclusion, we demonstrated that neuro-glial co-cultures show many features of cellular senescence and respond to the exposure to a known anti-aging/neuro-protective substance such as resveratrol. The comparison of global miRNA expression *in vitro* and *in vivo* suggests that neuro-glial co-cultures resemble pathological more than normal brain aging. These findings may provide insights into the epigenetic regulatory mechanisms of age-induced brain alterations, and help identify miRNAs involved in these processes. Thus, this model can be useful for investigating the cellular and molecular mechanisms involved in neuronal aging, and for the screening of anti-aging/neuro-protective compounds.

Bibliography

Abbas T, Faivre E, Hölscher C. Impairment of synaptic plasticity and memory formation in GLP-1 receptor KO mice: Interaction between type 2 diabetes and Alzheimer's disease. Behav Brain Res. 2009 Dec 14;205(1):265-271.

Abbott NJ, Rönnbäck L, Hansson E. Astrocyte-endothelial interactions at the blood-brain barrier. Nat Rev Neurosci. 2006 Jan;7(1):41-53.

Abuznait AH, Qosa H, Busnena BA, El Sayed KA, Kaddoumi A. Olive-oil-derived oleocanthal enhances β-amyloid clearance as a potential neuroprotective mechanism against Alzheimer's disease: in vitro and in vivo studies. ACS Chem Neurosci. 2013 Jun 19;4(6):973-982.

Aksenova MV, Aksenov MY, Markesbery WR, Butterfield DA. Aging in a dish: age-dependent changes of neuronal survival, protein oxidation, and creatine kinase BB expression in long-term hippocampal cell culture. J Neurosci Res. 1999;58:308-317.

Aksoy O, Chicas A, Zeng T, Zhao Z, McCurrach M, Wang X, Lowe SW. The atypical E2F family member E2F7 couples the p53 and RB pathways during cellular senescence. Genes Dev. 2012 Jul 15;26(14):1546-1557.

Alajez NM, Shi W, Hui AB, Bruce J, Lenarduzzi M, Ito E, Yue S, O'Sullivan B, Liu FF. Enhancer of Zeste homolog 2 (EZH2) is overexpressed in recurrent nasopharyngeal carcinoma and is regulated by miR-26a, miR-101, and miR-98. Cell Death Dis. 2010 Oct 21;1:1-10.

Ambros V. The functions of animal microRNAs. Nature. 2004 Sep 16;431(7006):350-355.

Amiot M.J., Fleuriet A., Macheix J.J. Importance and evolution of phenolic compounds in olive during growth and maturation. J Agric Food Chem.1996; 34:823–826.

Arola-Arnal A, Bladé C. Proanthocyanidins modulate microRNA expression in human HepG2 cells. PLoS One. 2011;6(10):1-7.

Bäckman L, Nyberg L, Lindenberger U, Li SC, Farde L. The correlative triad among aging, dopamine, and cognition: current status and future prospects. Neurosci Biobehav Rev. 2006;30(6):791-807.

Bae S, Lee EM, Cha HJ, Kim K, Yoon Y, Lee H, Kim J, Kim YJ, Lee HG, Jeung HK, Min YH, An S. Resveratrol alters microRNA expression profiles in A549 human non-small cell lung cancer cells. Mol Cells. 2011 Sep;32(3):243-249.

Bai XY, Ma Y, Ding R, Fu B, Shi S, Chen XM. miR-335 and miR-34a Promote renal senescence by suppressing mitochondrial antioxidative enzymes. J Am Soc Nephrol. 2011 Jul;22(7):1252-1261.

Balasubramanyam M, Aravind S, Gokulakrishnan K, Prabu P, Sathishkumar C, Ranjani H, Mohan V. Impaired miR-146a expression links subclinical inflammation and insulin resistance in Type 2 diabetes. Mol Cell Biochem. 2011 May;351(1-2):197-205.

Ballard C, Gauthier S, Corbett A, Brayne C, Aarsland D, Jones E. Alzheimer's disease. Lancet. 2011 Mar 19;377(9770):1019-1031.

Bao X, Pal R, Hascup KN, Wang Y, Wang WT, Xu W, Hui D, Agbas A, Wang X, Michaelis ML, Choi IY, Belousov AB, Gerhardt GA, Michaelis EK. Transgenic expression of Glud1 (glutamate dehydrogenase 1) in neurons: in vivo model of enhanced glutamate release, altered synaptic plasticity, and selective neuronal vulnerability. J Neurosci. 2009 Nov 4;29(44):13929-13944.

Baraibar MA, Friguet B. Oxidative proteome modifications target specific cellular pathways during oxidative stress, cellular senescence and aging. Exp Gerontol. 2013 Jul;48(7):620-625.

Barberger-Gateau P. Nutrition and brain aging: how can we move ahead? Eur J Clin Nutr. 2014 Nov;68(11):1245-1249.

Barral S, Beltramo R, Salio C, Aimar P, Lossi L, Merighi A. Phosphorylation of histone H2AX in the mouse brain from development to senescence. Int J Mol Sci. 2014 Jan 21;15(1):1554-1573.

Bartel DP. MicroRNAs: genomics, biogenesis, mechanism, and function. Cell. 2004 Jan 23;116(2):281-297.

Barzilai N, Huffman DM, Muzumdar RH, Bartke A. The critical role of metabolic pathways in aging. Diabetes. 2012 Jun;61(6):1315-1322.

Baselga-Escudero L, Bladé C, Ribas-Latre A, Casanova E, Salvadó MJ, Arola L, Arola-Arnal A. Grape seed proanthocyanidins repress the hepatic lipid regulators miR-33 and miR-122 in rats. Mol Nutr Food Res. 2012 Nov;56(11):1636-1646.

Baselga-Escudero L, Blade C, Ribas-Latre A, Casanova E, Suárez M, Torres JL, Salvadó MJ, Arola L, Arola-Arnal A. Resveratrol and EGCG bind directly and distinctively to miR-33a and miR-22 and modulate divergently their levels in hepatic cells. Nucleic Acids Res. 2014 Jan;42(2):882-892.

Bastianetto S, Ménard C, Quirion R. Neuroprotective action of resveratrol. Biochim Biophys Acta. 2014 Oct 2.

Bates DJ, Liang R, Li N, Wang E. The impact of noncoding RNA on the biochemical and molecular mechanisms of aging. Biochim Biophys Acta. 2009 Oct;1790(10):970-979.

Baur JA, Pearson KJ, Price NL, Jamieson HA, Lerin C, Kalra A, Prabhu VV, Allard JS, Lopez-Lluch G, Lewis K, Pistell PJ, Poosala S, Becker KG, Boss O, Gwinn D, Wang M, Ramaswamy S, Fishbein KW, Spencer RG, Lakatta EG, Le Couteur D, Shaw RJ, Navas P, Puigserver P, Ingram DK, de Cabo R, Sinclair DA. Resveratrol improves health and survival of mice on a high-calorie diet. Nature. 2006 Nov 16;444(7117):337-342.

Baur JA, Sinclair DA. Therapeutic potential of resveratrol: the in vivo evidence. Nat Rev Drug Discov 2006;5:493-506

Baur JA. Resveratrol, sirtuins, and the promise of a DR mimetic. Mech Ageing Dev 2010;3:261-269.

Bayram B, Ozcelik B, Grimm S, Roeder T, Schrader C, Ernst IM, Wagner AE, Grune T, Frank J, Rimbach G. A diet rich in olive oil phenolics reduces oxidative stress in the heart of SAMP8 mice by induction of Nrf2-dependent gene expression. Rejuvenation Res. 2012 Feb;15(1):71-81.

Beauchamp GK, Keast RS, Morel D, Lin J, Pika J, Han Q, Lee CH, Smith AB, Breslin PA. Phytochemistry: ibuprofen-like activity in extra-virgin olive oil. Nature. 2005 Sep 1;437(7055):45-46.

Becker and Haferkamp. Molecular Mechanisms of Cellular Senescence http://dx.doi.org/10.5772/54120

Bellucci A, Luccanini F, Scali C, Prosperi C, Giovannini MG, Pepeu G, Casamenti F. Cholinergic dysfunction, neuronal damage and axonal loss in TgCRND8 mice. Neurobiology of Disease. 2006;23:260-272.

Bertrand SJ, Aksenova MV, Aksenov MY, Mactutus CF, Booze RM. Endogenous amyloidogenesis in long-term rat hippocampal cell cultures. BMC Neurosci. 2011;12:38-39.

Bezprozvanny I, Mattson MP. Neuronal calcium mishandling and the pathogenesis of Alzheimer's disease. Trends Neurosci. 2008 Sep;31(9):454-463.

Bhanu MU, Mandraju RK, Bhaskar C, Kondapi AK. Cultured cerebellar granule neurons as an in vitro aging model: topoisomerase IIbeta as an additional biomarker in DNA repair and aging. Toxicol In Vitro. 2010;24:1935-1945.

Bhaumik D, Scott GK, Schokrpur S, Patil CK, Orjalo AV, Rodier F, Lithgow GJ, Campisi J. MicroRNAs miR-146a/b negatively modulate the senescence-associated inflammatory mediators IL-6 and IL-8. Aging (Albany NY). 2009 Apr;1(4):402-411.

Bickford P. Motor learning deficits in aged rats are correlated with loss of cerebellar noradrenergic function. Brain Res 1993;620:133–138.

Bladé C, Baselga-Escudero L, Salvadó MJ, Arola-Arnal A. miRNAs, polyphenols, and chronic disease. Mol Nutr Food Res. 2013 Jan;57(1):58-70.

Blalock EM, Chen KC, Sharrow K, Herman JP, Porter NM, Foster TC, Landfield PW. Gene microarrays in hippocampal aging: statistical profiling identifies novel processes correlated with cognitive impairment. J Neurosci. 2003 May 1;23(9):3807-3819.

Borgdorff V, Lleonart ME, Bishop CL, Fessart D, Bergin AH, Overhoff MG, Beach DH. Multiple microRNAs rescue from Ras-induced senescence by inhibiting p21(Waf1/Cip1). Oncogene. 2010 Apr 15;29(15):2262-2271.

Bosch A, Suau P. Changes in core histone variant composition in differentiating neurons: the roles of differential turnover and synthesis rates. Eur J Cell Biol. 1995 Nov;68(3):220-225.

Brosh R, Shalgi R, Liran A, Landan G, Korotayev K, Nguyen GH, Enerly E, Johnsen H, Buganim Y, Solomon H, Goldstein I, Madar S, Goldfinger N, Borresen-Dale AL, Ginsberg D, Harris CC, Pilpel Y, Oren M, Rotter V. p53-Repressed miRNAs are involved with E2F in a feed-forward loop promoting proliferation. Mol Syst Biol. 2008;4:229-232.

Broughton S, Partridge L. Insulin/IGF-like signalling, the central nervous system and aging. Biochem J. 2009 Feb 15;418(1):1-12.

Bruni N, Cortesi N, Fiorino P. Influence of agricultural techniques, cultivar and area of origin on characteristics of virgin olive oil and levels of some of its “minor” components. Olivae. 994:28–34.

Buckland G, Mayen AL, Agudo A, Travier N, Navarro C, Huerta JM, Chirlaque MD, Barricarte A, Ardanaz E, Moreno-Iribas C, Marin P, Quiros JR, Redondo ML, Amiano P, Dorronsoro M, Arriola L, Molina E, Sanchez MJ, Gonzalez CA: Olive oil intake and mortality within the Spanish population (EPIC-Spain). Am J Clin Nutr 2012, 96:142-149.

Burch JB, Augustine AD, Frieden LA, Hadley E, Howcroft TK, Johnson R, Khalsa PS, Kohanski RA, Li XL, Macchiarini F, Niederehe G, Oh YS, Pawlyk AC, Rodriguez H, Rowland JH, Shen GL, Sierra F, Wise BC. Advances in geroscience: impact on healthspan and chronic disease. J Gerontol A Biol Sci Med Sci. 2014 Jun;69 Suppl 1:S1-S3.

Burnett C, Valentini S, Cabreiro F, Goss M, Somogyvári M, Piper MD, Hoddinott M, Sutphin GL, Leko V, McElwee JJ, Vazquez-Manrique RP, Orfila AM, Ackerman D, Au C, Vinti G, Riesen M, Howard K, Neri C, Bedalov A, Kaeberlein M, Soti C, Partridge L, Gems D. Absence of effects of Sir2 overexpression on lifespan in C. elegans and Drosophila. Nature. 2011 Sep 21;477(7365):482-485.

Cakatay U, Telci A, Kayali R, Tekeli F, Akcay T, Sivas A. Relation of oxidative protein damage and nitrotyrosine levels in the aging rat brain. Exp Gerontol. 2001;36:221-229.

Campisi J, d'Adda di Fagagna F. Cellular senescence: when bad things happen to good cells. Nat Rev Mol Cell Biol. 2007 Sep;8(9):729-740.

Campisi J. Cancer and ageing: rival demons? Nat Rev Cancer. 2003 May;3(5):339-349.

Campisi J. Cellular senescence as a tumor-suppressor mechanism. Trends Cell Biol. 2001 Nov;11(11):S27-31.

Campuzano O, Castillo-Ruiz MM, Acarin L, Castellano B, Gonzalez B. Increased levels of proinflammatory cytokines in the aged rat brain attenuate injury-induced cytokine response after excitotoxic damage. J Neurosci Res. 2009 Aug 15;87(11):2484-2497.

Carmignoto G, Gómez-Gonzalo M. The contribution of astrocyte signalling to neurovascular coupling. Brain Res Rev. 2010 May;63(1-2):138-148.

Chang C-F, Lin S-Z, Chiang Y-H, Morales M, Chou J, Lein P, Chen H-L, Hoffer BJ, Wang Y. Intravenous administration of bone morphogenetic protein-7 after ischemia improves motor function in stroke rats. Stroke. 2003;15(2):558–564.

Chen Q, Xu J, Li L, Li H, Mao S, Zhang F, Zen K, Zhang CY, Zhang Q. MicroRNA-23a/b and microRNA-27a/b suppress Apaf-1 protein and alleviate hypoxia-induced neuronal apoptosis. Cell Death Dis. 2014 Mar 20;5:e1132.

Chen X, Ba Y, Ma L, Cai X, Yin Y, Wang K, Guo J, Zhang Y, Chen J, Guo X, Li Q, Li X, Wang W, Wang J, Jiang X, Xiang Y, Xu C, Zheng P, Zhang J, Li R, Zhang H, Shang X, Gong T, Ning G, Zen K, Zhang CY (2008) Characterization of microRNAs in serum: a novel class of biomarkers for diagnosis of cancer and other diseases. Cell Res 18(10):997–1006.

Chernova T, Nicotera P, Smith AG. Heme deficiency is associated with senescence and causes suppression of N-methyl-D-aspartate receptor subunits expression in primary cortical neurons. Mol Pharmacol. 2006 Mar;69(3):697-705.

Chiamulera C, Di Chio M, Tedesco V, Cantù C, Formaggio E, Fumagalli G. Nicotine-induced phosphorylation of phosphorylated cyclic AMP response element-binding protein (pCREB) in hippocampal neurons is potentiated by agrin. Neurosci Lett. 2008 Sep 19;442(3):234-238.

Cicerale S, Lucas L, Keast R. Biological activities of phenolic compounds present in virgin olive oil. Int J Mol Sci. 2010 Feb 2;11(2):458-479.

Cimato A., Mattei A., Osti M. Variation of polyphenol composition with harvesting period. Acta Horticulturae. 990; 286: 453–456.

Cocco S, Diaz G, Stancampiano R, Diana A, Carta M, Curreli R, Sarais L, Fadda F. Vitamin A deficiency produces spatial learning and memory impairment in rats. Neuroscience. 2002;115(2):475-482.

Colman RJ, Anderson RM, Johnson SC, Kastman EK, Kosmatka KJ, Beasley TM, Allison DB, Cruzen C, Simmons HA, Kemnitz JW, Weindruch R Caloric restriction delays disease onset and mortality in rhesus monkeys. Science. 2009 Jul 10; 325(5937):201-204.

Coppe JP, Desprez PY, Krtolica A, Campisi J. The Senescence-Associated Secretory Phenotype: The Dark Side of Tumor Suppression. Annual Review of Pathology-Mechanisms of Disease. 2010;5:99-118.

Corona G, Tzounis X, Assunta Dessì M, Deiana M, Debnam ES, Visioli F, Spencer JP. The fate of olive oil polyphenols in the gastrointestinal tract: implications of gastric and colonic microflora-dependent biotransformation. Free Radic Res. 2006 Jun;40(6):647-658.

Correa-Salde V Albesa I. Reactive oxidant species and oxidation of protein and heamoglobin as biomarkers of susceptibility to stress caused by chloramphenicol. Biomedicine & Pharmacotherapy. 2009;63:100-104.

Costa RM, Honjo T, Silva AJ. Learning and memory deficits in Notch mutant mice. Curr Biol. 2003 Aug 5;13(15):1348-1354.

Covas MI, Nyyssönen K, Poulsen HE, Kaikkonen J, Zunft HJ, Kiesewetter H, Gaddi A, de la Torre R, Mursu J, Bäumler H, Nascetti S, Salonen JT, Fitó M, Virtanen J, Marrugat J; EUROLIVE Study Group. The effect of polyphenols in olive oil on heart disease risk factors: a randomized trial. Ann Intern Med. 2006 Sep 5;145(5):333-341.

Covas MI. Olive oil and the cardiovascular system. Pharmacol Res. 2007 Mar; 55(3):75-86.

Cox S, Harvey BK, Sanchez JF, Wang JY, Wang Y. Mediation of BMP7 neuroprotection by MAPK and PKC IN rat primary cortical cultures. Brain Res. 2004 Jun 4;1010(1-2):55-61.

Goldberg DM, Yan J, Soleas GJ. Absorption of three wine-related polyphenols in three different matrices by healthy subjects. Clin Biochem. 2003 Feb;36(1):79-87.

D'Angelo S, Manna C, Migliardi V, Mazzoni O, Morrica P, Capasso G, Pontoni G, Galletti P, Zappia V. Pharmacokinetics and metabolism of hydroxytyrosol, a natural antioxidant from olive oil. Drug Metab Dispos. 2001 Nov;29(11):1492-1498.

Daccache A, Lion C, Sibille N, Gerard M, Slomianny C, Lippens G, Cotelle P. Oleuropein and derivatives from olives as Tau aggregation inhibitors. Neurochem Int. 2011 May;58(6):700-707.

d'Adda di Fagagna F. Living on a break: cellular senescence as a DNA-damage response. Nat Rev Cancer. 2008 Jul;8(7):512-522.

Davidson LA, Wang N, Shah MS, Lupton JR, Ivanov I, Chapkin RS. n-3 Polyunsaturated fatty acids modulate carcinogen-directed non-coding microRNA signatures in rat colon. Carcinogenesis. 2009 Dec;30(12):2077-2084.

Davis CD, Ross SA. Evidence for dietary regulation of microRNA expression in cancer cells. Nutr Rev. 2008;66(8):477–482.

Debacq-Chainiaux F1, Erusalimsky JD, Campisi J, Toussaint O. Protocols to detect senescence-associated beta-galactosidase (SA-betagal) activity, a biomarker of senescent cells in culture and in vivo. Nat Protoc. 2009;4(12):1798-1806.

Dell'agnello C, Leo S, Agostino A, Szabadkai G, Tiveron C, Zulian A, Prelle A, Roubertoux P, Rizzuto R, Zeviani M. Increased longevity and refractoriness to Ca(2+)-dependent neurodegeneration in Surf1 knockout mice. Hum Mol Genet. 2007 Feb 15;16(4):431-444.

Djarmati A, Dobricić V, Kecmanović M, Marsh P, Jancić-Stefanović J, Klein C, Djurić M, Romac S. MECP2 mutations in Serbian Rett syndrome patients. Acta Neurol Scand. 2007 Dec;116(6):413-419.

Dong W, Cheng S, Huang F, Fan W, Chen Y, Shi H, He H. Mitochondrial dysfunction in long-term neuronal cultures mimics changes with aging. Med Sci Monit. 2011 Apr;17(4):91-96.

Doxakis E. Post-transcriptional regulation of alpha-synuclein expression by mir-7 and mir-153. The Journal of Biological Chemistry. 2010; 285(17):12726–12734.

Dranovsky A, Hen R. Hippocampal neurogenesis: regulation by stress and antidepressants. Biol Psychiatry. 2006 Jun 15;59(12):1136-1143.

Drummond MJ, Glynn EL, Fry CS, Dhanani S, Volpi E, et al. Essential amino acids increase microRNA-499, -208b, and -23a and downregulate myostatin and myocyte enhancer factor 2C mRNA expression in human skeletal muscle. J Nutr. 2009;39:2279–2284.

Eacker SM, Dawson TM, Dawson VL. Understanding microRNAs in neurodegeneration. Nat Rev Neurosci. 2009 Dec;10(12):837-841.

Earls LR, Westmoreland JJ, Zakharenko SS. Non-coding RNA regulation of synaptic plasticity and memory: implications for aging. Ageing Res Rev. 2014 Sep;17:34-42.

Ebi H, Sato T, Sugito N, Hosono Y, Yatabe Y, Matsuyama Y, Yamaguchi T, Osada H, Suzuki M, Takahashi T. Counterbalance between RB inactivation and miR-17-92 overexpression in reactive oxygen species and DNA damage induction in lung cancers. Oncogene. 2009;28:3371-3379.

Eda A, Takahashi M, Fukushima T, Hohjoh H. Alteration of microRNA expression in the process of mouse brain growth. Gene. 2011 Oct 1;485(1):46-52.

Edgecombe SC, Stretch GL, Hayball PJ. Oleuropein, an antioxidant polyphenol from olive oil, is poorly absorbed from isolated perfused rat intestine. J Nutr. 2000 Dec; 30(2):2996-3002.

EFSA Panel on Dietetic Products, Nutrition and Allergies (NDA). EFSA Journal 2011;9(4):2033-2058. http://www.efsa.europa.eu/

ElSharawy A, Keller A, Flachsbart F, Wendschlag A, Jacobs G, Kefer N, Brefort T, Leidinger P, Backes C, Meese E, Schreiber S, Rosenstiel P, Franke A, Nebel A. Genome-wide miRNA signatures of human longevity. Aging Cell. 2012;11:607-616.

Enokido Y, Yoshitake A, Ito H, Okazawa H. Age-dependent change of HMGB1 and DNA double-strand break accumulation in mouse brain. Biochem Biophys Res Commun. 2008 Nov 7;376(1):128-133.

Esiri MM. Ageing and the brain. J Pathol. 2007 Jan; 211(2):181-187.

Estruch R, Ros E, Salas-Salvadó J, Covas MI, Corella D, Arós F, Gómez-Gracia E, Ruiz-Gutiérrez V, Fiol M, Lapetra J, Lamuela-Raventos RM, Serra-Majem L, Pintó X, Basora J, Muñoz MA, Sorlí JV, Martínez JA, Martínez-González MA; PREDIMED Study Investigators. Primary prevention of cardiovascular disease with a Mediterranean diet. N Engl J Med. 2013 Apr 4;368(14):1279-1290.

Fabbri M, Garzon R, Cimmino A, Liu Z, Zanesi N, Callegari E, Liu S, Alder H, Costinean S, Fernandez-Cymering C, Volinia S, Guler G, Morrison CD, Chan KK, Marcucci G, Calin GA, Huebner K, Croce CM. MicroRNA-29 family reverts aberrant methylation in lung cancer by targeting DNA methyltransferases 3A and 3B. Proc Natl Acad Sci U S A. 2007 Oct 2;104(40):15805-15810.

Fabbri M, Paone A, Calore F, Galli R, Gaudio E, Santhanam R, Lovat F, Fadda P, Mao C, Nuovo GJ, Zanesi N, Crawford M, Ozer GH, Wernicke D, Alder H, Caligiuri MA, Nana-Sinkam P, Perrotti D, Croce CM. MicroRNAs bind to Toll-like receptors to induce prometastatic inflammatory response. Proc Natl Acad Sci U S A. 2012 Jul 31;109(31):2110-2116.

Fang M, Wang J, Zhang X, Geng Y, Hu Z, Rudd JA, Ling S, Chen W, Han S. The miR-124 regulates the expression of BACE1/β-secretase correlated with cell death in Alzheimer's disease. Toxicol Lett. 2012 Feb 25;209(1):94-105.

Faraonio R, Salerno P, Passaro F, Sedia C, Iaccio A, Bellelli R, Nappi TC, Comegna M, Romano S, Salvatore G, Santoro M, Cimino F. A set of miRNAs participates in the cellular senescence program in human diploid fibroblasts. Cell Death Differ. 2012 Apr;19(4):713-721.

Farr SA, Price TO, Dominguez LJ, Motisi A, Saiano F, Niehoff ML, Morley JE, Banks WA, Ercal N, Barbagallo M. Extra virgin olive oil improves learning and memory in SAMP8 mice. J Alzheimers Dis. 2012;28(1):81-92.

Fiacco TA, Agulhon C, McCarthy KD. Sorting out astrocyte physiology from pharmacology. Annu Rev Pharmacol Toxicol. 2009;49:151-174.

Finch CE, Morgan TE. Systemic inflammation, infection, ApoE alleles, and Alzheimer disease: a position paper. Curr Alzheimer Res. 2007 Apr;4(2):185-9.

Finch CE. Neurons, glia, and plasticity in normal brain aging. Neurobiol Aging. 2003 May-Jun;24 Suppl 1:S123-7;

Fischer DF, van Dijk R, van Tijn P, Hobo B, Verhage MC, van der Schors RC, Li KW, van Minnen J, Hol EM, van Leeuwen FW. Long-term proteasome dysfunction in the mouse brain by expression of aberrant ubiquitin. Neurobiol Aging. 2009 Jun;30(6):847-863.

Frozza RL, Bernardi A, Hoppe JB, Meneghetti AB, Matté A, Battastini AM, Pohlmann AR, Guterres SS, Salbego C. Neuroprotective effects of resveratrol against Aβ administration in rats are improved by lipid-core nanocapsules. Mol Neurobiol. 2013 Jun;47(3):1066-1080.

Furuta M, Kozaki KI, Tanaka S, Arii S, Imoto I, Inazawa J. miR-124 and miR-203 are epigenetically silenced tumor-suppressive microRNAs in hepatocellular carcinoma. Carcinogenesis. 2010 May;31(5):766-776.

Gabuzda D, Yankner BA. Physiology: Inflammation links ageing to the brain. Nature. 2013 May 9;497(7448):197-8.

Gao J, Wang WY, Mao YW, Gräff J, Guan JS, Pan L, Mak G, Kim D, Su SC, Tsai LH. A novel pathway regulates memory and plasticity via SIRT1 and miR-134. Nature. 2010 Aug 26;466(7310):1105-1109.

García-Cañas V, Simó C, León C, Cifuentes A. Advances in Nutrigenomics research: novel and future analytical approaches to investigate the biological activity of natural compounds and food functions. J Pharm Biomed Anal. 2010 Jan 20;51(2):290-304.

García-Segura L, Pérez-Andrade M, Miranda-Ríos J. The emerging role of MicroRNAs in the regulation of gene expression by nutrients. J Nutrigenet Nutrigenomics. 2013;6(1):16-31.

Garinis GA, van der Horst GT, Vijg J, Hoeijmakers JH. DNA damage and ageing: new-age ideas for an age-old problem. Nat Cell Biol. 2008 Nov;10(11):1241-1247.

Gascon E, Gao FB. Cause or Effect: Misregulation of microRNA Pathways in Neurodegeneration. Front Neurosci. 2012; 6(48):1-6.

Gaughwin PM, Ciesla M, Lahiri N, Tabrizi SJ, Brundin P, Bjorkqvist M. Hsa-miR-34b is a plasma-stable microRNA that is elevated in pre-manifest Huntington's disease. Hum Mol Genet. 2011;20:2225–2237.

Genade T Lang DM. Resveratrol extends lifespan and preserves glia but not neurons of the Nothobranchius guentheri optic tectum. Exp Gerontol. 2013;48:202-212.

Geng YQ, Guan JT, Xu XH, Fu YC. Senescence-associated beta-galactosidase activity expression in aging hippocampal neurons. Biochem Biophys Res Commun. 2010;396:866-869.

Gillette Guyonnet S, Abellan Van Kan G, Andrieu S, Barberger Gateau P, Berr C, Bonnefoy M, Dartigues JF, de Groot L, Ferry M, Galan P, Hercberg S, Jeandel C, Morris MC, Nourhashemi F, Payette H, Poulain JP, Portet F, Roussel AM, Ritz P, Rolland Y, Vellas B. IANA task force on nutrition and cognitive decline with aging. J Nutr Health Aging. 2007 Mar-Apr; (2):32-52.

Gingras J, Rassadi S, Cooper E, Ferns M. Synaptic transmission is impaired at neuronal autonomic synapses in agrin-null mice. Dev Neurobiol. 2007 Apr; 67(5):521-534.

Giovannelli L, Pitozzi V, Jacomelli M, Mulinacci N, Laurenzana A, Dolara P, Mocali A. Protective effects of resveratrol against senescence-associated changes in cultured human fibroblasts. J Gerontol A Biol Sci Med Sci. 2011 Jan;66(1):9-18.

Glorioso C, Sibille E. Between destiny and disease: genetics and molecular pathways of human central nervous system aging. Prog Neurobiol. 2011 Feb;93(2):165-181.

Goll MG, Bestor TH. Eukaryotic cytosine methyltransferases. Annu Rev Biochem. 2005;74:481-514.

González-Correa JA, Navas MD, Muñoz-Marín J, Trujillo M, Fernández-Bolaños J, de la Cruz JP. Effects of hydroxytyrosol and hydroxytyrosol acetate administration to rats on platelet function compared to acetylsalicylic acid. J Agric Food Chem. 2008 Sep 10;56(17):7872-7876.

Goyarzu P, Malin DH, Lau FC, Taglialatela G, Moon WD, Jennings R, Moy E, Moy D, Lippold S, Shukitt-Hale B, Joseph JA. Blueberry supplemented diet: effects on object recognition memory and nuclear factor-kappa B levels in aged rats. Nutr Neurosci. 2004 Apr;7(2):75-83.

Granados-Soto V. Pleiotropic effects of resveratrol. Drug News Perspect. 2003;6(5):299-307.

Grewal SI, Jia S. Heterochromatin revisited. Nat Rev Genet. 2007 Jan;8(1):35-46.

Griggs EM, Young EJ, Rumbaugh G, Miller CA. MicroRNA-182 regulates amygdala-dependent memory formation. J Neurosci. 2013 Jan 23;33(4):1734-1740.

Grillari J, Hackl M, Grillari-Voglauer R. miR-17-92 cluster: ups and downs in cancer and aging. Biogerontology. 2010 Aug;11(4):501-506.

Grossi C, Rigacci S, Ambrosini S, Ed Dami T, Luccarini I, Traini C, Failli P, Berti A, Casamenti F, Stefani M. The polyphenol oleuropein aglycone protects TgCRND8 mice against Aß plaque pathology. PLoS One. 2013 Aug 8;8(8):e71702.

Guarente L. Franklin H. Epstein Lecture: Sirtuins, aging, and medicine. N Engl J Med. 2011 Jun 9;364(23):2235-2244.

Hackl M, Brunner S, Fortschegger K, Schreiner C, Micutkova L, Muck C, Laschober GT, Lepperdinger G, Sampson N, Berger P, Herndler-Brandstetter D, Wieser M, Kuhnel H, Strasser A, Rinnerthaler M, Breitenbach M, Mildner M, Eckhart L, Tschachler E, Trost A, Bauer JW, Papak C, Trajanoski Z, Scheideler M, Grillari-Voglauer R, Grubeck-Loebenstein B, Jansen-Durr P, Grillari J. miR-17, miR-19b, miR-20a, and miR-106a are down-regulated in human aging. Aging Cell. 2010;9:291-296.

Haigis MC, Guarente LP Mammalian sirtuins emerging roles in physiology, aging, and calorie restriction. Genes Dev. 2006 Nov 1; 20(21):2913-2921.

Halagappa VK, Guo Z, Pearson M, Matsuoka Y, Cutler RG, Laferla FM, Mattson MP Intermittent fasting and caloric restriction ameliorate age-related behavioral deficits in the triple-transgenic mouse model of Alzheimer's disease. Neurobiol Dis. 2007 Apr; 26(1):212-220.

Halicka HD, Zhao H, Li J, Lee YS, Hsieh TC, Wu JM, Darzynkiewicz Z. Potential anti-aging agents suppress the level of constitutive mTOR- and DNA damage- signaling. Aging (Albany NY). 2012;4:952-965.

Han S, Brunet A. Histone methylation makes its mark on longevity. Trends Cell Biol. 2012 Jan;22(1):42-49.

Hansen KF, Sakamoto K, Wayman GA, Impey S, Obrietan K. Transgenic miR132 alters neuronal spine density and impairs novel object recognition memory. PLoS One. 2010 Nov 29;5(11):e15497.

Hao PP, Chen YG, Wang JL, Wang XL, Zhang Y Meta-analysis of aldehyde dehydrogenase 2 gene polymorphism and Alzheimer's disease in East Asians. Can J Neurol Sci. 2011 May; 38(3):500-506.

Hardy TM, Tollefsbol TO. Epigenetic diet: impact on the epigenome and cancer. Epigenomics. 2011 Aug;3(4):503-518.

Harman D. The free radicals theory of aging: effect of age on serum copper levels. J Gerontol. 1965 Apr;20:151-153.

Harper CR, Edwards MC, Jacobson TA. Flaxseed oil supplementation does not affect plasma lipoprotein concentration or particle size in human subjects. J. Nutr. 2006;36:2844–2848.

Harrison DE, Strong R, Sharp ZD, Nelson JF, Astle CM, Flurkey K, Nadon NL, Wilkinson JE, Frenkel K, Carter CS, Pahor M, Javors MA, Fernandez E, Miller RA. Rapamycin fed late in life extends lifespan in genetically heterogeneous mice. Nature. 2009 Jul 16;460(7253):392-395.

Hartl FU, Bracher A, Hayer-Hartl M. Molecular chaperones in protein folding and proteostasis. Nature. 2011 Jul 20;475(7356):324-332.

Hayflick L.The limited in vitro lifetime of human diploid cell strains. Exp Cell Res. 1965; 37:614-636.

Hébert SS, Horré K, Nicolaï L, Papadopoulou AS, Mandemakers W, Silahtaroglu AN, Kauppinen S, Delacourte A, De Strooper B. Loss of microRNA cluster miR-29a/b-1 in sporadic Alzheimer's disease correlates with increased BACE1/beta-secretase expression. Proc Natl Acad Sci U S A. 2008 Apr 29;105(17):6415-6420.

Hébert SS, Papadopoulou AS, Smith P, Galas MC, Planel E, Silahtaroglu AN, Sergeant N, Buée L, De Strooper B. Genetic ablation of Dicer in adult forebrain neurons results in abnormal tau hyperphosphorylation and neurodegeneration. Hum Mol Genet. 2010 Oct 15;19(20):3959-3969.

Heinonen AM, Rahman M, Dogbevia G, Jakobi H, Wölfl S, Sprengel R, Schwaninger M. Neuroprotection by rAAV-mediated gene transfer of bone morphogenic protein 7. BMC Neurosci. 2014 Mar 11;15:38.

Hekimi S, Lapointe J, Wen Y. Taking a "good" look at free radicals in the aging process. Trends Cell Biol. 2011 Oct;21(10):569-576.

Hermeking H. The miR-34 family in cancer and apoptosis. Cell Death Differ. 2010; 17: 193–199.

Herranz D, Serrano M. SIRT1: recent lessons from mouse models. Nat Rev Cancer. 2010 Dec;10(12):819-823.

Herskovits AZ, Guarente L. SIRT1 in neurodevelopment and brain senescence. Neuron. 2014 Feb 5;81(3):471-483.

Hinkal GW, Gatza CE, Parikh N, Donehower LA. Altered senescence, apoptosis, and DNA damage response in a mutant p53 model of accelerated aging. Mech Ageing Dev. 2009 Apr;130(4):262-271.

Hitoshi S, Alexson T, Tropepe V, Donoviel D, Elia AJ, Nye JS, Conlon RA, Mak TW, Bernstein A, van der Kooy D. Notch pathway molecules are essential for the maintenance, but not the generation, of mammalian neural stem cells. Genes Dev. 2002 Apr 1; 16(7):846-858.

Ho DJ, Calingasan NY, Wille E, Dumont M, Beal MF. Resveratrol protects against peripheral deficits in a mouse model of Huntington's disease. Exp Neurol. 2010 Sep;225(1):74-84.

Hoeijmakers JH. DNA damage, aging, and cancer. N Engl J Med. 2009 Oct 8;361(15):1475-1485.

Hof PR, Duan H, Page TL, Einstein M, Wicinski B, He Y, Erwin JM, Morrison JH. Age-related changes in GluR2 and NMDAR1 glutamate receptor subunit protein immunoreactivity in corticocortically projecting neurons in macaque and patas monkeys. Brain Res. 2002 Feb 22;928(1-2):175-186.

Houtkooper RH, Pirinen E, Auwerx J. Sirtuins as regulators of metabolism and healthspan. Nat Rev Mol Cell Biol. 2012 Mar 7;13(4):225-238.

Hu H, Du L, Nagabayashi G, Seeger RC, Gatti RA. ATM is down-regulated by N-Myc-regulated microRNA-421. Proc Natl Acad Sci U S A. 2010 Jan 26;107(4):1506-1511.

Hubbard BP, Sinclair DA Small molecule SIRT1 activators for the treatment of aging and age-related diseases. Trends Pharmacol Sci. 2014 Mar;35(3):146-154.

Huber K Superti-Furga G. After the grape rush: sirtuins as epigenetic drug targets in neurodegenerative disorders. Bioorg Med Chem. 2011;19:3616-3624.

Hung TM, Ho CM2, Liu YC1, Lee JL3, Liao YR3, Wu YM3, Ho MC3, Chen CH4, Lai HS3, Lee PH5. Up-regulation of microRNA-190b plays a role for decreased IGF-1 that induces insulin resistance in human hepatocellular carcinoma. PLoS One. 2014 Feb 20;9(2):e89446.

Iser WB, Gami MS, Wolkow CA. Insulin signaling in Caenorhabditis elegans regulates both endocrine-like and cell-autonomous outputs. Dev Biol. 2007 Mar 15;303(2):434-447.

Jacobs S, Lie DC, DeCicco KL, Shi Y, DeLuca LM, Gage FH, Evans RM. Retinoic acid is required early during adult neurogenesis in the dentate gyrus. Proc Natl Acad Sci U S A. 2006 Mar 7;103(10):3902-3907.

Jacomelli M, Pitozzi V, Zaid M, Larrosa M, Tonini G, Martini A, Urbani S, Taticchi A, Servili M, Dolara P, Giovannelli L. Dietary extra-virgin olive oil rich in phenolic antioxidants and the aging process: long-term effects in the rat. J Nutr Biochem. 2010 Apr;21(4):290-296.

Jeyapalan JC, Sedivy JM. Cellular senescence and organismal aging. Mech Ageing Dev. 2008 Jul-Aug;129(7-8):467-474.

Jiang CH, Tsien JZ, Schultz PG, Hu Y. The effects of aging on gene expression in the hypothalamus and cortex of m ice. Proc Natl Acad Sci U S A. 2001 Feb 13;98(4):1930-1934.

Jiang T, Yu JT, Tan MS, Zhu XC, Tan L. β-Arrestins as potential therapeutic targets for Alzheimer's disease. Mol Neurobiol. 2013 Dec;48(3):812-818.

Jimenez-Mateos EM, Engel T, Merino-Serrais P, McKiernan RC, Tanaka K, Mouri G, Sano T, O'Tuathaigh C, Waddington JL, Prenter S, Delanty N, Farrell MA, O'Brien DF, Conroy RM, Stallings RL, DeFelipe J, Henshall DC. Silencing microRNA-134 produces neuroprotective and prolonged seizure-suppressive effects. Nat Med. 2012 Jul;18(7):1087-1094.

Jin C, Li J, Green CD, Yu X, Tang X, Han D, Xian B, Wang D, Huang X, Cao X, Yan Z, Hou L, Liu J, Shukeir N, Khaitovich P, Chen CD, Zhang H, Jenuwein T, Han JD. Histone demethylase UTX-1 regulates C. elegans life span by targeting the insulin/IGF-1 signaling pathway. Cell Metab. 2011 Aug 3;14(2):161-172.

Johnson SC, Rabinovitch PS, Kaeberlein M. mTOR is a key modulator of ageing and age-related disease. Nature. 2013;493:338-345.

Joseph JA, Shukitt-Hale B, Denisova NA, Bielinski D, Martin A, Mcewen JJ, Bickford PC. Reversals of age-related declines in neuronal signal transduction, cognitive, and motor behavioral deficits with blueberry, spinach, or strawberry dietary supplementation. J Neurosci 1999;19:8114–8121.

Junn E, Lee KW, Jeong BS, Chan TW, Im JY, Mouradian MM.Repression of alpha-synuclein expression and toxicity by microRNA-7. Proc Natl Acad Sci U S A. 2009 Aug 4;106(31):13052-13057.

Jurk D, Wang C, Miwa S, Maddick M, Korolchuk V, Tsolou A, Gonos ES, Thrasivoulou C, Saffrey MJ, Cameron K, von Zglinicki T. Postmitotic neurons develop a p21-dependent senescence-like phenotype driven by a DNA damage response. Aging Cell. 2012 Dec;11(6):996-1004.

Kaeberlein M, McVey M, Guarente L. The SIR2/3/4 complex and SIR2 alone promote longevity in Saccharomyces cerevisiae by two different mechanisms. Genes Dev. 1999 Oct 1;13(19):2570-2580.

Kanwal R, Gupta S. Epigenetic modifications in cancer. Clin Genet. 2012 Apr;81(4):303-311.

Kennedy DO, Wightman EL, Reay JL, Lietz G, Okello EJ, Wilde A, Haskell CF. Effects of resveratrol on cerebral blood flow variables and cognitive performance in humans: a double-blind, placebo-controlled, crossover investigation. Am J Clin Nutr. 2010 Jun;91(6):1590-1597.

Khanna A, Muthusamy S, Liang R, Sarojini H, Wang E Gain of survival signaling by down-regulation of three key miRNAs in brain of calorie-restricted mice. Aging (Albany NY). 2011 Mar;3(3):223-236.

Koga H, Kaushik S, Cuervo AM. Protein homeostasis and aging: The importance of exquisite quality control. Ageing Res Rev. 2011 Apr;10(2):205-215.

Komatsu M, Waguri S, Chiba T, Murata S, Iwata J, Tanida I, Ueno T, Koike M, Uchiyama Y, Kominami E, Tanaka K. Loss of autophagy in the central nervous system causes neurodegeneration in mice. Nature. 2006 Jun 15;441(7095):880-884.

Konstantinidou V, Covas MI, Muñoz-Aguayo D, Khymenets O, de la Torre R, Saez G, Tormos Mdel C, Toledo E, Marti A, Ruiz-Gutiérrez V, Ruiz Mendez MV, Fito M. In vivo nutrigenomic effects of virgin olive oil polyphenols within the frame of the Mediterranean diet: a randomized controlled trial. FASEB J. 2010 Jul;24(7):2546-2557.

Kortlever RM, Higgins PJ, Bernards R. Plasminogen activator inhibitor-1 is a critical downstream target of p53 in the induction of replicative senescence. Nat Cell Biol. 2006;8:877-884.

Kremsky I, Morgan TE, Hou X, Li L, Finch CE. Age-changes in gene expression in primary mixed glia cultures from young vs. old rat cerebral cortex are modified by interactions with neurons. Brain Behav Immun. 2012 Jul;26(5):797-802.

Lai EC. Micro RNAs are complementary to 3' UTR sequence motifs that mediate negative post-transcriptional regulation. Nat Genet. 2002 Apr;30(4):363-364.

Lal A, Kim HH, Abdelmohsen K, Kuwano Y, Pullmann R Jr, Srikantan S, Subrahmanyam R, Martindale JL, Yang X, Ahmed F, Navarro F, Dykxhoorn D, Lieberman J, Gorospe M. p16(INK4a) translation suppressed by miR-24. PLoS One. 2008 Mar 26;3(3):e1864.

Lal A, Pan Y, Navarro F, Dykxhoorn DM, Moreau L, Meire E, Bentwich Z, Lieberman J, Chowdhury D. miR-24-mediated downregulation of H2AX suppresses DNA repair in terminally differentiated blood cells. Nat Struct Mol Biol. 2009 May;16(5):492-8.

Lau GC, Saha S, Faris R, Russek SJ. Up-regulation of NMDAR1 subunit gene expression in cortical neurons via a PKA-dependent pathway. J Neurochem. 2004 Feb;88(3):564-575.

Lee BY, Han JA, Im JS, Morrone A, Johung K, Goodwin EC, et al. Senescence-associated beta-galactosidase is lysosomal beta-galactosidase. Aging Cell. 2006;5(2):187-195.

Lee JS, Ward WO, Ren H, Vallanat B, Darlington GJ, Han ES, Laguna JC, DeFord JH, Papaconstantinou J, Selman C, Corton JC. Meta-analysis of gene expression in the mouse liver reveals biomarkers associated with inflammation increased early during aging. Mech Ageing Dev. 2012 Jul;133(7):467-78.

Lee K, Kim JH, Kwon OB, An K, Ryu J, Cho K, Suh YH, Kim HS. An activity-regulated microRNA, miR-188, controls dendritic plasticity and synaptic transmission by downregulating neuropilin-2. J Neurosci. 2012 Apr 18;32(16):5678-5687.

Lesuisse C, Martin LJ. Long-term culture of mouse cortical neurons as a model for neuronal development, aging, and death. J Neurobiol. 2002;51:9–23.

Lewis BP, Shih IH, Jones-Rhoades MW, Bartel DP, Burge CB. Prediction of mammalian microRNA targets. Cell. 2003 Dec 26;115(7):787-798.

Li G, Luna C, Qiu J, Epstein DL, Gonzalez P. Alterations in microRNA expression in stress-induced cellular senescence. Mech Ageing Dev. 2009;130:731-741.

Li M, Linseman DA, Allen MP, Meintzer MK, Wang X, Laessig T, Wierman ME, Heidenreich KA. Myocyte enhancer factor 2A and 2D undergo phosphorylation and caspase-mediated degradation during apoptosis of rat cerebellar granule neurons. J Neurosci. 2001 Sep 1;21(17):6544-6552.

Li N, Bates DJ, An J, Terry DA, Wang E. Up-regulation of key microRNAs, and inverse down-regulation of their predicted oxidative phosphorylation target genes, during aging in mouse brain. Neurobiol Aging. 2011 May;32(5):944-955.

Li X, Khanna A, Li N, Wang E. Circulatory miR34a as an RNA based, noninvasive biomarker for brain aging. Aging (Albany NY). 2011 Oct;3(10):985-1002.

Li Y, Kong D, Wang Z, Sarkar FH. Regulation of microRNAs by natural agents: an emerging field in chemoprevention and chemotherapy research. Pharm Res. 2010 Jun;27(6):1027-1041.

Li Z, Rana TM. Therapeutic targeting of microRNAs: current status and future challenges. Nat Rev Drug Discov. 2014 Aug;13(8):622-638.

Liang R, Bates DJ, Wang E. Epigenetic Control of MicroRNA Expression and Aging. Curr Genomics. 2009 May;10(3):184-193.

Lindow M, Kauppinen, S. Discovering the first microRNA-targeted drug. J. Cell Biol. 2012; 199: 407–412.

Liu CG, Wang JL, Li L, Wang PC (2014) MicroRNA-384 regulates both amyloid precursor protein and beta-secretase expression and is a potential biomarker for Alzheimer's disease. International Journal of Molecular Medicine 34(1):160–166.

Liu GS, Zhang ZS, Yang B, He W. Resveratrol attenuates oxidative damage and ameliorates cognitive impairment in the brain of senescence-accelerated mice Life Sci., 2012 9: 872–877.

Liu N, Landreh M, Cao K, Abe M, Hendriks GJ, Kennerdell JR, Zhu Y, Wang LS, Bonini NM. The microRNA miR-34 modulates ageing and neurodegeneration in Drosophila. Nature. 2012 Feb 15;482(7386):519-523.

Liu RM, van Groen T, Katre A, Cao D, Kadisha I, Ballinger C, Wang L, Carroll SL, Li L. Knockout of plasminogen activator inhibitor 1 gene reduces amyloid beta peptide burden in a mouse model of Alzheimer's disease. Neurobiol Aging. 2011;32:1079-1089.

Loerch PM, Lu T, Dakin KA, Vann JM, Isaacs A, Geula C, Wang J, Pan Y, Gabuzda DH, Li C, Prolla TA, Yankner BA. Evolution of the aging brain transcriptome and synaptic regulation. PLoS One. 2008 Oct 2;3(10):e3329.

Long JM, Lahiri DK. Current drug targets for modulating Alzheimer's amyloid precursor protein: role of specific micro-RNA species. Curr Med Chem. 2011;18(22):3314-3321.

López-Otín C, Blasco MA, Partridge L, Serrano M, Kroemer G. The hallmarks of aging. Cell. 2013 Jun 6;153(6):1194-1217.

Lu T, Pan Y, Kao SY, Li C, Kohane I, Chan J, Yankner BA. Gene regulation and DNA damage in the ageing human brain. Nature. 2004 Jun 24;429(6994):883-891.

Lugli G, Torvik VI, Larson J, Smalheiser NR. Expression of microRNAs and their precursors in synaptic fractions of adult mouse forebrain. J Neurochem. 2008 Jul;106(2):650-661.

Luo Y, Roth GS. The roles of dopamine oxidative stress and dopamine receptor signaling in aging and age-related neurodegeneration. Antioxid Redox Signal. 2000 Fall;2(3):449-460.

Madabhushi R, Pan L, Tsai LH. DNA damage and its links to neurodegeneration. Neuron. 2014 Jul 16;83(2):266-282.

Magill ST, Cambronne XA, Luikart BW, Lioy DT, Leighton BH, Westbrook GL, Mandel G, Goodman RH. microRNA-132 regulates dendritic growth and arborization of newborn neurons in the adult hippocampus. Proc Natl Acad Sci U S A. 2010 Nov 23;107(47):20382-20387.

Mah LJ, El-Osta A, Karagiannis TC. GammaH2AX as a molecular marker of aging and disease. Epigenetics. 2010 Feb 16;5(2):129-136.

Manna C, Galletti P, Maisto G, Cucciolla V, D'Angelo S, Zappia V Transport mechanism and metabolism of olive oil hydroxytyrosol in Caco-2 cells. FEBS Lett. 2000 Mar 3; 470(3):34-40.

Markowska AL, Koliatsos VE, Breckler SJ, Price DL, Olton DS. Human nerve growth factor improves spatial memory in aged but not in young rats. J Neurosci. 1994 Aug;14(8):4815-4824.

Marrugat J, Covas MI, Fitó M, Schröder H, Miró-Casas E, Gimeno E, López-Sabater MC, de la Torre R, Farré M; SOLOS Investigators. Effects of differing phenolic content in dietary olive oils on lipids and LDL oxidation--a randomized controlled trial. Eur J Nutr. 2004 Jun;43(3):140-7.

Martinez I, Cazalla D, Almstead LL, Steitz JA, DiMaio D. miR-29 and miR-30 regulate B-Myb expression during cellular senescence. Proc Natl Acad Sci U S A. 2011 Jan 11;108(2):522-527.

Martínez-González MÁ, Toledo E, Arós F, Fiol M, Corella D, Salas-Salvadó J, Ros E, Covas MI, Fernández-Crehuet J, Lapetra J, Muñoz MA, Fitó M, Serra-Majem L, Pintó X, Lamuela-Raventós RM, Sorlí JV, Babio N, Buil-Cosiales P, Ruiz-Gutierrez V, Estruch R, Alonso A; PREDIMED Investigators.Extravirgin olive oil consumption reduces risk of atrial fibrillation: the PREDIMED (Prevención con Dieta Mediterránea) trial. Circulation. 2014 Jul ;30(1):18-26.

Martínez-Lapiscina EH, Clavero P, Toledo E, San Julián B, Sanchez-Tainta A, Corella D, Lamuela-Raventós RM, Martínez JA, Martínez-Gonzalez MÁ. Virgin olive oil supplementation and long-term cognition: the PREDIMED-NAVARRA randomized, trial. J Nutr Health Aging. 2013;17(6):544-552.

Masala G, Ceroti M, Pala V, Krogh V, Vineis P, Sacerdote C, Saieva C, Salvini S, Sieri S, Berrino F, Panico S, Mattiello A, Tumino R, Giurdanella MC, Bamia C, Trichopoulou A, Riboli E, Palli D. A dietary pattern rich in olive oil and raw vegetables is associated with lower mortality in Italian elderly subjects. Br J Nutr. 2007 Aug;98(2):406-415.

Mattson MP, Duan W, Chan SL, Cheng A, Haughey N, Gary DS, Guo Z, Lee J, Furukawa K. Neuroprotective and neurorestorative signal transduction mechanisms in brain aging: modification by genes, diet and behavior. Neurobiol Aging. 2002 Sep-Oct;23(5):695-705.

Mattson MP, Maudsley S, Martin B. A neural signaling triumvirate that influences ageing and age-related disease: insulin/IGF-1, BDNF and serotonin. Ageing Res Rev. 2004 Nov;3(4):445-464.

Mattson MP. Glutamate and neurotrophic factors in neuronal plasticity and disease. Ann N Y Acad Sci. 2008 Nov;1144:97-112.

Mercken EM, Majounie E, Ding J, Guo R, Kim J, Bernier M, Mattison J, Cookson MR, Gorospe M, de Cabo R, Abdelmohsen K Age-associated miRNA alterations in skeletal muscle from rhesus monkeys reversed by caloric restriction. Aging (Albany NY). 2013 Sep;5(9):692-703.

Michaelis EK, Wang X, Pal R, Bao X, Hascup KN, Wang Y, Wang WT, Hui D, Agbas A, Choi IY, Belousov A, Gerhardt GA. Neuronal Glud1 (glutamate dehydrogenase 1) over-expressing mice: increased glutamate formation and synaptic release, loss of synaptic activity, and adaptive changes in genomic expression. Neurochem Int. 2011;59:473-481.

Middeldorp J, Hol EM. GFAP in health and disease. Prog Neurobiol. 2011 Mar;93(3):421-443.

Milenkovic D, Deval C, Gouranton E, Landrier JF, Scalbert A, Morand C, Mazur A. Modulation of miRNA expression by dietary polyphenols in apoE deficient mice: a new mechanism of the action of polyphenols. PLoS One. 2012;7(1):e29837.

Milenkovic D, Jude B, Morand C. miRNA as molecular target of polyphenols underlying their biological effects. Free Radic Biol Med. 2013 Sep;64:40-51.

Mitchell PS, Parkin RK, Kroh EM, Fritz BR, Wyman SK, Pogosova-Agadjanyan EL, Peterson A, Noteboom J, O'Briant KC, Allen A, Lin DW, Urban N, Drescher CW, Knudsen BS, Stirewalt DL, Gentleman R, Vessella RL, Nelson PS, Martin DB, Tewari M. Circulating microRNAs as stable blood-based markers for cancer detection. Proc Natl Acad Sci U S A. 2008 Jul 29;105(30):10513-10518.

Molofsky AV, Slutsky SG, Joseph NM, He S, Pardal R, Krishnamurthy J, Sharpless NE, Morrison SJ. Increasing p16INK4a expression decreases forebrain progenitors and neurogenesis during ageing. Nature. 2006 Sep 28;443(7110):448-452.

Moskalev AA, Shaposhnikov MV, Plyusnina EN, Zhavoronkov A, Budovsky A, Yanai H, Fraifeld VE. The role of DNA damage and repair in aging through the prism of Koch-like criteria. Ageing Res Rev. 2013 Mar;12(2):661-84.

Muñoz-Najar U, Sedivy JM. Epigenetic control of aging. Antioxid Redox Signal. 2011 Jan 15;14(2):241-259.

Murai KK, Pasquale EB. Eph receptors and ephrins in neuron-astrocyte communication at synapses Glia. 2011 Nov;59(11):1567-1578.

Murase T, Haramizu S, Ota N, Hase T. Suppression of the aging-associated decline in physical performance by a combination of resveratrol intake and habitual exercise in senescence-accelerated mice. Biogerontology. 2009 Aug;10(4):423-434.

Musolino C, Allegra A, Saija A, Alonci A, Russo S, Spatari G, Penna G, Gerace D, Cristani M, David A, Saitta S, Gangemi S. Changes in advanced oxidation protein products, advanced glycation end products, and s-nitrosylated proteins, in patients affected by polycythemia vera and essential thrombocythemia. Clin Biochem. 2012;45:1439-1443.

Naesens M. Replicative senescence in kidney aging, renal disease, and renal transplantation. Discov Med. 2011 Jan;11(56):65-75.

Narita M, Nũnez S, Heard E, Narita M, Lin AW, Hearn SA, Spector DL, Hannon GJ, Lowe SW. Rb-mediated heterochromatin formation and silencing of E2F target genes during cellular senescence. Cell. 2003 Jun 13;113(6):703-716.

Nonaka M, Kim R, Fukushima H, Sasaki K, Suzuki K, Okamura M, Ishii Y, Kawashima T, Kamijo S, Takemoto-Kimura S, Okuno H, Kida S, Bito H. Region-specific activation of CRTC1-CREB signaling mediates long-term fear memory. Neuron. 2014 Oct 1;84(1):92-106.

Noren HN, Abdelmohsen K, Gorospe M, Ejiogu N, Zonderman AB, Evans MK. microRNA expression patterns reveal differential expression of target genes with age. Plos One. 2010;5:e10724.

Nudelman AS, DiRocco DP, Lambert TJ, Garelick MG, Le J, Nathanson NM, Storm DR. Neuronal activity rapidly induces transcription of the CREB-regulated microRNA-132, in vivo. Hippocampus. 2010 Apr;20(4):492-498.

Ogunshola OO Antoniou X. Contribution of hypoxia to Alzheimer's disease: is HIF-1alpha a mediator of neurodegeneration? Cell Mol Life Sci. 2009;66:3555-3563.

Olivieri F, Rippo MR, Procopio AD, Fazioli F. Circulating inflamma-miRs in aging and age-related diseases. Front Genet. 2013 Jun 26;4:121-129.

Onodera T, Sakudo A, Tsubone H, Itohara S Review of studies that have used knockout mice to assess normal function of prion protein under immunological or pathophysiological stress. Microbiol Immunol. 2014 Jul;58(7):361-374.

Oomen CA, Farkas E, Roman V, van der Beek EM, Luiten PG, Meerlo P. Resveratrol preserves cerebrovascular density and cognitive function in aging mice. Front Aging Neurosci. 2009;1:4-7.

Osterfield M, Egelund R, Young LM, Flanagan JG. Interaction of amyloid precursor protein with contactins and NgCAM in the retinotectal system. Development. 2008;135:1189-1199.

Owen RW, Mier W, Giacosa A, Hull WE, Spiegelhalder B, Bartsch H. Phenolic compounds and squalene in olive oils: the concentration and antioxidant potential of total phenols, simple phenols, secoiridoids, lignansand squalene. Food Chem Toxicol. 2000 Aug;38(8):647-659.

Page MM, Richardson J, Wiens BE, Tiedtke E, Peters CW, Faure PA, Burness G, Stuart JA. Antioxidant enzyme activities are not broadly correlated with longevity in 14 vertebrate endotherm species. Age (Dordr). 2010 Jun;32(2):255-270.

Park SK, Kim K, Page GP, Allison DB, Weindruch R, Prolla TA Gene expression profiling of aging in multiple mouse strains: identification of aging biomarkers and impact of dietary antioxidants. Aging Cell. 2009 Aug; 8(4):484-495.

Pearson KJ, Baur JA, Lewis KN, Peshkin L, Price NL, Labinskyy N, Swindell WR, Kamara D, Minor RK, Perez E, Jamieson HA, Zhang Y, Dunn SR, Sharma K, Pleshko N, Woollett LA, Csiszar A, Ikeno Y, Le Couteur D, Elliott PJ, Becker KG, Navas P, Ingram DK, Wolf NS, Ungvari Z, Sinclair DA, de Cabo R. Resveratrol delays age-related deterioration and mimics transcriptional aspects of dietary restriction without extending life span. Cell Metab. 2008 Aug;8(2):157-168.

Pellegrini-Giampietro DE, Peruginelli F, Meli E, Cozzi A, Albani-Torregrossa S, Pellicciari R, Moroni F. Protection with metabotropic glutamate 1 receptor antagonists in models of ischemic neuronal death: time-course and mechanisms. Neuropharmacology. 1999;38:1607-1619.

Persengiev S, Kondova I, Otting N, Koeppen AH, Bontrop RE. Genome-wide analysis of miRNA expression reveals a potential role for miR-144 in brain aging and spinocerebellar ataxia pathogenesis. Neurobiol Aging. 2011 Dec;32(12):2316.e17-27.

Persengiev SP, Kondova II, Bontrop RE. The Impact of MicroRNAs on Brain Aging and Neurodegeneration. Curr Gerontol Geriatr Res. 2012;2012:359369-359378.

Pertusa M, García-Matas S, Rodríguez-Farré E, Sanfeliu C, Cristòfol R. Astrocytes aged in vitro show a decreased neuroprotective capacity. J Neurochem. 2007 May;101(3):794-805.

Pitozzi V, Jacomelli M, Catelan D, Servili M, Taticchi A, Biggeri A, Dolara P, Giovannelli L. Long-term dietary extra-virgin olive oil rich in polyphenols reverses age-related dysfunctions in motor coordination and contextual memory in mice: role of oxidative stress. Rejuvenation Res. 2012 Dec;15(6):601-612.

Pitozzi V, Jacomelli M, Zaid M, Luceri C, Bigagli E, Lodovici M, Ghelardini C, Vivoli E, Norcini M, Gianfriddo M, Esposto S, Servili M, Morozzi G, Baldi E, Bucherelli C, Dolara P, Giovannelli L. Effects of dietary extra-virgin olive oil on behaviour and brain biochemical parameters in ageing rats. Br J Nutr. 2010 Jun;103(11):1674-1683.

Poirazi P, Mel BW. Impact of active dendrites and structural plasticity on the memory capacity of neural tissue. Neuron. 2001 Mar; 29(3):779-796.

Pollock A, Bian S, Zhang C, Chen Z, Sun T. Growth of the developing cerebral cortex is controlled by microRNA-7 through the p53 pathway. Cell Rep. 2014;7:1184-1196.

Powers ET, Morimoto RI, Dillin A, Kelly JW, Balch WE. Biological and chemical approaches to diseases of proteostasis deficiency. Annu Rev Biochem. 2009;78:959-991.

Provost P. Interpretation and applicability of microRNA data to the context of Alzheimer's and age-related diseases. Aging (Albany NY). 2010;2:166-169.

Psaltopoulou T, Kyrozis A, Stathopoulos P, Trichopoulos D, Vassilopoulos D, Trichopoulou A. Diet, physical activity and cognitive impairment among elders: the EPIC-Greece cohort (European Prospective Investigation into Cancer and Nutrition). Public Health Nutr. 2008 Oct; (0):054-062.

Rahmadi A, Steiner N, Munch G. Advanced glycation endproducts as gerontotoxins and biomarkers for carbonyl-based degenerative processes in Alzheimer's disease. Clin Chem Lab Med. 2011;49:385-391.

Ravikumar B, Vacher C, Berger Z, Davies JE, Luo S, Oroz LG, Scaravilli F, Easton DF, Duden R, O'Kane CJ, Rubinsztein DC. Inhibition of mTOR induces autophagy and reduces toxicity of polyglutamine expansions in fly and mouse models of Huntington disease. Nat Genet. 2004 Jun;36(6):585-595.

Rimer M. Emerging roles for MAP kinases in agrin signaling. Commun Integr Biol. 2011 Mar;4(2):143-146.

Rodríguez JJ, Noristani HN, Verkhratsky A. The serotonergic system in ageing and Alzheimer's disease. Prog Neurobiol. 2012 Oct;99(1):15-41.

Rollo CD. Dopamine and aging: intersecting facets. Neurochem Res. 2009 Apr;34(4):601-629.

Salas-Salvadó J, Bulló M, Estruch R, Ros E, Covas MI, Ibarrola-Jurado N, Corella D, Arós F, Gómez-Gracia E, Ruiz-Gutiérrez V, Romaguera D, Lapetra J, Lamuela-Raventós RM, Serra-Majem L, Pintó X, Basora J, Muñoz MA, Sorlí JV, Martínez-González MA. Prevention of diabetes with Mediterranean diets: a subgroup analysis of a randomized trial. Ann Intern Med. 2014 Jan 7;160(1):1-10.

Salminen A, Ojala J, Kaarniranta K, Haapasalo A, Hiltunen M, Soininen H. Astrocytes in the aging brain express characteristics of senescence-associated secretory phenotype. Eur J Neurosci. 2011 Jul;34(1):3-11.

Salta E, De Strooper B. Non-coding RNAs with essential roles in neurodegenerative disorders. Lancet Neurol. 2012 Feb;11(2):189-200.

Samieri C, Grodstein F, Rosner BA, Kang JH, Cook NR, Manson JE, Buring JE, Willett WC, Okereke OI. Mediterranean diet and cognitive function in older age. Epidemiology. 2013 Jul;24(4):490-499.

Sangiao-Alvarellos S, Pena-Bello L, Manfredi-Lozano M, Tena-Sempere M, Cordido F. Perturbation of hypothalamic microRNA expression patterns in male rats after metabolic

distress: impact of obesity and conditions of negative energy balance. Endocrinology. 2014 May;55(5):838-850.

Sayed AS, Xia K, Salma U, Yang T, Peng J. Diagnosis, prognosis and therapeutic role of circulating miRNAs in cardiovascular diseases. Heart Lung Circ. 2014 Jun;23(6):503-510.

Scharfman HE, Chao MV. The entorhinal cortex and neurotrophin signaling in Alzheimer's disease and other disorders. Cogn Neurosci. 2013;4(3-4):123-135.

Schieke SM, Finkel T. Mitochondrial signaling, TOR, and life span. Biol Chem. 2006 Oct-Nov;387(10-11):1357-1361

Schipper HM, Maes OC, Chertkow HM, Wang E. MicroRNA expression in Alzheimer blood mononuclear cells. Gene Regulation and Systems Biology. 2009; 1:263–274

Schmatz R, Mazzanti CM, Spanevello R, Stefanello N, Gutierres J, Corrêa M, da Rosa MM, Rubin MA, Chitolina Schetinger MR, Morsch VM. Resveratrol prevents memory deficits and the increase in acetylcholinesterase activity in streptozotocin-induced diabetic rats. Eur J Pharmacol. 2009 May 21;610(1-3):42-8.

Schriner SE, Linford NJ, Martin GM, Treuting P, Ogburn CE, Emond M, Coskun PE, Ladiges W, Wolf N, Van Remmen H, Wallace DC, Rabinovitch PS. Extension of murine life span by overexpression of catalase targeted to mitochondria. Science. 2005 Jun 24;308(5730):1909-1911.

Schumacher B, Garinis GA, Hoeijmakers JH. Age to survive: DNA damage and aging. Trends Genet. 2008 Feb;24(2):77-85.

Schwarzenbach H, Nishida N, Calin GA, Pantel K. Clinical relevance of circulating cell-free microRNAs in cancer. Nat Rev Clin Oncol. 2014 Mar;11(3):145-156.

Sedelnikova OA, Horikawa I, Zimonjic DB, Popescu NC, Bonner WM, Barrett JC. Senescing human cells and ageing mice accumulate DNA lesions with unrepairable double-strand breaks. Nat Cell Biol. 2004 Feb;6(2):168-170.

Sedensky MM, Morgan PG. Mitochondrial respiration and reactive oxygen species in mitochondrial aging mutants. Exp Gerontol. 2006 Mar;41(3):237-245.

Serra A, Rubió L, Borràs X, Macià A, Romero MP, Motilva MJ. Distribution of olive oil phenolic compounds in rat tissues after administration of a phenolic extract from olive cake. Mol Nutr Food Res. 202 Mar;56(3):486-496.

Sestan N, Artavanis-Tsakonas S, Rakic P. Contact-dependent inhibition of cortical neurite growth mediated by notch signaling. Science. 1999 Oct 22; 286(5440):741-746.

Shan Q, Lu J, Zheng Y, Li J, Zhou Z, Hu B, Zhang Z, Fan S, Mao Z, Wang YJ, Ma D. Purple sweet potato color ameliorates cognition deficits and attenuates oxidative damage and inflammation in aging mouse brain induced by d-galactose. J. Biomed. Biotechnol. 2009;2009:564-573.

Sheinerman KS, Tsivinsky VG, Abdullah L, Crawford F, Umansky SR. Plasma microRNA biomarkers for detection of mild cognitive impairment: biomarker validation study. Aging (Albany NY). 2013 Dec;5(12):925-938.

Shin CM, Chung YH, Kim MJ, Lee EY, Kim EG, Cha CI. Age-related changes in the distribution of nitrotyrosine in the cerebral cortex and hippocampus of rats. Brain Res. 2002;931:194-199.

Shors TJ, Miesegaes G, Beylin A, Zhao M, Rydel T, Gould E. Neurogenesis in the adult is involved in the formation of trace memories. Nature. 2001 Mar 15; 410(6826):372-376.

Siegel G, Obernosterer G, Fiore R, Oehmen M, Bicker S, Christensen M, Khudayberdiev S, Leuschner PF, Busch CJ, Kane C, Hübel K, Dekker F, Hedberg C, Rengarajan B, Drepper C, Waldmann H, Kauppinen S, Greenberg ME, Draguhn A, Rehmsmeier M, Martinez J, Schratt GM. A functional screen implicates microRNA-138-dependent regulation of the depalmitoylation enzyme APT1 in dendritic spine morphogenesis. Nat Cell Biol. 2009 Jun;11(6):705-716.

Sikora E, Arendt T, Bennett M, Narita M. Impact of cellular senescence signature on ageing research. Ageing Res Rev. 2011 Jan;10(1):146-152.

Sikora E, Bielak-Zmijewska A, Mosieniak G. Cellular senescence in ageing, age-related disease and longevity. Curr Vasc Pharmacol. 2014;12(5):698-706.

Simonsen A, Cumming RC, Brech A, Isakson P, Schubert DR, Finley KD. Promoting basal levels of autophagy in the nervous system enhances longevity and oxidant resistance in adult Drosophila. Autophagy. 2008 Feb;4(2):176-184.

Sinclair DA. Toward a unified theory of caloric restriction and longevity regulation. Mech Ageing Dev 2005;26:987-1002

Singhal G, Jaehne EJ, Corrigan F, Toben C, Baune BT. Inflammasomes in neuroinflammation and changes in brain function: a focused review. Front Neurosci. 2014 Oct 7;8:315-320.

Sinha K, Chaudhary G, Gupta YK. Protective effect of resveratrol against oxidative stress in middle cerebral artery occlusion model of stroke in rats. Life Sci. 2002 Jun 28;71(6):655-665.

Smith-Vikos T, Slack FJ. MicroRNAs and their roles in aging. J Cell Sci. 2012 Jan 1;125(Pt 1):7-17.

Sofi F, Cesari F, Abbate R, Gensini GF, Casini A. Adherence to Mediterranean diet and health status: meta-analysis. BMJ. 2008 Sep 11;337:a1344.

Solfrizzi V, Colacicco AM, D'Introno A, Capurso C, Torres F, Rizzo C, Capurso A, Panza F. Dietary intake of unsaturated fatty acids and age-related cognitive decline: a 8.5-year follow-up of the Italian Longitudinal Study on Aging. Neurobiol Aging. 2006 Nov;27(11):1694-1704.

Sordet O, Redon CE, Guirouilh-Barbat J, Smith S, Solier S, Douarre C, Conti C, Nakamura AJ, Das BB, Nicolas E, Kohn KW, Bonner WM, Pommier Y. Ataxia telangiectasia mutated activation by transcription- and topoisomerase I-induced DNA double-strand breaks. EMBO Rep. 2009 Aug;10(8):887-893.

Spencer JP. Beyond antioxidants: the cellular and molecular interactions of flavonoids and how these underpin their actions on the brain. Proc. Nutr. Soc. 2010; 69: 244–260.

Spencer JP. The interactions of flavonoids within neuronal signalling pathways. Genes Nutr.2007; 2:257–273.

Stewart J, Mitchell J, Kalant N The effects of life-long food restriction on spatial memory in young and aged Fischer 344 rats measured in the eight-arm radial and the Morris water mazes. Neurobiol Aging. 1989 Nov-Dec; 10(6):669-675

St-Laurent-Thibault, C., Arseneault, M., Longpre, F., Ramassamy, C. Tyrosol and hydroxytyrosol two main components of olive oil, protect N2a cells against amyloid-beta-induced toxicity. Involvement of the NF-kappa B signaling. Curr. Alzh. Res. 20; 8: 543–555.

Strosznajder JB, Czapski GA, Adamczyk A, Strosznajder RP. Poly(ADP-ribose) polymerase-1 in amyloid beta toxicity and Alzheimer's disease. Mol Neurobiol. 2012;46:78-84.

Suárez M, Valls RM, Romero MP, Macià A, Fernández S, Giralt M, Solà R, Motilva MJ. Bioavailability of phenols from a phenol-enriched olive oil. Br J Nutr. 20 Dec;06:69-70.

Sulli G, Di Micco R, d'Adda di Fagagna F. Crosstalk between chromatin state and DNA damage response in cellular senescence and cancer. Nat Rev Cancer. 2012 Oct;12(10):709-720.

Sun CY, Qi SS, Sun SH. Effect of curcumin on the learning, memory and hippocampal Ca+/CaMK II level in senescence-accelerated mice. Zhongguo Zhong Xi Yi Jie He Za Zhi. 2011 Mar;31(3):376-80.

Sun W, McConnell E, Pare JF, Xu Q, Chen M, Peng W, Lovatt D, Han X, Smith Y, Nedergaard M. Glutamate-dependent neuroglial calcium signaling differs between young and adult brain. Science. 2013 Jan 11;339(6116):197-200.

Swarup V, Srivastava AK, Rajeswari MR. Identification and quantification of differentially expressed proteins in plasma of spinocerebellar ataxia type 12. Neurosci Res. 2012 Jun;73(2):161-167.

Taguchi A, Wartschow LM, White MF. Brain IRS2 signaling coordinates life span and nutrient homeostasis. Science. 2007 Jul 20;317(5836):369-372.

Tanaka J, Horiike Y, Matsuzaki M, Miyazaki T, Ellis-Davies GC, Kasai H. Protein synthesis and neurotrophin-dependent structural plasticity of single dendritic spines. Science. 2008 Mar 21;319(5870):1683-1687.

Tapia-Arancibia L, Aliaga E, Silhol M, Arancibia S. New insights into brain BDNF function in normal aging and Alzheimer disease. Brain Res Rev. 2008 Nov;59(1):201-220.

Tissenbaum HA, Guarente L. Increased dosage of a sir-2 gene extends lifespan in Caenorhabditis elegans. Nature. 2001 Mar 8;410(6825):227-230.

Tomaru U, Takahashi S, Ishizu A, Miyatake Y, Gohda A, Suzuki S, Ono A, Ohara J, Baba T, Murata S, Tanaka K, Kasahara M. Decreased proteasomal activity causes age-related phenotypes and promotes the development of metabolic abnormalities. Am J Pathol. 2012 Mar;180(3):963-972.

Trifunovic A, Wredenberg A, Falkenberg M, Spelbrink JN, Rovio AT, Bruder CE, Bohlooly-Y M, Gidlöf S, Oldfors A, Wibom R, Törnell J, Jacobs HT, Larsson NG. Premature ageing in mice expressing defective mitochondrial DNA polymerase. Nature. 2004 May 27;429(6990):417-423.

Tripoli E, Giammanco M, Tabacchi G, Di Majo D, Giammanco S, La Guardia M. The phenolic compounds of olive oil: structure, biological activity and beneficial effects on human health. Nutr. Res. Rev. 2005;8:98–102.

Tsang J, Zhu J, van Oudenaarden A. MicroRNA-mediated feedback and feed forward loops are recurrent network motifs in mammals. Mol Cell. 2007;26:753–767.

Tsang WP, Kwok TT. Epigallocatechin gallate up-regulation of miR-16 and induction of apoptosis in human cancer cells. J Nutr Biochem. 2010 Feb;21(2):140-146.

Tsivgoulis G, Judd S, Letter AJ, Alexandrov AV, Howard G, Nahab F, Unverzagt FW, Moy C, Howard VJ, Kissela B, Wadley VG. Adherence to a Mediterranean diet and risk of incident cognitive impairment. Neurology. 2013 Apr 30;80(18):1684-1692.

Valls-Pedret C, Lamuela-Raventos RM, Medina-Remon A, Quintana M, Corella D, Pinto X, Martinez-Gonzalez MA, Estruch R, Ros E: Polyphenol-rich foods in the Mediterranean diet are associated with better cognitive function in elderly subjects at high cardiovascular risk. J Alzheimers Dis. 2012, 29:773-782.

Van der Heide LP, Ramakers GM, Smidt MP. Insulin signaling in the central nervous system: learning to survive. Prog Neurobiol. 2006 Jul;79(4):205-221.

Van Raamsdonk JM, Hekimi S. Deletion of the mitochondrial superoxide dismutase sod-2 extends lifespan in Caenorhabditis elegans. PLoS Genet. 2009 Feb;5(2):e1000361.

Vauzour D. Dietary polyphenols as modulators of brain functions: biological actions and molecular mechanisms underpinning their beneficial effects. Oxid Med Cell Longev. 2012;2012:914273.

Verkhratsky A, Parpura V. Recent advances in (patho)physiology of astroglia. Acta Pharmacol Sin. 2010 Sep;31(9):1044-1054.

Vijg J, Suh Y. Genome instability and aging. Annu Rev Physiol. 2013;75:645-668.

Virgili M, Contestabile A. Partial neuroprotection of in vivo excitotoxic brain damage by chronic administration of the red wine antioxidant agent, trans-resveratrol in rats. Neurosci Lett. 2000 Mar 10;281(2-3):123-126.

Visioli F, De La Lastra CA, Andres-Lacueva C, Aviram M, Calhau C, Cassano A, D'Archivio M, Faria A, Favé G, Fogliano V, Llorach R, Vitaglione P, Zoratti M, Edeas M. Polyphenols and human health: a prospectus. Crit Rev Food Sci Nutr. 2011 Jul;51(6):524-546.

Visioli F, Galli C, Bornet F, Mattei A, Patelli R, Galli G, Caruso D Olive oil phenolics are dose-dependently absorbed in humans. FEBS Lett. 2000 Feb 25; 468(2-3):59-60.

Visioli F, Galli C. Biological properties of olive oil phytochemicals. Crit Rev Food Sci Nutr. 2002;42(3):209-212.

Visioli F, Galli C. Natural antioxidants and prevention of coronary heart disease: the potential role of olive oil and its minor constituents. Nutr. Metab. Cardio. Dis. 995;5:306–34.

Visioli F, Poli A, Gall C. Antioxidant and other biological activities of phenols from olives and olive oil. Med Res Rev. 2002 Jan;22(1):65-75.

Vissers MN, Zock PL, Katan MB. Bioavailability and antioxidant effects of olive oil phenols in humans: a review. Eur J Clin Nutr. 2004 Jun;58(6):955-965.

Viswanathan M, Guarente L. Regulation of Caenorhabditis elegans lifespan by sir-2.1 transgenes. Nature. 2011 Sep 21;477(7365):E1-2.

Waki T, Tamura G, Sato M, Motoyama T. Age-related methylation of tumor suppressor and tumor-related genes: an analysis of autopsy samples. Oncogene. 2003 Jun 26;22(26):4128-4133.

Walle T. Bioavailability of resveratrol. Ann N Y Acad Sci. 20;25:9-5.

Wang C, Jurk D, Maddick M, Nelson G, Martin-Ruiz C, von Zglinicki T. DNA damage response and cellular senescence in tissues of aging mice. Aging Cell. 2009 Jun;8(3):311-323.

Wang Q, Xu J, Rottinghaus GE, Simonyi A, Lubahn D, Sun GY, Sun AY. Resveratrol protects against global cerebral ischemic injury in gerbils. Brain Res. 2002 Dec 27;958(2):439-447.

Wang WX, Huang Q, Hu Y, Stromberg AJ, Nelson PT. Patterns of microRNA expression in normal and early Alzheimer's disease human temporal cortex: white matter versus gray matter. Acta Neuropathol. 2011 Feb;121(2):193-205.

Wang X, Liu P, Zhu H, Xu Y, Ma C, Dai X, Huang L, Liu Y, Zhang L, Qin C. miR-34a, a microRNA up-regulated in a double transgenic mouse model of Alzheimer's disease, inhibits bcl2 translation. Brain Res Bull. 2009 Oct 28;80(4-5):268-273.

Wayman GA, Davare M, Ando H, Fortin D, Varlamova O, Cheng HY, Marks D, Obrietan K, Soderling TR, Goodman RH, Impey S. An activity-regulated microRNA controls dendritic plasticity by down-regulating p250GAP. Proc Natl Acad Sci U S A. 2008 Jul 1;105(26):9093-9098.

Weinbrenner T, Fitó M, de la Torre R, Saez GT, Rijken P, Tormos C, Coolen S, Albaladejo MF, Abanades S, Schroder H, Marrugat J, Covas MI. Olive oils high in phenolic compounds modulate oxidative/antioxidative status in men. J Nutr. 2004 Sep;134(9):2314-2321.

Wey MC, Fernandez E, Martinez PA, Sullivan P, Goldstein DS, Strong R. Neurodegeneration and motor dysfunction in mice lacking cytosolic and mitochondrial aldehyde dehydrogenases: implications for Parkinson's disease. PLoS One. 2012;7(2):e31522.

Willett WC, Sacks F, Trichopoulou A, Drescher G, Ferro-Luzzi A, Helsing E, Trichopoulos D. Mediterranean diet pyramid: a cultural model for healthy eating. Am J Clin Nutr. 1995 Jun;61(6 Suppl):1402S-1406S.

Willi R, Winter C, Wieske F, Kempf A, Yee BK, Schwab ME, Singer P., Loss of EphA4 impairs short-term spatial recognition memory performance and locomotor habituation. Genes Brain Behav. 2012 Aug; 11(8):1020-1031

Williams RJ, Spencer JP. Flavonoids, cognition, and dementia: actions, mechanisms, and potential therapeutic utility for Alzheimer disease. Free Radic Biol Med. 2012 Jan 1;52(1):35-45.

Witte AV, Fobker M, Gellner R, Knecht S, Flöel A. Caloric restriction improves memory in elderly humans. Proc Natl Acad Sci U S A. 2009 Jan 27; 106(4):1255-1260.

Wong MY, Yu Y, Walsh WR, Yang JL. microRNA-34 family and treatment of cancers with mutant or wild-type p53 (Review). Int J Oncol. 2011 May;38(5):1189-1195.

Wong RH, Coates AM, Buckley JD, Howe PR. Evidence for circulatory benefits of resveratrol in humans. Ann N Y Acad Sci. 2013 Jul;1290:52-58.

Wood JG, Rogina B, Lavu S, Howitz K, Helfand SL, Tatar M, Sinclair D. Sirtuin activators mimic caloric restriction and delay ageing in metazoans. Nature. 2004 Aug 5;430(7000):686-689.

Xie J, Zhang X, Zhang L. Negative regulation of inflammation by SIRT1. Pharmacol Res. 2013 Jan;67(1):60-67.

Yang J, Chen D, He Y, Meléndez A, Feng Z, Hong Q, Bai X, Li Q, Cai G, Wang J, Chen X. MiR-34 modulates Caenorhabditis elegans lifespan via repressing the autophagy gene atg9. Age (Dordr). 2013 Feb;35(1):11-22.

Yankner BA, Lu T, Loerch P. The aging brain. Annu Rev Pathol. 2008;3:41-66.

Zhang H, Yang H, Zhang C, Jing Y, Wang C, Liu C, Zhang R, Wang J, Zhang J, Zen K, Zhang C, Li D. Investigation of MicroRNA Expression in Human Serum During the Aging Process. J Gerontol A Biol Sci Med Sci. 2015 Jan;70(1):102-109.

Zhang R, Poustovoitov MV, Ye X, Santos HA, Chen W, Daganzo SM, Erzberger JP, Serebriiskii IG, Canutescu AA, Dunbrack RL, Pehrson JR, Berger JM, Kaufman PD, Adams PD. Formation of MacroH2A-containing senescence-associated heterochromatin foci and senescence driven by ASF1a and HIRA. Dev Cell. 2005;8:19-30.

Zhang Y, Ikeno Y, Qi W, Chaudhuri A, Li Y, Bokov A, Thorpe SR, Baynes, JW, Epstein C, Richardson A, Van Remmen H. Mice deficient in both Mn superoxide dismutase and glutathione peroxidase-1 have increased oxidative damage and a greater incidence of pathology but no reduction in longevity. J. Gerontol. A Biol. Sci. Med. Sci. 2009; 64, 1212–1220.

Zhao YN, Li WF, Li F, Zhang Z, Dai YD, Xu AL, Qi C, Gao JM, Gao J. Resveratrol improves learning and memory in normally aged mice through microRNA-CREB pathway. Biochem Biophys Res Commun. 2013 Jun 4;435(4):597-602.

Zhu HC, Wang LM, Wang M, Song B, Tan S, Teng JF, Duan DX. MicroRNA-195 downregulates Alzheimer's disease amyloid-β production by targeting BACE1. Brain Res Bull. 2012 Sep 1;88(6):596-601.

Zovoilis A, Agbemenyah HY, Agis-Balboa RC, Stilling RM, Edbauer D, Rao P, Farinelli L, Delalle I, Schmitt A, Falkai P, Bahari-Javan S, Burkhardt S, Sananbenesi F, Fischer A. microRNA-34c is a novel target to treat dementias. EMBO J. 2011 Sep 23;30(20):4299-4308.